2023

Ecology Of Larval Fishes Along The Western Antarctic Peninsula: Climate-Change Impact, Taxonomy, Phenology, And Thermal Tolerance

Andrew Derik Corso
William & Mary - Virginia Institute of Marine Science, 705adc@gmail.com

Recommended Citation

Corso, Andrew Derik, "Ecology Of Larval Fishes Along The Western Antarctic Peninsula: Climate-Change Impact, Taxonomy, Phenology, And Thermal Tolerance" (2023). *Dissertations, Theses, and Masters Projects.* William & Mary. Paper 1697552482.
https://dx.doi.org/10.25773/v5-nq6n-y836

Ecology of larval fishes along the western Antarctic Peninsula: climate-change impact, taxonomy, phenology, and thermal tolerance

A Dissertation

Presented to

The Faculty of the School of Marine Science

The College of William and Mary in Virginia

In Partial Fulfillment

of the Requirements for the Degree of

Doctor of Philosophy

by

Andrew Derik Corso

August 2023

APPROVAL PAGE

This dissertation is submitted in partial fulfillment of

the requirements for the degree of

Doctor of Philosophy

Andrew Derik Corso

Approved by the Committee, August 2023

Eric J. Hilton, Ph.D.
Committee Co-Chair / Co-Advisor

Deborah K. Steinberg, Ph.D.
Committee Co-Chair / Co-Advisor

Jan R. McDowell, Ph.D.

Michael Vecchione, Ph.D.

Christopher D. Jones, Ph.D.
National Oceanic and Atmospheric Administration, National Marine Fisheries Service,
Southwest Fisheries Science Center
La Jolla, California, USA

For my father, Dr. William Corso.

TABLE OF CONTENTS

CHAPTER 6

CHAPTER 7

ACKNOWLEDGEMENTS

I am grateful for the support and friendship of many wonderful people during my Ph.D. program. Firstly, I thank my amazing co-advisors, Drs. Eric J. Hilton and Deborah K. Steinberg. Their encouragement, knowledge, patience, and wonderful personalities created a fun and productive research environment. They both welcomed me into their labs as an undergraduate volunteer and I will forever appreciate their mentorship and friendship. I am also thankful for an excellent committee – Drs. Jan R. McDowell, Michael Vecchione, and Christopher D. Jones. Whether it was hosting me at the Smithsonian, providing invaluable genetic advice and expertise, or answering my excessive emails about Antarctic fishes, my committee has helped me in countless ways over the last six years.

The Virginia Institute of Marine Science (VIMS) is a great place to conduct graduate research for several reasons, not the least of which being the community. I have met several lifelong friends at VIMS. I cherish the friendship and support of Drs. Adena Schonfeld, Kyle Hinson, Stephanie Wilson, Jack Conroy, Patricia Thibodeau, Kate Bemis, Laur Ferris, and many other fellow VIMS graduates. I also value the friendship and help of Joe Cope, Tor Mowatt-Larssen, Miguel Montalvo, Maya Thomas, Brian Kim, Kristen Sharpe, Drs. Dan Crear and Willie Goldsmith, Meredith Nolan, and others who made my time at VIMS so fun. I have received immeasurable guidance at VIMS, but I would especially like to thank Drs. Robert Latour, Sarah Huber, Peter Konstantinidis, Linda Schaffner, Iris Anderson, and Bongkeun Song, and Ellen Biesack, Jennifer Hay, and Catherine Cake.

Beyond VIMS, I am thankful for the many wonderful people who I have had the pleasure to work with in Antarctica, including Drs. Ben Van Mooy, Megan Cimino, Oscar Schofield, Carlos Moffat, Hugh Ducklow, and Bill Fraser, Ross Nichols, Arianna Torello, Leigh West, Josh Mitchell, Tepper Rasmussen, Diane Hutt, Julian Race, Captains Ernest Stelly and Matt Gosselin, Megan and Darren Roberts, and Maggie Amsler. I also appreciate the dedication of other captains, crew, and staff of the ASRV *Laurence M. Gould* and at Palmer Station for making a harsh environment not only safe to conduct research, but enjoyable. I benefitted from the mentorship of several other collaborators, including Drs. Sharon Stammerjohn, Thomas Desvignes, Chuck Amsler, Marino Vacchi, Laura Ghigliotti, and Mario La Mesa.

My parents, Adrienne and Bill Corso, shaped my passion for science, and my brother, Jack Corso, helped maintain my sanity during graduate school. I am enormously appreciative of their love and help through the ups and downs of life. I am also grateful for the love of my new family, Tucker and Mark Schrage and numerous other Schrages, Nortons, and Bryans.

Finally, I want to thank my partner, Kharis Schrage. Her love and unwavering commitment to furthering my interests has been nothing short of extraordinary, especially during our many months in opposite hemispheres. I am a better scientist and person from her influence.

The research associated with this dissertation was supported by the National Science Foundation Office of Polar Programs (OPP-1440435 and 2026045) and Division of Biological Infrastructure (DBI-1349327), VIMS Office of Academic Studies, the VIMS John Olney Fellowship, the Explorers Club, and the Scientific Committee on Antarctic Research.

LIST OF TABLES

Chapter 2

Chapter 3

Chapter 4

Chapter 5

Chapter 6

LIST OF FIGURES

Chapter 2

Chapter 3

Chapter 4

Chapter 5

Chapter 6

ABSTRACT

The Antarctic fish fauna is unique, with approximately 88% of the ~375 known species endemic to the Southern Ocean. One group, the perciform suborder Notothenioidei, dominates fish richness and biomass. These fishes possess several traits that allow existence in frigid conditions, but also limit their ability to cope with temperature increases due to climate change. In the western Antarctic Peninsula (WAP) region, a combination of anthropogenic impacts, including climate change and fishing pressure, threaten these fishes. The WAP is one of the most rapidly warming regions globally (3.4 °C per century) and has the highest fishing pressure for Antarctic krill in the Southern Ocean, which can result in the bycatch of larval notothenioids. The goal of my dissertation is to utilize interdisciplinary techniques to better understand the diversity of these unique fishes, as well as more accurately predict how their early life stages will respond to future conditions. Data in my dissertation are sourced from the Palmer Antarctica Long-Term Ecological Research (Palmer LTER) program, established in 1990 to study the pelagic ecosystem of the WAP. Larval fishes are captured annually as bycatch in Palmer LTER zooplankton net tows and represent the longest running (30+ years), fisheries-independent time series of Antarctic fishes. In Chapter 2, I utilize this novel time series to model the impacts of environmental change on *Pleuragramma antarctica* (Nototheniidae) larvae. Adult *P. antarctica* use sea ice as spawning habitat and are important prey for penguins and other predators. I show that warmer sea surface temperature and decreased sea ice are associated with reduced larval abundance, indicating these keystone fish could disappear regionally in the near future. In Chapter 3, I employ a combination of morphological and genetic analyses to describe unknown early life stages of a rare notothenioid genus (*Akarotaxis*; Bathydraconidae), which led to the discovery of a new species, *Akarotaxis* n. sp., that is described in Chapter 4. These two Chapters provide information on the evolution of notothenioids and biology of *Akarotaxis* n. sp., which appears to be endemic to the WAP region. In Chapter 5, I model biotic and abiotic drivers of phenology and growth of the larval fish assemblage near Palmer Station on the WAP. Several fish species are positively correlated with copepod and diatom abundances, which are modulated by interannual changes in sea ice. In addition, I model dispersion pathways of nototheniid yolk-sac larvae to locate their potential spawning areas. In Chapter 6, I use thermal tolerance experiments to study the physiological vulnerability to warming of larvae from three notothenioid families (Nototheniidae, Channichthyidae, and Artedidraconidae). Thermal tolerance increases with body length in larval channichthyids, suggesting that younger, less motile larvae may be especially susceptible to rapid warming events such as marine heatwaves. Results also indicate that the artedidraconid species *Neodraco skottsbergi* possesses one of the highest thermal tolerances reported for endemic notothenioids of any life stage. I offer ecological and evolutionary hypotheses that may explain this remarkable tolerance. My research provides multifaceted information on the vulnerable early life stages of fishes in a rapidly changing ecosystem. These insights inform future research priorities and will significantly contribute to the ongoing development of Marine Protected Areas in the Southern Ocean.

Ecology of larval fishes along the western Antarctic Peninsula: climate-change impact, taxonomy, phenology, and thermal tolerance

CHAPTER 1

Introduction to the dissertation

Warming and climatic variability of the western Antarctic Peninsula

The western Antarctic Peninsula (WAP) region has experienced rapid environmental change over the last century. From 1951 to 2000, there was an increase in annual mean surface air temperature of 2.8° C (Turner et al. 2016), classifying the WAP as one of the fastest warming regions on Earth during this period (Vaughan et al. 2003). Beginning around 1999, the WAP entered a cooling phase with a decadal decrease in air temperature of – 0.47° C (Turner et al. 2016; Oliva et al. 2017). Regional ice core records from the Antarctic Peninsula (AP) indicate this variability is likely a result of natural decadal oscillations rather than global warming (Turner et al. 2016). However, it appears anthropogenically-induced Antarctic ozone losses and greenhouse gas emissions magnified the WAP warming phase by inducing a trend in positive Southern Annular Mode (SAM) events (Thompson and Solomon 2002; Turner et al. 2016). Due to a continuation of positive SAM events and increasing variability in other teleconnections, the WAP is projected to continue a long-term trend of ocean warming (Cai et al. 2023).

Three atmospheric teleconnections predominantly influence the WAP climate – the SAM, the Amundsen Sea Low (ASL), and the El Niño Southern Oscillation (ENSO). Their linkages are complex and seasonally variable (Raphael et al. 2016). Positive SAM events cause the Antarctic Circumpolar Current (ACC) to contract closer to the continent and spin-up (i.e., deepen) the ASL, a cyclonic low-pressure system (Maksym et al. 2012; Coggins and McDonald 2015). A deepened ASL draws down more warm northerly winds along the AP. Ozone depletion over Antarctica resulted in a trend of positive SAM events and deepened ASL that was partially responsible for the warming phase (Turner et al. 2016; Henley et al. 2019). The ENSO phenomenon can magnify or dampen the effects of SAM (Clem and Fogt 2013). The La Niña (El

Niño) phase of ENSO brings warmer (cooler) air to the Bellingshausen Sea (Yuan 2004, p. 20; Wang et al. 2023).

There are indications that the recent recovery of the ozone hole led to more neutral or negative SAM events, a weaker ASL, and the cooling phase over the WAP (Henley et al. 2019). However, greenhouse gas emissions also lead to positive SAM events (Gille et al. 2016). The Antarctic ozone hole is predicted to recover entirely by about the year 2100, while most scenarios predict increasing greenhouse gas emissions through 2100 (Szulejko et al. 2017; Screen et al. 2018). It is unclear how these counteracting forces will impact future SAM events (Arblaster et al. 2011). The effects of medium emission scenarios would possibly be cancelled out by ozone recovery, while high emission scenarios will likely result in a prolonged trend of positive SAM events and atmospheric warming (Rintoul et al. 2018; Screen et al. 2018).

Cryospheric (ice) and physical dynamics

The WAP is unique among Antarctic geographic features as it lies closer to the ACC than any other Antarctic land mass (Ducklow et al. 2012; Martinson 2012). Westerly winds will often create subsurface eddies that transport some of the warmer ACC water towards the continental shelf (Henley et al. 2019). This warm water, referred to as Circumpolar Deep Water (CDW), is a major factor in controlling the near-shore environment of the WAP (Martinson et al. 2008). As the WAP shelf region is approached from the continental slope, depths rise from 3000 to 500 meters. The average depth of the Antarctic shelf (~500m) is several times greater than the global average, primarily due to weight from the continental ice sheet (Anderson 1999; Eastman and McCune 2000).

The WAP coastal region is made up of many islands, fjords, submarine canyons, and deep channels. The only area of the WAP coastal region where the Weddell Sea exchanges with the Bellingshausen Sea is through the Bransfield Strait, located at the northernmost tip of the WAP. During most years, several localized gyres also develop on the WAP shelf. Gyres and submarine canyons (450 to 1000 m deep) transport nutrient-rich CDW onto the shelf (Martinson et al. 2008; Gille et al. 2016). The volume and depth of CDW inputs partially determine annual gyre intensity (Martinson et al. 2008).

In addition to rising air temperature during the 20th century, the Bellingshausen Sea also warmed significantly (Meredith and King 2005; Schmidtko et al. 2014). Increased westerlies associated with positive SAM events theoretically increase eddy kinetic energy and poleward heat transport towards the WAP (Schmidtko et al. 2014; Gille et al. 2016). As a result, mean ocean temperatures at 150 m increased by ~1° C from 1945 to 2009 and mean CDW temperature warmed at 0.1° C per decade (Schmidtko et al. 2014; Cook et al. 2016). Additional investigations, especially on the impacts of winds on CDW, are necessary to elucidate the suite of mechanisms behind these ocean warming events and future scenarios (Gille et al. 2016). It is clear, however, that trends in SAM and warming water parcels during the late 20th century have significantly impacted the WAP cryosphere (Schmidtko et al. 2014; Cook et al. 2016; Stammerjohn and Maksym 2017).

The WAP sea ice system is primarily controlled by ocean heat flux, precipitation, and atmospheric teleconnections (Maksym et al. 2012; Stammerjohn and Maksym 2017). The northerly winds associated with a deepened ASL push sea ice southward away from the WAP (Henley et al. 2019). Resultingly, the WAP experienced a decline in sea ice duration coinciding with the late 20th century warming phase. In the WAP region, sea ice advances during autumn, reaches peak extent in winter, and begins to retreat in spring. From 1979 – 2004, mean sea ice retreat became 31 days earlier and mean advance 54 days later (Stammerjohn et al. 2008). The overall reduction in WAP sea ice duration during this period was greater than any other region on Earth (Ducklow et al. 2012). There has also been significant glacial retreat in the WAP region. Approximately 90% of 674 marine-terminating glaciers examined on the WAP retreaded from 1945 to 2009 (Cook et al. 2016). In the Bellingshausen Sea, wind-driven eddy transport of CDW is basally melting marine-terminating Antarctic ice shelves (Pritchard et al. 2012).

Although trends in glacial and sea ice dynamics are variable in the WAP region, especially during the early 21st century, long-term declines in ice will continue through 2100 regardless of emission scenarios (Intergovernmental Panel on Climate Change (IPCC) 2022). Following pervasive ice mass loses and retreat during the late 20th century, most glaciers in the northern WAP have experienced ice mass gains from the early 2000s to 2019, partially due to increased snowfall (Oliva et al. 2017) and anomalous sea ice circulation (Christie et al. 2022). However, glacial mass losses in the WAP region have presently resumed (Zemp et al. 2021; Engel et al. 2023). Sea ice duration also increased for a period due to the trend of negative and neutral SAM events (Schofield et al. 2018; Henley et al. 2019). However, the warming trend has returned, and in 2022, the WAP experienced the highest winter air temperature and shortest sea ice season on record– of only 70 days duration (S. Stammerjohn pers. Comm, 2023). While significant losses in sea ice are likely by 2100 (Intergovernmental Panel on Climate Change

(IPCC) 2022), system feedbacks may increase variability in this trend (Bintanja et al. 2013). Future atmospheric warming could stabilize the water column surrounding the WAP and reduce incursions of CDW, increasing sea ice duration and thickness due to a reduction in basal melting (Maksym et al. 2012). Additional research and longer data sets, especially on sea ice thickness, are necessary to accurately predict the scale of future WAP sea ice losses (Maksym et al. 2012; Oliva et al. 2017; Stammerjohn and Maksym 2017).

Phytoplankton and zooplankton dynamics

Sea ice dynamics strongly impact the ecology of the WAP region. Sea ice retreat during austral spring increases available solar illumination and consequent meltwater stratifies the water column (Ducklow et al. 2012; Trimborn et al. 2015), initiating a successional bloom that initially consists of primarily of autotrophic flagellates originating from the sea ice community (van Leeuwe et al. 2020) and centric diatoms (Nardelli et al. 2023). Sea ice melt also releases nutrients into the water column that additionally seed phytoplankton blooms (Ducklow et al. 2007). Higher surface temperatures and surface salinities during mid-summer are associated with cryptophytes, mixed flagellates, and pennate diatoms (Nardelli et al. 2023). Towards the end of the summer, centric diatoms and mixed flagellates are the most abundant (Nardelli et al. 2023). There are regional and bathymetric gradients to the composition of WAP primary production as well. Following increases in day length, offshore production peaks around November, while shelf primary production peaks much later, during late January (Trimborn et al. 2015; Arrigo et al. 2017). While diatoms dominate the phytoplankton community throughout the WAP, generally cryptophytes and *Phaeocystis antarctica* are more common in northern WAP (Trimborn et al. 2015; Schofield et al. 2017; Nardelli et al. 2023).

Primary production declined significantly in the northern WAP from 1979 – 2006, while increasing in the southern WAP. These opposing trends are largely attributed to differing impacts from sea ice decline (Montes-Hugo et al. 2009; Ferreira et al. 2020). Reductions in sea ice during this period exposed the northern WAP coastal waters to more winds, which deepened the mixed layer leading to light limitation for phytoplankton. In the southern WAP, decreased sea ice during summer months allows for more light, promoting phytoplankton growth (Montes-Hugo et al. 2009). Sea ice and glacial loss also impacts the upper mixed layer depth (MLD) and stability of the water column, with a nearly two-fold decrease in MLD in the southern WAP from 1993 to 2017 (Schofield et al. 2018). Phytoplankton community structure is also changing in the WAP region (Montes-Hugo et al. 2009; van Leeuwe et al. 2020), with larger diatoms decreasing and smaller cyrptophytes increasing in the north (Saba et al. 2014). Primary production increased significantly during the temporary recovery of sea ice in the WAP region from 2008 – 2017 (Schofield et al. 2018; Henley et al. 2019), though recent historical sea ice lows have likely altered this trend. Continued glacial retreat will shallow the MLD, which favors taxa that prefer higher light (e.g., cryptophytes), but stronger westerly winds and sea ice losses will deepen the MLD, which favors taxa that prefer low light (e.g., haptophytes) (Ferreira et al. 2020; Mendes et al. 2023). Therefore, future trends in the WAP phytoplankton community remain challenging to predict (Ferreira et al. 2020).

Epipelagic zooplankton (> 2mm) of the WAP region are composed mainly of euphausiids (e.g., *Euphausia superba*, *Thysanoessa marcrura,* and *Euphausia crystallorophias*), calanoid copepods (e.g., *Calanoides acutus* and *Calanus propinquus*), pteropods (e.g., *Limacina rangii*), salps (mostly *Salpa thompsoni*), chaetognaths, polychaetes, and amphipods (Steinberg et al. 2015; Pinkerton et al. 2020; Johnston et al. 2022; Conroy et al. 2023). In the summer, salps prefer ice-free conditions and are generally found farther offshore (Ross et al. 2008; Bernard et al. 2012; Steinberg et al. 2015). Summer pteropod abundance is affected by climatic variability and increases following warmer winters with more ice-free conditions associated with La Niña and positive SAM (Steinberg et al. 2015; Thibodeau et al. 2019). Copepods are the numerically dominant group in the WAP region (Gleiber 2014), while krill and salps represent the majority of biomass in tows (Steinberg et al. 2015).

Due to their key roles in the Antarctic marine food web and harvest pressure by an international fishery, the population dynamics of *E. superba* is an area of substantial research (Johnston et al. 2022). Abundance of *E. superba* from 1926 – 2016 has decreased in the northern WAP. Their range has contracted poleward towards the Antarctic shelves (Atkinson et al. 2019). In the mid-WAP study region of the Palmer Antarctica Long-Term Ecological Research (Palmer LTER) program, *E. superba* has a 5-year cycle in abundance peaks but no long-term directional trend in abundance (Steinberg et al. 2015). There is also evidence of reduced survival of eggs and larval *E. superba* during positive SAM events, leading to reduced recruitment (Atkinson et al. 2019). Larval krill develop under the protection of sea ice during winter, feeding on under-ice algae (Meyer et al. 2017). Therefore, an overall negative trend in the abundance of *E. superba* is partly attributed to reduced sea ice cover (Atkinson et al. 2019). There is also evidence for strong bottom-up control of *E. superba* and other zooplankton species (Saba et al. 2014; Steinberg et al. 2015; Schofield et al. 2017). A shift from diatoms to smaller flagellates (cryptophytes) less accessible to krill, which feed less efficiently on these small prey, could also negatively affect krill stocks (Henley et al. 2019).

Benthic community and upper trophic levels

Approximately 80% of the WAP neritic benthos (< 30 m depth) is covered with macroalgae, rivalling the biomass of dense temperate kelp forests (Wiencke and Amsler 2012; Alder et al. 2017). These macroalgal communities provide critically important habitat for WAP benthic organisms such as gastropods, annelids, crustaceans, and fishes (Huang et al. 2007). Ice scouring, which extends to depths of 500m but primarily occurs at 5m, strongly impacts the WAP nearshore benthic community, a single scouring event can result in >95% reduction in local species abundances (Smale et al. 2008; Alder et al. 2017). At depths below macroalgal coverage and the effects of ice scouring, there is a diverse community of sessile invertebrates that arrange into structures that provide habitat for mobile benthic fauna such as amphipods, isopods, and fishes (McClintock et al. 2010; Alder et al. 2017)

The dominant higher predators of the WAP are penguins (Adélie, Gentoo, and Chinstrap), other seabirds (e.g., south polar skuas), seals, and whales (Ducklow et al. 2012). Penguins in the WAP have been dramatically impacted by climate change. Since 1975, ice-dependent Adélie penguins have decreased by 80%, while ice-intolerant Chinstrap and Genoo penguins have increased (Ducklow et al. 2012). The decrease in Adélie penguins in the northern WAP is primarily due to chick mortality resulting from a continued shift to subpolar conditions (i.e., increased precipitation and reduce sea ice extent) due to climate change (Chapman et al. 2011; Cimino et al. 2016; Cimino et al. 2019; Cimino et al. 2023). However, the decline is also attributed to decreases in one of their main prey items – fishes (Chapman et al. 2011; Cimino et al. 2016).

Fishes of the western Antarctic Peninsula

Fishes form an important yet understudied link in the WAP food web (Ducklow et al. 2012). The Antarctic fish fauna (~370 species) is unique (Duhamel et al. 2014). While these fishes represent only about 2% of global fish diversity, nearly 90% of Antarctic fishes are endemic to the Southern Ocean (Duhamel et al. 2014). The rapid cooling and isolation of Antarctica during the Miocene (20 – 25 million years ago) led to mass extinction of local fauna and reduction of diversity (Eastman 2005, p. 200). As a result, there was an adaptive radiation of the suborder Notothenioidei, one of the only examples of a marine species flock (Eastman and McCune 2000).

Notothenioids represent the majority (~ 75%) of fish diversity in the WAP (Barrera-Oro 2002; Dornburg et al. 2016a). They are also significantly more prevalent than most other taxa, often accounting for ~90% of fish abundance and ~90% of fish biomass (Eastman 2005; Dornburg et al. 2016b; Daane and Detrich 2022). Several major revisions to notothenioid taxonomy based on genetic analyses have been proposed (Near et al. 2012; Duhamel et al. 2014; Near et al. 2018). However, I follow the taxonomy and nomenclature described in Eastman and Eakin (2021). In their species checklist, Eastman and Eakin (2021) state the validity of these genetic-based revisions must be replicated and expanded to include broader taxonomic coverage prior to widespread adoption.

Most notothenioids are circumpolarly distributed and their diversity is greatest in the continental shelf and coastal regions of the Southern Ocean (Duhamel et al. 2014). Five notothenioid families are grouped together in the Cryonotothenioidea (Near et al. 2015): Nototheniidae, Channichthyidae, Bathydraconidae, Artedidraconidae, and Harpagiferidae. All five families lack swim bladders; buoyancy is primarily regulated by differences in bone density and lipid deposits (Near et al. 2012). As a result, most cryonotothenioids are demersal as juveniles and adults, however nearly all species have pelagic larval stages (Gon and Heemstra 1990). From benthic ancestors, species of the family Nototheniidae radiated to occupy different portions of the water column as adults, an example of pelagicism (Eastman and McCune 2000). Consequently, nototheniids are the most abundant fishes near the WAP and the most well-studied (La Mesa et al. 2004).

Due to their availability to predators near the surface, pelagic nototheniids are especially important as prey. The only nototheniid that remains pelagic for its entire life cycle is *Pleuragramma antarctica* (La Mesa and Eastman 2012), which functions as a keystone species and accounts for a major portion of diets for sea birds (e.g., south polar skuas and Adélie penguins) and seals (e.g., Weddell, leopard, and crabeater seals)(Barrera-Oro 2002; Parker et al. 2015). Other nototheniids and channichthyids also commonly consume *P. antarctica* (La Mesa et al. 2004). Zooplankton (e.g., euphausiids [*E. crystallorophias* and *E. superba*] and amphipods normally are the main prey of mature pelagic nototheniids (Barrera-Oro 2002).

Prominent nototheniids near the WAP include *Lepidonotothen* spp., *Trematomus* spp., and *Notothenia* species. These fishes predominantly consume polychaetes, gammarids, isopods, and euphausiids (Barrera-Oro 2002). Several nototheniids appear omnivorous; *Notothenia coriiceps* has repeatedly been observed intentionally ingesting macroalgae (Iken et al. 1997; Amsler et al. 2005). Benthic nototheniids are consumed by seals and seabirds during diving forays. However, their main predators are other fishes (La Mesa et al. 2004). Many neritic nototheniid species, and other cryonotothenioids, may use the dense macroalgal forests as cover from seals and birds while also targeting the amphipods associated with the algae (Amsler et al. 2014).

Channichthyids, especially *Chionodraco* spp. and *Chaenocephalus* spp., commonly occur near the WAP. Channichthyids, or the white-blooded icefishes, are the only known vertebrates that lack the expression of hemoglobin, a protein normally found in red blood cells responsible for transporting oxygen (Beers and Jayasundara 2015). They cope with this loss by directly diffusing oxygen across their thin skin and gills into solution in the plasma of an enlarged circulatory system that can transport larger volumes of blood and oxygen than other notothenioid groups (Beers and Jayasundara 2015). With these adaptations, their oxygen carrying capacity is still < 10% of the red-blooded Antarctic fishes (Beers and Jayasundara 2015). As a result, they are especially slow moving and do not feed extensively (Kock 2005). Based on limited sampling, channichthyids generally consume euphausiids and mesopelagic fishes (Kock 2005).

Significantly less is known about other notothenioid families. Artedidraconids, bathydraconids, and harpagiferids are predominantly sluggish and they are assumed to be sit-and-wait predators (Wyanski and Targett 1981; Barrera-Oro 2002). Artedidraconids and bathydraconids generally occur on the outer edge of the WAP shelf region and are infrequently sampled as adults.

Early life history and reproductive biology of notothenioids

Cryonotothenioid spawning generally occurs during the austral autumn and winter (La Mesa et al. 2021). Due to difficulties associated with sampling during these months, relatively little is known about their reproductive biology. Most cryonotothenioids appear to migrate inshore to lay large eggs on the benthos, presumably to protect them from predators (Loeb et al. 1993; La Mesa et al. 2021). However, *P. antarctica* will lay eggs at the surface within sea ice (La Mesa and Eastman 2012). Incubation can last from 2 – 5 months and hatching largely peaks during spring and summer but can occur throughout the year (Loeb et al. 1993)

Loeb et al. (1993) hypothesized there is a distinct temporal hatching sequence near the WAP that matches peaks in copepod reproduction (Cushing 1990). Most notothenioid larvae can actively feed after absorbing their yolk-sac. Small larvae feed on phytoplankton, especially diatoms (Koubbi et al. 2007) and all life stages of cyclopoid and calanoid copepods (Kellermann 1996). Furcilia stage euphausiid larvae are also important prey for channichthyids, especially for species that hatch in late winter and spring while there is still significant sea ice. Some larval channichthyid species also prey on nototheniid larvae and may have simultaneous hatching events to maximize their overlap. Most notothenioids have abnormally large, yolky eggs that may help yolk-sac larvae survive mismatches with prey (Kellermann 1996). If a notothenioid hatch is decoupled from copepod reproduction, the large yolk-sac can serve as a source of lipids for more than 40 days post-hatch (Kellermann 1996).

Near the WAP, most larvae occur at depths of 0 – 200 m. Fishes generally migrate to the benthos and offshore as they become juveniles (Loeb et al. 1993). Cryonotothenioids have low fecundity, delayed maturation, and abnormally lengthy larval development compared to temperate fishes (Di Prisco et al. 1998; Balushkin 2000). For example, *P. antarctica* develops for over one year as larvae and post-larvae before entering its juvenile stage (La Mesa and Eastman 2012). A later onset of development, or post-displacement, is a heterochronic trait that allows notothenioids to occupy the pelagic niche for longer periods (Voskoboinikova 2001; La Mesa and Eastman 2012).

The location of fish larvae near the WAP is predominantly controlled by physical factors. The intensity of localized gyres affect local retention and distribution of larvae, especially during pre-flexion stages when swimming ability is limited (Loeb et al. 1993; Parker et al. 2015). Additionally, the "larval pump" hypothesis suggests that the Bransfield Strait is a major source of larvae transported from the Weddell Sea (Loeb et al. 1993; Parker et al. 2015). Kellermann (1996) hypothesizes sea ice extent and duration strongly controls notothenioid year classes. In the 1980s near the WAP, he observed similar trends in *P. antarctica* abundance and ice coverage. Poor sea ice conditions could reduce prey and lead to starvation in larval fishes despite their large yolk-sac reserves (Kellermann 1996).

Larvae of sub-Antarctic notothenioids (e.g., *Lepidonotothen squamifrons*) are frequently transported onto the shelf via CDW. The WAP is the southern-most range for many of these sub-Antarctic species (Loeb et al. 1993). The CDW also transports larvae normally found in slope regions onto the WAP shelf. As a result, several species are commonly found in the WAP larval assemblage that do not belong to Notothenioidei (Loeb et al. 1993; Kellermann 1996).

Non-notothenioid fishes

Except for the family Myctophidae (Woods et al. 2023), information on non-notothenioids near the WAP is lacking. Myctophids are mesopelagic and occur on the slope and shelf of the WAP. They predominantly consume euphausiids, copepods, and other fishes (Barrera-Oro 2002). The common species (e.g., *Electrona antarctica*) are important prey for seabirds and seals. Due to their greater energy content, myctophids are preferred by several predators over krill (Barrera-Oro 2002; Ruck et al. 2014). They are also slow growing, with larval stages between one and two years (Greely et al. 1999). Two species (*Notolepis annulata* and *Notolepis coatsorum*) from the family Paralepididae are also frequently found near the WAP. Relatively little is known on the life histories and ecology of *Notolepis*. They are mesopelagic and seem to feed predominantly on krill and amphipods (Hoddell et al. 2000). In the South Shetland Islands, *N. coatsorum* is recognized as one of the most important prey items for the Antarctic Fur seal. Despite their apparent importance, the two species are indistinguishable as larvae (Hoddell et al. 2000).

Other non-notothenioid Antarctic families near the WAP include: Bathylagidae, Gonostomatidae, Macrouridae, and Muraenolepididae (Kellermann 1990; Duhamel et al. 2014; Konstantinidis et al. 2016). These species are rarely encountered as adults and little is known about their diversity, biology, and range, though larvae of each family are annually found near the WAP. Deep water (>500 m) benthic fishes near the WAP primarily belong to the families

Liparidae and Zoarcidae (Eastman 2005). These two families are respectively the first and third most speciose of Southern Ocean fishes. However, minimal deep-water sampling efforts limits knowledge on their biology and population dynamics (Duhamel et al. 2014)

Structure of dissertation

This dissertation examines the ecology, diversity, and phenology of Antarctic fishes, primarily during the larval stages. Much of this research and data collection is affiliated with the Palmer Antarctica Long Term Ecological Research (PAL LTER) program, established in 1990 to study the pelagic ecosystem of the WAP (Ducklow et al. 2007). Larval fishes are captured annually as bycatch in PAL LTER net tows targeting zooplankton and preserved at the Virginia Institute of Marine Science (VIMS) Nunnally Ichthyology Collection. Through a comprehensive effort to sort and identify these larvae as part of this dissertation, the previously unused specimens now represent the longest running (30+ years), fisheries-independent time series of Antarctic fishes.

The dissertation is separated into five main chapters, examining long-term trends in the abundance of *P. antarctica* along the WAP in Chapter 2 (published in *Nature Communications Biology*), the cryptic diversity and biology of lesser known bathydraconid species in Chapters 3 (*published in the Journal of Fish Biology*) and 4, the phenology and seasonal predator-prey interactions of a larval fish assemblage in the coastal WAP region in Chapter 5, and the thermal tolerance of larval cryonotothenioids in Chapter 6, which provides insights into their physiology. The collective impacts of these studies (Chapter 7) are summarized, with suggestions for future research efforts focused on the unique, and potentially imperiled, fishes of the Southern Ocean.

References

Alder V, Azzaro M, Hucke-Gaete R, Mosetti R, Orgeira JL, Quartino L, Rey AR, Schejter L, Secchione M, Marschoff ER. 2017. Southern Ocean. First Global Marine Assessment.:41.

Amsler CD, Iken K, McClintock JB, Amsler MO, Peters KJ, Hubbard JM, Furrow FB, Baker BJ. 2005. Comprehensive evaluation of the palatability and chemical defenses of subtidal macroalgae from the Antarctic Peninsula. Marine Ecology Progress Series. 294:141–159.

Amsler CD, McClintock JB, Baker BJ. 2014. Chemical mediation of mutualistic interactions between macroalgae and mesograzers structure unique coastal communities along the western Antarctic Peninsula. Journal of Phycology. 50(1):1–10.

Anderson JB. 1999. Antarctic marine geology. Cambridge: Cambridge University Press.

Arblaster JM, Meehl GA, Karoly DJ. 2011. Future climate change in the Southern Hemisphere: Competing effects of ozone and greenhouse gases. Geophysical Research Letters. 38(2).

Arrigo KR, van Dijken GL, Alderkamp A-C, Erickson ZK, Lewis KM, Lowry KE, Joy-Warren HL, Middag R, Nash-Arrigo JE, Selz V. 2017. Early spring phytoplankton dynamics in the Western Antarctic Peninsula. Journal of Geophysical Research: Oceans. 122(12):9350–9369.

Atkinson A, Hill SL, Pakhomov EA, Siegel V, Reiss CS, Loeb VJ, Steinberg DK, Schmidt K, Tarling GA, Gerrish L, Sailley SF. 2019. Krill (*Euphausia superba*) distribution contracts southward during rapid regional warming. Nature Climate Change. 9(2):142–147. https://doi.org/10.1038/s41558-018-0370-z

Balushkin AV. 2000. Morphology, classification, and evolution of notothenioid fishes of the Southern Ocean (Notothenioidei, Perciformes). Journal of Ichthyology. 40(1):S74.

Barrera-Oro E. 2002. The role of fish in the Antarctic marine food web: differences between inshore and offshore waters in the southern Scotia Arc and west Antarctic Peninsula. Antarctic Science. 14(4):293–309. https://doi.org/10.1017/S0954102002000111

Beers JM, Jayasundara N. 2015. Antarctic notothenioid fish: what are the future consequences of 'losses' and 'gains' acquired during long-term evolution at cold and stable temperatures? Journal of Experimental Biology. 218(12):1834–1845.

Bernard KS, Steinberg DK, Schofield OM. 2012. Summertime grazing impact of the dominant macrozooplankton off the Western Antarctic Peninsula. Deep Sea Research Part I: Oceanographic Research Papers. 62:111–122.

Bintanja R, van Oldenborgh GJ, Drijfhout SS, Wouters B, Katsman CA. 2013. Important role for ocean warming and increased ice-shelf melt in Antarctic sea-ice expansion. Nature Geoscience. 6(5):376–379. https://doi.org/10.1038/ngeo1767

Cai W, Jia F, Li S, Purich A, Wang G, Wu L, Gan B, Santoso A, Geng T, Ng B, et al. 2023. Antarctic shelf ocean warming and sea ice melt affected by projected El Niño changes. Nature Climate Change. 13(3):235–239. https://doi.org/10.1038/s41558-023-01610-x

Chapman EW, Hofmann EE, Patterson DL, Ribic CA, Fraser WR. 2011. Marine and terrestrial factors affecting Adélie -penguin Pygoscelis adeliae chick growth and recruitment off the western Antarctic Peninsula. Marine Ecology Progress Series. 436:273–289. https://doi.org/10.3354/meps09242

Christie FDW, Benham TJ, Batchelor CL, Rack W, Montelli A, Dowdeswell JA. 2022. Antarctic ice-shelf advance driven by anomalous atmospheric and sea-ice circulation. Nat Geoscience. 15(5):356–362. https://doi.org/10.1038/s41561-022-00938-x

Cimino MA, Conroy JA, Connors E, Bowman J, Corso A, Ducklow H, Fraser W, Friedlaender A, Kim HH, Larsen GD. 2023. Long-term patterns in ecosystem phenology near Palmer Station, Antarctica, from the perspective of the Adélie penguin. Ecosphere. 14(2):e4417.

Cimino MA, Lynch HJ, Saba VS, Oliver MJ. 2016. Projected asymmetric response of Adélie penguins to Antarctic climate change. Scientific Reports. 6(1):28785. https://doi.org/10.1038/srep28785

Cimino MA, Patterson-Fraser DL, Stammerjohn S, Fraser WR. 2019. The interaction between island geomorphology and environmental parameters drives Adélie penguin breeding phenology on neighboring islands near Palmer Station, Antarctica. Ecology and Evolution. 9(16):9334–9349. https://doi.org/10.1002/ece3.5481

Clem KR, Fogt RL. 2013. Varying roles of ENSO and SAM on the Antarctic Peninsula climate in austral spring. Journal of Geophysical Research: Atmospheres. 118(20):11,481-11,492. https://doi.org/10.1002/jgrd.50860

Coggins JHJ, McDonald AJ. 2015. The influence of the Amundsen Sea Low on the winds in the Ross Sea and surroundings: Insights from a synoptic climatology. Journal of Geophysical Research: Atmospheres. 120(6):2167–2189. https://doi.org/10.1002/2014JD022830

Conroy JA, Steinberg DK, Thomas MI, West LT. 2023. Seasonal and interannual changes in a coastal Antarctic zooplankton community. Marine Ecology Progress Series. 706:17–32. https://doi.org/10.3354/meps14256

Cook AJ, Holland PR, Meredith MP, Murray T, Luckman A, Vaughan DG. 2016. Ocean forcing of glacier retreat in the western Antarctic Peninsula. Science. 353(6296):283–286.

Cushing DH. 1990. Plankton Production and Year-class Strength in Fish Populations: An Update of the Match/Mismatch Hypothesis. In: Blaxter JHS, Southward AJ, editors. Advances in

Marine Biology. Vol. 26. Academic Press; p. 249–293. https://doi.org/10.1016/S0065-2881(08)60202-3

Daane JM, Detrich HW. 2022. Adaptations and Diversity of Antarctic Fishes: A Genomic Perspective. Annual Review of Animal Biosciences. 10(1):39–62. https://doi.org/10.1146/annurev-animal-081221-064325

Di Prisco G, Pisano E, Clarke A, White MG. 1998. Development, dispersal and recruitment: a paradox for survival among Antarctic fish. Fishes of Antarctica: a biological overview.:53–62.

Dornburg A, Federman S, Eytan RI, Near TJ. 2016a. Cryptic species diversity in sub-Antarctic islands: A case study of Lepidonotothen. Molecular Phylogenetics and Evolution. 104:32–43. https://doi.org/10.1016/j.ympev.2016.07.013

Dornburg A, Federman S, Eytan RI, Near TJ. 2016b. Cryptic species diversity in sub-Antarctic islands: A case study of Lepidonotothen. Molecular Phylogenetics and Evolution. 104:32–43. https://doi.org/10.1016/j.ympev.2016.07.013

Ducklow H, Clarke A, Dickhut R, Doney SC, Geisz H, Huang K, Martinson DG, Meredith MP, Moeller HV, Montes-Hugo M. 2012. The marine system of the Western Antarctic Peninsula. Antarctic ecosystems: an extreme environment in a changing world.:121–159.

Ducklow HW, Baker K, Martinson DG, Quetin LB, Ross RM, Smith RC, Stammerjohn SE, Vernet M, Fraser W. 2007. Marine pelagic ecosystems: the West Antarctic Peninsula. Philosophical Transactions of the Royal Society B: Biological Sciences. 362(1477):67–94. https://doi.org/10.1098/rstb.2006.1955

Duhamel G, Hulley P-A, Causse R, Koubbi P, Vacchi M, Pruvost P, Vigetta S, Irisson J-O, Mormede S, Belchier M. 2014. Biogeographic patterns of fish.

Eastman JT. 2005. The nature of the diversity of Antarctic fishes. Polar biology. 28:93–107.

Eastman JT, Eakin RR. 2021. Checklist of the species of notothenioid fishes. Antarctic Science. 33(3):273–280. https://doi.org/10.1017/S0954102020000632

Eastman JT, McCune AR. 2000. Fishes on the Antarctic continental shelf: evolution of amarine species flock? Journal of Fish Biology. 57:84–102.

Engel Z, Láska K, Kavan J, Smolíková J. 2023. Persistent mass loss of Triangular Glacier, James Ross Island, north-eastern Antarctic Peninsula. Journal of Glaciology. 69(273):27–39. https://doi.org/10.1017/jog.2022.42

Ferreira A, Costa RR, Dotto TS, Kerr R, Tavano VM, Brito AC, Brotas V, Secchi ER, Mendes CRB. 2020. Changes in Phytoplankton Communities Along the Northern Antarctic Peninsula: Causes, Impacts and Research Priorities. Frontiers in Marine Science. 7. https://www.frontiersin.org/articles/10.3389/fmars.2020.576254

Gille ST, McKee DC, Martinson DG. 2016. Temporal Changes in the Antarctic Circumpolar Current: Implications for the Antarctic Continental Shelves. Oceanography. 29(4):96–105.

Gleiber M. 2014. Long-Term Change in Copepod Community Structure in the Western Antarctic Peninsula: Linkage to Climate and Implications for Carbon Cycling. Dissertations, Theses, and Masters Projects. https://dx.doi.org/doi:10.25773/v5-we5s-aq55

Gon O, Heemstra PC. 1990. Fishes of the Southern Ocean. JLB Smith Institute of Ichthyology Grahamstown.

Greely TM, Gartner Jr JV, Torres JJ. 1999. Age and growth of Electrona antarctica (Pisces: Myctophidae), the dominant mesopelagic fish of the Southern Ocean. Marine Biology. 133(1):145–158. https://doi.org/10.1007/s002270050453

Henley SF, Schofield OM, Hendry KR, Schloss IR, Steinberg DK, Moffat C, Peck LS, Costa DP, Bakker DC, Hughes C. 2019. Variability and change in the west Antarctic Peninsula marine system: research priorities and opportunities. Progress in Oceanography. 173:208–237.

Hoddell RJ, Crossley AC, Williams R, Hosie GW. 2000. The distribution of Antarctic pelagic fish and larvae (CCAMLR division 58.4. 1). Deep Sea Research Part II: Topical Studies in Oceanography. 47(12–13):2519–2541.

Huang YM, Amsler MO, McClintock JB, Amsler CD, Baker BJ. 2007. Patterns of gammaridean amphipod abundance and species composition associated with dominant subtidal macroalgae from the western Antarctic Peninsula. Polar Biology. 30:1417–1430.

Iken K, Barrera-Oro ER, Quartino ML, Casaux RJ, Brey T. 1997. Grazing by the Antarctic fish *Notothenia coriiceps*: evidence for selective feeding on macroalgae. Antarctic Science. 9(4):386–391.

Intergovernmental Panel on Climate Change (IPCC). 2022. The Ocean and Cryosphere in a Changing Climate: Special Report of the Intergovernmental Panel on Climate Change. Cambridge: Cambridge University Press; [accessed 2023 Jun 25]. https://doi.org/10.1017/9781009157964

Johnston NM, Murphy EJ, Atkinson A, Constable AJ, Cotté C, Cox M, Daly KL, Driscoll R, Flores H, Halfter S. 2022. Status, change, and futures of zooplankton in the Southern Ocean. Frontiers in Ecology and Evolution. 9:1039.

Kellermann AK. 1990. Identification key and catalogue of larval Antarctic fishes. Ber Polarforsch.(67):1–138.

Kellermann AK. 1996. Midwater fish ecology. Foundations for ecological research west of the Antarctic Peninsula. 70:231–256.

Kock K-H. 2005. Antarctic icefishes (Channichthyidae): a unique family of fishes. A review, Part I. Polar biology. 28(11):862–895.

Konstantinidis P, Hilton EJ, Matarese AC. 2016. New records of larval stages of the eel cod genus Muraenolepis Günther 1880 (Gadiformes: Muraenolepididae) from the western Antarctic Peninsula. Journal of Fish Biology. 89(2):1494–1500.

Koubbi P, Vallet C, Razouls S, Grioche A, Hilde D, Courcot L, Janquin MA, Vacchi M. 2007. Condition and diet of larval *Pleuragramma antarcticum* (Nototheniidae) from Terre Adélie (Antarctica) during summer.

La Mesa M, Eastman JT. 2012. Antarctic silverfish: life strategies of a key species in the high-Antarctic ecosystem. Fish and Fisheries. 13(3):241–266.

La Mesa M, Eastman JT, Vacchi M. 2004. The role of notothenioid fish in the food web of the Ross Sea shelf waters: a review. Polar Biolgy. 27(6):321–338. https://doi.org/10.1007/s00300-004-0599-z

La Mesa M, Llompart F, Riginella E, Eastman JT. 2021. Parental care and reproductive strategies in notothenioid fishes. Fish and Fisheries. 22(2):356–376.

van Leeuwe MA, Webb AL, Venables HJ, Visser RJW, Meredith MP, Elzenga JTM, Stefels J. 2020. Annual patterns in phytoplankton phenology in Antarctic coastal waters explained by environmental drivers. Limnology and Oceanography. 65(7):1651–1668. https://doi.org/10.1002/lno.11477

Loeb VJ, Kellermann AK, Koubbi P, North AW, White MG. 1993. Antarctic larval fish assemblages: a review. Bulletin of Marine Science. 53(2):416–449.

Maksym T, Stammerjohn SE, Ackley S, Massom R. 2012. Antarctic Sea Ice: A Polar Opposite? Oceanography. 25(3):140–151.

Martinson DG. 2012. Antarctic circumpolar current's role in the Antarctic ice system: An overview. Palaeogeography, Palaeoclimatology, Palaeoecology. 335:71–74.

Martinson DG, Stammerjohn SE, Iannuzzi RA, Smith RC, Vernet M. 2008. Western Antarctic Peninsula physical oceanography and spatio–temporal variability. Deep Sea Research Part II: Topical Studies in Oceanography. 55(18–19):1964–1987.

McClintock JB, Amsler CD, Baker BJ. 2010. Overview of the chemical ecology of benthic marine invertebrates along the Western Antarctic Peninsula. Integrative and comparative biology. 50(6):967–980.

Mendes CRB, Costa RR, Ferreira A, Jesus B, Tavano VM, Dotto TS, Leal MC, Kerr R, Islabão CA, Franco A de O da R, et al. 2023. Cryptophytes: An emerging algal group in the rapidly changing Antarctic Peninsula marine environments. Global Change Biology. 29(7):1791–1808. https://doi.org/10.1111/gcb.16602

Meredith MP, King JC. 2005. Rapid climate change in the ocean west of the Antarctic Peninsula during the second half of the 20th century. Geophysical Research Letters. 32(19). https://doi.org/10.1029/2005GL024042

Meyer B, Freier U, Grimm V, Groeneveld J, Hunt BP, Kerwath S, King R, Klaas C, Pakhomov E, Meiners KM. 2017. The winter pack-ice zone provides a sheltered but food-poor habitat for larval Antarctic krill. Nature Ecology & Evolution. 1(12):1853–1861.

Montes-Hugo M, Doney SC, Ducklow HW, Fraser W, Martinson D, Stammerjohn SE, Schofield O. 2009. Recent Changes in Phytoplankton Communities Associated with Rapid

Regional Climate Change Along the Western Antarctic Peninsula. Science. 323(5920):1470–1473. https://doi.org/10.1126/science.1164533

Nardelli SC, Gray PC, Stammerjohn SE, Schofield O. 2023. Characterizing coastal phytoplankton seasonal succession patterns on the West Antarctic Peninsula. Limnology & Oceanography. https://doi.org/10.1002/lno.12314

Near TJ, Dornburg A, Harrington RC, Oliveira C, Pietsch TW, Thacker CE, Satoh TP, Katayama E, Wainwright PC, Eastman JT, Beaulieu JM. 2015. Identification of the notothenioid sister lineage illuminates the biogeographic history of an Antarctic adaptive radiation. BMC Evolutionary Biology. 15(1):109. https://doi.org/10.1186/s12862-015-0362-9

Near TJ, Dornburg A, Kuhn KL, Eastman JT, Pennington JN, Patarnello T, Zane L, Fernández DA, Jones CD. 2012. Ancient climate change, antifreeze, and the evolutionary diversification of Antarctic fishes. Proceedings of the National Academy of Sciences. USA. 109(9):3434–3439. https://doi.org/10.1073/pnas.1115169109

Near TJ, MacGuigan DJ, Parker E, Struthers CD, Jones CD, Dornburg A. 2018. Phylogenetic analysis of Antarctic notothenioids illuminates the utility of RADseq for resolving Cenozoic adaptive radiations. Molecular Phylogenetics and Evolution. 129:268–279. https://doi.org/10.1016/j.ympev.2018.09.001

Oliva M, Navarro F, Hrbáček F, Hernandéz A, Nỳvlt D, Pereira P, Ruiz-Fernandéz J, Trigo R. 2017. Recent regional climate cooling on the Antarctic Peninsula and associated impacts on the cryosphere. Science of the Total Environment. 580:210–223.

Parker ML, Fraser WR, Ashford J, Patarnello T, Zane L, Torres JJ. 2015. Assemblages of micronektonic fishes and invertebrates in a gradient of regional warming along the Western Antarctic Peninsula. Journal of Marine Systems. 152:18–41.

Pinkerton MH, Décima M, Kitchener JA, Takahashi KT, Robinson KV, Stewart R, Hosie GW. 2020. Zooplankton in the Southern Ocean from the continuous plankton recorder: Distributions and long-term change. Deep Sea Research Part I: Oceanographic Research Papers. 162:103303. https://doi.org/10.1016/j.dsr.2020.103303

Pritchard Hd, Ligtenberg SR, Fricker HA, Vaughan DG, van den Broeke MR, Padman L. 2012. Antarctic ice-sheet loss driven by basal melting of ice shelves. Nature. 484(7395):502–505.

Raphael MN, Marshall GJ, Turner J, Fogt RL, Schneider D, Dixon DA, Hosking JS, Jones Jm, Hobbs WR. 2016. The Amundsen Sea low: Variability, change, and impact on Antarctic climate. Bulletin of the American Meteorological Society. 97(1):111–121.

Rintoul SR, Chown SL, DeConto RM, England MH, Fricker HA, Masson-Delmotte V, Naish TR, Siegert MJ, Xavier JC. 2018. Choosing the future of Antarctica. Nature. 558(7709):233–241. https://doi.org/10.1038/s41586-018-0173-4

Ross RM, Quetin LB, Martinson DG, Iannuzzi RA, Stammerjohn SE, Smith RC. 2008. Palmer LTER: Patterns of distribution of five dominant zooplankton species in the epipelagic zone west of the Antarctic Peninsula, 1993–2004. Deep Sea Research Part II: Topical Studies in Oceanography. 55(18–19):2086–2105.

Ruck KE, Steinberg DK, Canuel EA. 2014. Regional differences in quality of krill and fish as prey along the Western Antarctic Peninsula. Marine Ecology Progress Series. 509:39–55. https://doi.org/10.3354/meps10868

Saba GK, Fraser WR, Saba VS, Iannuzzi RA, Coleman KE, Doney SC, Ducklow HW, Martinson DG, Miles TN, Patterson-Fraser DL, et al. 2014. Winter and spring controls on the summer food web of the coastal West Antarctic Peninsula. Nature Communications. 5(1):4318. https://doi.org/10.1038/ncomms5318

Schmidtko S, Heywood KJ, Thompson AF, Aoki S. 2014. Multidecadal warming of Antarctic waters. Science. 346(6214):1227–1231.

Schofield O, Brown M, Kohut J, Nardelli S, Saba G, Waite N, Ducklow H. 2018. Changes in the upper ocean mixed layer and phytoplankton productivity along the West Antarctic Peninsula. Philosophical Transactions of the Royal Society A: Mathematical, Physical and Engineering Sciences. 376(2122):20170173. https://doi.org/10.1098/rsta.2017.0173

Schofield O, Saba G, Coleman K, Carvalho F, Couto N, Ducklow H, Finkel Z, Irwin A, Kahl A, Miles T. 2017. Decadal variability in coastal phytoplankton community composition in a changing West Antarctic Peninsula. Deep Sea Research Part I: Oceanographic Research Papers. 124:42–54.

Screen JA, Bracegirdle TJ, Simmonds I. 2018. Polar Climate Change as Manifest in Atmospheric Circulation. Current Climate Change Reports. 4(4):383–395. https://doi.org/10.1007/s40641-018-0111-4

Smale DA, Barnes DK, Fraser KP, Peck LS. 2008. Benthic community response to iceberg scouring at an intensely disturbed shallow water site at Adelaide Island, Antarctica. Marine Ecology Progress Series. 355:85–94.

Stammerjohn S, Maksym T. 2017. Gaining (and losing) Antarctic sea ice: variability, trends and mechanisms. Sea ice.:261–289.

Stammerjohn SE, Martinson DG, Smith RC, Yuan X, Rind D. 2008. Trends in Antarctic annual sea ice retreat and advance and their relation to El Niño–Southern Oscillation and

Southern Annular Mode variability. Journal of Geophysical Research: Oceans. 113(C3). https://doi.org/10.1029/2007JC004269

Steinberg DK, Ruck KE, Gleiber MR, Garzio LM, Cope JS, Bernard KS, Stammerjohn SE, Schofield OME, Quetin LB, Ross RM. 2015. Long-term (1993–2013) changes in macrozooplankton off the Western Antarctic Peninsula. Deep Sea Research Part I: Oceanographic Research Papers. 101:54–70. https://doi.org/10.1016/j.dsr.2015.02.009

Szulejko JE, Kumar P, Deep A, Kim K-H. 2017. Global warming projections to 2100 using simple CO2 greenhouse gas modeling and comments on CO2 climate sensitivity factor. Atmospheric Pollution Research. 8(1):136–140.

Thibodeau PS, Steinberg DK, Stammerjohn SE, Hauri C. 2019. Environmental controls on pteropod biogeography along the Western Antarctic Peninsula. Limnology and Oceanography. 64(S1):S240–S256.

Thompson DW, Solomon S. 2002. Interpretation of recent Southern Hemisphere climate change. Science. 296(5569):895–899.

Trimborn S, Hoppe CJ, Taylor BB, Bracher A, Hassler C. 2015. Physiological characteristics of open ocean and coastal phytoplankton communities of Western Antarctic Peninsula and Drake Passage waters. Deep Sea Research Part I: Oceanographic Research Papers. 98:115–124.

Turner J, Lu H, White I, King JC, Phillips T, Hosking JS, Bracegirdle TJ, Marshall GJ, Mulvaney R, Deb P. 2016. Absence of 21st century warming on Antarctic Peninsula consistent with natural variability. Nature. 535(7612):411–415.

Vaughan DG, Marshall GJ, Connolley WM, Parkinson C, Mulvaney R, Hodgson DA, King JC, Pudsey CJ, Turner J. 2003. Recent rapid regional climate warming on the Antarctic Peninsula. Climatic change. 60:243–274.

Voskoboinikova OS. 2001. Evolutionary significance of heterochronies in the development of the bony skeleton in fishes of the suborder Notothenioidei (Perciformes). Journal of Ichthyology. 41(6):415–424.

Wang J, Luo H, Yu L, Li X, Holland PR, Yang Q. 2023. The impacts of combined SAM and ENSO on seasonal Antarctic sea ice changes. Journal of Climate. 1(aop):1–35. https://doi.org/10.1175/JCLI-D-22-0679.1

Wiencke C, Amsler CD. 2012. Seaweeds and their communities in polar regions. Seaweed biology: novel insights into ecophysiology, ecology and utilization.:265–291.

Woods BL, Van de Putte AP, Hindell MA, Raymond B, Saunders RA, Walters A, Trebilco R. 2023. Species distribution models describe spatial variability in mesopelagic fish abundance in the Southern Ocean. Frontiers in Marine Science. 9:2650.

Wyanski DM, Targett TE. 1981. Feeding biology of fishes in the endemic Antarctic Harpagiferidae. Copeia.:686–693.

Yuan X. 2004. ENSO-related impacts on Antarctic sea ice: a synthesis of phenomenon and mechanisms. Antarctic Science. 16(4):415–425.

Zemp M, Nussbaumer SU, Gärtner-Roer I, Bannwart J, Paul F, Hoelzle M. 2021. Global Glacier Change Bulletin Nr. 4 (2018-2019). WGMS. 4.

CHAPTER 2
Climate drives long-term change in Antarctic Silverfish along the western Antarctic Peninsula

Please cite this chapter as: Corso AD, Steinberg DK, Stammerjohn SE, Hilton EJ. 2022. Climate drives long-term change in Antarctic Silverfish along the western Antarctic Peninsula. *Communications Biology*. 5.1: 104. https://doi-org/10.1038/s42003-022-03042-3

Abstract

Over the last half of the 20th century, the western Antarctic Peninsula has been one of the most rapidly warming regions on Earth, leading to substantial reductions in regional sea ice coverage. These changes are modulated by atmospheric forcing, including the Amundsen Sea Low (ASL) pressure system. We utilized a novel 25-year (1993-2017) time series to model the effects of environmental variability on larvae of a keystone species, the Antarctic Silverfish (*Pleuragramma antarctica*). Antarctic Silverfish use sea ice as spawning habitat and are important prey for penguins and other predators. We show that warmer sea surface temperature and decreased sea ice are associated with reduced larval abundance. Variability in the ASL modulates both sea surface temperature and sea ice; a strong ASL is associated with reduced larvae. These findings support a narrow sea ice and temperature tolerance for adult and larval fish. Further regional warming predicted to occur during the 21st century could displace populations of Antarctic Silverfish, altering this pelagic ecosystem.

1. Introduction

The Antarctic Silverfish (*Pleuragramma antarctica;* Notothenioidei) can comprise over 90% of adult and larval fish biomass in coastal areas of the Southern Ocean (DeWitt 1970; Guglielmo et al. 1997), and is the only endemic Southern Ocean fish that maintains an entirely pelagic life history (La Mesa and Eastman 2012). Due to their abundance and availability within the upper water column, Antarctic Silverfish are important prey for higher predators, such as seals, penguins, other seabirds, and other fishes (La Mesa et al. 2004; Pinkerton et al. 2010). Antarctic Silverfish have a circumpolar distribution with populations having genetic connectivity along the continental shelf (Caccavo et al. 2018). However, the absence of an Antarctic Slope Front Current in the western Antarctic Peninsula (WAP) region (Fig. 1) has isolated this Antarctic Silverfish population from other established areas of reproduction in the species (Caccavo et al. 2018).

The central role of Antarctic Silverfish in the WAP food web has led to concern over the health of this isolated population due to regional climate change. Physiological adaptations that allow endemic fishes (most notably, members of Notothenioidei) to survive in the cold waters surrounding Antarctica also make them susceptible to ocean warming. Manipulation experiments show that an increase in water temperature of 5°C can result in mortality (Bilyk and DeVries 2011; Beers and Jayasundara 2015) and reduced food assimilation rate (Sandersfeld et al. 2015) in some notothenioid fishes. From 1945-2009, the mean ocean temperature at mid-depths (100-300m) along the WAP increased by 1°C, noting these mid-depth ocean waters are already 4°C warmer than the seawater freezing temperature (Cook et al. 2016). Concurrently, mean annual and winter air temperature increased by 3°C and 6°C, respectively (Henley et al. 2019;

Stammerjohn and Scambos 2020). Although this rapid warming likely caused no direct mortality in adult Antarctic Silverfish, it may have led to detrimental physiological responses at all life stages, especially in the less mobile larval stages (Mintenbeck and Torres 2017).

Regional warming in the WAP, combined with changes in winds, have also led to a decrease in sea ice, which plays a key and unique role in Antarctic Silverfish life history. These fish deposit their eggs within sea ice, which also serves as a nursery area for newly hatched larvae (Vacchi et al. 2004; La Mesa and Eastman 2012; Vacchi et al. 2012). The total elapsed days between sea ice advance and retreat, or annual sea ice duration, is used to monitor trends in the cryosphere. Between 1979 and 2018, annual sea ice duration along the WAP decreased by about 2 months (Henley et al. 2019). Therefore, recent declines in sea ice and thus spawning habitat have been implicated in diminished Antarctic Silverfish abundance in the WAP region (Kellermann 1996; Ross et al. 2014; La Mesa et al. 2015; Parker et al. 2015; Mintenbeck and Torres 2017) and other coastal areas of the Southern Ocean (La Mesa et al. 2010; Koubbi et al. 2011; Davis et al. 2017). However, abundance data of sufficient temporal and spatial scale for Antarctic Silverfish was previously unavailable to test this hypothesis.

Three atmospheric circulation patterns predominantly influence climate change in the WAP region – the Southern Annular Mode (SAM), El Niño Southern Oscillation (ENSO), and Amundsen Sea Low (ASL). Interconnections among these are complex, seasonally variable, and tied to anthropogenic impacts such as global greenhouse gas emissions (Raphael et al. 2016). The ASL, a climatological low-pressure center located in the Amundsen Sea (Fig. 1), has only recently been identified as a main factor behind WAP ocean warming (Fogt et al. 2012; Hosking et al. 2013; Hosking et al. 2016), sea ice loss (Stammerjohn et al. 2015; Hobbs et al. 2016; Holland et al. 2018), and glacial retreat (Thoma et al. 2008; Dotto et al. 2020) over the last century.

The strength and location of the ASL influences meridional winds east and west of the ASL center (Hosking et al. 2013) (Fig. 1a, b); stronger (i.e., deeper or spun-up) ASL events in the Amundsen Sea, for example, increase warm northerly airflow over the WAP region (i.e., along the eastern limb of the clockwise rotating low-pressure center), which reduces sea ice extent and concentration (Fig. 1b) and increases temperature at the surface along the WAP (Hobbs et al. 2016). In addition, the strength and location of the ASL influences zonal winds to the north and south of the ASL center. For example, an ASL that is centered southward (i.e., poleward) in the Amundsen Sea increases westerly wind anomalies near the continental shelf break (Hosking et al. 2016), enhancing the flow of warm Circumpolar Deep Water (CDW) southward onto the shelf (Thoma et al. 2008; Holland et al. 2019; Dotto et al. 2020). Although less is known regarding the impact of the ASL on CDW intrusions in the Bellingshausen Sea, a similar relationship is probable (Dinniman et al. 2011; Dinniman et al. 2012; Spence et al. 2014; Nakayama et al. 2018). While several studies examined the effects of SAM and ENSO oscillations on Antarctic phytoplankton and zooplankton (Greaves et al. 2020; Steinberg et al. 2015; La et al. 2019), no previous analyses focus on the potential impacts of the ASL strength or location on any organism.

Here we investigate connections between Antarctic Silverfish and the WAP environment across more than two decades. Specifically, we evaluate the impact of ocean temperature, sea ice dynamics, atmospheric circulation patterns, chlorophyll, and salinity on larval Antarctic Silverfish abundance. We use results from this analysis to offer predictions of regional pelagic food web response to future climate change.

2. Results and Discussion

Ocean temperature and larval abundance

We sorted, identified, and enumerated Antarctic Silverfish larvae (n = 7086) collected in a 25-year time series (1993 – 2017; Fig. 2a) of plankton net tows (see Materials and Methods) as part of the Palmer Antarctica Long-Term Ecological Research Program (Palmer LTER; Supplemental Fig. 1) and archived in the Nunnally Ichthyology Collection at the Virginia Institute of Marine Science. Zero-inflated Generalized Linear Mixed-Effects model predictions show the abundance of larvae during this period is closely tied to sea surface temperature, with higher abundance in colder water ($p < 0.001$; Fig. 2b; Supplemental Table 1). Approximately 45% of Antarctic Silverfish larvae were collected at sea surface temperatures ranging from - 2° to 0°C, and 95% of larvae were captured in waters colder than 1.5°C. Based on estimated marginal means, we predict that no larvae occur at sea surface temperatures of 1.7°C or greater (see Materials and Methods).

Based on the time series, at least two consecutive years of anomalously cold surface temperatures are necessary to produce peaks in larval abundance (Fig. 2a). Palmer LTER net tows are deployed to a depth of 120 meters, encompassing the majority of habitat occupied by Antarctic Silverfish larvae (Granata et al. 2009; La Mesa et al. 2010). Using data derived from CTD casts paired with net tows, we found Antarctic Silverfish abundance was significantly linked to colder temperatures averaged over the 120 m water column. However, sea surface temperature yielded optimal model performance (see Materials and Methods).

Impact of sea ice on spawning

We next isolated the effects of sea ice dynamics and climatic variability on Antarctic Silverfish adults by lagging variables in the model (Bhaskaran et al. 2013; Steinberg et al. 2015). Model results indicate the timing of sea ice advance during austral autumn (March to May) controls larval abundance in the following year ($p < 0.001$; Fig. 2c; Supplemental Table 1). Model performance (see Materials and Methods) was considerably reduced when sea ice advance was lagged two years, or when there was no lag (Supplemental Table 2). To our knowledge, this is the first statistically significant relationship reported between sea ice and the long-term abundance of any Antarctic fish species.

There are relatively sparse data on the reproductive biology of Antarctic Silverfish, especially in the WAP region (La Mesa et al. 2015). Adult fish likely spawn during late austral winter to early spring (July to September), eggs develop for approximately four months and hatch in November and December (Fig. 3a). Larvae are then sampled annually by the Palmer LTER during January and February. However, there is evidence from the Ross Sea that Antarctic Silverfish are skip spawners (Ghigliotti et al. 2017). In austral autumn, adult fish migrate from their offshore pelagic habitat to coastal areas. Adults then improve their nutritional condition for a year before spawning the next season (Fig. 3a) (La Mesa et al. 2015; Ghigliotti et al. 2017).

We suggest that adult Antarctic Silverfish select their spawning area along the WAP based in part on the presence of sufficient sea ice cover during austral autumn (Fig. 2a, Fig. 3b, c). An early sea ice advance in late April or early May (days 110 to 130 in Fig. 2c) acts as a positive cue for migrating adults and increases spawning habitat (Fig. 3b). If advance is delayed, spawning habitat is reduced (Fig. 3c) and could cause adults to travel elsewhere or continue to postpone spawning. We therefore predict that sea ice advance beginning on day 157 or earlier is necessary for spawning to successfully occur in this region (see Materials and Methods). Seasonal sea ice variability during the last 20 million years in the Southern Ocean has led to a high level of life-history plasticity among Antarctic Silverfish (Kellermann 1996; La Mesa and Eastman 2012). However, given the sea ice dependence indicated by our model, it is likely that the acute reduction in sea ice during the 20th century has significantly decreased spawning in the northern WAP. Consequently, there has been a lower abundance of mature adults observed in the northern WAP for several decades (Chapman et al. 2011; La Mesa et al. 2015; Parker et al. 2015).

Connections with ASL strength and location

Larval Antarctic Silverfish abundance was also significantly correlated with the ASL relative central pressure (RCP), an index of ASL strength, ($p = 0.006$; Fig. 4a; Supplemental Table 1) (Hosking et al. 2016) and the latitudinal location of the ASL ($p = 0.005$; Fig. 4b; Supplemental Table 1). We considered ASL RCP and latitude averaged over summer (DJF), autumn (MAM), winter (JJA), and spring (SON) months. Longitudinal location of the ASL was not included in this analysis because it exhibits a strong negative correlation with RCP during most of the year (Coggins and McDonald 2015). Lagged ASL strength and latitude averaged over autumn produced optimal model AIC (see Materials and Methods). These relationships further support our hypothesis that adult Antarctic Silverfish are selecting their spawning habitat during autumn, when sea ice is also beginning to advance (Fig. 3a). Autumn seasons with stronger (more negative) RCPs (Fig. 4a) and a poleward ASL location (Fig. 4b) were associated with diminished spawning success reflected by lower abundance of the larvae sampled in the following year. There was no correlation between larval abundance and lagged ENSO indices during any season. We observed a non-significant negative relationship between lagged Marshall SAM index and larval abundance during autumn ($p = 0.10$) and summer ($p = 0.09$); larval abundance was higher following years with a more negative SAM. However, including the SAM index for any season did not improve model performance (Supplemental Table 3) and thus was not included in the final model (see Materials and Methods; Supplemental Fig. 2a).

The positive relationship between the lagged latitude of the ASL and larval abundance is suggestive of CDW intrusions impacting adult fish. Increased intrusions of CDW onto the Amundsen continental shelf that occur during a poleward shift in the ASL (Fig. 3c) are well below the thermocline (Holland et al. 2019), with the CDW temperature maximum around 400 m (Assmann et al. 2013). This warm layer of water, with temperatures approaching 2°C (Moffat et al. 2009), expands as more CDW is transported onto the shelf (Holland et al. 2019). This water mass is well above the optimal thermal environment for Antarctic Silverfish, particularly as the physiological costs of spawning further impact their limited thermal tolerance (Dahlke et al. 2020). Adult Antarctic Silverfish, which occupy a depth range of 0 to 900 m (La Mesa and Eastman 2012), might therefore delay spawning or attempt to relocate when oceanic and sea ice conditions are unfavorable in the Bellingshausen Sea due to ASL strength and location (Fig. 3c).

However, additional ocean modeling is required to verify specific causes of the correlation between ASL strength, location, and adult fish.

Although there are connections between the West Antarctic cryosphere inclusive of the WAP and ASL (Stammerjohn et al. 2015; Hobbs et al. 2016), there were no indications of collinearity between WAP ice advance, sea surface temperature, autumn ASL RCP, and the ASL latitudinal location in this analysis (see Materials and Methods). The positive correlation between ASL RCP and larval abundance is likely due to the warm northerly winds associated with strong (deep) RCPs affecting sea ice in pathways that are not captured by the ice advance parameter.

One such pathway is that strong ASL events reduce the areal extent of sea ice by advecting and compacting the ice edge southward in the Bellingshausen Sea (Holland et al. 2014; Regan et al. 2018), which also reduces frazil ice production, the overall impact being less ideal spawning habitat for Antarctic Silverfish. In more southerly locations (e.g., the coastal Ross Sea), Antarctic Silverfish eggs are usually associated with the presence of a sub-ice platelet layer (SIPL) (Vacchi et al. 2012). The SIPL is highly porous, which facilitates nutrient exchange with seawater and supports exceptionally high algal biomass (Arrigo 2014; Hoppmann et al. 2020). This productive habitat is an ideal nursery area for larval Antarctic Silverfish. However, frequent intrusions of warm CDW in the Bellingshausen Sea likely prevent SIPLs from forming (Hoppmann et al. 2020), and platelet crystals have been observed only once in this region (Veazey et al. 1994). Instead, Antarctic Silverfish in the WAP area likely search for similarly highly porous and productive habitat, such as dense aggregations of frazil ice (Garrison et al. 1983; Quetin and Ross 2009).

Furthermore, sea surface temperatures (< 20m) increased in the WAP region by approximately 2°C during the 20th century (1955 – 1998) (Meredith and King 2005). Although this abrupt warming has recently slowed (Turner et al. 2016), it is expected to intensify in coming decades (Rintoul et al. 2018; Holland et al. 2019). The altered near-surface winds associated with prolonged deepening and a poleward shift in the ASL, modulated by the SAM (Turner et al. 2013) and Pacific variability (Ding et al. 2011), contributes to past and future surface warming in the WAP region (Hosking et al. 2016). Therefore, we posit that long-term strengthening of the ASL creates unfavorable water temperatures for Antarctic Silverfish larvae in the WAP region (Fig. 3c) (Rintoul et al. 2018; Holland et al. 2019).

Impact of chlorophyll and salinity on larval abundance

In addition to sea surface temperature, larval Antarctic Silverfish abundance was positively correlated with chlorophyll concentration ($p < 0.001$; Supplemental Fig. 3a; Supplemental Table 1), indicating bottom-up control in this food web. Phytoplankton are grazed by the early life stages of copepods (i.e., copepodites) which in turn are the primary prey of larval Antarctic Silverfish (La Mesa and Eastman 2012). While the focus of the present study is on modeling environmental variables, confounding influences of prey field dynamics due to a changing climate are also possible. The phytoplankton community shifts during warmer years with low sea ice (Moline et al. 2004; Henley et al. 2019), potentially altering copepod abundance and composition (Gleiber 2014). In addition to the physiological cost of warmer waters on larval

Antarctic Silverfish, climate change could cause their hatching period to become out of sync with peak abundances of their prey (Wöhrmann et al. 1997; La Mesa et al. 2010; Mintenbeck and Torres 2017).

Higher abundance of larvae also occurred in areas of lower surface salinity ($p < 0.001$; Supplemental Fig. 3b; Supplemental Table 1). Surface freshwater inputs from melting sea ice and glaciers lead to a more stratified surface layer and increased chlorophyll (Venables et al. 2013); such a stratified environment with ample food could be preferred by Antarctic Silverfish larvae. The relationship between salinity and larval abundance also points to the importance of sufficient sea ice cover. High-salinity brine is exported downwards in the water column during autumn sea ice growth and advance (Meredith et al. 2008; Venables et al. 2013). Consequently, surface salinity is fresher following winters with high sea ice extent (Meredith et al. 2008).

Slósarczyk (Slosarczyk 1986) found Antarctic Silverfish larvae were more abundant in areas of high salinity in the WAP region (34.1 to 34.6) (Mintenbeck and Torres 2017). However, their analysis used a single year of pelagic net tows, and the mean standard length (SL) of post-larval and juvenile Antarctic Silverfish they collected (75 mm) was over five times the mean SL of larvae used in our study (11.9 mm; Supplemental Fig. 4). Osmoregulation functions change in fishes during their development (Varsamos et al. 2005); therefore, post-larval Antarctic Silverfish could possess a greater ability to tolerate more saline water (Mintenbeck and Torres 2017). No experiments to date address the salinity thresholds of Antarctic Silverfish during any stage in their life history.

Outlook of WAP climate and Antarctic Silverfish

Our results support the hypothesis that sea ice and ocean temperatures, modulated by the ASL, impact Antarctic Silverfish spawning behavior, resulting in changes in abundance of their larvae along the WAP. Two anthropogenic forces jointly influence the prevailing circumpolar westerly winds and the strengthening/weakening of the ASL: the ozone hole located over Antarctica and greenhouse gas emissions; both tend to strengthen the westerly winds poleward and deepen the ASL (Thompson et al. 2011; Gille et al. 2016; Hosking et al. 2016). However, Antarctic climate is characterized by high regional and seasonal variability, both natural and forced, making it challenging to identify attribution (Hobbs et al. 2016). For example, a recent cooling along the WAP and increases in sea ice extent were attributed to Pacific decadal variability (Stammerjohn and Scambos 2020), though other factors were likely also at play. Nonetheless, it is expected that the recent reversal in WAP climate trends will not persist with continued increases in greenhouse gas emissions. The Antarctic ozone hole is predicted to recover entirely by ~2100, while most scenarios predict increasing greenhouse gas emissions through 2100 (Allen et al. 2019). High carbon dioxide emission scenarios will likely result in a prolonged trend of strong ASL events and atmospheric warming in the WAP region despite ozone recovery (Rintoul et al. 2018; Screen et al. 2018; Gao et al. 2021). Antarctic Silverfish have encountered periods of cyclic warming during their evolutionary history (Mintenbeck and Torres 2017). However, with precipitous climate warming due to continuing greenhouse gas emissions, Antarctic Silverfish could disappear from the WAP region entirely, triggering changes in other components of the pelagic food web.

Possible ecosystem responses to Antarctic Silverfish decline

For the last 6,000 years, Antarctic Silverfish have dominated Adélie penguin diets in the WAP region during periods of especially cold temperatures (Emslie and McDaniel 2002). Furthermore, the substantial decline of Adélie penguins in the northern WAP (Fraser and Trivelpiece 1996) is coincident with a long-term decrease in Antarctic Silverfish in their diet (Chapman et al. 2011). While there are several causal mechanisms driving population changes in Adélie penguins (Cimino et al. 2016; Ainley et al. 2018), these changes are possibly exacerbated by diminished Antarctic Silverfish abundance resulting from recent warming and reduced sea ice (Cimino et al. 2016). Antarctic Silverfish, especially spawning adults, are high-energy prey items (Chapman et al. 2011; Ruck et al. 2014). Penguins are known to switch to an entirely invertebrate-based diets (e.g., krill or squid) during warm periods (Chapman et al. 2011). However, the loss of lipid-rich Antarctic Silverfish in Adélie penguin chick diets induces low fledging weights, a vital determinant of future recruitment (Chapman et al. 2011; Ainley et al. 2018).

Antarctic Silverfish are also a primary prey item for the commercially important Antarctic Toothfish (*Dissostichus mawsoni*) in the Ross Sea (Eastman 1985, p. 19; La Mesa et al. 2004; Pinkerton et al. 2007; Ainley et al. 2013; Hanchet et al. 2015) and likely in other coastal Antarctic regions including the Bellingshausen and Amundsen Seas. There are many remaining gaps in knowledge regarding the life history of the Antarctic Toothfish; however, Antarctic Silverfish are likely to be an especially important component of their diet as they prepare for the migratory phase of their life history (Hanchet and Rickard 2008; Ainley et al. 2013). Shifts in the migratory behavior of Antarctic Silverfish due to changes in environmental conditions could have bottom-up effects on the condition and location of regional populations of Antarctic Toothfish (Fuiman et al. 2002). Furthermore, some species of seals, especially the Weddell seal (*Leptonychotes weddellii*), heavily consume both Antarctic Toothfish and Silverfish (Casaux et al. 2006; Ponganis and Stockard 2007; Rumolo et al. 2020). Changes in the occurrence of Antarctic Silverfish could cause Weddell seal populations to increase their predation pressure on Antarctic Toothfish, or other fishes.

It is challenging to predict specific top-down effects of a severe reduction in Antarctic Silverfish on the regional zooplankton community as the dietary preferences of Antarctic Silverfish broaden across ontogeny (La Mesa and Eastman 2012), with adults maintaining dietary flexibility by consuming a wide size range of copepods, pteropods, euphausiids, amphipods, other zooplankton, and early life stages of notothenioid fishes (Hubold and Ekau 1990; La Mesa and Eastman 2012). Some abundant copepod species, particularly *Metridia gerlachei*, could experience a positive shift in abundance due to reduced predation from Antarctic Silverfish (Moreno et al. 1986; Granata et al. 2009). With one of the highest grazing rates of Antarctic copepods (Gleiber et al. 2016), an increase in *M. gerlachei* abundance could significantly alter microbial food web composition (Garzio et al. 2013; Gleiber et al. 2016).

Trophic relationships and life history of Antarctic Silverfish are mostly known from the Ross and Weddell seas, thus it will be critical to further characterize the role of this keystone fish in the vulnerable WAP pelagic ecosystem. This study also demonstrates the value and importance of both long-term sampling programs (Hobbie 2003; Hughes et al. 2017) and natural history collections (Hilton et al. 2021). Curated time-series of larval fishes are rare but invaluable resources to determine causes of adult population changes (Houde 2008; Hoey et al. 2020). Finally, the ecosystem-level consequences of climate change must be considered in the context of air-sea interactions, such as the ASL, to predict food web shifts more accurately and manage natural resources in the region.

3. Materials and Methods

Sampling

Larval fishes used in this study were collected in accordance with the protocols of the Palmer Antarctica Long-Term Ecological Research (Palmer LTER) program (Steinberg et al. 2015) and were obtained as preserved specimens cataloged in the Virginia Institute of Marine Science (VIMS) Nunnally Ichthyology Collection. Scientists on Palmer LTER cruises collect multidisciplinary data in a fixed-sampling grid in the Bellingshausen Sea along the western Antarctic Peninsula (WAP; Supplemental Fig. 1) (Smith et al. 1995; Ducklow et al. 2007). Zooplankton and larval fishes are sampled annually (for this study, years included 1993 to 2017) during austral summer (January to February) using a 2-m^2 frame Metro net (700-µm mesh) towed to ~120m depth. A General Oceanics flowmeter positioned in the center of the net mouth was used to calculate each tow volume. All organisms in the tows are identified to family-level, measured in volume, and preserved in a formaldehyde solution.

From 1993 to 2007, tows were conducted from the 600 grid line to the 200 grid line (Steinberg et al. 2015). In 2008, the ‘far south’ lines (100, 000, and -100) were added to the Palmer LTER grid (Supplemental Fig. 1). The far south stations were included in this analysis and temporal autocorrelation was accounted for (see Model development). We included additional tows that were conducted from 1993 to 2017 at Process Study stations located between grid lines. We ran the final model without these Process Study and far south stations and the relationships were unchanged.

As larvae in this study are collected during the same fixed two-month period annually, it is important to note Antarctic Silverfish could be altering the timing of spawning during reduced sea ice conditions, resulting in modified hatching and subsequent peaks in larval abundance (Kellermann 1996). However, there has been minimal deviation in the standard length of Antarctic Silverfish larvae during the Palmer LTER (Supplemental Fig. 4) and no yolk-sac larvae have been sampled.

Identification

Antarctic Silverfish is among the most easily identified of the known larval fishes endemic to the Southern Ocean due to possession of two distinct dorsal pigment rows and a lack of abdominal pigmentation. All larvae in this study were identified based on Kellermann (Kellermann 1990). The majority (>70%) were identified to species level by Andrew D. Corso, and the remaining fishes were identified by Dr. Peter Konstantinidis (OSU) and other scientists associated with the VIMS Nunnally Ichthyology Collection.

Statistics and Reproducibility

The density (abundance divided by tow volume [in units of 1000 m^3]) of Antarctic Silverfish for each tow from 1993 – 2017 was modeled against environmental variables. We considered ocean temperatures and salinity from near the sea surface (5 m depth), the bottom of the tow depth (120 m), and averaged from 120 m to the surface. All temperature and salinity measurements were collected using CTD casts that were spatially and temporally paired with net tows. Discrete measurements of Chlorophyll a concentration measured in water collected in CTD casts were integrated to 100 m and also paired spatially and temporally with net tows. Bathymetry and time of day during net tows were also evaluated. Sea ice variables considered were derived from satellite imagery (Scanning Multichannel Microwave Radiometer and Special Sensor Microwave/Imager; SMMR-SSM/I) (Stammerjohn et al. 2008) and included duration, extent, day of retreat, and day of advance.

Annual indices of climatic teleconnections (e.g., ENSO, SAM, and ASL) were included in the model. The ENSO index is based on sea surface temperatures (referred to as the multivariate ENSO index [MEI]; https://psl.noaa.gov/enso/mei/) and the SAM (http://www.antarctica.ac.uk/met/gjma/sam.html) index is based on sea level pressure. These climate indices are seasonally adjusted (Hurrell 1995). The RCP and latitudinal location of the ASL were obtained from Hosking et al. (Hosking and National Center for Atmospheric Research Staff 2020, p. 20). The RCPs from all four seasons (DJF, MAM, JJA, and SON) were evaluated. Multicollinearity between the conditional model parameters was tested for with the Variance Inflation Factor (VIF) and correlation coefficient (O'brien 2007). All parameters in the final model had VIF values of less than 2, well under cutoff range for moderate correlation (5 – 10) (Gareth et al. 2013).

Zero-inflated Generalized Linear Mixed-Effects Models (GLMMs) following a Tweedie distribution (Shono 2008) were developed in R (R Core Team 2022) and used to model the relationships between environmental variables and larval abundances. Antarctic larval fishes primarily exist in the upper 300-m of the water column (La Mesa et al. 2010) and are incidentally captured by Palmer LTER trawls targeting zooplankton (e.g., krill, salps, copepods). Resultingly, there is significant overrepresentation of "zero fishes captured" each year at stations along the Palmer LTER sampling grid. Zero-inflated GLMMs were selected over zero-altered, as any zeros in the larval Antarctic Silverfish time series are likely 'false', resulting from an imperfect sampling design (Denes et al. 2015).

Using an autocorrelation function (ACF) and partial autocorrelation function (PACF), temporal autocorrelation was observed, likely due to the fixed-sampling grid design (Zuur and Ieno 2016). An autoregressive covariance (AR1) is used in the GLMMs to accommodate the temporal autocorrelation between contiguous years (Barnett et al. 2010). There are no indications of spatial autocorrelation in the time-series, although "nuggets" detected using variograms suggest fine-scale spatial variation and measurement noise (Clark 2010). Palmer LTER sampling stations (i.e., net tow coordinates) were treated as a random effect to account for unobserved spatial heterogeneity (Gschlößl and Czado 2008). Generalized Additive Mixed-Effects Models (GAMMs) were also considered as several environmental variables exhibit marginal non-linearity. However, the lack of combined zero-inflation and autocorrelation structures for GAMMs limited their performance compared to GLMMs that account for these complexities (Brooks et al. 2017). The final model (Supplemental Fig. 2a; Supplemental Table 1) was selected based on hypothesis testing, parsimony, and minimizing the Akaike information criterion (AIC) (Aho et al. 2014). Diagnostic residual plots (Supplemental Fig. 5) were also used to evaluate the model performance.

Predicted values (or estimated marginal means) were developed using the ggeffects package (Lüdecke 2018) in R (R Core Team 2022). The predicted values of larval density were conditioned on the fixed effects, zero-inflation, and random effects components of the final model (i.e., “re.zi”) (Lüdecke 2018). The 95% prediction intervals surrounding the predictions consider the mean random effect variance and are generally larger than confidence intervals due to this additional level of uncertainty (Lüdecke 2018; Francq et al. 2019; Spineli and Pandis 2020). Predictions of environmental cutoff values where no larvae occur were determined when the upper 95% prediction interval included 0.000 larvae / 1000 m^3.

Figure development

Figure 1. Monthly sea ice concentration anomalies are derived from the Scanning Multi-channel Microwave Radiometer-Special Sensor Microwave/Imager (SMMR/SSM/I) satellite time series based on the Goddard Space Flight Center (GSFC) Bootstrap algorithm (Comiso 2000; Comiso and Nishio 2008). The sea ice concentration data are gridded to 25 km and are provided by the EOS Distributed Active Archive Center (DAAC) at the National Snow and Ice Data Center (NSIDC, University of Colorado at Boulder, http://nsidc.org). The numerically-analyzed monthly 10-m height winds and sea-level pressure anomalies are from the fifth generation European Centre for Medium Range Weather Forecasts (ECMWF) Reanalysis (ERA-5) (Hersbach et al. 2019) and are provided by the Climate Data Store (CDS, https://cds.climate.copernicus.eu/).

Figure 2. Sea surface temperatures for the Palmer LTER study region were determined by the NOAA optimal interpolation (OI) sea surface temperature analysis (version Reyn_SmithOI.v2) using in situ and satellite sea surface temperatures (Reynolds et al. 2002), plus sea surface temperatures simulated by sea ice cover. Annual anomalies of larval density and sea surface temperature were standardized by subtracting the sample mean then dividing by the sample standard deviation.

Data availability

All data analyzed in this study are publicly available. The Antarctic Silverfish larvae are archived in the VIMS Nunnally Ichthyology Collection and data are publicly available on the VIMS Specify web portal (https://www.vims.edu/research/facilities/fishcollection/search_collection/index.php). The associated Palmer LTER environmental variables are available online from the Datazoo web portal. See https://pal.lternet.edu/data for more information.

Acknowledgements

We would like to thank Joseph Cope (VIMS) for assisting in the collection of fishes and data analysis. We also thank: Sarah Huber (VIMS) and Peter Konstantinidis (Oregon State University) for their contributions to the identification of fishes and curatorial support; Adena Schonfeld (VIMS) and Robert Latour (VIMS) for their assistance in statistical analysis; Carlos Moffat (University of Delaware), Scott Hosking (British Antarctic Survey), William Fraser (Polar Oceans Research Group), and Christopher Jones (NOAA SWFC) for their aid in the interpretation of results. We are grateful for the multiple contributions of Marino Vacchi, Laura

Ghigliotti, and their colleagues (Institute of Marine Sciences – National Research Council) regarding the life history of the Antarctic Silverfish. We thank the captains, crew, and support staff of the R/V *Polar Duke* and ASRV *Laurence M. Gould*, the support of personnel at Palmer Station, Antarctica, and the Leidos Antarctic Support Contractors. This work was funded by the National Science Foundation Antarctic Organisms and Ecosystems Program (PLR-1440435 and OPP-2026045 for specimen and environmental data collection) and Division of Biological Infrastructure (DBI-1349327 for specimen preservation and analysis), and the VIMS John Olney Fellowship. This is contribution 4067 of the Virginia Institute of Marine Science, William & Mary.

References

Aho K, Derryberry D, Peterson T. 2014. Model selection for ecologists: the worldviews of AIC and BIC. Ecology. 95(3):631–636. https://doi.org/10.1890/13-1452.1

Ainley DG, Dugger KM, Mesa ML, Ballard G, Barton KJ, Jennings S, Karl BJ, Lescroël A, Lyver PO, Schmidt A, Wilson P. 2018. Post-fledging survival of Adélie penguins at multiple colonies: chicks raised on fish do well. Marine Ecology Progress Series. 601:239–251. https://doi.org/10.3354/meps12687

Ainley DG, Nur N, Eastman JT, Ballard G, Parkinson CL, Evans CW, DeVries AL. 2013. Decadal trends in abundance, size and condition of Antarctic toothfish in McMurdo Sound, Antarctica, 1972–2011. Fish and Fisheries. 14(3):343–363. https://doi.org/10.1111/j.1467-2979.2012.00474.x

Allen M, Antwi-Agyei P, Aragon-Durand F, Babiker M, Bertoldi P, Bind M, Brown S, Buckeridge M, Camilloni I, Cartwright A, et al. 2019. Technical Summary: Global warming of 1.5°C. An IPCC Special Report on the impacts of global warming of 1.5°C above pre-industrial levels and related global greenhouse gas emission pathways, in the context of strengthening the global response to the threat of climate change, sustainable development, and efforts to eradicate poverty. https://www.ipcc.ch/site/assets/uploads/sites/2/2018/12/SR15_TS_High_Res.pdf

Arrigo KR. 2014. Sea Ice Ecosystems. Annu Rev Mar Sci. 6(1):439–467. https://doi.org/10.1146/annurev-marine-010213-135103

Assmann KM, Jenkins A, Shoosmith DR, Walker DP, Jacobs SS, Nicholls KW. 2013. Variability of Circumpolar Deep Water transport onto the Amundsen Sea Continental shelf through a shelf break trough. Journal of Geophysical Research: Oceans. 118(12):6603–6620. https://doi.org/10.1002/2013JC008871

Barnett AG, Koper N, Dobson AJ, Schmiegelow F, Manseau M. 2010. Using information criteria to select the correct variance–covariance structure for longitudinal data in ecology. Methods in Ecology and Evolution. 1(1):15–24. https://doi.org/10.1111/j.2041-210X.2009.00009.x

Beers JM, Jayasundara N. 2015. Antarctic notothenioid fish: what are the future consequences of 'losses' and 'gains' acquired during long-term evolution at cold and stable temperatures? Journal of Experimental Biology. 218(12):1834–1845.

Bhaskaran K, Gasparrini A, Hajat S, Smeeth L, Armstrong B. 2013. Time series regression studies in environmental epidemiology. International Journal of Epidemiology. 42(4):1187–1195. https://doi.org/10.1093/ije/dyt092

Bilyk KT, DeVries AL. 2011. Heat tolerance and its plasticity in Antarctic fishes. Comparative Biochemistry and Physiology Part A: Molecular & Integrative Physiology. 158(4):382–390.

Brooks ME, Kristensen K, van Benthem KJ, Magnusson A, Berg CW, Nielsen A, Skaug HJ, Machler M, Bolker BM. 2017. glmmTMB balances speed and flexibility among packages for zero-inflated generalized linear mixed modeling. The R journal. 9(2):378–400. https://doi.org/10.3929/ethz-b-000240890

Caccavo JA, Papetti C, Wetjen M, Knust R, Ashford JR, Zane L. 2018. Along-shelf connectivity and circumpolar gene flow in Antarctic silverfish (Pleuragramma antarctica). Scientific reports. 8(1):1–16.

Casaux R, Baroni A, Ramón A. 2006. The diet of the Weddell Seal Leptonychotes weddellii at the Danco Coast, Antarctic Peninsula. Polar Biol. 29(4):257–262. https://doi.org/10.1007/s00300-005-0048-7

Chapman EW, Hofmann EE, Patterson DL, Ribic CA, Fraser WR. 2011. Marine and terrestrial factors affecting Adélie -penguin Pygoscelis adeliae chick growth and recruitment off the western Antarctic Peninsula. Marine Ecology Progress Series. 436:273–289. https://doi.org/10.3354/meps09242

Cimino MA, Lynch HJ, Saba VS, Oliver MJ. 2016. Projected asymmetric response of Adélie penguins to Antarctic climate change. Scientific Reports. 6(1):28785. https://doi.org/10.1038/srep28785

Clark I. 2010. Statistics or geostatistics? Sampling error or nugget effect? Journal of the Southern African Institute of Mining and Metallurgy. 110(6):307–312.

Coggins JHJ, McDonald AJ. 2015. The influence of the Amundsen Sea Low on the winds in the Ross Sea and surroundings: Insights from a synoptic climatology. Journal of Geophysical Research: Atmospheres. 120(6):2167–2189. https://doi.org/10.1002/2014JD022830

Comiso JC. 2000. Variability and Trends in Antarctic Surface Temperatures from In Situ and Satellite Infrared Measurements. Journal of Climate. 13(10):1674–1696. https://doi.org/10.1175/1520-0442(2000)013<1674:VATIAS>2.0.CO;2

Comiso JC, Nishio F. 2008. Trends in the sea ice cover using enhanced and compatible AMSR-E, SSM/I, and SMMR data. Journal of Geophysical Research: Oceans. 113(C2). https://doi.org/10.1029/2007JC004257

Cook AJ, Holland PR, Meredith MP, Murray T, Luckman A, Vaughan DG. 2016. Ocean forcing of glacier retreat in the western Antarctic Peninsula. Science. 353(6296):283–286.

Dahlke FT, Wohlrab S, Butzin M, Pörtner H-O. 2020. Thermal bottlenecks in the life cycle define climate vulnerability of fish. Science. 369(6499):65–70. https://doi.org/10.1126/science.aaz3658

Davis LB, Hofmann EE, Klinck JM, Piñones A, Dinniman MS. 2017. Distributions of krill and Antarctic silverfish and correlations with environmental variables in the western Ross Sea, Antarctica. Marine Ecology Progress Series. 584:45–65.

Denes FV, Silveira LF, Beissinger SR. 2015. Estimating abundance of unmarked animal populations: accounting for imperfect detection and other sources of zero inflation. Methods in Ecology and Evolution. 6(5):543–556.

DeWitt HH. 1970. The character of the midwater fish fauna of the Ross Sea, Antarctica. Antarctic ecology. 1:305–314.

Ding Q, Steig EJ, Battisti DS, Küttel M. 2011. Winter warming in West Antarctica caused by central tropical Pacific warming. Nature Geoscience. 4(6):398–403. https://doi.org/10.1038/ngeo1129

Dinniman MS, Klinck JM, Hofmann EE. 2012. Sensitivity of Circumpolar Deep Water Transport and Ice Shelf Basal Melt along the West Antarctic Peninsula to Changes in the Winds. Journal of Climate. 25(14):4799–4816. https://doi.org/10.1175/JCLI-D-11-00307.1

Dinniman MS, Klinck JM, Smith WO. 2011. A model study of Circumpolar Deep Water on the West Antarctic Peninsula and Ross Sea continental shelves. Deep Sea Research Part II: Topical Studies in Oceanography. 58(13):1508–1523. https://doi.org/10.1016/j.dsr2.2010.11.013

Dotto TS, Naveira Garabato AC, Wåhlin AK, Bacon S, Holland PR, Kimura S, Tsamados M, Herraiz-Borreguero L, Kalén O, Jenkins A. 2020. Control of the Oceanic Heat Content of the Getz-Dotson Trough, Antarctica, by the Amundsen Sea Low. Journal of Geophysical Research: Oceans. 125(8). https://doi.org/10.1029/2020JC016113

Ducklow HW, Baker K, Martinson DG, Quetin LB, Ross RM, Smith RC, Stammerjohn SE, Vernet M, Fraser W. 2007. Marine pelagic ecosystems: the West Antarctic Peninsula. Philosophical Transactions of the Royal Society B: Biological Sciences. 362(1477):67–94. https://doi.org/10.1098/rstb.2006.1955

Eastman JT. 1985. *Pleuragramma antarcticum* (Pisces, Nototheniidae) as food for other fishes in McMurdo Sound, Antarctica. Polar Biol. 4(3):155–160. https://doi.org/10.1007/BF00263878

Emslie SD, McDaniel JD. 2002. Adélie penguin diet and climate change during the middle to late Holocene in northern Marguerite Bay, Antarctic Peninsula. Polar Biol. 25(3):222–229. https://doi.org/10.1007/s00300-001-0334-y

Fogt RL, Wovrosh AJ, Langen RA, Simmonds I. 2012. The characteristic variability and connection to the underlying synoptic activity of the Amundsen-Bellingshausen Seas Low. Journal of Geophysical Research: Atmospheres. 117(D7).

Francq BG, Lin D, Hoyer W. 2019. Confidence, prediction, and tolerance in linear mixed models. Statistics in Medicine. 38(30):5603–5622. https://doi.org/10.1002/sim.8386

Fraser WR, Trivelpiece WZ. 1996. Factors Controlling the Distribution of Seabirds: Winter-Summer Heterogeneity in the Distribution of AdéLie Penguin Populations. In: Foundations for Ecological Research West of the Antarctic Peninsula. American Geophysical Union (AGU. p. 257–272. https://doi.org/10.1029/AR070p0257

Fuiman L, Davis R, Williams T. 2002. Behavior of midwater fishes under the Antarctic ice: observations by a predator. Marine Biology. 140(4):815–822.

Gao M, Kim S-J, Yang J, Liu J, Jiang T, Su B, Wang Y, Huang J. 2021. Historical fidelity and future change of Amundsen Sea Low under 1.5 °C-4 °C global warming in CMIP6. Atmospheric Research. 255:105533. https://doi.org/10.1016/j.atmosres.2021.105533

Gareth J, Daniela W, Trevor H, Robert T. 2013. An Introduction to Statistical Learning: with Applications in R. Spinger; [accessed 2021 May 14]. http://dspace.agu.edu.vn:8080/handle/AGU_Library/13322

Garrison DL, Ackley SF, Buck KR. 1983. A physical mechanism for establishing algal populations in frazil ice. Nature. 306(5941):363–365. https://doi.org/10.1038/306363a0

Garzio L, Steinberg D, Erickson M, Ducklow H. 2013. Microzooplankton grazing along the Western Antarctic Peninsula. Aquat Microb Ecol. 70(3):215–232. https://doi.org/10.3354/ame01655

Ghigliotti L, Ferrando S, Carlig E, Di Blasi D, Gallus L, Pisano E, Hanchet S, Vacchi M. 2017. Reproductive features of the Antarctic silverfish (Pleuragramma antarctica) from the western Ross Sea. Polar Biol. 40(1):199–211. https://doi.org/10.1007/s00300-016-1945-7

Gille ST, McKee DC, Martinson DG. 2016. Temporal Changes in the Antarctic Circumpolar Current: Implications for the Antarctic Continental Shelves. Oceanography. 29(4):96–105.

Gleiber M. 2014. Long-Term Change in Copepod Community Structure in the Western Antarctic Peninsula: Linkage to Climate and Implications for Carbon Cycling. Dissertations, Theses, and Masters Projects. https://dx.doi.org/doi:10.25773/v5-we5s-aq55

Gleiber MR, Steinberg DK, Schofield OME. 2016. Copepod summer grazing and fecal pellet production along the Western Antarctic Peninsula. Journal of Plankton Research. 38(3):732–750. https://doi.org/10.1093/plankt/fbv070

Granata A, Zagami G, Vacchi M, Guglielmo L. 2009. Summer and spring trophic niche of larval and juvenile Pleuragramma antarcticum in the Western Ross Sea, Antarctica. Polar Biol. 32(3):369–382. https://doi.org/10.1007/s00300-008-0551-8

Greaves BL, Davidson AT, Fraser AD, McKinlay JP, Martin A, McMinn A, Wright SW. 2020. The Southern Annular Mode (SAM) influences phytoplankton communities in the seasonal ice zone of the Southern Ocean. Biogeosciences. 17(14):3815–3835. https://doi.org/10.5194/bg-17-3815-2020

Gschlößl S, Czado C. 2008. Modelling count data with overdispersion and spatial effects. Statistical Papers. 49(3):531–552. https://doi.org/10.1007/s00362-006-0031-6

Guglielmo L, Granata A, Greco S. 1997. Distribution and abundance of postlarval and juvenile Pleuragramma antarcticum (Pisces, Nototheniidae) off Terra Nova bay (Ross sea, antarctica). Polar Biology. 19(1):37–51.

Hanchet S, Dunn A, Parker S, Horn P, Stevens D, Mormede S. 2015. The Antarctic toothfish (Dissostichus mawsoni): biology, ecology, and life history in the Ross Sea region. Hydrobiologia. 761(1):397–414. https://doi.org/10.1007/s10750-015-2435-6

Hanchet SM, Rickard GJ. 2008. A hypothetical life cycle for Antarctic toothfish (Dissostichus mawsoni) in the Ross Sea region. CCAMLR Science. 15:35–53.

Henley SF, Schofield OM, Hendry KR, Schloss IR, Steinberg DK, Moffat C, Peck LS, Costa DP, Bakker DC, Hughes C. 2019. Variability and change in the west Antarctic Peninsula marine system: research priorities and opportunities. Progress in Oceanography. 173:208–237.

Hersbach H, Bell B, Berrisford P, Biavati G, Horányi A, Muñoz Sabater J, Nicolas J, Peubey C, Radu R, Rozum I, Schepers D. 2019. ERA5 monthly averaged data on single levels from 1979 to present. https://doi.org/10.24381/CDS.F17050D7

Hilton EJ, Watkins-Colwell GJ, Huber SK. 2021. The Expanding Role of Natural History Collections. Ichthyology & Herpetology. 109(2):379–391. https://doi.org/10.1643/t2020018

Hobbie JE. 2003. Scientific Accomplishments of the Long Term Ecological Research Program: An Introduction. BioScience. 53(1):17–20. https://doi.org/10.1641/0006-3568(2003)053[0017:SAOTLT]2.0.CO;2

Hobbs WR, Massom R, Stammerjohn S, Reid P, Williams G, Meier W. 2016. A review of recent changes in Southern Ocean sea ice, their drivers and forcings. Global and Planetary Change. 143:228–250.

Hoey JA, Fodrie FJ, Walker QA, Hilton EJ, Kellison GT, Targett TE, Taylor JC, Able KW, Pinsky ML. 2020. Using multiple natural tags provides evidence for extensive larval dispersal across space and through time in summer flounder. Molecular Ecology. 29(8):1421–1435. https://doi.org/10.1111/mec.15414

Holland MM, Landrum L, Raphael MN, Kwok R. 2018. The regional, seasonal, and lagged influence of the Amundsen Sea Low on Antarctic sea ice. Geophysical Research Letters. 45(20):11–227.

Holland PR, Bracegirdle TJ, Dutrieux P, Jenkins A, Steig EJ. 2019. West Antarctic ice loss influenced by internal climate variability and anthropogenic forcing. Nature Geoscience. 12(9):718–724. https://doi.org/10.1038/s41561-019-0420-9

Holland PR, Bruneau N, Enright C, Losch M, Kurtz NT, Kwok R. 2014. Modeled trends in Antarctic sea ice thickness. Journal of Climate. 27(10):3784–3801.

Hoppmann M, Richter ME, Smith IJ, Jendersie S, Langhorne PJ, Thomas DN, Dieckmann GS. 2020. Platelet ice, the Southern Ocean's hidden ice: a review. Annals of Glaciology. 61(83):341–368. https://doi.org/10.1017/aog.2020.54

Hosking JS, National Center for Atmospheric Research Staff, editors. 2020. The Climate Data Guide: Amundsen Sea Low indices.

Hosking JS, Orr A, Bracegirdle TJ, Turner J. 2016. Future circulation changes off West Antarctica: Sensitivity of the Amundsen Sea Low to projected anthropogenic forcing. Geophysical Research Letters. 43(1):367–376.

Hosking JS, Orr A, Marshall GJ, Turner J, Phillips T. 2013. The influence of the Amundsen–Bellingshausen Seas low on the climate of West Antarctica and its representation in coupled climate model simulations. Journal of Climate. 26(17):6633–6648.

Houde ED. 2008. Emerging from Hjort's Shadow. J Northw Atl Fish Sci. 41:53–70. https://doi.org/10.2960/J.v41.m634

Hubold G, Ekau W. 1990. Feeding patterns of post-larval and juvenile notothenioids in the southern Weddell Sea (Antarctica). Polar Biology. 10(4). https://doi.org/10.1007/BF00238422

Hughes BB, Beas-Luna R, Barner AK, Brewitt K, Brumbaugh DR, Cerny-Chipman EB, Close SL, Coblentz KE, de Nesnera KL, Drobnitch ST, et al. 2017. Long-Term Studies

Contribute Disproportionately to Ecology and Policy. BioScience. 67(3):271–281. https://doi.org/10.1093/biosci/biw185

Hurrell JW. 1995. Decadal Trends in the North Atlantic Oscillation: Regional Temperatures and Precipitation. Science. 269(5224):676–679. https://doi.org/10.1126/science.269.5224.676

Kellermann AK. 1990. Identification key and catalogue of larval Antarctic fishes. Ber Polarforsch.(67):1–138.

Kellermann AK. 1996. Midwater fish ecology. Foundations for ecological research west of the Antarctic Peninsula. 70:231–256.

Koubbi P, O'Brien C, Loots C, Giraldo C, Smith M, Tavernier E, Vacchi M, Vallet C, Chevallier J, Moteki M. 2011. Spatial distribution and inter-annual variations in the size frequency distribution and abundances of *Pleuragramma antarcticum* larvae in the Dumont d'Urville Sea from 2004 to 2010. Polar Science. 5(2):225–238.

La HS, Park K, Wåhlin A, Arrigo KR, Kim DS, Yang EJ, Atkinson A, Fielding S, Im J, Kim T-W, et al. 2019. Zooplankton and micronekton respond to climate fluctuations in the Amundsen Sea polynya, Antarctica. Scientific Reports. 9(1):10087. https://doi.org/10.1038/s41598-019-46423-1

La Mesa M, Catalano B, Russo A, Greco S, Vacchi M, Azzali M. 2010. Influence of environmental conditions on spatial distribution and abundance of early life stages of Antarctic silverfish, Pleuragramma antarcticum (Nototheniidae), in the Ross Sea. Antarctic Science. 22(3):243.

La Mesa M, Eastman JT. 2012. Antarctic silverfish: life strategies of a key species in the high-Antarctic ecosystem. Fish and Fisheries. 13(3):241–266.

La Mesa M, Eastman JT, Vacchi M. 2004. The role of notothenioid fish in the food web of the Ross Sea shelf waters: a review. Polar Biol. 27(6):321–338. https://doi.org/10.1007/s00300-004-0599-z

La Mesa M, Riginella E, Mazzoldi C, Ashford J. 2015. Reproductive resilience of ice-dependent Antarctic silverfish in a rapidly changing system along the Western Antarctic Peninsula. Marine Ecology. 36(2):235–245.

Lüdecke D. 2018. ggeffects: Tidy Data Frames of Marginal Effects from Regression Models. JOSS. 3(26):772. https://doi.org/10.21105/joss.00772

Meredith MP, Brandon MA, Wallace MI, Clarke A, Leng MJ, Renfrew IA, van Lipzig NPM, King JC. 2008. Variability in the freshwater balance of northern Marguerite Bay, Antarctic Peninsula: Results from δ18O. Deep Sea Research Part II: Topical Studies in Oceanography. 55(3):309–322. https://doi.org/10.1016/j.dsr2.2007.11.005

Meredith MP, King JC. 2005. Rapid climate change in the ocean west of the Antarctic Peninsula during the second half of the 20th century. Geophysical Research Letters. 32(19). https://doi.org/10.1029/2005GL024042

Mintenbeck K, Torres JJ. 2017. Impact of climate change on the Antarctic silverfish and its consequences for the Antarctic ecosystem. In: The Antarctic silverfish: a keystone species in a changing ecosystem. Springer; p. 253–286.

Moffat C, Owens B, Beardsley RC. 2009. On the characteristics of Circumpolar Deep Water intrusions to the west Antarctic Peninsula Continental Shelf. Journal of Geophysical Research: Oceans. 114(C5). https://doi.org/10.1029/2008JC004955

Moline MA, Claustre H, Frazer TK, Schofield O, Vernet M. 2004. Alteration of the food web along the Antarctic Peninsula in response to a regional warming trend. Global Change Biology. 10(12):1973–1980. https://doi.org/10.1111/j.1365-2486.2004.00825.x

Moreno C, Rueda T, Asencio G. 1986. The Trophic Niche of Pleuragramma antarcticum in the Bransfield Strait, Antarctica: Quantitative Comparison with other Areas of the Southern Ocean.

Nakayama Y, Menemenlis D, Zhang H, Schodlok M, Rignot E. 2018. Origin of Circumpolar Deep Water intruding onto the Amundsen and Bellingshausen Sea continental shelves. Nature Communications. 9(1):3403. https://doi.org/10.1038/s41467-018-05813-1

O'brien RM. 2007. A Caution Regarding Rules of Thumb for Variance Inflation Factors. Qual Quant. 41(5):673–690. https://doi.org/10.1007/s11135-006-9018-6

Parker ML, Fraser WR, Ashford J, Patarnello T, Zane L, Torres JJ. 2015. Assemblages of micronektonic fishes and invertebrates in a gradient of regional warming along the Western Antarctic Peninsula. Journal of Marine Systems. 152:18–41.

Pinkerton M, Hanchet S, Bradford-Grieve J. 2007. Finding the role of Antarctic toothfish in the Ross Sea ecosystem. Water and Atmosphere. 15:20–21.

Pinkerton MH, Bradford-Grieve JM, Hanchet SM. 2010. A balanced model of the food web of the Ross Sea, Antarctica. CCAMLR Science. 17:1–31.

Ponganis PJ, Stockard TK. 2007. Short Note: The Antarctic toothfish: how common a prey for Weddell seals? Antarctic Science. 19(4):441–442. http://dx.doi.org/10.1017/S0954102007000715

Quetin LB, Ross RM. 2009. Life under Antarctic pack ice: a krill perspective. Smithsonian at the Poles: Contributions to International Polar Year Science.

R Core Team. 2022. R: A language and environment for statistical computing. https://www.R-project.org/

Raphael MN, Marshall GJ, Turner J, Fogt RL, Schneider D, Dixon DA, Hosking JS, Jones Jm, Hobbs WR. 2016. The Amundsen Sea low: Variability, change, and impact on Antarctic climate. Bulletin of the American Meteorological Society. 97(1):111–121.

Regan HC, Holland PR, Meredith MP, Pike J. 2018. Sources, variability and fate of freshwater in the Bellingshausen Sea, Antarctica. Deep Sea Research Part I: Oceanographic Research Papers. 133:59–71.

Reynolds RW, Rayner NA, Smith TM, Stokes DC, Wang W. 2002. An Improved In Situ and Satellite SST Analysis for Climate. Journal of Climate. 15(13):1609–1625. https://doi.org/10.1175/1520-0442(2002)015<1609:AIISAS>2.0.CO;2

Rintoul SR, Chown SL, DeConto RM, England MH, Fricker HA, Masson-Delmotte V, Naish TR, Siegert MJ, Xavier JC. 2018. Choosing the future of Antarctica. Nature. 558(7709):233–241. https://doi.org/10.1038/s41586-018-0173-4

Ross RM, Quetin LB, Newberger T, Shaw CT, Jones JL, Oakes SA, Moore KJ. 2014. Trends, cycles, interannual variability for three pelagic species west of the Antarctic Peninsula 1993-2008. Marine Ecology Progress Series. 515:11–32.

Ruck KE, Steinberg DK, Canuel EA. 2014. Regional differences in quality of krill and fish as prey along the Western Antarctic Peninsula. Marine Ecology Progress Series. 509:39–55. https://doi.org/10.3354/meps10868

Rumolo P, Zappes IA, Fabiani A, Barra M, Rakaj A, Palozzi R, Allegrucci G. 2020. The diet of Weddell seals (Leptonychotes weddellii) in Terra Nova Bay using stable isotope analysis. The European Zoological Journal. 87(1):94–104. https://doi.org/10.1080/24750263.2020.1720832

Sandersfeld T, Davison W, Lamare MD, Knust R, Richter C. 2015. Elevated temperature causes metabolic trade-offs at the whole-organism level in the Antarctic fish Trematomus bernacchii. Journal of Experimental Biology. 218(15):2373–2381.

Screen JA, Bracegirdle TJ, Simmonds I. 2018. Polar Climate Change as Manifest in Atmospheric Circulation. Curr Clim Change Rep. 4(4):383–395. https://doi.org/10.1007/s40641-018-0111-4

Shono H. 2008. Application of the Tweedie distribution to zero-catch data in CPUE analysis. Fisheries Research. 93(1):154–162. https://doi.org/10.1016/j.fishres.2008.03.006

Slosarczyk W. 1986. Attempts at a quantitative estimate by trawl sampling of distribution of postlarval and juvenile notothenioids (Pisces, Perciformes) in relation to environmental conditions in the Antarctic Peninsula region during SIBEX 1983-84. 40:299–315.

Smith RC, Baker KS, Fraser WR, Hofmann EE, Karl DM, Klinck JM, Quetin LB, Prézelin BB, Ross RM, Trivelpiece WZ. 1995. The Palmer LTER: A long-term ecological research program at Palmer Station, Antarctica. Oceanography. 8(3):77–86.

Spence P, Griffies SM, England MH, Hogg AM, Saenko OA, Jourdain NC. 2014. Rapid subsurface warming and circulation changes of Antarctic coastal waters by poleward shifting winds. Geophysical Research Letters. 41(13):4601–4610. https://doi.org/10.1002/2014GL060613

Spineli LM, Pandis N. 2020. Prediction interval in random-effects meta-analysis. American Journal of Orthodontics and Dentofacial Orthopedics. 157(4):586–588. https://doi.org/10.1016/j.ajodo.2019.12.011

Stammerjohn SE, Maksym T, Massom RA, Lowry KE, Arrigo KR, Yuan X, Raphael M, Randall-Goodwin E, Sherrell RM, Yager PL. 2015. Seasonal sea ice changes in the Amundsen Sea, Antarctica, over the period of 1979–2014. Elementa: Science of the Anthropocene. 3.

Stammerjohn SE, Martinson DG, Smith RC, Iannuzzi RA. 2008. Sea ice in the western Antarctic Peninsula region: Spatio-temporal variability from ecological and climate change perspectives. Deep Sea Research Part II: Topical Studies in Oceanography. 55(18):2041–2058. https://doi.org/10.1016/j.dsr2.2008.04.026

Stammerjohn SE, Scambos TA. 2020. Warming reaches the South Pole. Nature Climate Change. 10(8):710–711. https://doi.org/10.1038/s41558-020-0827-8

Steinberg DK, Ruck KE, Gleiber MR, Garzio LM, Cope JS, Bernard KS, Stammerjohn SE, Schofield OME, Quetin LB, Ross RM. 2015. Long-term (1993–2013) changes in macrozooplankton off the Western Antarctic Peninsula. Deep Sea Research Part I: Oceanographic Research Papers. 101:54–70. https://doi.org/10.1016/j.dsr.2015.02.009

Thoma M, Jenkins A, Holland D, Jacobs S. 2008. Modelling Circumpolar Deep Water intrusions on the Amundsen Sea continental shelf, Antarctica. Geophysical Research Letters. 35(18). https://doi.org/10.1029/2008GL034939

Thompson DWJ, Solomon S, Kushner PJ, England MH, Grise KM, Karoly DJ. 2011. Signatures of the Antarctic ozone hole in Southern Hemisphere surface climate change. Nature Geoscience. 4(11):741–749. https://doi.org/10.1038/ngeo1296

Turner J, Lu H, White I, King JC, Phillips T, Hosking JS, Bracegirdle TJ, Marshall GJ, Mulvaney R, Deb P. 2016. Absence of 21st century warming on Antarctic Peninsula consistent with natural variability. Nature. 535(7612):411–415.

Turner J, Phillips T, Hosking JS, Marshall GJ, Orr A. 2013. The Amundsen Sea low. International Journal of Climatology. 33(7):1818–1829. https://doi.org/10.1002/joc.3558

Vacchi M, DeVries AL, Evans CW, Bottaro M, Ghigliotti L, Cutroneo L, Pisano E. 2012. A nursery area for the Antarctic silverfish Pleuragramma antarcticum at Terra Nova Bay (Ross Sea): first estimate of distribution and abundance of eggs and larvae under the seasonal sea-ice. Polar Biol. 35(10):1573–1585. https://doi.org/10.1007/s00300-012-1199-y

Vacchi M, La Mesa M, Dalu M, Macdonald J. 2004. Early life stages in the life cycle of Antarctic silverfish, Pleuragramma antarcticum in Terra Nova Bay, Ross Sea. Antartic science. 16(3):299–305. https://doi.org/10.1017/S0954102004002135

Varsamos S, Nebel C, Charmantier G. 2005. Ontogeny of osmoregulation in postembryonic fish: A review. Comparative Biochemistry and Physiology Part A: Molecular & Integrative Physiology. 141(4):401–429. https://doi.org/10.1016/j.cbpb.2005.01.013

Veazey AL, Jeffries MO, Morris K. 1994. Small-Scale variability of physical properties and structural characteristics of Antarctic fast ice. Annals of Glaciology. 20:61–66. https://doi.org/10.3189/1994AoG20-1-61-66

Venables HJ, Clarke A, Meredith MP. 2013. Wintertime controls on summer stratification and productivity at the western Antarctic Peninsula. Limnology and Oceanography. 58(3):1035–1047. https://doi.org/10.4319/lo.2013.58.3.1035

Wöhrmann AP, Hagen W, Kunzmann A. 1997. Adaptations of the Antarctic silverfish Pleuragramma antarcticum (Pisces: Nototheniidae) to pelagic life in high-Antarctic waters. Marine Ecology Progress Series. 151:205–218.

Zuur AF, Ieno EN. 2016. Beginner´s guide to zero-inflated models with R. Newburgh: Highland Statistics Ltd.

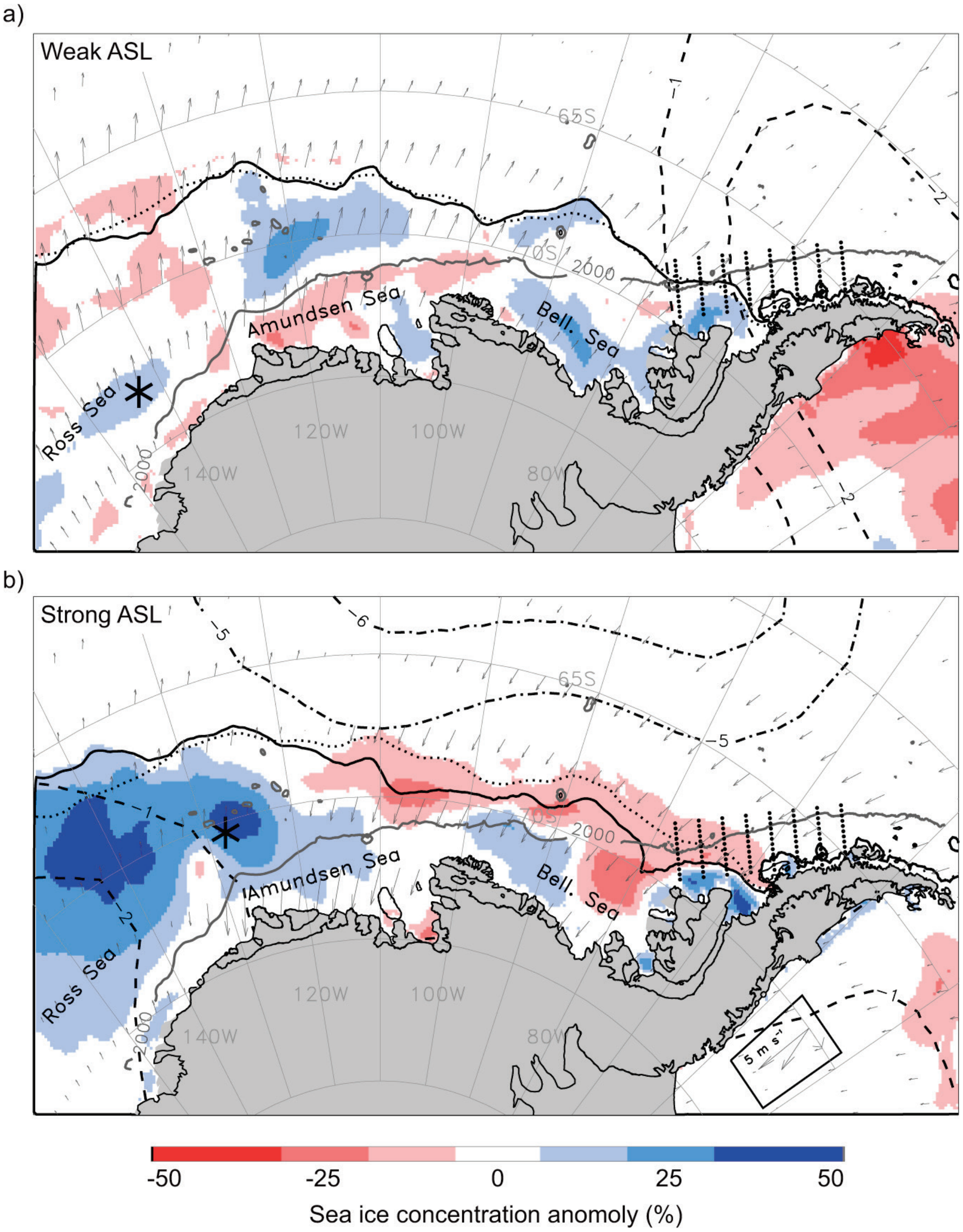

Figure 1. (a) Averaged environmental conditions for the duration of an especially weak (shallow; relative central pressure, RCP, of -6) ASL event during March-April-May (MAM) 1993. The ASL central location is marked by the black asterisk and the Palmer Antarctica Long-Term Ecological Research program study region and sampling stations is depicted by eight lines of small black dots. Sea ice concentration anomalies are color shaded and the MAM 1993 mean ice edge contour (solid black line) and long-term (1979 – 2019) mean contour (dotted black line) are also marked. Subsampled wind anomalies are shown in vector format. The negative sea-level pressure (SLP) anomalies are shown for the most negative feature during MAM 1993 (dashed concentric contours). (b) The same averaged environmental conditions and symbology as in (a), but for the duration of an especially strong (deep; RCP of -16) ASL event during MAM 1996. The wind-vector legend for both 1993 and 1996 is boxed in the lower right corner.

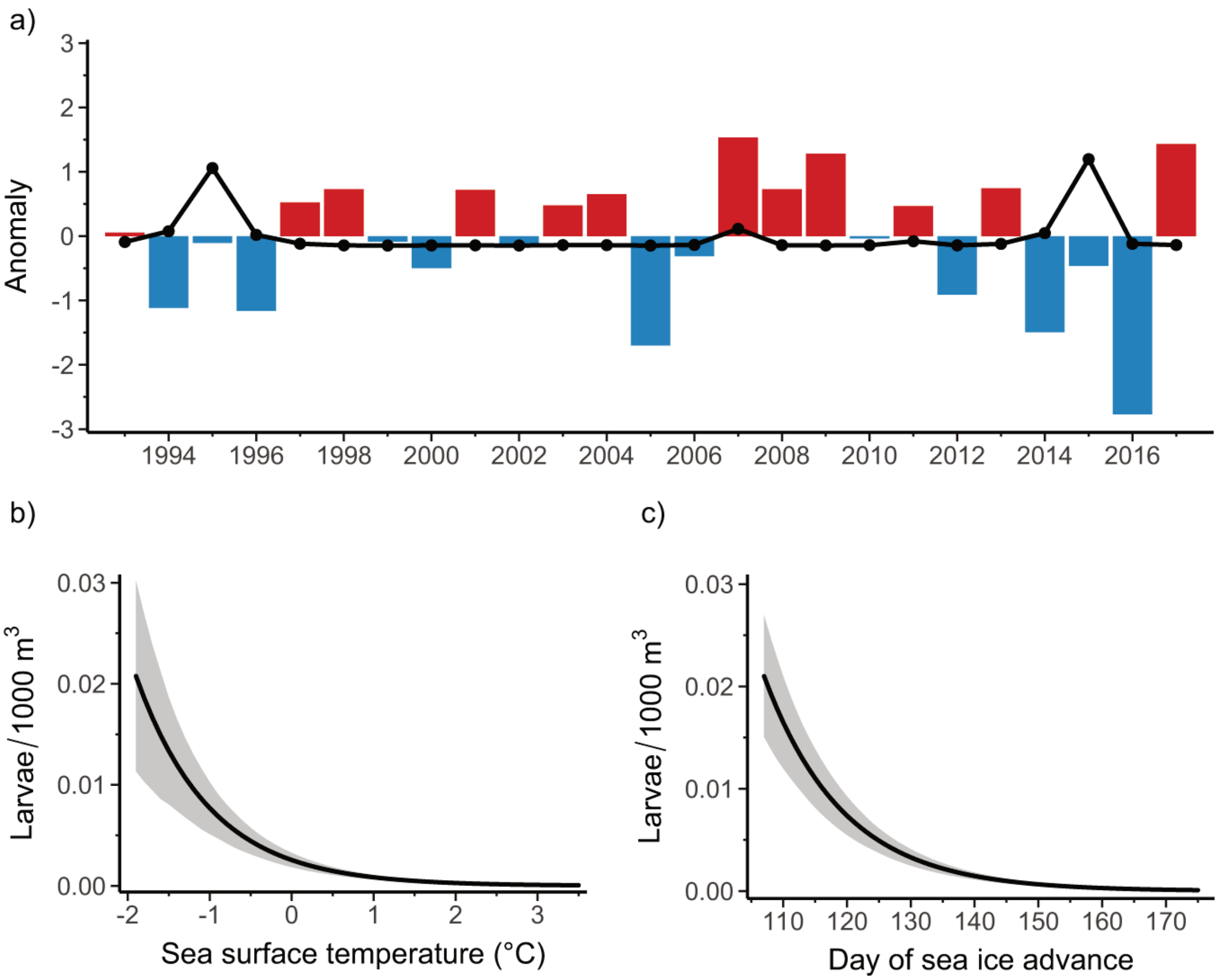

Figure 2. (a) Positive (red; warmer temperatures) and negative (blue; cooler temperatures) anomalies in the standardized mean sea surface temperature (see Materials and Methods) for the Palmer LTER study region (Supplemental Fig. 1) during austral summer (December, January, February). Standardized anomalies in mean annual larval Antarctic Silverfish abundance (larvae/1000 m^3) that were captured during January and February are overlaid (black dotted line). b-c, Predicted impact (solid black lines) on larval Antarctic Silverfish abundance from (b) sea surface temperature ($p < 0.001$) and **(c),** lagged day of sea ice advance ($p < 0.001$) from the model (see Materials and Methods). Sea ice advance was temporally lagged in the model to align with life history patterns in adult Antarctic Silverfish abundance. The shaded regions represent the 95% prediction interval, which considers uncertainty from the fixed effects, zero-inflation, and random effects components of the final model (Supplemental Fig. 2a (Lüdecke 2018), see Materials and Methods).

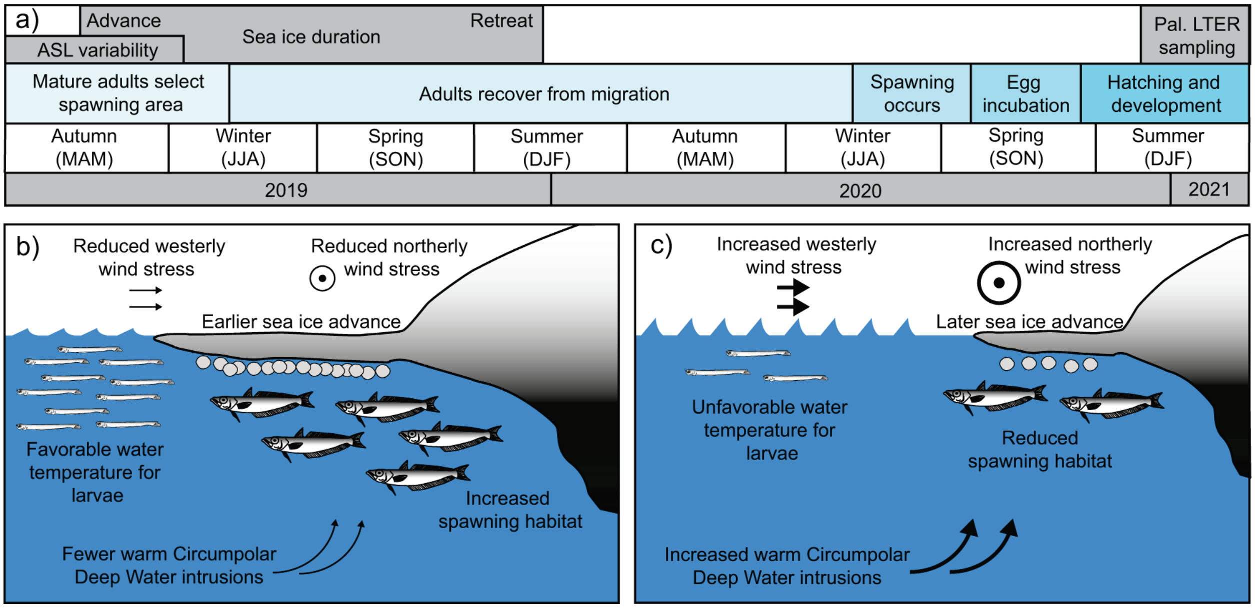

Figure 3. (a) A timeline of Antarctic Silverfish skip-spawning behavior and proposed relationships with Amundsen Sea Low (ASL) variability and sea ice advance. b-c, Schematic of (b) optimal and (c) suboptimal environmental conditions for larval and spawning adult Antarctic Silverfish near the WAP. Northerly and westerly wind stresses are both modulated by the ASL strength (i.e., RCP) and location (i.e., latitude). Intrusions of Circumpolar Deep Water (CDW) are associated with anomalous westerly winds; sea ice advance is influenced by a combination of wind stress, CDW, precipitation, and other factors; and near-surface water temperatures are determined by atmospheric heat, CDW intrusions, ice melt, and other factors.

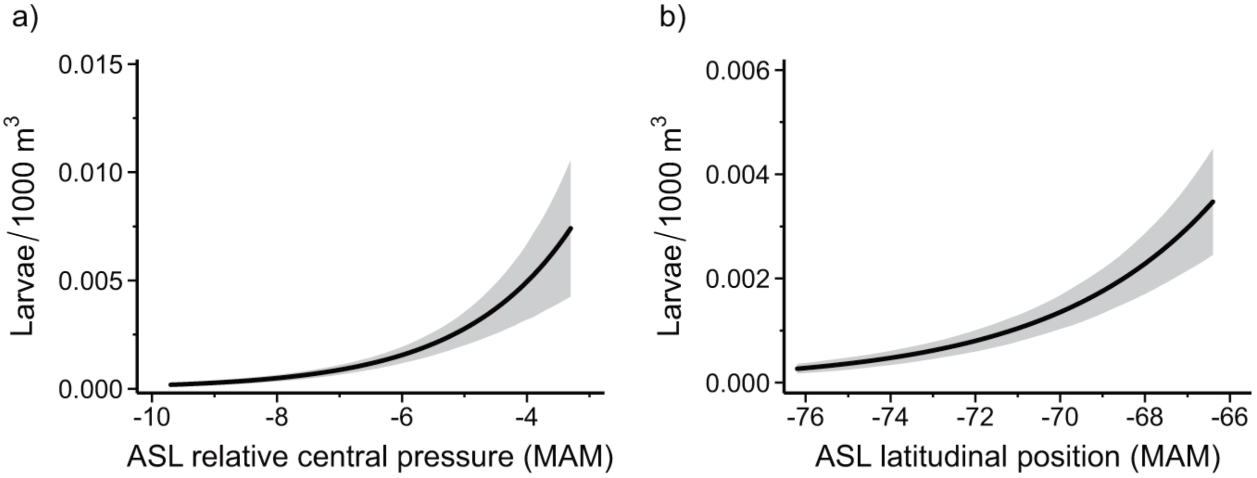

Figure 4. a-b, Predicted impact (solid black lines) on larval Antarctic Silverfish abundance from (a) the relative central pressure (RCP) of the Amundsen Sea Low (ASL) during austral autumn (March-April-May [MAM]; *p* = 0.006) and (b) the latitudinal location of the ASL during austral autumn (*p* = 0.004) from the model (see Materials and Methods). Smaller RCP values correspond with stronger (i.e., deeper) ASL events and smaller latitudinal values correspond with southward (i.e., poleward) locations of the ASL. The ASL RCPs and locations were temporally lagged in the model to align with life history patterns in adult Antarctic Silverfish abundance. The shaded regions represent the 95% prediction interval, which considers uncertainty from the fixed effects, zero-inflation, and random effects components of the final model (Supplemental Fig. 2a (Lüdecke 2018), see Materials and Methods). It is important to note only one value of ASL RCP was greater (less negative) than -4.5, which accounts for the increased uncertainty at less negative values (> -4.5). Additionally, we observed no significant collinearity between ASL RCP and latitude in this analysis (see Materials and Methods).

Supplemental Table 1. Results from the conditional component of the final model. While several other variables were tested during the model development process (see Materials and Methods), only estimates for the parameters in the selected final model (Supplemental Fig. 2a) are displayed.

Variable	Estimate	Std. Error	Wald z	*p*-value
Sea surface temperature	-1.10	0.28	-4.00	< 0.001
Lagged sea ice advance	-0.08	0.01	-5.77	< 0.001
Lagged ASL MAM RCP	0.58	0.21	2.73	0.006
Lagged ASL MAM Lat.	0.26	0.09	2.83	0.005
Sea surface salinity	-2.43	0.44	-5.48	< 0.001
Log(Chlorophyll conc.)	1.47	0.30	4.92	< 0.001

Supplemental Table 2. Impact of temporal lagging strategy on model performance. In each identical final model (Supplemental Fig. 2a), sea ice advance, ASL RCP, and ASL latitude are either not lagged (0-years), lagged by one year (1-year), or lagged by two years (2-year). Number of parameters (No. par), Akaike information criterion (AIC), the difference in AIC score (ΔAIC) between the given model and the best performing model, and the model deviance (Dev.) are displayed for comparison.

Model structure	No. par	AIC	ΔAIC	Dev.
Final model (0-year lag)	8	1143.3	24.7	1117.2
Final model (1-year lag)	8	1118.6	0	1092.6
Final model (2-year lag)	8	1134.0	15.4	1108.0

Supplemental Table 3. Impact of the ASL, SAM, and ENSO on model performance. Annual indices of ASL, SAM, and ENSO (MEI) were each added to a base model (Supplemental Fig. 2b) to illustrate the relative impact of each climatic teleconnection on model performance. For this comparison, annual indices were used to partially account for differing seasonality of the three systems. The location of the ASL was also excluded from the base model. However, the final model (Supplemental Fig. 2a) contains ASL RCP and latitudinal location for the MAM period. Number of parameters (No. par), Akaike information criterion (AIC), the difference in AIC score (ΔAIC) between the given model and the best performing model, and the model deviance (Dev.) are displayed for comparison.

Model structure	No. par	AIC	ΔAIC	Dev.
Base (no clim. indices)	6	1128.8	10.2	1106.8
Base + annual ASL	7	1122.4	3.8	1098.4
Base + annual SAM	7	1127.9	9.3	1103.9
Base + annual MEI	7	1130.8	12.2	1106.8
Final model	8	1118.6	0	1092.6

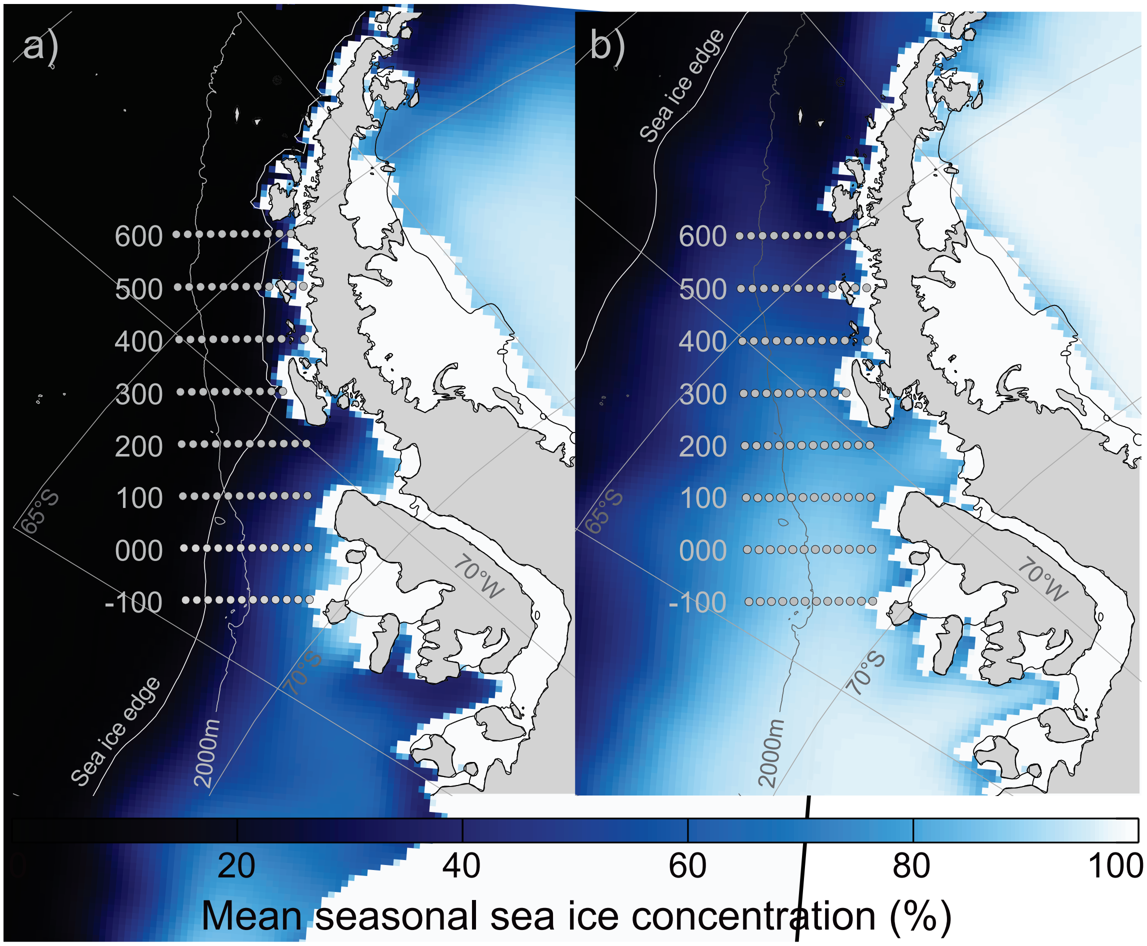

Supplemental Figure 1. (a) The Palmer LTER sampling grid with mean (1979 to 2020) sea ice concentration during the summer (DJF). The boundary between sea ice and open water is represented by the sea ice edge line. Stations are shown as circles and are spaced 20 km apart along grid lines (600 to -100) arranged perpendicular to the peninsula. Each grid line is spaced 100 km apart for a total sampling grid length of 700 km. The continental shelf boundary is also depicted by the 2000 m bathymetric contour line (b) The sampling grid with mean (1979 to 2020) sea ice concentrations shown during the winter (JJA).

a) Final model = glmmTMB(CPUE ~ sea surface temperature + 1-year lag sea ice advance + 1-year lag ASL MAM RCP + 1-year lag ASL MAM latitude + sea surface salinity + log(chlorophyll concentration) + AR1(year) + (1 | net tow coordinates), ziformula = all observations, family = tweedie(link = “log”))

b) Base model = glmmTMB(CPUE ~ sea surface temperature + sea surface salinity + log(chlorophyll concentration) + AR1(year) + (1 | net tow coordinates), ziformula = all observations, family = tweedie(link = “log”))

Supplemental Figure 2. (a) The structure for the final model, which was developed in R1 using glmmTMB2. Acronyms not discussed previously are defined as: catch per unit effort (cpue; larvae 1000m3), zero-inflation argument (ziformula), random effect (1 | …). (b) The structure of the base model, which was used to illustrate the influence of the ASL, SAM, and ENSO on model performance (Supplemental Table 3).

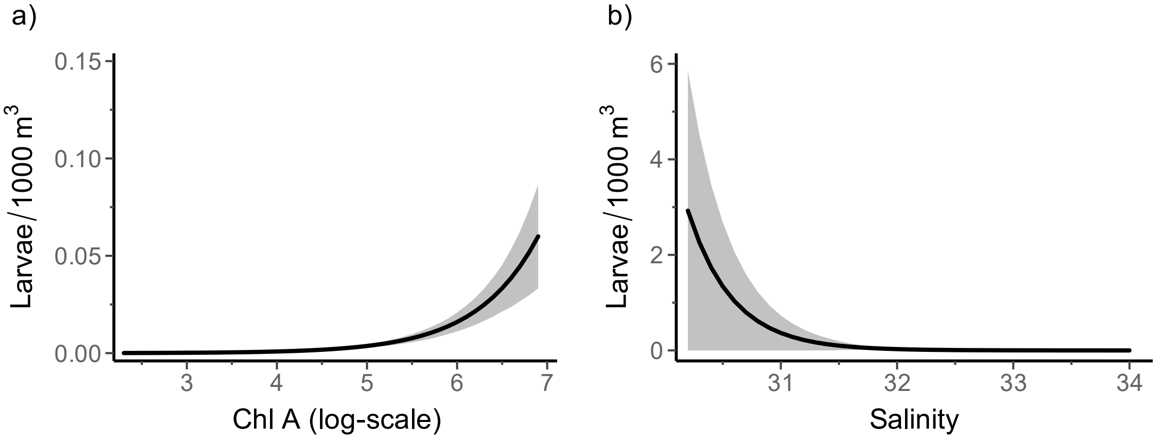

Supplemental Figure 3. Predicted impact (solid black lines) on larval Antarctic Silverfish abundance from (a) log-transformed chlorophyll concentration ($p < 0.001$) and (b) sea surface salinity ($p < 0.001$) from the final model (Supplemental Fig. 2a). The shaded regions represent the 95% prediction interval, which considers uncertainty from the fixed effects, zero-inflation, and random effects components of the final model (Supplemental Fig. 2a 3, see Materials and Methods).

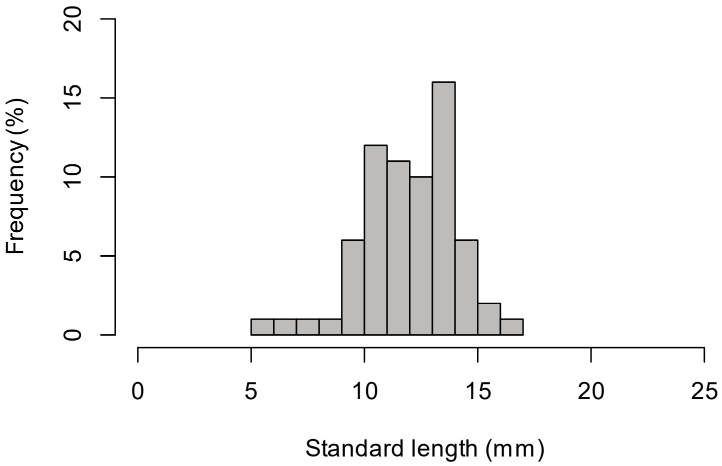

Supplemental Figure 4. Length distribution of Antarctic Silverfish larvae (n = 71) caught by the Palmer Antarctica Long-Term Ecological Research Program (Palmer LTER) off the western Antarctic Peninsula. The mean is 11.9 mm with a standard deviation of 2.1 mm. A subsample of larvae were randomly selected from the 7,093 fish used in this study to be measured. Note: the poor condition of the larvae prevented reliable measurements past the tenths place.

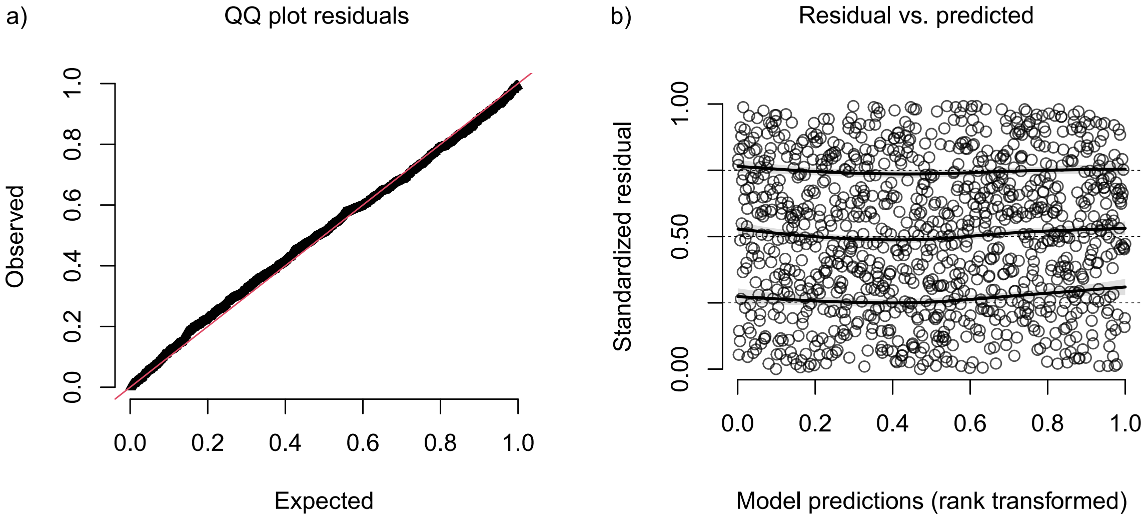

Supplemental Figure 5. (a) A uniform quantile-quantile (QQ) plot for a uniform distribution created from a DHARMa simulation output 4 of the final model (Supplemental Fig. 2a). (b) A plot comparing simulated quantile residuals, which have been standardized between 0 and 1 for ease of interpretation 4, to the rank-transformed predicted values from the fixed-effect component of the final model. Quantile regressions have been added (solid black lines) for the 0.25, 0.5, and 0.75 quantiles, which are represented by the dashed lines.

CHAPTER 3

Larval stages of the Antarctic dragonfish *Akarotaxis nudiceps* (Waite, 1916) with comments on the larvae of the morphologically similar species *Prionodraco evansii* Regan 1914 (Notothenioidei; Bathydraconidae)

Please cite this chapter as: Corso AD, McDowell JR, Biesack EE, Muffelman SC, Hilton EJ. Larval stages of the Antarctic dragonfish *Akarotaxis nudiceps* (Waite, 1916), with comments on the larvae of the morphologically similar species *Prionodraco evansii* Regan 1914 (Notothenioidei: Bathydraconidae). 2023. Journal of Fish Biology. 102.2: 395-402. https://doi.org/10.1111/jfb.15267

Abstract

The notothenioid family Bathydraconidae is a poorly understood family of fishes endemic to the Southern Ocean. There is especially little information on *Akarotaxis nudiceps*, one of the deepest-dwelling and least fecund bathydraconid species. Using genetic and morphological data, we document and describe the larval stages of this unique species, offer a novel characteristic to distinguish it from the morphologically similar bathydraconid *Prionodraco evansii* and use the sampling locations to infer a possible spawning area of *A. nudiceps* along the western Antarctic Peninsula. These results provide important baseline information for locating, identifying and studying the biology of *A. nudiceps*, an important component of the Southern Ocean ecosystem.

1. Introduction

Bathydraconidae, the Antarctic Dragonfishes, are one of five families of Notothenioidei endemic to the Southern Ocean. The family currently includes 16 species in 11 genera (Eastman and Eakin 2021). All bathydraconids have an elongate and slender appearance at maturity (Gon and Heemstra 1990). Morphological analysis suggests bathydraconids are monophyletic, primarily based on the synapomorphic loss of the first spinous dorsal fin (Derome et al. 2002). Although genetic analyses based on sequencing the mitochondrial 16S and 12S regions have suggested that the family is paraphyletic (Bargelloni et al. 2000; Near et al. 2004; Near et al. 2012; Daane et al. 2019; Bista et al. 2022), a recent analysis of ~100,000 single nuclear polymorphism (SNP) loci recovered a monophyletic Bathydraconidae as a sister lineage of the Channichthyidae (Near et al. 2018).

As adults, most bathydraconids are found on the continental shelf and upper slope (de Broyer and Koubbi 2014) at depths ranging from 500 to 1000m, although they have been collected from the surface to a maximum depth of 3000m (Eastman 2017). Most bathydraconid species likely spawn during austral autumn and early winter (Kock and Kellermann 1991; Loeb et al. 1993; Evans et al. 2005; Kuhn et al. 2011). However, analysis of oogenesis and observations by SCUBA divers indicate several species also spawn during the summer in the southern Scotia Arc (Barrera-Oro and Lagger 2010; La Mesa et al. 2012), Ross Sea (La Mesa et al. 2007), and the Weddell Sea (Van der Molen and Matallanas 2003; La Mesa, Riginella, et al. 2018; La Mesa, Calì, et al. 2018). Egg guarding has been reported for several species of bathydraconids; adults generally deposit 200 to 20,000 eggs measuring 1 to 4 mm in diameter onto rocks (Kock and Kellermann 1991; Evans et al. 2005; Barrera-Oro and Lagger 2010; Kuhn et al. 2011; La Mesa et al. 2021). Eggs will develop for 5 to 10 months (Kock and Kellermann 1991; Evans et al. 2005), with most larvae hatching in late spring during October and November (Kellermann 1990).

With just 200 to 300 oocytes, *Akarotaxis nudiceps* (Waite 1916) has one of the lowest absolute fecundities of all Antarctic notothenioids (Kock and Kellermann 1991; La Mesa et al. 2007). Adults have been recorded in the Weddell, Ross, Bellingshausen, and Davis Seas; the species likely has a circumpolar distribution on the Antarctic shelf (Gon and Heemstra 1990; Ekau 1990; La Mesa et al. 2019). With a depth range of 371 – 1191m, *A. nudiceps* is also among the deepest living bathydraconids (Eastman 2017). In deep coastal areas of the Weddell Sea, *A. nudiceps* has been reported as one of the most dominant fish species, although very little is known about its biology (Ekau 1990; La Mesa et al. 2019). It has been suggested that *A. nudiceps* exhibits nest guarding due to its low fecundity (La Mesa et al. 2007), although this behavior has not yet been observed. Given the limited number of eggs per female and the inherent challenges of sampling in the Southern Ocean, it is not surprising that the earliest life history stages of *A. nudiceps* are largely unknown.

In this study, we document and describe the larval stages of *A. nudiceps* caught in the Bellingshausen Sea off the coast of the western Antarctic Peninsula (WAP) based on morphological and genetic data. We also describe characters that differentiate *A. nudiceps* from the morphologically similar, sympatric bathydraconid *Prionodraco evansii* (Regan 1914) . Finally, we map the sampling locations of *A. nudiceps* larvae and discuss possible spawning areas.

2. Materials and Methods

Sample collection, measurements, and photography

Larval *A. nudiceps* and *P. evansii* were collected using a 2-m^2 frame Metro net (700-µm mesh) towed to ~120m depth. The net tows were conducted during austral summer (January – February) as part of the Palmer Antarctica Long-Term Ecological Research (Palmer LTER) Program. Scientists on Palmer LTER cruises collect multidisciplinary data in a fixed-sampling grid (see Smith *et al.*, 1995) in the Bellingshausen Sea along the WAP (Ducklow et al. 2007). Specimens were preserved in a formaldehyde (1995 – 2013) or 95% ethanol (2014 – present) solution and cataloged in the Nunnally Ichthyology Collection at the Virginia Institute of Marine Science (VIMS), William & Mary (Gloucester Point, Virginia, U.S.A.). We used Mitutoyo 500-752-20 digital calipers for all measurements and photographed larvae with a high-resolution AxioCam digital camera mounted on a Zeiss Discovery V20 stereomicroscope, and used Z-stacking to increase depth of field. Photoshop© was used to adjust color and contrast of images, clean the background (e.g., remove dust from the background; no alteration of the subject was made), and assemble the photographic figures.

DNA Extraction

We extracted DNA from single eyeballs of larvae following a modified magnetic bead-based protocol. Due to the extended preservation period for several specimens (up to 25 years) and the relatively small size of the eye in these specimens, incubations for several components of the protocol were extended to 24-hour periods to ensure successful DNA recovery. Samples were digested in a standard digestion buffer for 24 hours at 55 C° and vortexed. For each sample, 10ul of carboxylated magnetic beads (McLab, San Francisco, CA) were cleaned 3x with 100ul of 0.5M EDTA, rehydrated in 100ul of NACL PEG solution, and incubated for 24 hours at 32 C°, followed by three 70% ethanol washes. Finally, DNA was eluted from the magnetic beads in 0.1 TE buffer for 24 hours at 32 C° prior to amplification.

Amplification and sequencing

The full-length mitochondrially-encoded NADH dehydrogenase subunit 2 gene (ND2; *mt-nd2*) and a fragment of the mitochondrial cytochrome oxidase I (COI; *mt-co1*) gene were amplified in a portion of specimens that were suspected to be *A. nudiceps*. We selected these gene regions because they have been demonstrated to distinguish closely-related notothenioid fishes (Near and Cheng 2008) and because of the availability of vouchered reference sequences on GenBank. The *mt-co1*region was amplified with the COI-3 primer set (Ivanova et al. 2007) and the *mt-nd2* region using primers GLN and ASN (Kocher et al. 1995). The PCR products were purified using the QIAquick PCR Purification Kit (Qiagen, Hilden, Germany). The purified PCR products were Sanger sequenced in the forward and reverse direction with an ABI BigDye Terminator v3.1 Cycle Sequencing Kit (Applied Biosystems, USA). The resulting fragments were electrophoresed on an ABI 3500 capillary sequencer and bases were called using the integrated Data Collection Software. The resulting sequences for each sample and locus were edited and assembled into contigs using Sequencher 5.3.6 (Gene Codes Corp., Ann Arbor, MI). NCBI-BLASTN searches (Altschul et al. 1990) were conducted with the edited sequences to identify sequences with the highest similarity within the database using MegaBLAST. Sequences without specimen vouchers were excluded from the analysis.

Ethical Statement

All *A. nudiceps* and *P. evansii* specimens were preserved and catalogued in the VIMS Nunnally Ichthyology Collection prior to this analysis. Therefore, an ethical statement is not applicable.

3. Results

Based on morphological characters, we identified 14 bathydraconid specimens as putatively representing *A. nudiceps* due to their overall similarity to previous descriptions of larger individuals (Kellermann 1990). The relatively long guts and slender body shape of the specimens suggested they were larval bathydraconids. Specimens were also heavily pigmented all over, but we ruled out the morphologically similar *Prionodraco evansii* based on the lack of dorsolateral and ventrolateral spines (Kellermann 1990). The 14 specimens were collected between 1997 and 2020 (Table 1) by the Palmer LTER (Figure 1) and ranged from 10.8 mm total length (L_{T}) to 22.7 mm L_{T}, with a mean length of 15.4 mm $L_{\mathrm{T}} \pm 4.0$ SD (Table 2).

We sequenced DNA from two of the 14 specimens (VIMS 43571a, 10.8 mm L_{T} and VIMS 43240, 19.2 mm L_{T}), and obtained *mt-nd2* and *mt-co1* sequences, trimmed to a final length of 1048 and 693 respectively. The *mt-nd2* region for both specimens most closely aligned with two *mt-nd2* sequences for *A. nudiceps* in GenBank from the same analysis (HQ170108.1 and HQ170109.1) with greater than 99% identity and 97% query coverage (accessed on 3 July 2022), supporting our initial morphologically based identification. As these results provided sufficiently clear support to our initial morphological identification of *A. nudiceps*, we opted to restrict genetic analysis to two specimens to limit dissection of these rare specimens. To confirm the morphological identification of preflexion *P. evansii* larvae, we also obtained an *mt-nd2* sequence (trimmed to a final length of 1048) from a preflexion specimen (VIMS 42468) which most closely aligned with *P. evansii mt-nd2* sequences in GenBank (HQ170126.1 and HQ170127.1) with greater than 99% identity and 91% query coverage (accessed 28 September 2022).

The *mt-co1* region for both specimens also most closely aligned with a *mt-co1* sequence for *A. nudiceps* (OK493722.1) with 96.9% identity and 94% query coverage (accessed on 3 July 2022). We are performing a separate concurrent analysis to evaluate population connectivity of *A. nudiceps* for the relatively large gap in sequence identity between our *A. nudiceps* larvae and the closest sequences available in GenBank for the *mt-co1* region.

The two smallest preflexion larvae (VIMS 43571a, 10.8 mm L_T and VIMS 43716, 10.9 mm L_T), were collected in 2019 near the mouth of Marguerite Bay over bottom depths ranging from 750 – 773 m (Figure 1). Two other small, preflexion larvae were also collected near the mouth of Marguerite Bay in 2006 (VIMS 41358, 14.9 mm L_T) and 2019 (VIMS 43571b, 11.8 mm L_T). We found one additional preflexion larvae (VIMS 24545, 11.4 mm L_T) that was collected farther south, near Wilkins Sound, over a bottom depth of 215 m (Figure 1).

The preflexion specimens all have a similar pigmentation pattern. Their bodies are heavily and uniformly pigmented from their jaw to their caudal peduncle (Figure 2). Pigmentation extends onto the base of the pectoral fins, although it is less dense than on the body. There is also pigmentation along the base of the dorsal and anal fin folds (Figure 2). The pectoral fins are well-developed in preflexion larvae, with pectoral-fin rays (P) ranging from 18 to 22 (Table 2). Fin rays were also present on the caudal fins of these preflexion specimens, ranging from eight to 11 (Table 2). However, the dorsal (D) and anal (A) fin folds are less developed and lack fin rays. The pelvic fins are not clearly visible at the preflexion stage.

Pigmentation pattern changes little during ontogeny (Figure 2). The largest specimen we studied (VIMS 22788a, 22.7 mm L_T) was pigmented similarly to the smaller stages, with pigment evenly covering the body. In postflexion specimens, pigmentation extends slightly past the caudal peduncle and onto the caudal-fin rays (Figure 2). The largest specimen examined (VIMS 22788a) had 21 pectoral-fin rays, but its anal and dorsal fins remained undeveloped, with no fin rays clearly present (Kellermann 1990) (Table 2). Adult *A. nudiceps* are known to have 29 – 33 D, 25 – 28 A, 22 – 24 P, and 56 – 65 vertebrate (V) (Gon and Heemstra 1990). We were unable to obtain a myomere count from any individual due to the condition of the specimens. However, we combined the preanal myomeres (17) from VIMS 24545 and the postanal myomeres (37) from VIMS 20913 to obtain a combined estimate of 54 myomeres (including those associated with three occipital myomeres).

4. Discussion

Early life history of Akarotaxis nudiceps

To our knowledge, there are four reports of the early life stages of *Akarotaxis nudiceps* in the literature. Kellermann (1990) describes two transforming juveniles (37.0 and 39.1 mm L_S) that were caught during early March and mid-February in the northeastern Weddell Sea. Fin-ray and vertebrate counts for the 39.1 mm L_S specimen were reported as D 26+, A 25+, P 24, V 49.

The pigmentation for these transforming specimens was described as being uniformly heavy on the body and lighter on the head. Voskoboinikova (2001) also describes one juvenile (43.1 mm L_S) caught in the Weddell Sea during late February. Fin-ray counts for this specimen are D 29, A 25, P 22 and the heavy pigmentation had begun transitioning to a grayish-brown coloration. Flores *et al.* (2008) found one larva from the Lazarev Sea during April 2004, but the description, length, and location were not reported. Finally, Vacchi *et al.* (1999) collected a small, 14 mm L_S specimen that they identified as *A. nudiceps* in the coastal Ross Sea near Zucchelli Station (74^o 48'75 S, 164^o 36' 90"E); however, this specimen was not described or illustrated. This larva was caught with a 5-m^2 Hamburg Plankton Net (mesh size of 500 mm) towed to 30 m over a bottom depth of 320 m (Vacchi et al. 1999).

Each of the 14 larval *A. nudiceps* identified in this study were collected at locations that are relatively nearshore, with most (n=10) occurring just outside Marguerite Bay (Figure 1). The Palmer LTER sampling grid extends approximately 240 kilometers offshore in this area (see Smith *et al.*, 1995), but *A. nudiceps* larvae have not been found in any other net tows during the more than 30-year time series. This suggests that adult *A. nudiceps* are likely spawning in neritic areas along the WAP. This is supported by the coastal association of the only other small *A. nudiceps* larva reported by Vacchi *et al.* (1999). Additionally, histological analysis and nesting behavior of *Parachaenichthys charcoti* in the South Shetland Islands region also indicates spawning occurs in nearshore habitat (Novillo et al. 2018).

In the relatively ice-free austral summer (i.e., December – February), one of the dominant currents of this region, the Antarctic Peninsula Coastal Current (APCC), is flowing in a southwest direction along the coast of the WAP (Moffat et al. 2008). The circulation pattern is less characterized within Marguerite Bay, but the APCC likely creates a cyclonic surface flow within the bay (Moffat and Meredith 2018). Based on the congregation of larval *A. nudiceps* across years and APCC flow, we hypothesize there is a recurring nesting area for *A. nudiceps* somewhere around the perimeter of Adelaide Island (Figure 1). With our limited data, it is not possible to determine whether the larvae collected farther north (VIMS 22690) and south (VIMS 33107, 24545, and 24518) originated from the Marguerite area or if there are multiple nesting sites along the coast. Yolk-sac lengths of *P. evansii* (12.0 to 14.2 mm SL), *Racovitzia glacialis* (12.0 to 13.2 mm SL), and *Gymnodraco acuticeps* (not reported), captured in similar areas along the WAP in November suggests hatching occurs in late spring (October – November)(Kellermann 1990). The mid-January sampling date for the seven larvae smaller than 14 mm LT (Table 1) in this study suggests hatching may occur in December. We also did not observe yolk remains on any larvae, indicating *A. nudiceps* may have a smaller length at hatch than other reported bathydraconids, or absorb their yolk-sac more quickly.

Differences between Akarotaxis nudiceps *and* Prionodraco evansii

Several specimens of *A. nudiceps* we identified in this study were previously misidentified as *P. evansii*. Although the pigmentation patterns of the two species are similar at early larval stages (Figure 3), there are a few key differences that separate the two species. *Prionodraco evansii* has two parallel rows of ventrolateral spiny scales that run from their hindgut to the caudal peduncle and two parallel rows of dorsolateral spines running from the nape to peduncle (Kellermann 1990). However, at early preflexion stages, or in the wrong light, these spiny scales are easily overlooked. The gut and abdomen are less pigmented in the larval stages of *P. evansii* when compared to the condition in *A. nudiceps* (Figure 3), although this difference is difficult to quantify. A second distinguishing characteristic between the two species involves their cranial pigmentation. Each of the 14 larval *A. nudiceps* we examined had dense, uniformly spaced pigmentation on the occipital region of the head (Figure 4a). In contrast, *P. evansii* is known to have a few large pigment spots on either side of the posterior portion of the head (Kellermann 1990) (Figure 4b). We have not yet conducted a thorough developmental analysis of *P. evansii*, but we estimate that most stages have 2 – 6 large pigment spots.

Conclusion

Through study of an existing collection of preserved larval fishes, we identified and described the early life history stages of the least fecund notothenioid, *Akarotaxis nudiceps,* based on morphological and genetic criteria. We provide the first documentation of preflexion and small post-flexion larvae for this species. Although relatively few specimens were collected in the more than 30-year time series that we examined, we conclude that spawning occurs near coastal islands and bays along the WAP. Future research is necessary to establish baseline information about the biology and life history of this important member of the benthic ecosystem. Given the paucity of understanding of the early life history of most Antarctic fishes, we suggest that archived larval collections such as this hold an under-sampled wealth of information on the biology, taxonomy, and distribution of this unique ichthyofauna.

Acknowledgements

We thank Sarah K. Huber for curatorial assistance, Mario La Mesa for discussion, and Miguel Montalvo for photography assistance. This work was funded by the National Science Foundation

Antarctic Organisms and Ecosystems Program (PLR-1440435 for specimen and environmental data collection) and Division of Biological Infrastructure (DBI-1349327 for specimen preservation and analysis), the Explorers Club, and the VIMS John Olney Fellowship.

References

Altschul SF, Gish W, Miller W, Myers EW, Lipman DJ. 1990. Basic local alignment search tool. Journal of molecular biology. 215(3):403–410.

Bargelloni L, Marcato S, Zane L, Patarnello T. 2000. Mitochondrial Phylogeny of Notothenioids: A Molecular Approach to Antarctic Fish Evolution and Biogeography. Systematic Biology. 49(1):114–129. https://doi.org/10.1080/10635150050207429

Barrera-Oro ER, Lagger C. 2010. Egg-guarding behaviour in the Antarctic bathydraconid dragonfish Parachaenichthys charcoti. Polar Biol. 33(11):1585–1587. https://doi.org/10.1007/s00300-010-0847-3

Bista I, Wood JM, Desvignes T, McCarthy SA, Matschiner M, Ning Z, Tracey A, Torrance J, Sims Y, Chow W. 2022. Genomics of cold adaptations in the Antarctic notothenioid fish radiation. bioRxiv.

de Broyer C, Koubbi P. 2014. Biogeographic atlas of the Southern Ocean.

Daane JM, Dornburg A, Smits P, MacGuigan DJ, Brent Hawkins M, Near TJ, Detrich III W, Harris MP. 2019. Historical contingency shapes adaptive radiation in Antarctic fishes. Nature ecology & evolution. 3(7):1102–1109.

Derome N, Chen W-J, Dettaï A, Bonillo C, Lecointre G. 2002. Phylogeny of Antarctic dragonfishes (Bathydraconidae, Notothenioidei, Teleostei) and related families based on their anatomy and two mitochondrial genes. Molecular Phylogenetics and Evolution. 24(1):139–152. https://doi.org/10.1016/S1055-7903(02)00223-3

Ducklow HW, Baker K, Martinson DG, Quetin LB, Ross RM, Smith RC, Stammerjohn SE, Vernet M, Fraser W. 2007. Marine pelagic ecosystems: the West Antarctic Peninsula.

Philosophical Transactions of the Royal Society B: Biological Sciences. 362(1477):67–94. https://doi.org/10.1098/rstb.2006.1955

Eastman JT. 2017. Bathymetric distributions of notothenioid fishes. Polar Biol. 40(10):2077–2095. https://doi.org/10.1007/s00300-017-2128-x

Eastman JT, Eakin RR. 2021. Checklist of the species of notothenioid fishes. Antarctic Science. 33(3):273–280. https://doi.org/10.1017/S0954102020000632

Ekau W. 1990. Demersal fish fauna of the Weddell Sea, Antarctica. Antartic science. 2(2):129–137. https://doi.org/10.1017/S0954102090000165

Evans CW, Cziko P, Cheng C-HC, Devries AL. 2005. Spawning behaviour and early development in the naked dragonfish Gymnodraco acuticeps. Antartic science. 17(3):319–327. https://doi.org/10.1017/S0954102005002749

Flores H, Van de Putte A, Siegel V, Pakhomov E, van Franeker J, Meesters H, Volckaert F. 2008. Distribution, abundance and ecological relevance of pelagic fishes in the Lazarev Sea, Southern Ocean. Mar Ecol Prog Ser. 367:271–282. https://doi.org/10.3354/meps07530

Gon O, Heemstra PC. 1990. Fishes of the Southern Ocean. JLB Smith Institute of Ichthyology Grahamstown.

Ivanova NV, Zemlak TS, Hanner RH, Hebert PD. 2007. Universal primer cocktails for fish DNA barcoding. Molecular Ecology Notes. 7(4):544–548.

Kellermann AK. 1990. Identification key and catalogue of larval Antarctic fishes. Ber Polarforsch. (67):1–138.

Kocher TD, Conroy JA, McKaye KR, Stauffer JR, Lockwood SF. 1995. Evolution of NADH Dehydrogenase Subunit 2 in East African Cichlid Fish. Molecular Phylogenetics and Evolution. 4(4):420–432. https://doi.org/10.1006/mpev.1995.1039

Kock K-H, Kellermann A. 1991. Reproduction in Antarctic notothenioid fish. Antarctic Science. 3:125–150. https://doi.org/10.1017/S0954102091000172

Kuhn KL, Near TJ, Detrich HW, Eastman JT. 2011. Biology of the Antarctic dragonfish Vomeridens infuscipinnis (Notothenioidei: Bathydraconidae). Antartic science. 23(1):18–26. https://doi.org/10.1017/S095410201000060X

La Mesa M, Calì F, Donato F, Riginella E, Mazzoldi C. 2018. Aspects of the biology of the Antarctic dragonfish Gerlachea australis (Notothenioidei: Bathydraconidae) in the Weddell Sea, Antarctica. Polar Biology. 41(4):793–803.

La Mesa M, Caputo V, Eastman JT. 2007. Gametogenesis in the dragonfishes Akarotaxis nudiceps and Bathydraco marri (Pisces, Notothenioidei: Bathydraconidae) from the Ross Sea. Antarctic Science. 19(1):64–70. https://doi.org/10.1017/S0954102007000090

La Mesa M, Catalano B, Kock K-H, Jones CD. 2012. Age and growth of the Antarctic dragonfish Parachaenichthys charcoti (Pisces, Bathydraconidae) from the southern Scotia Arc. Polar Biol. 35(10):1545–1553. https://doi.org/10.1007/s00300-012-1194-3

La Mesa M, Llompart F, Riginella E, Eastman JT. 2021. Parental care and reproductive strategies in notothenioid fishes. Fish and Fisheries. 22(2):356–376.

La Mesa M, Piepenburg D, Pineda-Metz SEA, Riginella E, Eastman JT. 2019. Spatial distribution and habitat preferences of demersal fish assemblages in the southeastern Weddell Sea (Southern Ocean). Polar Biol. 42(5):1025–1040. https://doi.org/10.1007/s00300-019-02495-3

La Mesa M, Riginella E, Donato F, Mazzoldi C. 2018. Life history traits of rare Antarctic dragonfishes from the Weddell Sea. Antarctic Science. 30(5):289–297.

Loeb VJ, Kellermann AK, Koubbi P, North AW, White MG. 1993. Antarctic larval fish assemblages: a review. Bulletin of Marine Science. 53(2):416–449.

Moffat C, Beardsley RC, Owens B, van Lipzig N. 2008. A first description of the Antarctic Peninsula Coastal Current. Deep Sea Research Part II: Topical Studies in Oceanography. 55(3):277–293. https://doi.org/10.1016/j.dsr2.2007.10.003

Moffat C, Meredith M. 2018. Shelf–ocean exchange and hydrography west of the Antarctic Peninsula: a review. Phil Trans R Soc A. 376(2122):20170164. https://doi.org/10.1098/rsta.2017.0164

Near TJ, Cheng C-HC. 2008. Phylogenetics of notothenioid fishes (Teleostei: Acanthomorpha): Inferences from mitochondrial and nuclear gene sequences. Molecular Phylogenetics and Evolution. 47(2):832–840. https://doi.org/10.1016/j.ympev.2007.11.027

Near TJ, Dornburg A, Kuhn KL, Eastman JT, Pennington JN, Patarnello T, Zane L, Fernández DA, Jones CD. 2012. Ancient climate change, antifreeze, and the evolutionary diversification of Antarctic fishes. Proc Natl Acad Sci USA. 109(9):3434–3439. https://doi.org/10.1073/pnas.1115169109

Near TJ, MacGuigan DJ, Parker E, Struthers CD, Jones CD, Dornburg A. 2018. Phylogenetic analysis of Antarctic notothenioids illuminates the utility of RADseq for resolving Cenozoic adaptive radiations. Molecular Phylogenetics and Evolution. 129:268–279. https://doi.org/10.1016/j.ympev.2018.09.001

Near TJ, Pesavento JJ, Cheng C-HC. 2004. Phylogenetic investigations of Antarctic notothenioid fishes (Perciformes: Notothenioidei) using complete gene sequences of the mitochondrial encoded 16S rRNA. Molecular Phylogenetics and Evolution. 32(3):881–891. https://doi.org/10.1016/j.ympev.2004.01.002

Novillo M, Moreira E, Macchi G, Barrera-Oro E. 2018. Reproductive biology in the Antarctic bathydraconid dragonfish Parachaenichthys charcoti. Polar Biol. 41(11):2239–2248. https://doi.org/10.1007/s00300-018-2359-5

Regan CT. 1914. II.—Diagnoses of new marine fishes collected by the British Antarctic ('Terra Nova') Expedition. Annals and magazine of Natural History. 13(73):11–17.

Smith RC, Baker KS, Fraser WR, Hofmann EE, Karl DM, Klinck JM, Quetin LB, Prézelin BB, Ross RM, Trivelpiece WZ. 1995. The Palmer LTER: A long-term ecological research program at Palmer Station, Antarctica. Oceanography. 8(3):77–86.

Vacchi M, La Mesa M, Greco S. 1999. Summer distribution and abundance of larval and juvenile fishes in the western Ross Sea. Antarctic Science. 11(1):54–60.

Van der Molen S, Matallanas J. 2003. Oocyte development and maturity classification of Gerlachea australis from the Weddell Sea, Antarctica. Polar Biol. 26(10):653–658. https://doi.org/10.1007/s00300-003-0542-8

Voskoboinikova OS. 2001. Juveniles of five species of Antarctic notothenioid fishes from the Weddell Sea. Russian Journal of Marine Biology. 27(6):397–400.

Waite ER. 1916. Fishes. Australasian Antarctic Expedition Scientific Reports. 3:1–92.

Table 1. The sampling dates, locations and map label key associated with the 14 larval specimens of *Akarotaxis nudiceps.*

Label #	VIMS #	Count	Sampling date	Latitude	Longitude	Bottom depth
1	20913	1	2/3/1997	-67.770	-69.921	711
2	22788a, b	2	2/4/1997	-68.151	-68.978	239
3	22690	1	2/7/1997	-66.550	-67.174	398
4	41368	1	1/26/2006	-67.649	-70.277	599
5	33107	1	1/29/2011	-70.076	-76.176	336
6	23177	1	1/17/2013	-68.038	-69.595	964
7	24545	1	1/24/2015	-68.958	-73.584	215
8	24518	1	1/26/2015	-69.387	-75.795	308
9	23274	1	1/21/2016	-67.465	-70.585	760
10	43571a, b	2	1/14/2019	-67.522	-70.591	773
11	43716	1	1/17/2019	-67.781	-69.958	750
12	43240	1	1/18/2020	-67.766	-68.241	387

Table 2. Morphometric and meristic data of the 14 *Akarotaxis nudiceps* larvae examined herein, including total length (L_{T}), standard length (L_{S}), notochord length (L_{N}), prepectoral length (L_{PP}), predorsal length (L_{PD}), preanal length (L_{PA}), head length (L_{H}), and preorbital length (L_{PO}). The stage, caudal (C) and pectoral (P) fin rays are also listed.

VIMS #	Stage	L_T	L_S	L_N	L_{PP} (%L_T)	L_{PD} (%L_T)	L_{PA} (%L_T)	L_H (%L_T)	L_{PO} (%L_T)	C	P
43571a	Preflexion	10.8	-	10.1	2.26 (21.0)	0.95 (8.8)	5.7 (52.9)	2.18 (20.2)	0.45 (4.2)	Broken	19/19
43716	Preflexion	10.9	-	10.7	Broken	Broken	Broken	Broken	Broken	Broken	Broken
24545	Preflexion	11.4	-	11.0	2.27 (19.9)	1.66 (14.5)	5.36 (46.9)	2.15 (18.8)	0.53 (4.6)	Broken	Broken
24518	Postflexion	11.8	11.3	-	2.01 (17.1)	Broken	Broken	1.63 (13.8)	0.27 (2.3)	Broken	9/Broken
43571b	Preflexion	11.8	-	11.8	2.44 (20.7)	1.01 (8.6)	5.69 (48.2)	2.28 (19.3)	0.6 (5.1)	8	19/18
23274	Postflexion	13.2	12.6	-	2.5 (19.0)	1.26 (9.6)	Broken	2.22 (16.9)	0.42 (3.2)	5	15/15
23177	Postflexion	13.4	12.1	-	2.99 (22.3)	2.13 (15.9)	6.62 (49.3)	2.92 (21.8)	0.69 (5.1)	13	20/21
41368	Preflexion	14.9	-	14.4	2.95 (19.9)	1.85 (12.4)	7.42 (49.9)	2.7 (18.2)	0.61 (4.1)	11	Broken/22
20913	Postflexion	17.3	16.7	-	3.49 (20.1)	2.65 (15.3)	8.53 (49.2)	3.14 (18.1)	0.77 (4.4)	11	19/19
33107	Postflexion	18.5	17.2	-	4.79 (25.8)	3.34 (18.0)	8.4 (45.3)	4.39 (23.7)	1.21 (6.5)	15	21/21
43240	Postflexion	19.2	17.2	-	4.15 (21.6)	2.84 (14.8)	9.04 (47.1)	3.94 (20.5)	1.13 (5.9)	13	19/18
22788b	Postflexion	19.5	17.6	-	3.77 (19.3)	2.14 (11.0)	8.22 (42.1)	3.24 (16.6)	1.06 (5.4)	12	21/20
22690	Postflexion	19.7	18.6	-	4.85 (24.6)	2.76 (14.0)	9.96 (50.6)	4.54 (23.0)	1.09 (5.5)	13	21/21
22788a	Postflexion	22.7	20.7	-	4.48 (19.7)	2.85 (12.5)	9.56 (42.1)	4.33 (19.1)	1.03 (4.5)	15	21/21

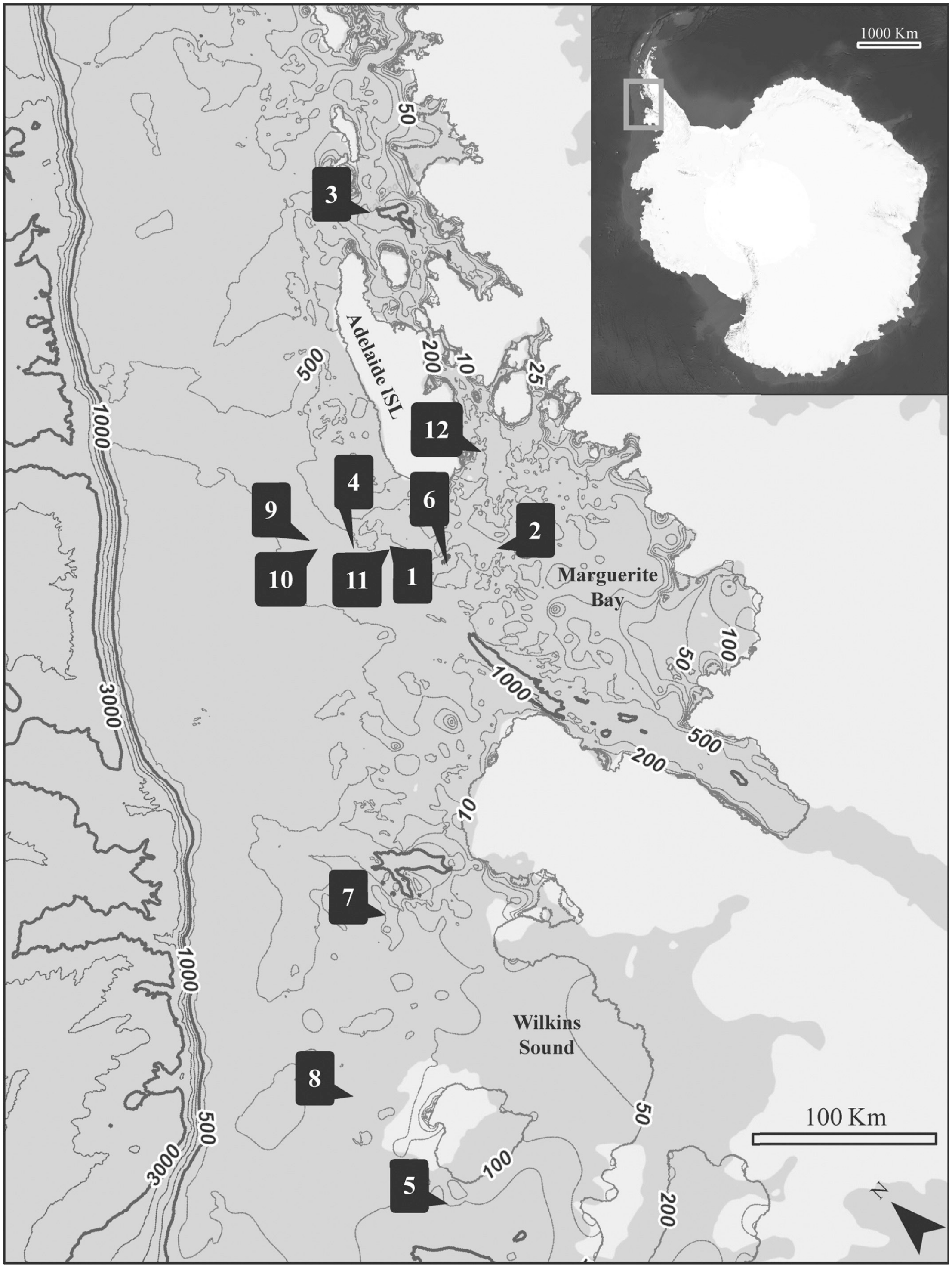

Figure 1. Map of a portion of the western Antarctic Peninsula showing the capture sites of the 14 larval specimens of *Akarotaxis nudiceps* examined herein with depth contours in meters. The inset shows Antarctica with the grey box indicating the map region. The specimens were collected by the Palmer Antarctica Long-Term Ecological Research (Palmer LTER) program during austral summer (January–February). The corresponding VIMS catalogue numbers to each of the shortened labels are given in Table 1.

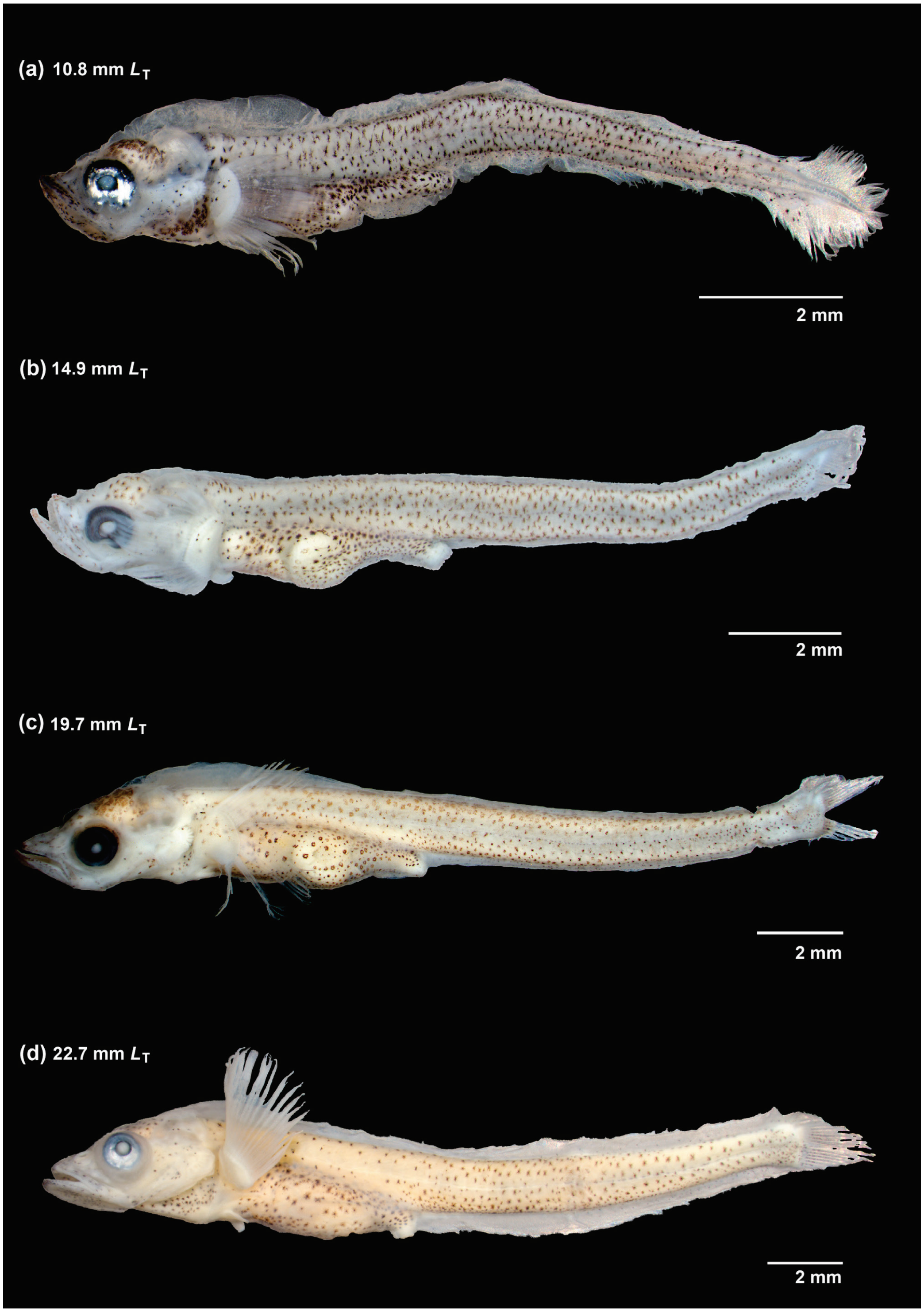

Figure 2. Development of *Akarotaxis nudiceps* in left lateral view. (a) VIMS 43571, 10.8 mm total length (L_T), preflexion. (b) VIMS41368, 14.9 mm L_T, postflexion. (c) VIMS 22690, 19.7 mm L_T, postflexion. (d) VIMS 22788a, 22.7 mm L_T, postflexion.

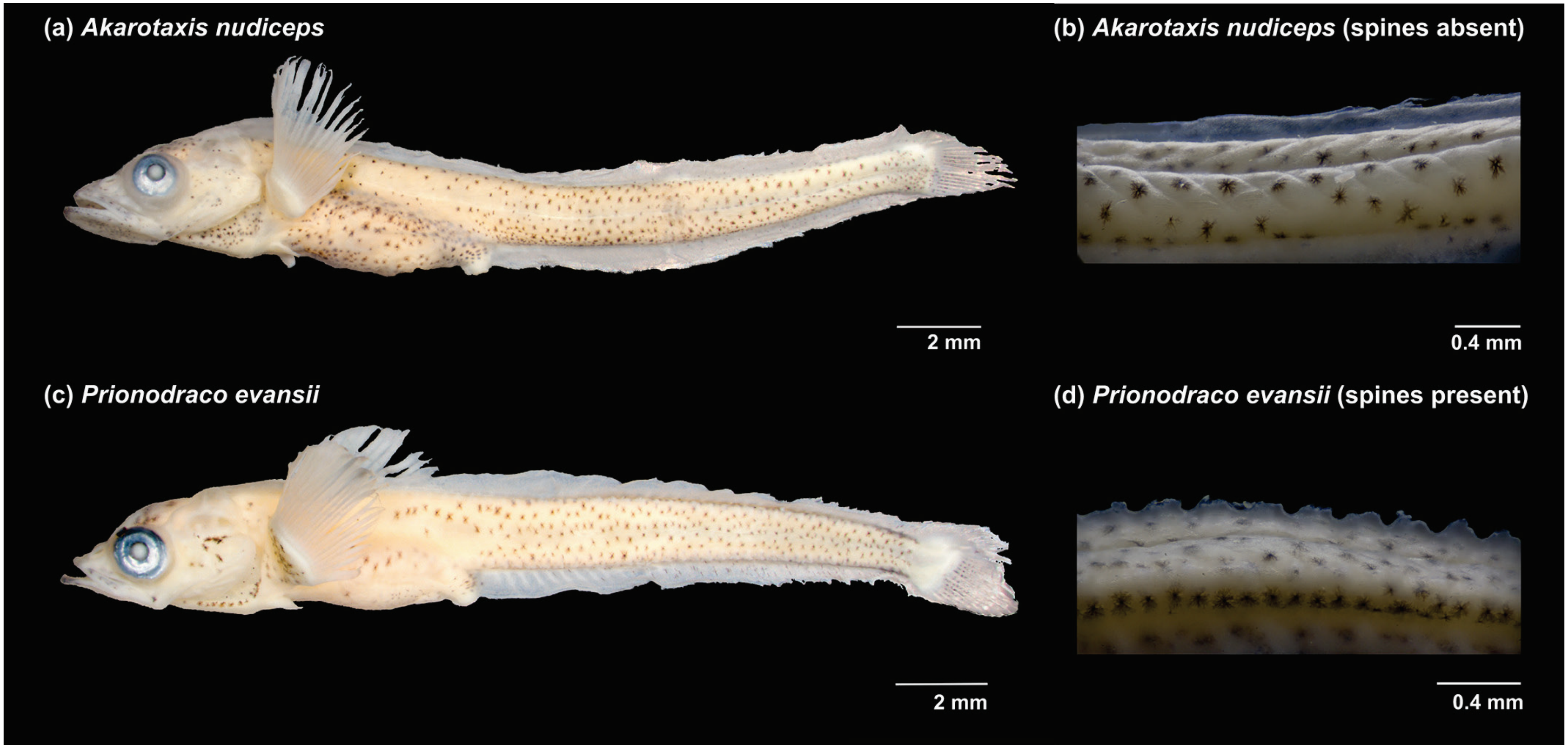

Figure 3. Comparison of (a) left lateral view and (b) dorsal view of lower tail of *Akarotaxis nudiceps* [VIMS 22788a, 22.7 mm total length (L_T)]to (c) left lateral view and (d) dorsal view of lower tail of *Prionodraco evansii* (VIMS 43603, 19.4mm L_T). Anterior faces left in both (b) and (d).

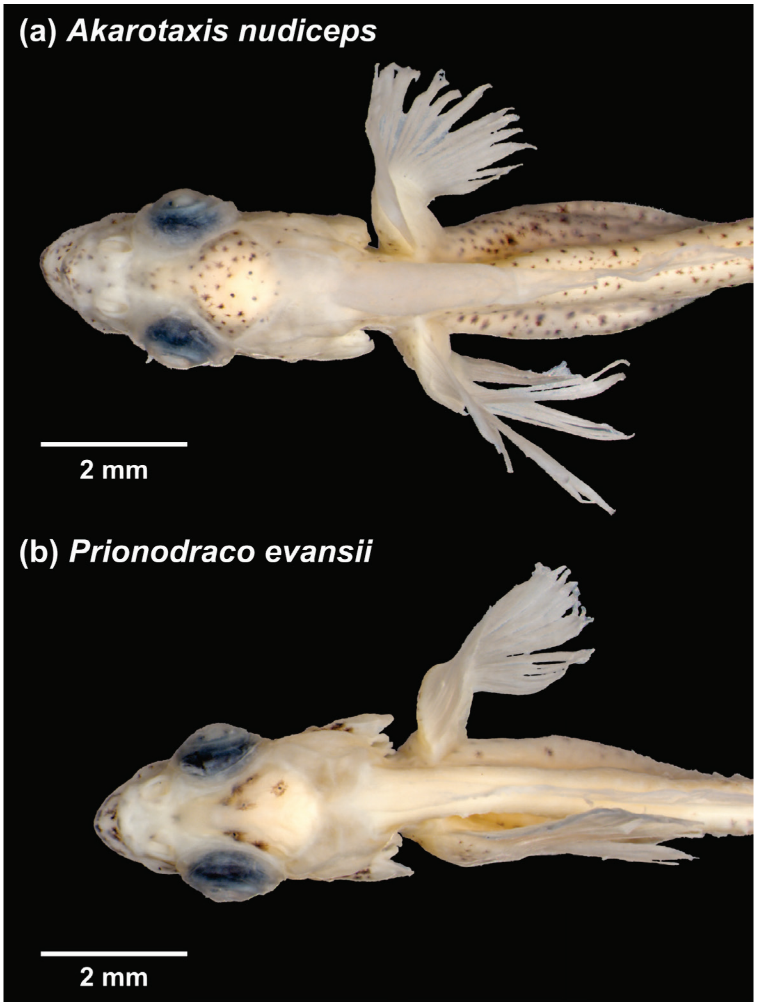

Figure 4. Comparison of (a) *Akarotaxis nudiceps* [VIMS 22788a, 22.7 mm total length (L_T)] and (b) *Prionodraco evansii* (VIMS 43603, 19.4 mm L_T). Dorsal view.

CHAPTER 4

A new species of Antarctic dragonfish (Notothenioidei: Bathydraconidae) in the genus *Akarotaxis*, from the western Antarctic Peninsula

This chapter is in preparation for submission to *Zootaxa* as: Corso AD, Desvignes T, McDowell JR, Christina Cheng CH, Biesack EE, Steinberg DK, Hilton EJ. A new species of Antarctic dragonfish (Notothenioidei: Bathydraconidae) in the genus *Akarotaxis*, from the western Antarctic Peninsula

Abstract

Bathydraconidae (Notothenioidei) are a group of rare benthic fishes endemic to the Southern Ocean. Because of their recent evolutionary radiation and limited sampling efforts due to their occurrence in remote regions, their diversity is likely underestimated. *Akarotaxis nudiceps*, the sole currently recognized member of its genus, is an especially poorly known bathydraconid. Although *Akarotaxis* has a circumpolar distribution on the Antarctic continental shelf, its deep habitat and rarity limit knowledge of its life history and biology. Using a combination of morphological and genetic analyses, we identified an undescribed species of this genus, herein named *Akarotaxis* n. sp. (Banded Dragonfish). The separation of this species was initially identified from archived larval specimens, highlighting the importance of early life stage taxonomy and natural history collections. Furthermore, all currently known adult and larval *Akarotaxis* n. sp. specimens have been collected from a restricted ~400 km coastal section of the western Antarctic Peninsula. This region is targeted by the epipelagic Antarctic krill fishery, which could potentially capture larval fishes as bycatch. Due to the extremely low fecundity of *Akarotaxis* n. sp. and near-surface occurrence of larvae, we suggest the growing Antarctic krill fishery could endanger the novel species.

1. Introduction

Notothenioidei are a suborder of Perciformes comprising eight families and about 140 species found throughout the Southern Ocean and nearby waters (Eastman and Eakin 2021). They form a unique radiation of fishes, representing one of the few recognized examples of a marine species flock, resulting from their recent endemic speciation and the oceanographic barriers of the Southern Ocean (Eastman and McCune 2000). Some notothenioid species, such as *Notothenia coriiceps* Richardson 1844, *Harpagifer antarcticus* Nybelin 1947*,* and *Chaenocephalus aceratus* (Lönnberg 1906), have been relatively well documented for their life history (Postlethwait et al. 2016; Novillo et al. 2019), sensitivity to stressors (O'Brien et al. 2018; Saravia et al. 2021), and genetics (Bilyk et al. 2019; Beck et al. 2022) because of their abundance, coastal habitats facilitating their capture, and research interest in their unique physiological adaptations. However, the diversity and biology of rare and deep-dwelling notothenioid taxa remain poorly understood. The presence of cryptic diversity among notothenioids has recently been reported (Dornburg et al. 2016; Ceballos et al. 2019). Sub-Antarctic islands, such as South Georgia, likely contain higher proportions of cryptic species compared to Antarctica because they may have served as habitat refugia and subsequently as source-populations during periods of glacial maxima (Dornburg et al. 2016; Dornburg et al. 2017). However, it also possible that the deepest regions of the continental shelf functioned as refugia, which could harbor unknown diversity in these hard-to-sample areas (Riddle et al. 2007; Dornburg et al. 2016).

Bathydraconidae, or Antarctic dragonfishes, are a notothenioid family first defined by Regan (1916) and now comprising 16 valid species (Eastman and Eakin 2021). Many of these species occur at depths greater than 500m, are small, and are rarely collected (Gon and Heemstra 1990; Eastman 2017). Thus, little is known about their biology, morphology, or population genetics. Recent studies focused on testing the monophyly of Bathydraconidae with respect to the Channichthyidae (Derome et al. 2002; Near et al. 2018), describing their biology (Barrera-Oro and Lagger 2010; Kuhn et al. 2011; La Mesa et al. 2018; La Mesa et al. 2018; Novillo et al. 2018), and on early life stages and biogeography (Mesa et al. 2017; Desvignes et al. 2020; Corso et al. 2023).

The bathydraconid genus *Akarotaxis* (DeWitt and Hureau 1980) currently contains a single recognized species, *A. nudiceps* (Waite 1916) known from the Bellingshausen, Weddell, Lazarev, Cooperation, Davis, D'Urville, Ross, and Amundsen seas (Ekau 1990; Gon and Heemstra 1990; Duhamel et al. 2014; La Mesa et al. 2019; Cao et al. 2022), suggesting a circumpolar distribution on the Antarctic continental shelf (Fig 1). Although most adult specimens were collected over bottom depths ranging from 370 to 600 m, specimens of *A. nudiceps* have been collected as deep as 1191 m (Eastman 2017). Due to the extremely low absolute fecundity of *A. nudiceps* (<300 oocytes), La Mesa *et al.* (2007) suggested that nest guarding is likely. The early life history stages of *A. nudiceps* are also poorly known, likely due in part to their low fecundity, though Corso *et al.* (2022) recently described the pelagic larval stages of *A. nudiceps* based on specimens derived from a long-term monitoring program along the western Antarctic Peninsula (WAP) coast (Fig 1).

As part of the larval description of *Akarotaxis nudiceps*, Corso *et al.* (2022a) sequenced two mitochondrial markers (*mt-nd2* and *mt-co1*) from two larval specimens of *A. nudiceps* collected in the Bellingshausen Sea (Fig 1). Several differences in conserved-nucleotides between these specimens, compared to sequences from specimens collected in other areas of the Southern Ocean, raised the possibility that the larvae represented either distinct populations or a separate species. In this study, we further explored these differences by combining morphological and genetic analyses of additional specimens, ultimately demonstrating the presence of a previously undescribed species of dragonfish in the genus *Akarotaxis*.

2. Materials and Methods

Morphological analysis.

Specimens for morphological analysis are from the collections of the Nunnally Ichthyology Collection at the Virginia Institute of Marine Science, William & Mary, Gloucester Point, Virginia, USA (VIMS), the Collection d'Ichthyologie at the Muséum national d'Histoire naturelle, Paris, France (MNHN), Oregon State University Ichthyology Collection, Corvallis, Oregon, USA (OS), and the Peabody Museum of Natural History at Yale University, New Haven, Connecticut, USA (YPM ICH); digital images and x-rays of two paratype specimens, AMS IA.484 and AMS IA.485, of *A. nudiceps* were obtained from Australian Museum, Sydney, N. S. W., Australia (AMS). Collection abbreviations follow Sabaj (2020). Information about the specimens used in the morphological analyses is provided in Table 1.

We used Mitutoyo 500-752-20 digital calipers for all measurements, which were recorded to the nearest 0.01 mm. We followed the methods of DeWitt & Hureau (1980), in which measurements are defined as follows: standard length (SL; from the tip of the upper jaw to the posterior end of the hypural bone), head length (HL; from the tip of the upper jaw to the posterior tip of the operculum), head width (HW; widest point of the head), head depth (HD; distance from dorsal to ventral sides of head at mid-orbit), orbital diameter (O; greatest distance between the eye socket rims), snout length (SnL; from the tip of the upper jaw to the most anterior portion of the orbit), interorbital space (IO; between the edges of the eye socket rim at mid-orbit on the dorsal portion of the head), jaw length (UJL; from tip of upper jaw to posterior end of maxilla), caudal peduncle length (CPL; posterior insertion of dorsal fin to the posterior end of the hypural bones), caudal peduncle depth (CPD; from the dorsal to ventral sides of caudal peduncle at the widest point), body depth [BD(AO); from the dorsal to ventral sides of the body at the anterior origin of the anal fin], predorsal-fin distance (Sn-D; from the tip of the upper jaw to the anterior origin of the dorsal fin), preanal-fin distance (Sn-AO; from the tip of the upper jaw to the anterior origin of the anal fin), distance between anal-fin origin and caudal-fin base (AO-C; anterior origin of anal fin to the posterior end of the hypural bones), distance between pelvic fin base and anal-fin origin (AO-V; anterior origin of anal fin to the anterior base of the pelvic fin), pectoral-fin length (PL; base to tip of fin rays with preference for the left side if available), pelvic-fin length (VL; base to tip of fin rays; on the left side if available), caudal-fin length (CL; distance from posterior end of the hypural bones to the tip of the fin rays). Mean (± standard deviation) for each measurement are reported in Table 2.

In addition to measurements, we also collected meristic data following DeWitt & Hureau (1980), including: anterior gill rakers (Ant GR; leading edge of first arch), posterior gill rakers (Post GR; trailing edge of first arch), dorsal-fin rays (D), anal-fin rays (A), caudal-fin rays (C), pectoral-fin rays (P), scales along the lateral line (LSc), scales along the upper lateral line (ULL; including tubular, t, and perforate, p), scales along the middle lateral line (MLL), branchiostegal rays (Br), pores in preoperculo-mandibular canal (PMP), pores in the infraorbital canal (IOP), supraorbital pores (SOP), temporal pores (TP), and pores in supratemporal canal (STP). Ranges for counts are reported in Table 2.

Mapping of catch sites

Maps were created in ArcGIS Pro (Version 3.1.1, Environmental Systems Research Institute) with bathymetry data from the International Bathymetric Chart of the Southern Ocean Version 2 (Dorschel et al. 2022). The Commission for the Conservation of Antarctic Marine Living Resources (CCAMLR) provided data to map Subarea 48.1.

Fecundity data.

One gravid female (Label #14, SL = 153 mm, Total weight = 29.93 g) was dissected to estimate fecundity and reproductive investment. This specimen was captured on 08-20-2017 in Hugo-Anvers Trough and was originally identified as *A. nudiceps*. Fresh ovaries weighing 5.1 g were fixed intact in Bouin's fixative. After fixation, the ovaries weighed 3.536 g. A portion of one ovary (0.384 g) was separated, rinsed in 70% ethanol, and oocytes of all stages were dissociated and imaged on a Leica M165 FC stereomicroscope equipped with a Leica DFC425 C digital camera. Absolute fecundity was estimated by scaling the number of developing oocytes counted in the studied fragment to the entire gonad weight. Egg diameter was measured using ImageJ and egg size distribution was studied using R.

Mitochondrial DNA amplification and sequencing.

We sequenced three mitochondrial genes – full length *NADH dehydrogenase 2* (*mt-nd2*), and partial length *cytochrome c oxidase I* (*mt-co1*) and *cytochrome b* (*mt-cyb*) from a total of 23 *Akarotaxis* specimens captured from WAP coastal sites. Specimen and catch locations are detailed in Table 3. DNA from six archival specimens from the YPM and VIMS collections were isolated with a Tris-buffer based digest, followed by magnetic bead purification (Corso et al 2022a). DNA from 17 individuals from the University of Illinois and University of Oregon collections captured from Lapeyrere Bay and Anvers-Hugo Trough were isolated using Qiagen DNAeasy Blood and Tissue Kit (Hilden, Germany). The *mt-co1* region was amplified with the CO1-3 primer set (Ivanova et al. 2007) and Noto-co1 (Desvignes et al. 2019), the *mt-nd2* gene using primers GLN and ASN (Kocher et al. 1995), and the *mt-cyb* region using primers NotCytBf, L14724t, and H15915t (Matschiner et al. 2011). PCR amplicons were purified, Sanger sequenced in the forward and reverse direction using BigDye Terminator v.3.1 Cycle Sequencing chemistry (Applied Biosciences, USA), and electrophoresed on an ABI 3500 or 3730xl capillary sequencer. The resulting sequences for each sample and locus were edited and assembled into contigs using Sequencher 5.3.6 (Gene Codes Corp., Ann Arbor, MI).

Phylogenetic analysis.

In addition to the newly generated sequences from the WAP, additional *Akarotaxis* mitochondrial sequences were sourced from GenBank (Table 3). To place the *Akarotaxis* specimens in a phylogenetic context spanning all Antarctic dragonfish species, a representative sequence of each species was also included when available (Supp. Table 1). A representative sequence from *N. coriiceps* served as an outgroup to root the trees. Combined sequences were aligned using MAFFT version 7 webserver (Katoh et al. 2019) and trimmed. Sequence alignments were analyzed in a Bayesian Inference framework using MrBayes v.3.2.7a (Huelsenbeck and Ronquist 2001) on the NGPhylogeny webserver (Lemoine et al. 2019) and using the best substitution model previously identified by ModelTest-NG (Darriba et al. 2020) based on the Bayesian information criterion (BIC) (HKY+I+G4 for *mt-co1*, TIM3+G4 for *mt-nd2*, and TIM3+I+G4 for *mt-cyb*). Posterior probabilities were estimated using a Metropolis-coupled Markov chain Monte Carlo (MCMCMC) algorithm running four chains of 50 million generations each with trees sampled every 5000 generations. The initial 10% of iterations was discarded as "burn-in". Convergence was assessed by checking that all parameters had Estimated Sample Size (ESS) > 200 in the run output. Sequence alignments were also analyzed in a Maximum-Likelihood (ML) framework using ModelTest-NG (Darriba et al. 2020) implemented in raxmlGUI 2.0 (Edler et al. 2021) to determine the best fitting substitution model based on the corrected Akaike information criterion (AICc) (TIM3+I+G4 for all three mitochondrial markers). ML trees were constructed using the RAxML-NG web-server (Kozlov et al. 2019) using 50 parsimony and 50 random starting trees and a bootstrapping cutoff of 0.03.

Genetic diversity and structure.

The level of genetic polymorphism was determined for each species and each locus using standard diversity indices including number of segregation sites (S), number of haplotypes (h), haplotype diversity (H_d), and nucleotide diversity (π) using ARLEQUIN v.3.5.2.2 (Excoffier and Lischer 2010). Tajima's D test of selective neutrality was performed to assess deviation from the neutral model of sequence evolution. The *mt-co1* locus was used to estimate the level of genetic differentiation between the two *Akarotaxis* species through mean pairwise differences (Φ_{ST}, using the Kimura-2P model) and haplotype frequencies (F_{ST}) in ARLEQUIN v3.5.2.2 (Excoffier and Lischer 2010), using 10,000 permutations to assess significance. Genealogical relationships were estimated for each mitochondrial marker by constructing a median-joining haplotype network (Bandelt et al. 1999) of all available *Akarotaxis* sequences using PopArt (Leigh and Bryant 2015).

Time calibrated phylogeny.

Phylogenetic reconstruction and divergence time analyses were performed with BEAST v.2.7.1 (Bouckaert et al. 2019) using a partitioned dataset of concatenated *mt-co1*, *mt-nd2*, and *mt-cyb* sequences and applying a relaxed lognormal molecular clock. The dataset included all seventeen bathydraconid species known to date (16 previously described and the described herein *Akarotaxis* n. sp.). Most species were represented by the three mitochondrial loci, except for *Psilodraco breviceps* Norman 1937 and *Bathydraco joannae* DeWitt 1985, which were represented by a single marker, and *Parachaenichthys georgianus* (Fischer 1885), *Vomeridens infuscipinnis* (DeWitt and Hureau 1980), *B. scotiae* Dollo 1906, and *B. antarcticus* Günther 1878, which were represented by two markers. Accession numbers of the sequences used in this analysis are provided in Supp. Table 1.

An Optimized Relaxed Clock model was used along with a nucleotide substitution model (HKY+G) and a Birth-Death model of speciation. Sequences from *N. coriiceps* were included as outgroup. Time calibration of the phylogeny used two Log Normal monophyletic priors based on estimates from the most-recent genome-wide time-calibrated phylogeny of notothenioids (Bista et al. 2023): divergence of *N. coriiceps* and bathydraconids around 7.24 MYA (2.5–97.5 interpercentile range: 5.38 – 9.76 MYA) and the origin of bathydraconid group around 4.75 MYA (3.34 – 6.76 MYA). BEAST2 was run for 100 million MCMC iterations sampled every 10,000 generations. Convergence was assessed using Tracer v.1.7 (Rambaut et al. 2018) and confirmed all ESS were > 2,500. A maximum clade credibility tree with common ancestor node heights was generated using TreeAnnotator 2.7.1 and visualized with FigTree 1.4.4.

To place the time-calibrated phylogeny in a paleoclimatic context, benthic δ^{18}O (‰) data were converted to sea-surface temperature anomalies in degrees Celsius (ºC) with respect to average global temperature from 1961-1990 (Westerhold et al. 2020) with overlaid Loess smoothed curves of sea surface temperature evolution with a window span corresponding to 40,000 years (blue curve) and 1 million years (red curve).

3. Taxonomy

Akarotaxis (DeWitt and Hureau 1980)

Figures 2 - 4

Bathydraco (Günther 1878)

Akarotaxis (DeWitt & Hureau 1980, see Sheiko 2019)

Type species. *Bathydraco nudiceps* (Waite 1916). Davis Sea, Antarctica.

Diagnosis. A genus of Bathydraconinae (Regan 1913) with the following combination of characters: body covered with ctenoid scales; presence of two lateral lines; a small hook on the posterodorsal end of the opercle; six branchiostegal rays; small, conical teeth present; gill rakers are well-developed (Gon & Heemstra 1990).

Remarks. The genus *Akarotaxis* was erected as monotypic by DeWitt & Hureau (1980) for a species of *Bathydraco* Günther 1878 described by Edgar R. Waite (Waite 1916) based on three specimens collected in January 1914 from a coastal area off the Davis Sea off east Antarctica (Fig 1; Table 1). Waite and others collected them while conducting benthic trawls to sample fishes of the "glacial ooze", or fine sediment deposited at the marine terminus of nearby glaciers (Waite 1916). The type specimen of *A. nudiceps* was collected at a depth of 439 m. After collecting *Bathydraco nudiceps* during an expedition to the Bellingshausen Sea off the western Antarctic Peninsula (WAP; Fig 1; Table 1), DeWitt & Hureau (1980) noticed several major differences between *B. nudiceps* and the other members of *Bathydraco* and erected the novel genus *Akarotaxis*. Most notably, *Bathydraco* spp. possess a single lateral line, whereas *A. nudiceps* has two. In the same report, DeWitt & Hureau (1980) also described the monotypic genus *Vomeridens* (Bathydraconidae), which possesses two lateral lines as well. However, the upper lateral line in *A. nudiceps* has 10 or fewer tubular scales, while *Vomeridens* possess 47 – 50 tubular scales.

Etymology. Combination of *akaro,* Greek, meaning "short" and *taxis*, Greek, meaning "line" referring to the short upper lateral line.

Akarotaxis n. sp.
Banded Dragonfish

Figures 2 - 4

Bathydraco nudiceps Waite 1916; original description of genus (DeWitt and Hureau 1980)

Bathydraco wohlschlagi DeWitt and Tyler 1960; (DeWitt 1962)

Akarotaxis nudiceps (Waite 1916); morphology (DeWitt and Hureau 1980; Gon and Heemstra 1990; Miller 1993; Sheiko 2019)

Akarotaxis nudiceps (Waite 1916); genetics (Near et al. 2012); (Bista et al. 2023)

Akarotaxis nudiceps (Waite 1916); early life history (Corso et al. 2023)

Holotype. YPM ICH 24241 (= YFTC 20826; OVERT 05053; Label #1; GenBank ##TBD), 140.8 mm SL, sex unknown, collected by Kuhn, K.L. and Detrich, H.W. aboard the ARSV *Laurence M. Gould* on 22 April 2010.

Paratypes. YPM ICH 36536; YFTC 20827; Label #2, GenBank ##TBD, 135.8 mm SL, sex unknown, collected by Kuhn, K.L. and Detrich, H.W. aboard the ARSV *Laurence M. Gould* on 22 April 2010; YPM ICH 20043; YFTC 12874, Label #3, GenBank ##TBD, 129.3 mm SL, sex unknown, collected by Detrich, H.W. aboard the ARSV *Laurence M. Gould* on 15 May 2008; YPM ICH 20045, YFTC 12876, Label #4, GenBank ##TBD, 127.3 mm SL, sex unknown, collected by Detrich, H.W. aboard the ARSV *Laurence M. Gould* on 15 May 2008; OS 26108, Label #5, GenBank ##TBD, 133 mm SL, male, collected by Desvignes, T. aboard the ARSV *Laurence M. Gould* on 20 August 2017; OS 26109, Label #6, GenBank ##TBD, 133 mm SL, male, collected by Desvignes, T. aboard the ARSV *Laurence M. Gould* on 20 August 2017;

VIMS 45856, Label #7, GenBank ##TBD, 136 mm SL, female, collected by Desvignes, T. aboard the ARSV *Laurence M. Gould* on 7 May 2018.

Diagnosis. A species of *Akarotaxis* distinguished from *A. nudiceps* by the presence of two dark vertical bands of pigment on the body (Figs 2, 3); wider body depth at the origin of the pelvic fins (Table 2; Fig 3); and a shorter snout and jaw length (Figs 3, 4; Table 2).

Description. Body slender, head depressed with wide snout and elongate mouth. Dentary extends slightly past the premaxilla, with dense array of small, conical teeth on jaws (Fig 4). Enlarged, bulbous eyes. Trapezoidal dorsal and anal fins, both extending posterior to the caudal region and commonly depressed in live and preserved animals (Fig 2). Pectoral fins long, extending to anus. Caudal fin truncate. Body covered in mostly ctenoid scales; cycloid scales on the breast anterior to pelvic fins, nape between head and dorsal fin, and on body at base of pectoral fin, no scales on head. Two lateral lines, one (middle) extending to the caudal peduncle and the other (upper) ending about halfway down the body (Fig 2). There are 3 to 5 tubular scales at the beginning of the upper lateral line. There are 84 – 91 scales on the lateral row (Table 2).

Head covered in enlarged cephalic canals (see Table 2) with large bony vacuities enclosed by a thin membrane that are mostly, though variably, open to the environment (i.e., true pores). No coronal pore present. Six branchiostegal rays. Posterior end of opercle terminates in a hook shape. Morphometric data from seven *Akarotaxis* n. sp. specimens summarized in Table 2.

Dorsal (D) 28 – 31; anal (A) 25 – 28; pectoral (P) 20 – 22; caudal (C) 12 – 13; anterior gill rakers (GRA) (7 – 9) + (18 – 20); posterior gill rakers (GRP) (3 – 4) + (14 – 18).

Color in life. Body pale brown with two dark vertical bands that extend down the sides of the body. Band width and location varies among specimens, but one band is centered above the hindgut while the other is positioned above the posterior area of the anal fin. Some specimens show one or two additional darker spots near the dorsal fin, but these do not extend downwards (Fig 3). Caudal, pectoral fins, and opercula are generally darker than the body. Pelvic and anal fins are occasionally darker as well. Abdominal cavity, or gut, area is generally lighter and more silvery than the rest of the body.

Color in alcohol. Body dark tan. Two vertical bands can be less apparent. Caudal, pectoral, anal, and pelvic fins range from tan to black (Figs 2,3).

Remarks. Measurements for the two specimens of *A. nudiceps* presented by DeWitt & Hureau (1980) do not closely align with our data for *A. nudiceps* collected in the D'Urville Sea (Table 2). For example, the caudal length (CL), pelvic length (VL), orbital diameter (O), and head depth (HD presented by Dewitt & Hureau (1980) are all substantially greater than our measurements for both species (Table 2). We did not have access to images or data taken directly from these specimens. However, we did obtain photographs of two paratypes of *A. nudiceps*, AMS IA.484 (Figs 3h and 4h) and AMS IA.485, that lack bands and resemble the morphology of *A. nudiceps*. These paratypes were collected January 29th, 1914 in same region as Waite's (1916) holotype. Online photographs of live *A. nudiceps* collected in the D'urville Sea also lack bands (https://v3.boldsystems.org/index.php/Taxbrowser_Taxonpage?taxid=159627). A complete reexamination of all *Akarotaxis* specimens should be prioritized in the future.

The smallest adult specimen of *Akarotaxis* n. sp. we examined was 127.3 mm SL, although the gender was not determined (based on YPM ICH 20045; Fig 3). It is unknown when the characteristic dark vertical bands develop in *Akarotaxis* n. sp., although they do not appear on larvae up to 20.7 mm SL (Corso et al. 2023). The presence of these bands was not reported by Waite (1916) or Dewitt & Hureau (1980) and are absent on two molecularly-verified *A. nudiceps* specimens (Fig 5).

4. Habitat, Genetics, Biogeography, and Speciation

Habitat and biology.

Akarotaxis nudiceps and *Akarotaxis* n. sp. display similar bathymetric distributions. The depth of capture of *Akarotaxis* n. sp. ranged from 600 to 705 m for adults and from 215 to 964 m for larvae (Tables 1, 3)(Corso et al. 2023). As adults, *A. nudiceps* has been found at depths ranging from 103 to 1191 m (Eastman 2017; Li et al. 2022). Habitats at these depths in coastal regions of Antarctica are likely composed of similar fine sediments, as noted by Waite (1916). The difference in jaw morphology between species suggests that trophic mode may differ. However, given probable habitat similarities *Akarotaxis* spp. would likely encounter similar prey types, especially as most smaller, deep-dwelling bathydraconids possess generalist “sit-and-wait” feeding strategies (La Mesa et al. 2004; La Mesa, Eastman, et al. 2007; Münster et al. 2017). An analysis of gut contents of *Akarotaxis* spp. is necessary to further examine this hypothesis.

We estimated that the absolute fecundity of the studied gravid female was approximately 322 eggs (35 maturing oocytes in the ovarian fragment representing ~11% of the complete ovaries weight). The bimodal size-frequency distribution of oocyte diameters aligns with observations in other bathydraconids, suggesting ovaries follow group synchronous development and a likely single spawning event (Fig 6) (La Mesa, Caputo, et al. 2007; La Mesa et al. 2018; La Mesa et al. 2021). The distribution of larger oocytes averaged 2.44 ± 0.15 mm (Fig 6), which indicates the fish was preparing to spawn based on egg size of *A. nudiceps* (1.6 – 2.6 mm) (La Mesa, Caputo, et al. 2007). The low fecundity of *Akarotaxis* n. sp. and high reproductive investment (Gonadosomatic Index of the maturing female GSI = 17%) may suggest a nesting behavior, similarly to what was proposed for *A. nudiceps* and has been observed in other bathydraconids (Evans et al. 2005; La Mesa, Caputo, et al. 2007; Barrera-Oro and Lagger 2010; La Mesa et al. 2021).

Bathydraconidae phylogeny and placement of Akarotaxis spp..

We produced and retrieved sequences for 23 specimens of *Akarotaxis* n. sp. and 19 specimens of *A. nudiceps* (Table 3), including 22 *mt-nd2*, 22 *mt-co1*, four *mt-cyb* of *Akarotaxis* n. sp. and one *mt-nd2*, 16 *mt-co1*, one *mt-cyb*, and one complete *mt* genome sequence of *Akarotaxis nudiceps* (Table 3). In addition, we included single *mt-nd2* and *mt-co1* sequences from 13 other bathydraconid species and single *mt-cyb* sequences from 11 other bathydraconid species (see Figs 7, Supp. Fig 1, Supp. Table 1).

Our phylogenetic analyses revealed that *Akarotaxis* n. sp. and *A. nudiceps* form two distinct sister species with Bayesian inference posterior probabilities of 1 for all three genes and both species (Fig 7) and with ML bootstrap supports of 100 for *mt-nd2* and *mt-cyb* for both species, and of 97 and 88 for *mt-co1* for *Akarotaxis* n. sp. and *A. nudiceps*, respectively (Supp. Fig 1). Corrected average pairwise difference Φ_{ST} and pairwise F_{ST} based on *mt-co1* confirms a significant difference between the two species ($\Phi_{ST} = 0.155$, $p = 0$; $F_{ST} = 0.157$, $p = <0.001$). Further, the sister species haplogroups were separated by many mutational steps: 17 for *mt-co1*, 29 for *mt-cyb*, and 43 for *mt-nd2* (Fig 7). Our analyses further support the monophyly of the *Akarotaxis* genus with a Bayesian inference posterior probability of 1 based on *mt-co1* and *mt-cytb*, of 0.93 for *mt-nd2* (Fig 7), and of 1 when all three markers were analyzed simultaneously (Fig 8) and with ML bootstrap support of 56, 82, and 91 for *mt-co1*, *mt-nd2*, and *mt-cyb*, respectively (Supp. Fig 1).

The *Akarotaxis* genus is resolved as the sister genus to the genus *Bathydraco* with a posterior probability of 1 in the three-marker time-calibrated phylogeny (Fig 8). *Akarotaxis* and *Bathydraco* compose the Bathydraconinae sub-family along with the monotypic genera *Racovitzia* (Dollo 1900), *Prionodraco* (Regan 1914) and *Vomeridens* (DeWitt and Hureau 1980). While the two other dragonfish sub-families Gymnodraconinae and Cygnodraconinae were also unambiguously resolved as monophyletic with posterior probabilities of 1, the position of the Bathydraconinae as sister to Gymnodraconinae and Cygnodraconinae is supported with a posterior probability of only 0.83 (Fig 7).

Biogeography of Akarotaxis spp.

A. nudiceps and *Akarotaxis* n. sp. have potentially allopatric distributions. All adult specimens of *Akarotaxis* n. sp. examined in this study and the larvae in Corso *et al.* (2022a) were captured along a ~400 km coastal section of the WAP between Lapeyrere Bay and Adelaide Island (Fig 1, 7). In contrast, *A. nudiceps* appears to possess a near circumpolar distribution in high-Antarctic coastal areas (Gon and Heemstra 1990; Duhamel et al. 2014). Only one specimen of *A. nudiceps* has been recorded in the coastal WAP region (DeWitt and Hureau 1980) and was used to describe the genus. This specimen, however, could not be observed, and it is possible that it is a member of *Akarotaxis* n. sp. based on its capture location (Label #9 in Fig 1). Depending on the identity of the Dewitt and Hureau specimen, *A. nudiceps* and *Akarotaxis* n. sp. may have allopatric distributions or parapatric distributions with small overlaps.

Timing and mode of speciation.

No population structure was observed within either species. H_d and π were comparable between species (Supp. Table 2). H_d was 0.79 for *mt-co1* in *Akarotaxis* n. sp. and 0.9 in *A. nudiceps*. π was 0.0021 for *mt-co1* in *Akarotaxis* n. sp. and 0.0029 in *A. nudiceps*. The star-like topology of the *mt-co1* haplotype network for *Akarotaxis* n. sp. (Fig 7) and significant Tajima's D test for neutrality (D = -2.05915, p = 0.0071, Supp. Table 2), suggests past contraction-expansion processes, such as population expansion following a genetic bottleneck due to drastic reductions in population size (Hewitt 2004; Provan and Bennett 2008; Marko et al. 2010; Maturana et al. 2022). While no population structure was observed in *A. nudiceps* either, the reticulated and expanded genealogy of the *mt-co1* haplotype network (Fig. 3) suggests a panmictic population that would not have undergone a similar bottleneck and would spread all around most of the continent. Consistently, Tajima's D test for neutrality was not significant for *A. nudiceps* (D = -0.32219, p = 0.4145, Supp. Table 2) suggesting that *A. nudiceps* population evolve neutrally with no evidence of selection.

The disruptive and relatively rapid expansion of ice sheets during intermediate to maximum glacial states has been shown to drive speciation among notothenioids by isolating populations in sub-Antarctic island refugia (Dornburg et al. 2017; Daane and Detrich 2022). Our divergence estimate of *Akarotaxis* n. sp., at approximately 0.78 MYA (95% highest posterior density interval (HPD): 0.33 – 1.25 MYA) (Fig 8), occurs during an especially volatile period of glacial growth and collapse in West Antarctica (Pollard and DeConto 2009; Collins et al. 2020). The Mid-Pleistocene Transition (MPT), from 1.2 to 0.7 Mya (Fig 8c), was characterized by a shift in Earth's climate cycles, changing from a periodicity of ~41 Kyr to 100 Kyr (Elderfield et al. 2012; Sutter et al. 2019). The warm, super-interglacial period, Marine Isotope Stage (MIS) 25 around 0.9 MYA was followed by the first 80 – 120 Kyr period of unperturbed Antarctic Ice Sheet growth (Sutter et al. 2019). Alternance of ice advances and retreats may have isolated *Akarotaxis* populations leading to the divergence of the two sister species by allopatric speciation.

Based on our time calibrated molecular phylogeny, which is the first to date to include all known Bathydraconidae, several lineages diversified during or immediately following the MPT (Fig 8). The congeneric species *Parachaenichthys charcoti* (Vaillant 1906) on the WAP and *P. georgianus* in South Georgia diverged around 1.1 MYA (95% HPD: 0.50 – 1.74 MYA), and the sister species *Acanthodraco dewitti* (Skóra 1995) in Antarctica and *Psilodraco breviceps* also in South Georgia diverged around 0.7 MYA (95% HPD: 0.23 – 1.24 MYA). Both sister species pairs thus fit the model of sub-Antarctic island refugia as a source of species diversity. In contrast, the diversification within Antarctic waters of *Akarotaxis*, and of the *Bathydraco* genus around 0.65 MYA (95% HPD: 0.28 – 1.0 MYA), suggests a mechanism of diversification during past glacial maxima differing from the sub-Antarctic island refugia hypothesis. The apparent isolation of *Akarotaxis* n. sp. in deep areas of the WAP and *Akarotaxis* and *Bathydraco* being the two deepest-dwelling bathydraconid genera (Eastman 2017), supports instead the in-shelf refugium hypothesis for these species (Barnes and Kuklinski 2010; Clarke and Crame 2010; Dornburg et al. 2016). In this scenario, an ancestral species of *Akarotaxis* was able to survive ice progression following MIS25 through an isolated population localized in deep areas (e.g., canyons) off the WAP which diverged from the other almost circumpolar population. Based on the current range, it is unclear why *Akarotaxis* n. sp. was unable to expand to a wider range outside the WAP region and did not interbreed with *A. nudiceps* during subsequent interglacial periods (Barnes and Hillenbrand 2010; Marino et al. 2013).

5. Policy Implications

Based on currently known occurrences, *Akarotaxis* n. sp. has one of the most limited distributions of fishes endemic to the Antarctic area of the Southern Ocean (Duhamel et al. 2014). Adults and larvae have all been captured in the coastal WAP area, which is located within the Commission for the Conservation of Antarctic Marine Living Resource's (CCAMLR) Subarea 48.1 (Fig 1)(CCAMLR 2017). This region, especially near the Bransfield Strait, is historically one of the regions most heavily targeted by the international fishery for Antarctic Krill (*Euphausia superba*) managed by CCAMLR (Meyer et al. 2020; CCAMLR Secretariat 2022 May 27). Fishing vessels capture krill in the epipelagic zone (0 – 250m) by using either midwater trawls, beam trawls, or a continuous method that pumps the net contents directly onto the ship (CCAMLR 2021). Although fishing effort was historically the greatest during austral summer (December – February), vessels have recently been fishing later into the austral autumn (March – May) to target more lipid-rich krill (Meyer et al. 2020; CCAMLR Secretariat 2022 May 27). Over the last five years (2017 – 2021), vessels averaged an aggregate annual harvest of 154, 972 tons of krill (CCAMLR Secretariat 2022 May 27).

Although there are efforts towards ecosystem-based management of Antarctic krill by CCAMLR, many current and proposed restrictions are focused on reducing the direct impact of the fishery on seabirds, adult finfishes, and marine mammals (Brooks et al. 2016; Nicol and Foster 2016; Meyer et al. 2020; Watters et al. 2020; Brooks et al. 2022; Trathan et al. 2022). In contrast, the potential impacts of the fishery on the early life stages of Antarctic finfishes are poorly understood. In 2005, observation of the bycatch of juvenile fishes was identified as a research priority by the CCAMLR Scientific Committee (SC) (Sabourenkov and Appleyard 2005). Over a decade later, the CCAMLR SC continues to emphasize the difficulties in correctly identifying larval and juvenile finfish bycatch based on morphology (SC CAMLR 2018), while the costs of genetic methods of species identification (e.g., DNA barcoding) prevent their widespread use by monitors.

The potential endemism of *Akarotaxis* n. sp. to Subarea 48.1 (Fig 1), its low fecundity, and the location of early life stages in the epipelagic zone suggests that this species could be impacted by the krill fishery. Although bathydraconid larvae are not listed as one of the frequently captured groups of finfish bycatch (CCAMLR Secretariat 2015), the early larval stages can easily be confused with other listed nototheniids. Corso *et al.* (2022a) found *Akarotaxis* n. sp. larvae from January – February, with several occurring near Marguerite Bay.

As CCAMLR continues to develop seasonal and regional closures for the krill fishery, we suggest considering the exceptionally high prevalence of larval *Akarotaxis* n. sp. and other notothenioid larvae during the austral summer near the coastal WAP region. It is critical that this vulnerable assemblage of unique fishes is protected from threats of bycatch as they are increasingly impacted by climate change (Mintenbeck et al. 2012; Corso et al. 2022).

Conclusions

The study of museum-archived *A. nudiceps* larvae by Corso et al. (2022a) led to the discovery of *Akarotaxis* n. sp., highlighting the importance of studying the early life stages of fishes to reach a comprehensive understanding of biodiversity. These combined efforts also demonstrate the continued importance of long-term ecological research and of natural history collections (O'Brien et al. 2022). Repeated annual sampling, such as that performed by NSF LTER, increases the likelihood of encountering rare organisms. Further, publicly available repositories allow researchers to study these organisms in perpetuity. With these structures in place, our understanding of Antarctic ichthyofaunal diversity will undoubtedly continue to expand.

Acknowledgements

We thank Marissa Goerke for the illustration of *Akarotaxis* n. sp., Sarah K. Huber, Gregory Watkins-Colwell, Peter Konstantinidis, Zouhaira Gabsi, Amanda Hay, Kerryn Parkinson, and Agnès Dettaï for access to specimens and curatorial assistance, Mario La Mesa, Christopher Jones, Adena Schonfeld, Joseph Cope, and Kharis Schrage for discussion, William H. Detrich and Kristen Kuhn for collection information, Katherine R. Murphy and Kevin Bilyk for photographs and collection information, Hai Li for gene sequences from Prydz Bay, and Stéphane Thanassekos for geographic information. We thank the captains, crew, and support staff of the R/V *Polar Duke* and ASRV *Laurence M. Gould*, the support of personnel at Palmer Station, Antarctica, and the Leidos Antarctic Support Contractors. This work was funded by the National Science Foundation Office of Polar Program (OPP-1440435, 2026045, and 1543383 for specimen and environmental data collection and OPP-1947040) and Division of Biological Infrastructure (DBI-1349327 for specimen preservation and analysis), the Explorers Club, and the VIMS John Olney Fellowship.

References

Bandelt HJ, Forster P, Röhl A. 1999. Median-joining networks for inferring intraspecific phylogenies. Molecular Biology and Evolution. 16(1):37–48. https://doi.org/10.1093/oxfordjournals.molbev.a026036

Barnes DKA, Hillenbrand C-D. 2010. Faunal evidence for a late quaternary trans-Antarctic seaway. Global Change Biology. 16(12):3297–3303. https://doi.org/10.1111/j.1365-2486.2010.02198.x

Barnes DKA, Kuklinski P. 2010. Bryozoans of the Weddell Sea continental shelf, slope and abyss: did marine life colonize the Antarctic shelf from deep water, outlying islands or in situ refugia following glaciations? Journal of Biogeography. 37(9):1648–1656. https://doi.org/10.1111/j.1365-2699.2010.02320.x

Barrera-Oro ER, Lagger C. 2010. Egg-guarding behaviour in the Antarctic bathydraconid dragonfish *Parachaenichthys charcoti*. Polar Biolgy 33(11):1585–1587. https://doi.org/10.1007/s00300-010-0847-3

Beck EA, Healey HM, Small CM, Currey MC, Desvignes T, Cresko WA, Postlethwait JH. 2022. Advancing human disease research with fish evolutionary mutant models. Trends in Genetics. 38(1):22–44. https://doi.org/10.1016/j.tig.2021.07.002

Bilyk KT, Zhuang X, Murphy KR, Cheng C-HC. 2019. A tale of two genes: divergent evolutionary fate of haptoglobin and hemopexin in hemoglobinless Antarctic icefishes. Journal of Experimental Biology. 222(6):jeb188573. https://doi.org/10.1242/jeb.188573

Bista I, Wood JMD, Desvignes T, McCarthy SA, Matschiner M, Ning Z, Tracey A, Torrance J, Sims Y, Chow W, et al. 2023. Genomics of cold adaptations in the Antarctic notothenioid fish radiation. Nat Communications 14(1):3412. https://doi.org/10.1038/s41467-023-38567-6

Bouckaert R, Vaughan TG, Barido-Sottani J, Duchêne S, Fourment M, Gavryushkina A, Heled J, Jones G, Kühnert D, Maio ND, et al. 2019. BEAST 2.5: An advanced software platform for Bayesian evolutionary analysis. PLOS Computational Biology. 15(4):e1006650. https://doi.org/10.1371/journal.pcbi.1006650

Brooks CM, Ainley DG, Jacquet J, Chown SL, Pertierra LR, Francis E, Rogers A, Chavez-Molina V, Teh L, Sumaila UR. 2022. Protect global values of the Southern Ocean ecosystem. Science. 378(6619):477–479. https://doi.org/10.1126/science.add9480

Brooks CM, Crowder LB, Curran LM, Dunbar RB, Ainley DG, Dodds KJ, Gjerde KM, Sumaila UR. 2016. Science-based management in decline in the Southern Ocean. Science. 354(6309):185–187.

Cao S, Li Y, Miao X, Zhang R, Lin L, Li H. 2022. DNA Barcoding Provides Insights Into Fish Diversity and Molecular Taxonomy of the Amundsen Sea: In Review; [accessed 2022 Mar 4]. https://doi.org/10.21203/rs.3.rs-1244705/v1

CCAMLR. 2017. Map of the CAMLR Convention Area. Last updated October 2017. [accessed 2022 Dec 1]. www.ccamlr.org/node/86816

CCAMLR. 2021. Krill fisheries. Last updated July 2021. [accessed 2022 Dec 1]. https://www.ccamlr.org/en/fisheries/krill

CCAMLR Secretariat. 2015. Common fish by-catch species in CCAMLR krill fisheries. Last modified on March 2015. [accessed 2022 Dec 1]. https://www.ccamlr.org/en/document/science/common-fish-catch-species-ccamlr-krill-fisheries

CCAMLR Secretariat. 2022. Fishery Report 2021: *Euphausia superba* in Area 48. :33.

Ceballos SG, Roesti M, Matschiner M, Fernández DA, Damerau M, Hanel R, Salzburger W. 2019. Phylogenomics of an extra-Antarctic notothenioid radiation reveals a previously unrecognized lineage and diffuse species boundaries. BMC Evolutionary Biology. 19(1):13. https://doi.org/10.1186/s12862-019-1345-z

Clarke A, Crame JA. 2010. Evolutionary dynamics at high latitudes: speciation and extinction in polar marine faunas. Philosophical Transactions of the Royal Society B. 365(1558):3655–3666. https://doi.org/10.1098/rstb.2010.0270

Collins GE, Hogg ID, Convey P, Sancho LG, Cowan DA, Lyons WB, Adams BJ, Wall DH, Green TGA. 2020. Genetic diversity of soil invertebrates corroborates timing estimates for past collapses of the West Antarctic Ice Sheet. Proceedings of the National Academy of Sciences. 117(36):22293–22302. https://doi.org/10.1073/pnas.2007925117

Corso AD, McDowell JR, Biesack EE, Muffelman SC, Hilton EJ. 2023. Larval stages of the Antarctic Dragonfish *Akarotaxis nudiceps* (Waite, 1916), with comments on the larvae of the morphologically similar species *Prionodraco evansii* Regan 1914 (Notothenioidei: Bathydraconidae). Journal of Fish Biology.

Corso AD, Steinberg DK, Stammerjohn SE, Hilton EJ. 2022. Climate drives long-term change in Antarctic Silverfish along the western Antarctic Peninsula. Communications biology. 5(1):1–10.

Daane JM, Detrich HW. 2022. Adaptations and Diversity of Antarctic Fishes: A Genomic Perspective. Annual Review of Animal Biosciences 10(1):39–62. https://doi.org/10.1146/annurev-animal-081221-064325

Darriba D, Posada D, Kozlov AM, Stamatakis A, Morel B, Flouri T. 2020. ModelTest-NG: A New and Scalable Tool for the Selection of DNA and Protein Evolutionary Models. Molecular Biology and Evolution. 37(1):291–294. https://doi.org/10.1093/molbev/msz189

Derome N, Chen W-J, Dettaï A, Bonillo C, Lecointre G. 2002. Phylogeny of Antarctic dragonfishes (Bathydraconidae, Notothenioidei, Teleostei) and related families based on their anatomy and two mitochondrial genes. Molecular Phylogenetics and Evolution. 24(1):139–152. https://doi.org/10.1016/S1055-7903(02)00223-3

Desvignes T, Postlethwait JH, Konstantinidis P. 2020. Biogeography of the Antarctic dragonfishes *Acanthodraco dewitti* and *Psilodraco breviceps* with re-description of *Acanthodraco dewitti* larvae (Notothenioidei: Bathydraconidae). Polar Biolgy. 43(5):565–572. https://doi.org/10.1007/s00300-020-02661-y

DeWitt HH. 1962. A New Antarctic Nototheniid Fish with Notes on Two Recently Described Nototheniiforms. Copeia. 1962(4):826–833. https://doi.org/10.2307/1440685

DeWitt HH. 1985. Reports on fishes of the university of southern California, Antarctic research program, 1962-1968. I: A review of the genus Bathydraco Gunther (Family Bathydraconidae). Cybium (Paris). 9(3):295–314.

DeWitt HH, Hureau JC. 1980. Fishes collected during" Hero" cruise 72-2 in the Palmer Archipelago, Antarctic, with the description of two new general and three new species. Bulletin du Museum National d’Histoire Naturelle Zoologie (France).

DeWitt HH, Tyler JC. 1960. Fishes of the Stanford Antarctic biological research program, 1958–1959. Stanford Ichthyology Bulletin. 7:162–199.

Dollo L. 1900. *Racovitzia glacialis*, poisson abyssal nouveau, recueilli par cette expédition. Expédition Antarctique Belge. Communication Préliminaire Bull Acad R Belg(Cl Sci). 4:316–327.

Dollo L, Traquair MRH. 1906. *Bathydraco Scotiæ*, Poisson abyssal nouveau recueilli par l'Expédition Antarctique Nationale Ecossaise. Proceedings of the Royal Society of Edinburgh. 26(1):65–75. https://doi.org/10.1017/S0370164600024433

Dornburg A, Federman S, Eytan RI, Near TJ. 2016. Cryptic species diversity in sub-Antarctic islands: A case study of *Lepidonotothen*. Molecular Phylogenetics and Evolution. 104:32–43. https://doi.org/10.1016/j.ympev.2016.07.013

Dornburg A, Federman S, Lamb AD, Jones CD, Near TJ. 2017. Cradles and museums of Antarctic teleost biodiversity. Nature Ecology and Evolution. 1(9):1379–1384. https://doi.org/10.1038/s41559-017-0239-y

Dorschel B, Hehemann L, Viquerat S, Warnke F, Dreutter S, Tenberge YS, Accettella D, An L, Barrios F, Bazhenova E, et al. 2022. The International Bathymetric Chart of the Southern Ocean Version 2. Sci Data. 9(1):275. https://doi.org/10.1038/s41597-022-01366-7

Duhamel G, Hulley P-A, Causse R, Koubbi P, Vacchi M, Pruvost P, Vigetta S, Irisson J-O, Mormede S, Belchier M. 2014. Biogeographic patterns of fish.

Eastman JT. 2017. Bathymetric distributions of notothenioid fishes. Polar Biolgy. 40(10):2077–2095. https://doi.org/10.1007/s00300-017-2128-x

Eastman JT, Eakin RR. 2021. Checklist of the species of notothenioid fishes. Antarctic Science. 33(3):273–280. https://doi.org/10.1017/S0954102020000632

Eastman JT, McCune AR. 2000. Fishes on the Antarctic continental shelf: evolution of amarine species flock? Journal of Fish Biology. 57:84–102.

Edler D, Klein J, Antonelli A, Silvestro D. 2021. raxmlGUI 2.0: A graphical interface and toolkit for phylogenetic analyses using RAxML. Methods in Ecology and Evolution. 12(2):373–377. https://doi.org/10.1111/2041-210X.13512

Ekau W. 1990. Demersal fish fauna of the Weddell Sea, Antarctica. Antartic Science. 2(2):129–137. https://doi.org/10.1017/S0954102090000165

Elderfield H, Ferretti P, Greaves M, Crowhurst S, McCave IN, Hodell D, Piotrowski AM. 2012. Evolution of Ocean Temperature and Ice Volume Through the Mid-Pleistocene Climate Transition. Science. 337(6095):704–709. https://doi.org/10.1126/science.1221294

Evans CW, Cziko P, Cheng C-HC, Devries AL. 2005. Spawning behaviour and early development in the naked dragonfish *Gymnodraco acuticeps*. Antartic Science. 17(3):319–327. https://doi.org/10.1017/S0954102005002749

Excoffier L, Lischer HEL. 2010. Arlequin suite ver 3.5: a new series of programs to perform population genetics analyses under Linux and Windows. Molecular Ecology Resources. 10(3):564–567. https://doi.org/10.1111/j.1755-0998.2010.02847.x

Fischer JG. 1885. Über Fische von Süd-Georgien. Ichthyologische und herpetologische Bemerkungen Jahrbuch der Hamburgischen Wissenschaftlichen Anstalten. 2:49–65.

Gon O, Heemstra PC. 1990. Fishes of the Southern Ocean.: JLB Smith Institute of Ichthyology Grahamstown.

Günther A. 1878. II.—Preliminary notices of Deep-Sea Fishes collected during the Voyage of HMS 'Challenger.' Journal of Natural History. 2(7):17–28.

Hewitt GM. 2004. Genetic consequences of climatic oscillations in the Quaternary. Philosophical Transactions of the Royal Society of London Series B: Biological Sciences. https://doi.org/10.1098/rstb.2003.1388

Huelsenbeck JP, Ronquist F. 2001. MRBAYES: Bayesian inference of phylogenetic trees. Bioinformatics. 17(8):754–755. https://doi.org/10.1093/bioinformatics/17.8.754

Katoh K, Rozewicki J, Yamada KD. 2019. MAFFT online service: multiple sequence alignment, interactive sequence choice and visualization. Briefings in Bioinformatics. 20(4):1160–1166. https://doi.org/10.1093/bib/bbx108

Kozlov AM, Darriba D, Flouri T, Morel B, Stamatakis A. 2019. RAxML-NG: a fast, scalable and user-friendly tool for maximum likelihood phylogenetic inference. Bioinformatics. 35(21):4453–4455. https://doi.org/10.1093/bioinformatics/btz305

Kuhn KL, Near TJ, Detrich HW, Eastman JT. 2011. Biology of the Antarctic dragonfish *Vomeridens infuscipinnis* (Notothenioidei: Bathydraconidae). Antarctic Science. 23(1):18–26.

La Mesa M, Calì F, Donato F, Riginella E, Mazzoldi C. 2018. Aspects of the biology of the Antarctic dragonfish *Gerlachea australis* (Notothenioidei: Bathydraconidae) in the Weddell Sea, Antarctica. Polar Biology. 41(4):793–803.

La Mesa M, Caputo V, Eastman JT. 2007. Gametogenesis in the dragonfishes Akarotaxis nudiceps and *Bathydraco marri* (Pisces, Notothenioidei: Bathydraconidae) from the Ross Sea. Antarctic Science. 19(1):64–70. https://doi.org/10.1017/S0954102007000090

La Mesa M, Eastman JT, Licandro P. 2007. Feeding habits of *Bathydraco marri* (Pisces, Notothenioidei, Bathydraconidae) from the Ross Sea, Antarctica. Polar Biolgy. 30(5):541–547. https://doi.org/10.1007/s00300-006-0211-9

La Mesa M, Eastman JT, Vacchi M. 2004. The role of notothenioid fish in the food web of the Ross Sea shelf waters: a review. Polar Biol. 27(6):321–338. https://doi.org/10.1007/s00300-004-0599-z

La Mesa M, Llompart F, Riginella E, Eastman JT. 2021. Parental care and reproductive strategies in notothenioid fishes. Fish and Fisheries. 22(2):356–376.

La Mesa M, Piepenburg D, Pineda-Metz SEA, Riginella E, Eastman JT. 2019. Spatial distribution and habitat preferences of demersal fish assemblages in the southeastern Weddell Sea (Southern Ocean). Polar Biolgy. 42(5):1025–1040. https://doi.org/10.1007/s00300-019-02495-3

Leigh JW, Bryant D. 2015. popart: full-feature software for haplotype network construction. Methods in Ecology and Evolution. 6(9):1110–1116. https://doi.org/10.1111/2041-210X.12410

Lemoine F, Correia D, Lefort V, Doppelt-Azeroual O, Mareuil F, Cohen-Boulakia S, Gascuel O. 2019. NGPhylogeny.fr: new generation phylogenetic services for non-specialists. Nucleic Acids Research. 47(W1):W260–W265. https://doi.org/10.1093/nar/gkz303

Li H, Cao S, Li Y, Song P, Zhang R, Wang R, Liu S, Miao X, Lin L. 2022. Molecular assessment of demersal fish diversity in Prydz Bay using DNA taxonomy. Deep Sea Research Part II: Topical Studies in Oceanography. 202:105140. https://doi.org/10.1016/j.dsr2.2022.105140

Lönnberg E. 1906. Contributions to the fauna of South Georgia. Almqvist & Wiksells.

Marino I a. M, Benazzo A, Agostini C, Mezzavilla M, Hoban SM, Patarnello T, Zane L, Bertorelle G. 2013. Evidence for past and present hybridization in three Antarctic icefish species provides new perspectives on an evolutionary radiation. Molecular Ecology. 22(20):5148–5161. https://doi.org/10.1111/mec.12458

Marko PB, Hoffman JM, Emme SA, Mcgovern TM, Keever CC, Nicole Cox L. 2010. The ‘Expansion–Contraction’ model of Pleistocene biogeography: rocky shores suffer a sea change? Molecular Ecology. 19(1):146–169. https://doi.org/10.1111/j.1365-294X.2009.04417.x

Maturana CS, Biersma EM, Díaz A, González-Wevar C, Contador T, Convey P, Jackson JA, Poulin E. 2022. Survivors and colonizers: Contrasting biogeographic histories reconciled in the Antarctic freshwater copepod *Boeckella poppei*. Frontiers in Ecology and Evolution. 10. https://www.frontiersin.org/articles/10.3389/fevo.2022.1012852

Mesa ML, Riginella E, Jones CD. 2017. Early life history traits and geographical distribution of *Parachaenichthys charcoti*. Antarctic Science. 29(5):410–416. https://doi.org/10.1017/S0954102017000189

Meyer B, Atkinson A, Bernard KS, Brierley AS, Driscoll R, Hill SL, Marschoff E, Maschette D, Perry FA, Reiss CS, et al. 2020. Successful ecosystem-based management of Antarctic krill should address uncertainties in krill recruitment, behaviour and ecological adaptation. Communications Earth and Environment. 1(1):1–12. https://doi.org/10.1038/s43247-020-00026-1

Miller RG. 1993. History and atlas of the fishes of the Antarctic Ocean.

Mintenbeck K, Barrera-Oro ER, Brey T, Jacob U, Knust R, Mark FC, Moreira E, Strobel A, Arntz WE. 2012. Impact of climate change on fishes in complex Antarctic ecosystems. In: Advances in ecological research. Vol. 46. Elsevier; p. 351–426.

Münster J, Kochmann J, Grigat J, Klimpel S, Kuhn T. 2017. Parasite fauna of the Antarctic dragonfish *Parachaenichthys charcoti* (Perciformes: Bathydraconidae) and closely related Bathydraconidae from the Antarctic Peninsula, Southern Ocean. Parasites Vectors. 10(1):1–9. https://doi.org/10.1186/s13071-017-2176-7

Near TJ, Dornburg A, Kuhn KL, Eastman JT, Pennington JN, Patarnello T, Zane L, Fernández DA, Jones CD. 2012. Ancient climate change, antifreeze, and the evolutionary diversification of Antarctic fishes. Proceedings of the National Academy of Sciences. 109(9):3434–3439. https://doi.org/10.1073/pnas.1115169109

Near TJ, MacGuigan DJ, Parker E, Struthers CD, Jones CD, Dornburg A. 2018. Phylogenetic analysis of Antarctic notothenioids illuminates the utility of RADseq for resolving Cenozoic adaptive radiations. Molecular Phylogenetics and Evolution. 129:268–279. https://doi.org/10.1016/j.ympev.2018.09.001

Nicol S, Foster J. 2016. The Fishery for Antarctic Krill: Its Current Status and Management Regime. In: Siegel V, editor. Biology and Ecology of Antarctic Krill. Cham: Springer International Publishing. p. 387–421. https://doi.org/10.1007/978-3-319-29279-3_11

Norman JR. 1937. LV.—Diagnoses of new Nototheniiform fishes collected by the 'Discovery' Expedition. Annals and Magazine of Natural History. 20(118):475–476. https://doi.org/10.1080/00222933708655368

Novillo M, Moreira E, Macchi G, Barrera-Oro E. 2018. Reproductive biology in the Antarctic bathydraconid dragonfish *Parachaenichthys charcoti*. Polar Biolgy. 41(11):2239–2248. https://doi.org/10.1007/s00300-018-2359-5

Novillo M, Moreira E, Macchi G, Barrera-Oro E. 2019. Reproductive effort in *Chaenocephalus aceratus* validated by gonadal histology: inshore sites serve as spawning grounds for some notothenioids. Polar Biolgy. 42(11):1959–1972. https://doi.org/10.1007/s00300-019-02571-8

Nybelin O. 1947. Antarctic fishes. Scientific Results of the Norwegian Antarctic Expeditions (1927-1931). 26(2):1–76.

O’Brien KM, Crockett EL, Adams BJ, Amsler CD, Appiah-Madson HJ, Collins A, Desvignes T, Detrich HW, Distel DL, Eppley SM, et al. 2022. The time is right for an Antarctic biorepository network. Proceedings of the National Academy of Sciences. 119(50):e2212800119. https://doi.org/10.1073/pnas.2212800119

O’Brien KM, Rix AS, Egginton S, Farrell AP, Crockett EL, Schlauch K, Woolsey R, Hoffman M, Merriman S. 2018. Cardiac mitochondrial metabolism may contribute to differences in thermal tolerance of red- and white-blooded Antarctic notothenioid fishes. Journal of Experimental Biology. 221(15):jeb177816. https://doi.org/10.1242/jeb.177816

Pollard D, DeConto RM. 2009. Modelling West Antarctic ice sheet growth and collapse through the past five million years. Nature. 458(7236):329–332. https://doi.org/10.1038/nature07809

Postlethwait JH, Yan Y, Desvignes T, Allard C, Titus T, Le François NR, Detrich III HW. 2016. Embryogenesis and early skeletogenesis in the Antarctic bullhead notothen, *Notothenia coriiceps*. Developmental Dynamics. 245(11):1066–1080. https://doi.org/10.1002/dvdy.24437

Provan J, Bennett KD. 2008. Phylogeographic insights into cryptic glacial refugia. Trends in Ecology & Evolution. 23(10):564–571. https://doi.org/10.1016/j.tree.2008.06.010

Rambaut A, Drummond AJ, Xie D, Baele G, Suchard MA. 2018. Posterior Summarization in Bayesian Phylogenetics Using Tracer 1.7. Systematic Biology. 67(5):901–904. https://doi.org/10.1093/sysbio/syy032

Regan CT. 1913. II.—The Antarctic Fishes of the Scottish National Antarctic Expedition. Earth and Environmental Science Transactions of The Royal Society of Edinburgh. 49(2):229–292.

Regan CT. 1914. II.—Diagnoses of new marine fishes collected by the British Antarctic ('Terra Nova') Expedition. Annals and Magazine of Natural History. 13(73):11–17.

Richardson J. 1844. Ichthyology of the Voyage of HMS Erebus & Terror, Under the Command of Captain Sir James Clark Ross. EW Janson, 28, Museum Street, WC.

Riddle MJ, Craven M, Goldsworthy PM, Carsey F. 2007. A diverse benthic assemblage 100 km from open water under the Amery Ice Shelf, Antarctica. Paleoceanography. 22(1). https://doi.org/10.1029/2006PA001327

Sabaj MH. 2020. Codes for Natural History Collections in Ichthyology and Herpetology. Copeia. 108(3):593–669. https://doi.org/10.1643/ASIHCODONS2020

Sabourenkov EN, Appleyard E. 2005. Scientific observations in CCAMLR fisheries–past, present and future. CCAMLR Science. 12:81–98.

Saravia J, Paschke K, Oyarzún-Salazar R, Cheng C-HC, Navarro JM, Vargas-Chacoff L. 2021. Effects of warming rates on physiological and molecular components of response to CTMax heat stress in the Antarctic fish Harpagifer antarcticus. Journal of Thermal Biology. 99:103021. https://doi.org/10.1016/j.jtherbio.2021.103021

SC CAMLR. 2018. Report of the thirty-seventh meeting of the Scientific Committee. Hobart, Australia: CCAMLR; [accessed 2022 Dec 1]. https://meetings.ccamlr.org/en/sc-camlr-xxxvii

Sheiko BA. 2019. Comments on the nomenclature of genus-and family-series taxa of notothenioid fishes (Perciformes, Notothenioidei). Bionomina. 16(1):46–82.

Skóra KE. 1995. *Acanthodraco dewitti* gen. et sp. n (Pisces, Bathydraconidae) from Admiral Bay (King George Island, South Shetland Islands, Antarctica). Archive of fishery and marine research. 42(3):283–289.

Sutter J, Fischer H, Grosfeld K, Karlsson NB, Kleiner T, Van Liefferinge B, Eisen O. 2019. Modelling the Antarctic Ice Sheet across the mid-Pleistocene transition – implications for Oldest Ice. The Cryosphere. 13(7):2023–2041. https://doi.org/10.5194/tc-13-2023-2019

Trathan PN, Warwick-Evans V, Young EF, Friedlaender A, Kim JH, Kokubun N. 2022. The ecosystem approach to management of the Antarctic krill fishery - the 'devils are in the detail' at small spatial and temporal scales. Journal of Marine Systems. 225:103598. https://doi.org/10.1016/j.jmarsys.2021.103598

Vaillant LL. 1906. Sur une nouvelle espèce de Chaenichthys provenant de l'expédition antarctique francaise sous le commandement du Dr. Jean Charcot. Bulletin du Muséum National d'Histoire Naturelle (Série 1). 12(5):246–247.

Waite ER. 1916. Fishes. Australasian Antarctic Expedition Scientific Reports. 3:1–92.

Watters GM, Hinke JT, Reiss CS. 2020. Long-term observations from Antarctica demonstrate that mismatched scales of fisheries management and predator-prey interaction lead to erroneous conclusions about precaution. Scientific Reports. 10(1):2314. https://doi.org/10.1038/s41598-020-59223-9

Westerhold T, Marwan N, Drury AJ, Liebrand D, Agnini C, Anagnostou E, Barnet JSK, Bohaty SM, De Vleeschouwer D, Florindo F, et al. 2020. An astronomically dated record of Earth's climate and its predictability over the last 66 million years. Science. 369(6509):1383–1387. https://doi.org/10.1126/science.aba6853

Table 1. Collection information of Akarotaxis spp. specimens examined morphologically in this study (*Akarotaxis* n. sp. and *A. nudiceps*). We were unable to measure the holotype for *A. nudiceps* (#8) and *Akarotaxis* (#9) directly, but used measurements published in Dewitt & Hureau (1979).

Label #	Taxa	Voucher #	Genetic analysis?	SL (MM)	Collection date	Location	Depth (m)	Latitude	Longitude
1	*Akarotaxis* n. sp.	YPM ICH 24241	Yes	140.8	22-Apr-2010	Hugo-Anvers Trough, WAP	675	-64.739	-65.433
2	*Akarotaxis* n. sp.	YPM ICH 36536	Yes	135.8	22-Apr-2010	Hugo-Anvers Trough, WAP	675	-64.739	-65.433
3	*Akarotaxis* n. sp.	YPM ICH 20043	Yes	129.3	15-May-2008	Banana Trench, WAP	692	-66.266	-66.546
4	*Akarotaxis* n. sp.	YPM ICH 20045	Yes	127.3	15-May-2008	Banana Trench, WAP	692	-66.266	-66.546
5	*Akarotaxis* n. sp.	VIMS 45856	Yes	136	9-May-2018	Hugo-Anvers Trough, WAP	698-700	-64.753	-65.505
6	*Akarotaxis* n. sp.	OS 26108	No	133	20-Aug-2017	Hugo-Anvers Trough, WAP	690-705	-64.746	-65.481
7	*Akarotaxis* n. sp.	OS 26109	No	133	20-Aug-2017	Hugo-Anvers Trough, WAP	690-705	-64.746	-65.481
8	*A. nudiceps* (holotype)	SAM F-369	No	119	28-Jan-1914	Shackleton Ice Shelf	439	-65.330	95.450
9	*A. nudiceps* (paratype)	UMOD 148-1	No	129	26-Feb-1972	Adelaide Island, WAP	630-650	-67.260	-70.200
10	*A. nudiceps*	MNHN-2009-1057	Yes	105.2	31-Dec-2007	D'Urville Sea	839-860	-66.737	144.640
11	*A. nudiceps*	MNHN-2009-1074	No	117.3	4-Jan-2008	D'Urville Sea	689-710	-66.316	143.301
12	*A. nudiceps*	MNHN-2009-1075	No	97.2	4-Jan-2008	D'Urville Sea	689-710	-66.316	143.301

Table 2. Mean (± Standard Deviation) and ranges of meristic information of all *Akarotaxis spp.* specimens listed in Table 1. Means are reported as a percentage of standard length (SL). Meristic data highlighted in the manuscript are italicized and followed by an asterisk.

Specimen Group	***Akarotaxis* n. sp. (n=7)**	***A. nudiceps* type specimens (n=2)**	***A. nudiceps* (n=3)**
	Mean (+/- SD)	Mean (+/- SD)	Mean (+/- SD)
Standard length (SL)	131.7 ± 5.4	124 ± 7.1	106.6 ± 10.1
Head length (HL)	33.3 ± 1.0	33.9 ± 2.7	33.8 ± 0.9
Head width (HW)	14.2 ± 0.4	15.9 ± 3.2	14.3 ± 0.6
Head depth (HD)	10.5 ± 1.4	12.5 ± 2.1	9.5 ± 0.8
*Orbital diameter (O)**	9.0 ± 0.4	9.4 ± 1.3	8.4 ± 0.5
*Snout length (SnL)**	10.3 ± 0.4	10.6 ± 0.9	11.0 ± 0.1
Interorbital space (IO)	2.7 ± 0.3	2.6 ± 0.4	3.1 ± <0.0
Jaw length (UJL)	10.7 ± 0.5	11.8 ± 1.8	11.3 ± 0.2
Caudal peduncle length (CPL)	7.7 ± 0.3	7.0 ± 0.8	6.7 ± 1.0
Caudal peduncle depth (CPD) max	4.1 ± 0.8	3.4 ± 0.1	5.0 ±0.7
*Body depth [BD(AO)]**	12.7 ± 2.7	10.5 ± 0.4	8.8 ± 0.3
Predorsal-fin distance (Sn-D)	42.1 ± 1.3	44.2 ± 3.1	44.9 ± 0.3
Preanal-fin distance (Sn-AO)	53.2 ± 2.3	53.4 ±3.4	53.3 ± 0.4
Dist. between A origin and C base (AO-C)	47.2 ± 1.2	43.9 ± 1.6	46.7 ± 0.8
Dist. between V base and A origin (AO-V)	25.0 ± 1.4	24.7 ± 0.3	23.1 ± 1.1
Pectoral length (PL)	21.7 ± 1.6	23.8 ±1.6	22.8 ± 1.0
Pelvic length (VL)	19.1 ± 0.8	21.0 ± 0.5	19.9 ± 2.0
Caudal length (CL)	15.0 ± 0.6	17.9 ± 0.4	15.3 ± 1.2
*Orbital diameter / snout length (O/SnL)**	87.7 ± 4.4	88.9 ± 4.3	76.5 ± 5.2
*Snout length / head length (SnL/HL)**	30.9 ± 1.2	31.1 ± 0.2	32.6 ± 1.2
*Jaw length / head length (UJL/HL)**	32.0 ± 1.5	34.7 ± 2.7	33.5 ± 0.5
	Range	Range	Range
Anterior gill rakers (Ant GR)	(7-9) + 0 + (18-20)	9 + 0 + (19-20)	(7-8) + 0 + (17-21)
Posterior gill rakers (Post GR)	(3-4) + 0 + (14-18)	4 + (0-1) + (17-18)	(3-4) + 0 + (14-15)
Dorsal fin rays (D)	28 - 31	33 - 31	27 - 28
Anal fin rays (A)	25 - 28	27 - 28	24 - 25
Caudal fin rays (C)	12 - 13	12 - 13	12
Pectoral fin rays (P)	20 - 22	22 - 23	21
Lateral scales (LSc)	84 - 91	86 - 88	71 - 74
Upper lateral line scales (ULL)	3 - 5t	4 - 5t	4 - 6t
Branchiostegal rays (Br)	6	6	6
Pores in preoperculo-mandibular canal (PMP)	(8-9) / (7-9)	8 / 8	(7-9) / (7-8)
Pores in infraorbital canal (IOP)	7 / 7	7 / 7	7 / 7
Supraorbital pores (SOP)	4 + 1 + 4	(3-4) + 0 + (3-4)	4 + 1 + 4
Temporal pores (TP)	4 / 4	(3-5) / (3-4)	4 / 4
Pores in supratemporal canal (STP)	(2.5-3) / (2.5-3)	3 / 0	(2.5-3) / (2.5-3)

Table 3. Collection information of *Akarotaxis spp.* that were examined genetically.

Species	Label #	Voucher ID, if any	Field ID	Collection Date	Capture Location	Depth (m)	Latitude	Longitude	*mt-co1*	*mt-nd2*	*mt-cyb*
Akarotaxis n. sp.	1	YPM ICH 24241	Corso_62	4/22/2010	Hugo-Anvers Trough, WAP	675	-64.739	-65.433	TBD	TBD	TBD
Akarotaxis n. sp.	2	YPM ICH 36536	Corso_63	4/22/2010	Hugo-Anvers Trough, WAP	675	-64.739	-65.433	N/A	N/A	TBD
Akarotaxis n. sp.	3	YPM ICH 20043	Corso_61	5/15/2008	Banana Trench, WAP	692	-66.266	-66.546	TBD	HQ170108	TBD
Akarotaxis n. sp.	4	YPM ICH 20045	Corso_60	5/15/2008	Banana Trench, WAP	692	-66.266	-66.546	TBD	HQ170109	TBD
Akarotaxis n. sp.	5	VIMS 45856	Aka_18_07	5/7/2018	Hugo-Anvers Trough, WAP	698-700	-64.753	-65.505	TBD	TBD	N/A
Akarotaxis n. sp.	13	N/A	Aka_17_05	8/20/2017	Hugo-Anvers Trough, WAP	692-704	-64.747	-65.498	TBD	TBD	N/A
Akarotaxis n. sp.	14	N/A	Aka_17_06	8/20/2017	Hugo-Anvers Trough, WAP	692-704	-64.747	-65.498	TBD	TBD	N/A
Akarotaxis n. sp.	15	N/A	Aka_18_03	4/30/2018	Hugo-Anvers Trough, WAP	698	-64.750	-65.500	TBD	TBD	N/A
Akarotaxis n. sp.	16	VIMS 43571a	Corso_18	1/14/2019	Adelaide Island, WAP	773	-67.522	-70.591	TBD	TBD	N/A
Akarotaxis n. sp.	17	VIMS 43240	Corso_19	1/18/2020	Adelaide Island, WAP	387	-67.766	-68.241	TBD	TBD	N/A
Akarotaxis n. sp.	18	N/A	2008_Aka_1_Hugo	7/23/2008	Hugo-Anvers Trough, WAP	600	-64.807	-65.387	TBD	TBD	N/A
Akarotaxis n. sp.	19	N/A	2008_Aka_2_Hugo	7/23/2008	Hugo-Anvers Trough, WAP	600	-64.807	-65.387	TBD	TBD	N/A
Akarotaxis n. sp.	20	N/A	2008_Aka_4_Hugo	7/23/2008	Hugo-Anvers Trough, WAP	600	-64.807	-65.387	TBD	TBD	N/A
Akarotaxis n. sp.	21	N/A	2008_Aka_5_Lapeyrere	9/2/2008	Lapeyrere Bay, WAP	650	-64.408	-63.267	TBD	TBD	N/A
Akarotaxis n. sp.	22	N/A	2008_Aka_6_Lapeyrere	9/2/2008	Lapeyrere Bay, WAP	650	-64.408	-63.267	TBD	TBD	N/A
Akarotaxis n. sp.	23	N/A	2014_Aka_1_Hugo	7/18 to 8/8/2014	Hugo-Anvers Trough, WAP	630-690	-64.841	-65.370	TBD	TBD	N/A
Akarotaxis n. sp.	24	N/A	2014_Aka_2_Hugo	7/18 to 8/8/2014	Hugo-Anvers Trough, WAP	630-690	-64.841	-65.370	TBD	TBD	N/A
Akarotaxis n. sp.	25	N/A	2014_Aka_3_Hugo	7/18 to 8/8/2014	Hugo-Anvers Trough, WAP	630-690	-64.841	-65.370	TBD	TBD	N/A
Akarotaxis n. sp.	26	N/A	2014_Aka_4_Hugo	7/18 to 8/8/2014	Hugo-Anvers Trough, WAP	630-690	-64.841	-65.370	TBD	TBD	N/A
Akarotaxis n. sp.	27	N/A	2014_Aka_5_Hugo	7/18 to 8/8/2014	Hugo-Anvers Trough, WAP	630-690	-64.841	-65.370	TBD	TBD	N/A
Akarotaxis n. sp.	28	N/A	2014_Aka_6_Hugo	7/18 to 8/8/2014	Hugo-Anvers Trough, WAP	630-690	-64.841	-65.370	TBD	TBD	N/A
Akarotaxis n. sp.	29	N/A	2014_Aka_9_Hugo	7/18 to 8/8/2014	Hugo-Anvers Trough, WAP	630-690	-64.841	-65.370	TBD	TBD	N/A
Akarotaxis n. sp.	30	N/A	2014_Aka_10_Hugo	7/18 to 8/8/2014	Hugo-Anvers Trough, WAP	630-690	-64.841	-65.370	TBD	TBD	N/A
A. nudiceps	10	MNHN-2009-1057	si195n1467	12/31/2007	D'Urville Sea	839-860	-66.737	144.640	HQ712805	N/A	N/A
A. nudiceps	31	MNHN-2009-1098	si462n3046	1/15/2008	D'Urville Sea	896	-66.404	139.794	HQ712806	N/A	N/A
A. nudiceps	32	AN102	N/A	2020	Amundsen Sea	627	-73.520	-113.350	OK493722	N/A	N/A
A. nudiceps	33	AN103	N/A	2020	Amundsen Sea	627	-73.520	-113.350	OK493723	N/A	N/A
A. nudiceps	34	AN123	N/A	2020	Amundsen Sea	627	-73.520	-113.350	OK493743	N/A	N/A
A. nudiceps	35	N/A	N/A	2012	Elephant Island, AP	N/A	N/A	N/A	NC_057664	NC_057664	NC_057664
A. nudiceps	36	TJN 1795	AnudA	NA, pre-2003	Terra Nova bay, Ross Sea	N/A	-75.033	166.267	N/A	AY249486	N/A
A. nudiceps	37	N/A	PS77-248-3	3/7/2011	Larsen Ice Shelf, Weddell Sea	430	-65.551	-60.197	N/A	N/A	KJ721597
A. nudiceps	38	N/A	CHINARE-31_136	2015	Prydz Bay	103	-67.242	73.045	*	N/A	N/A
A. nudiceps	39	N/A	CHINARE-31_137	2015	Prydz Bay	103	-67.242	73.045	*	N/A	N/A
A. nudiceps	40	N/A	CHINARE-31_143	2015	Prydz Bay	103	-67.242	67.978	*	N/A	N/A
A. nudiceps	41	N/A	CHINARE-31_144	2015	Prydz Bay	103	-67.242	67.978	*	N/A	N/A
A. nudiceps	42	N/A	CHINARE-31_145	2015	Prydz Bay	103	-67.242	67.978	*	N/A	N/A
A. nudiceps	43	N/A	CHINARE-31_146	2015	Prydz Bay	103	-67.242	65.481	*	N/A	N/A
A. nudiceps	44	N/A	CHINARE-31_147	2015	Prydz Bay	103	-67.242	65.481	*	N/A	N/A
A. nudiceps	45	N/A	CHINARE-31_148	2015	Prydz Bay	103	-67.242	65.481	*	N/A	N/A
A. nudiceps	46	N/A	CHINARE-31_149	2015	Prydz Bay	103	-67.242	65.481	*	N/A	N/A
A. nudiceps	47	N/A	CHINARE-31_150	2015	Prydz Bay	653	-69.120	65.481	*	N/A	N/A
A. nudiceps	48	N/A	CHINARE-29_S20	2013	Prydz Bay	735	-67.999	65.481	*	N/A	N/A

** mt-co1 sequences not publicly available but obtained from the authors of Li et al. (2022) (https://doi.org/10.1016/j.dsr2.2022.105140)*

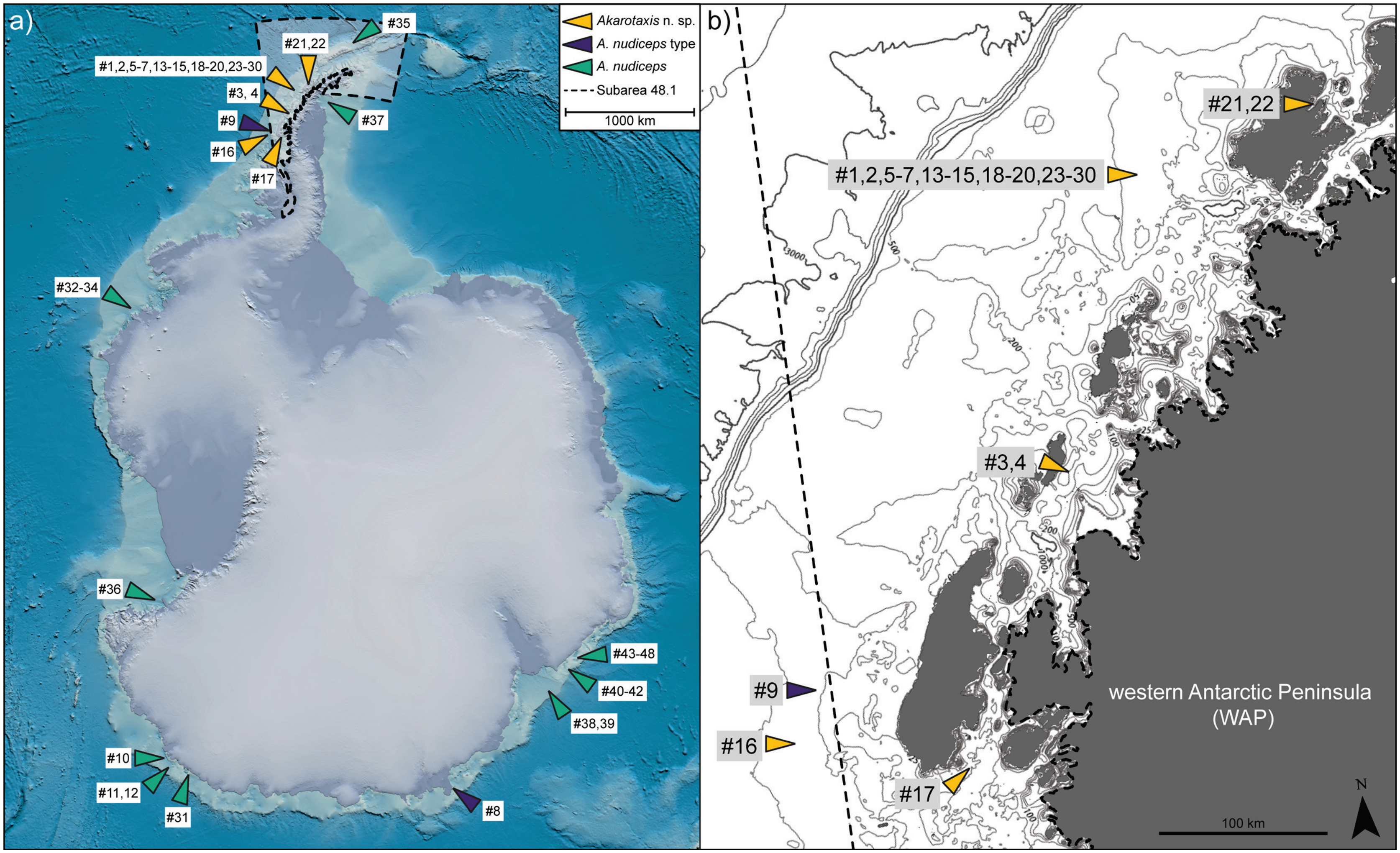

Figure 1. Maps of a) all *Akarotaxis* spp. collection sites, with *Akarotaxis* n. sp. market by yellow arrows, the holotype and paratypes of *A. nudiceps* (#8) and *Akarotaxis* (#9) by purple, and all other *A. nudiceps* marked by green; b) a magnified visualization of all known *Akarotaxis* n. sp. collection sites near the western Antarctic Peninsula (WAP), with bathymetric information in meters. In both maps, numbers for each location correspond to the Label #'s in Tables 1 and 3 and the CCAMLR subarea 48.1 is shown by a dashed line.

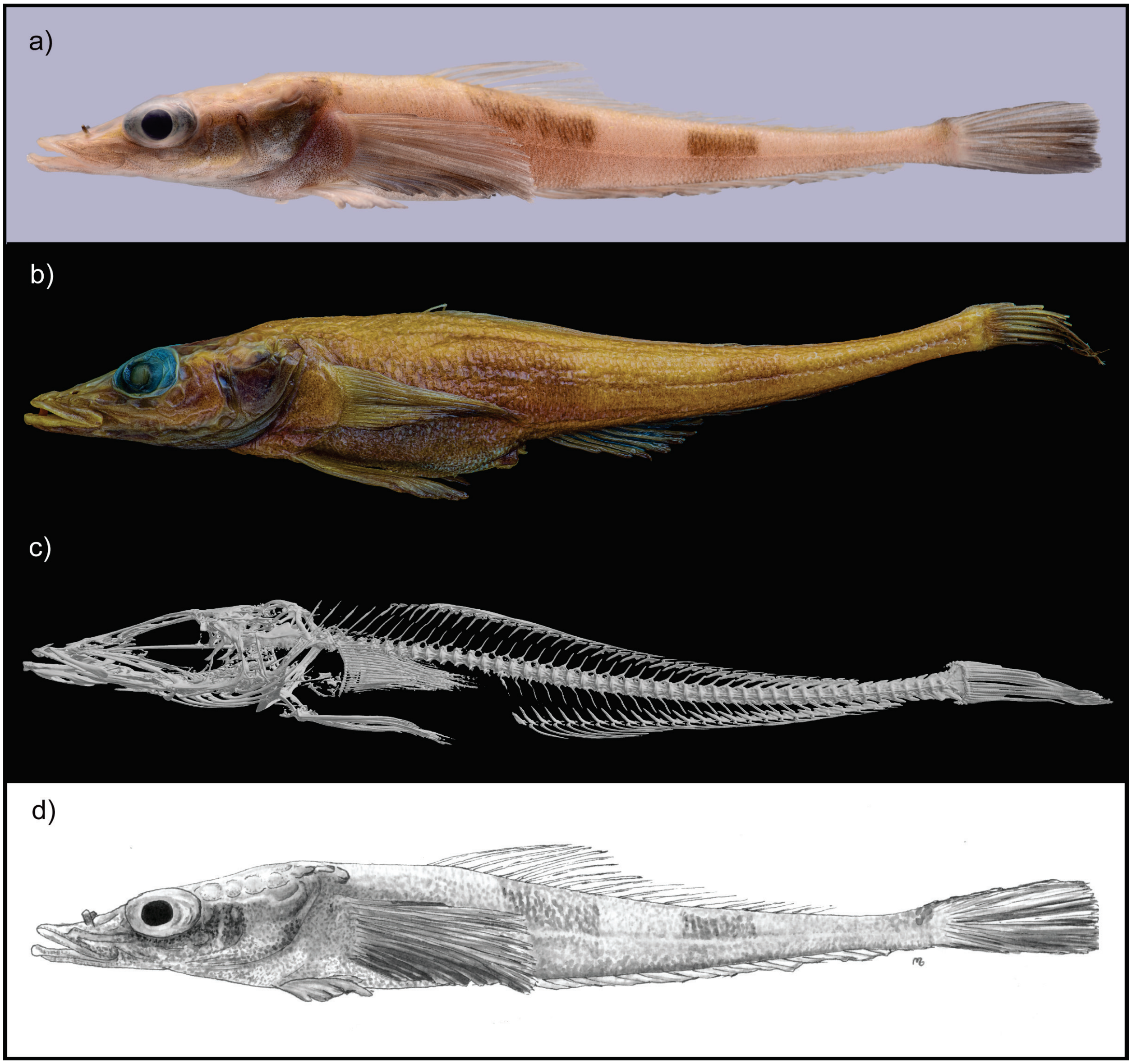

Figure 2. *Akarotaxis* n. sp. a) alive, collected and photographed by C.H. Cheng off the western Antarctic Peninsula (WAP) on 08-09-2014 but not preserved, b) YPM ICH 24241 (holotype), c) CT scan of YPM ICH 24241 (OVERT 05053), and d) illustration by Marissa Goerke.

Figure 3. Images of preserved *Akarotaxis* n. sp., a) YPM ICH 20043, b) YPM ICH 20045, c) YPM ICH 24241, and ICH 36536, and *Akarotaxis nudiceps,* e) MNHN 2009-1057, f) MNHN 2009-1074, g) MNHN 2009-1075, and h) AMS IA.484. All scale bars are 1 cm.

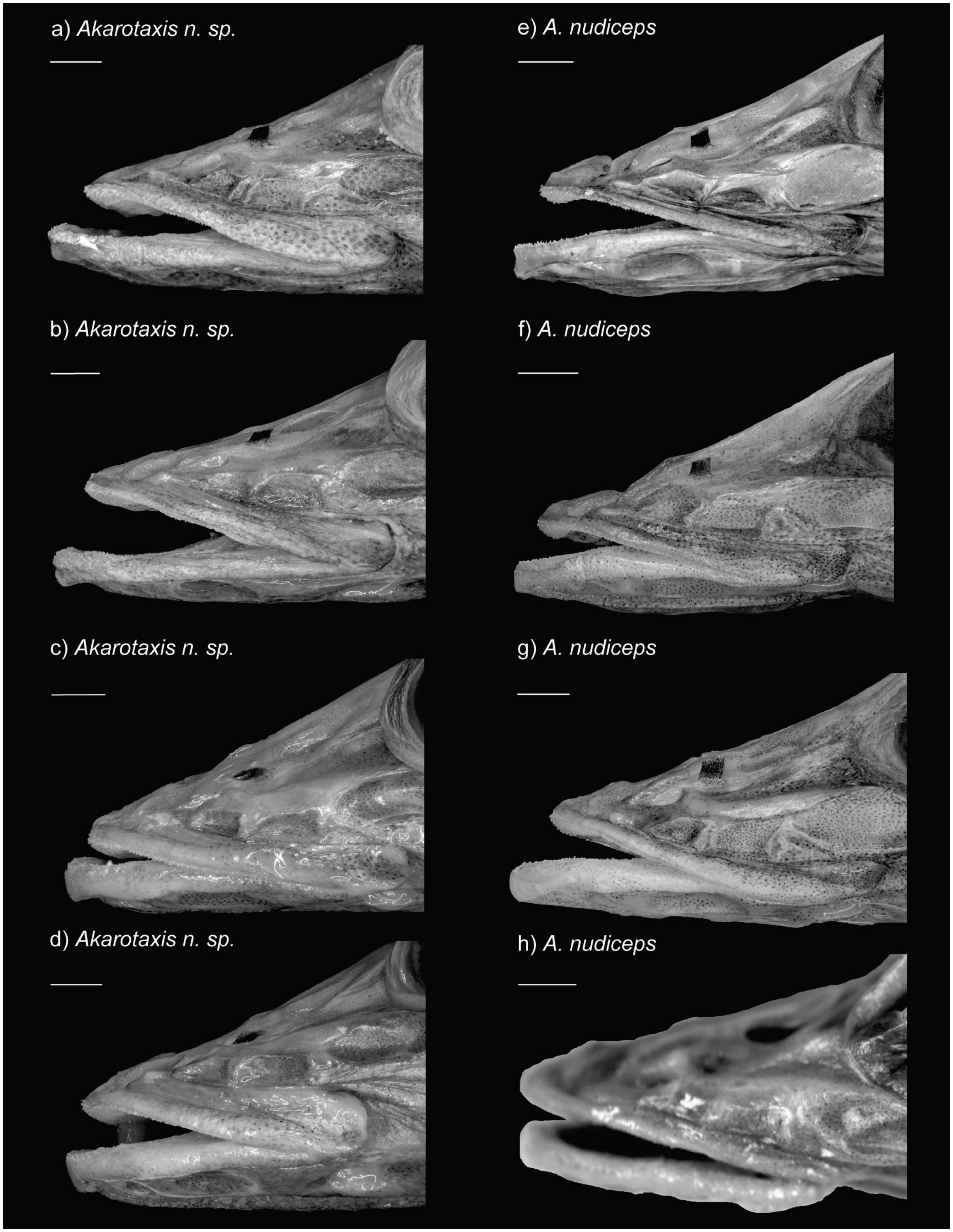

Figure 4. Snout comparison of *Akarotaxis* n. sp. [a) YPM ICH 20043, b) YPM ICH 20045, c) YPM ICH 24241, and ICH 36536] and *Akarotaxis nudiceps* [e) MNHN 2009-1057, f) MNHN 2009-1074, g) MNHN 2009-1075, h) AMS IA.484]. All scale bars are 2 mm, color images were converted to grayscale in order to highlight morphology.

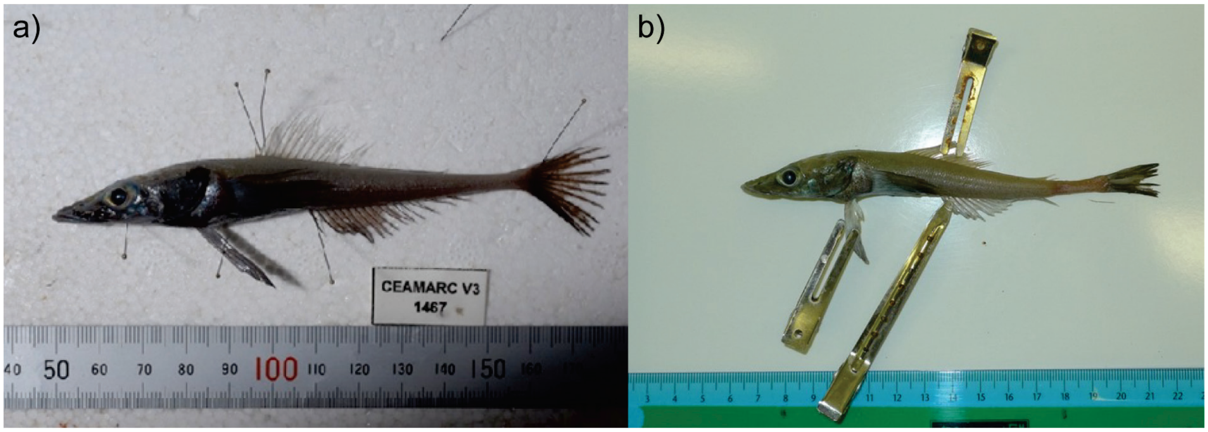

Figure 5. Live photographs of two specimens that were molecularly verified as *A. nudiceps* a) MNHN-2009-1057, Label #10 (**Tables 1 – 3**) and b) PS77-248-3, Label #37 (**Table 3**). Note the absence of dark bands on both specimens.

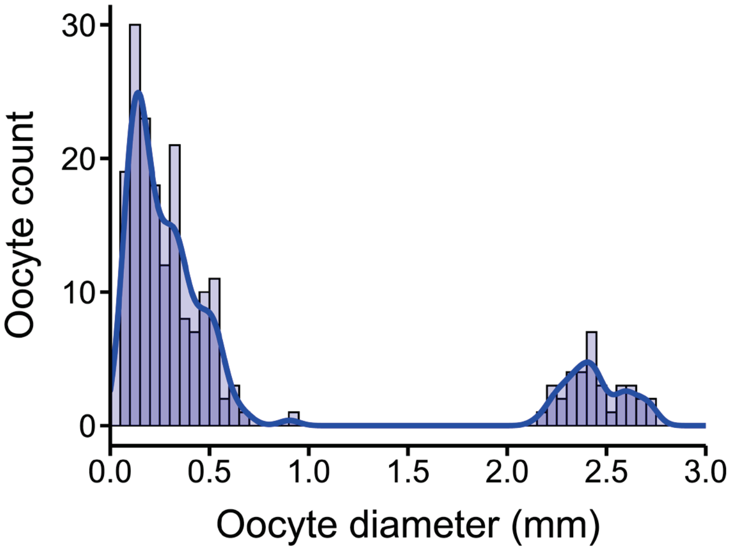

Figure 6. Oocyte (egg) diameter of one gravid *Akarotaxis* n. sp. (Aka_17_6, SL = 153 mm).

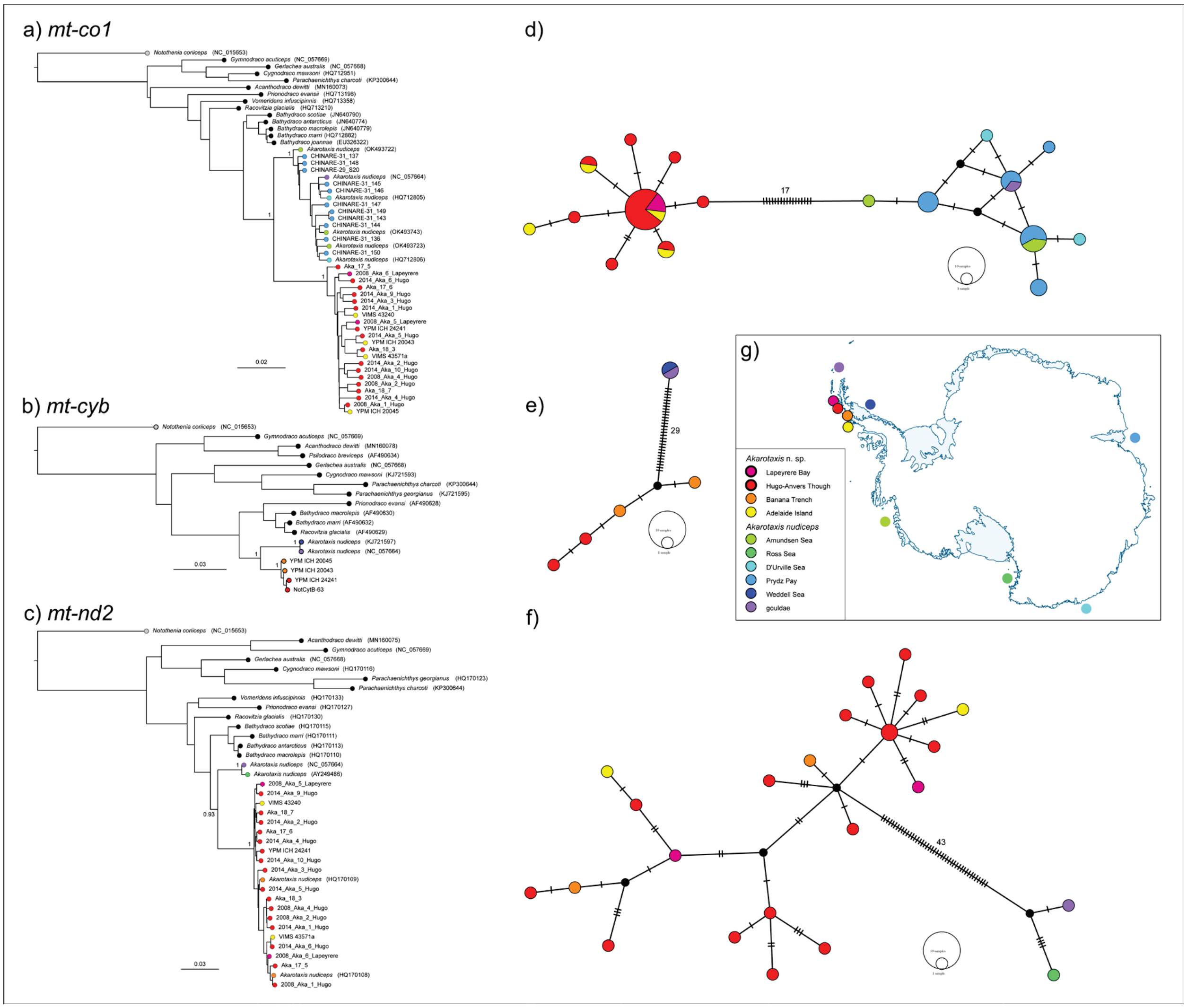

Figure 7. Bayesian-estimated phylogenetic trees (a-c) and haplotype networks (d-f) for mitochondrial genes used in this study – *mt-co1* (a, d), *mt-cyb*, (b, e), and *mt-nd2* (c, f). Circles corresponding to *Akarotaxis* spp. in the trees are colored to match the haplotype diagrams and distribution map (g). Scales bars for trees indicate substitution rate and scale circles for haplotype networks indicate sample size for each haplotype.

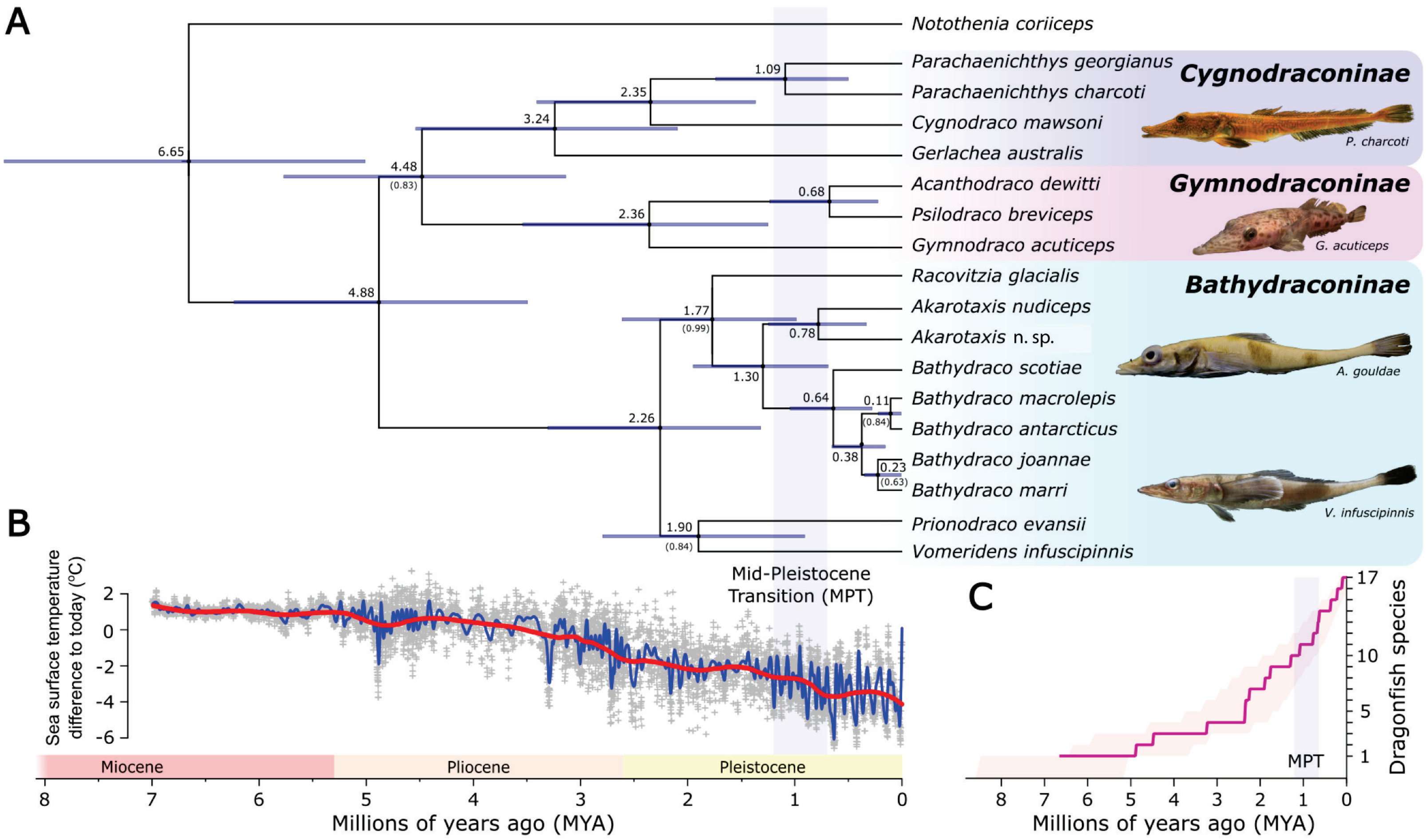

Figure 8. a) Time-calibrated phylogeny of Bathydraconidae based on three markers (*mt-nd2*, 22 *mt-co1*, and *mt-cyb*). Divergence estimates are labeled, with blue shading representing the 95% highest posterior density interval (HPD). b) Sea surface temperature anomalies with respect to average global temperature from 1961-1990 following (Westerhold et al. 2020). Loess smoothed curves are overlaid with a window span corresponding to 40,000 years (blue) and 1 million years (red). c) Divergence of Bathydraconidae based on the time-calibrated phylogeny, with the Mid-Pleistocene Transition (MPT) highlighted.

Supplemental Table 1. Accession numbers of additional sequences used in the phylogenetic analyses.

Species	*mt-co1*	*mt-nd2*	*mt-cyb*
Acanthodraco dewitti	MN160073	MN160075	MN160078
Bathydraco antarcticus	JN640774	HQ170113	N/A
Bathydraco joannae	EU326322	N/A	N/A
Bathydraco macrolepis	JN640779	HQ170110	AF490630
Bathydraco marri	HQ712882	HQ170111	AF490632
Bathydraco scotiae	JN640790	HQ170115	N/A
Cygnodraco mawsoni	HQ712951	HQ170116	KJ721593
Gerlachea australis	NC_057668	NC_057668	NC_057668
Gymnodraco acuticeps	NC_057669	NC_057669	NC_057669
Parachaenichthys charcoti	KP300644	KP300644	KP300644
Parachaenichthys georgianus	N/A	HQ170123	KJ721595
Prionodraco evansii	HQ713198	HQ170127	AF490628
Psilodraco breviceps	N/A	N/A	AF490634
Racovitzia glacialis	HQ713210	HQ170130	AF490629
Vomeridens infuscipinnis	HQ713358	HQ170133	N/A
Notothenia corriceps	NC_015653	NC_015653	NC_015653
Akarotaxis n. sp. *	COI_62_4	AK17-6	NotCytB-60
Akarotaxis nudiceps *	NC_057664	NC_057664	NC_057664

* Sequences used for the time-calibrated phylogeny.

Supplemental Table 2. Results of the genetic polymorphism analysis. Grey cells highlight results of analyses performed for thoroughness but however unreliable due to extremely small sample sizes.

		Sequences #	Segregating sites	Haplotype #	Haplotype Diversity	Nucleotide Diversity	Tajima's Test	
Marker	Species	N	S	h	H_d	π	D	p-value
mt-co1	*A. nudiceps*	16	7	9	0.9	0.002949	-0.32219	0.4145
	Akarotaxis n. sp.	19	11	11	0.7895	0.002069	-2.05915	0.0071
mt-nd2	*A. nudiceps*	2	5	2	1	0.004808	0	1
	Akarotaxis n. sp.	22	29	21	0.9957	0.005179	-1.24154	0.0956
mt-cyb	*A. nudiceps*	2	0	1	0	0	0	1
	Akarotaxis n. sp.	4	4	4	1	0.002016	-0.06501	0.5894

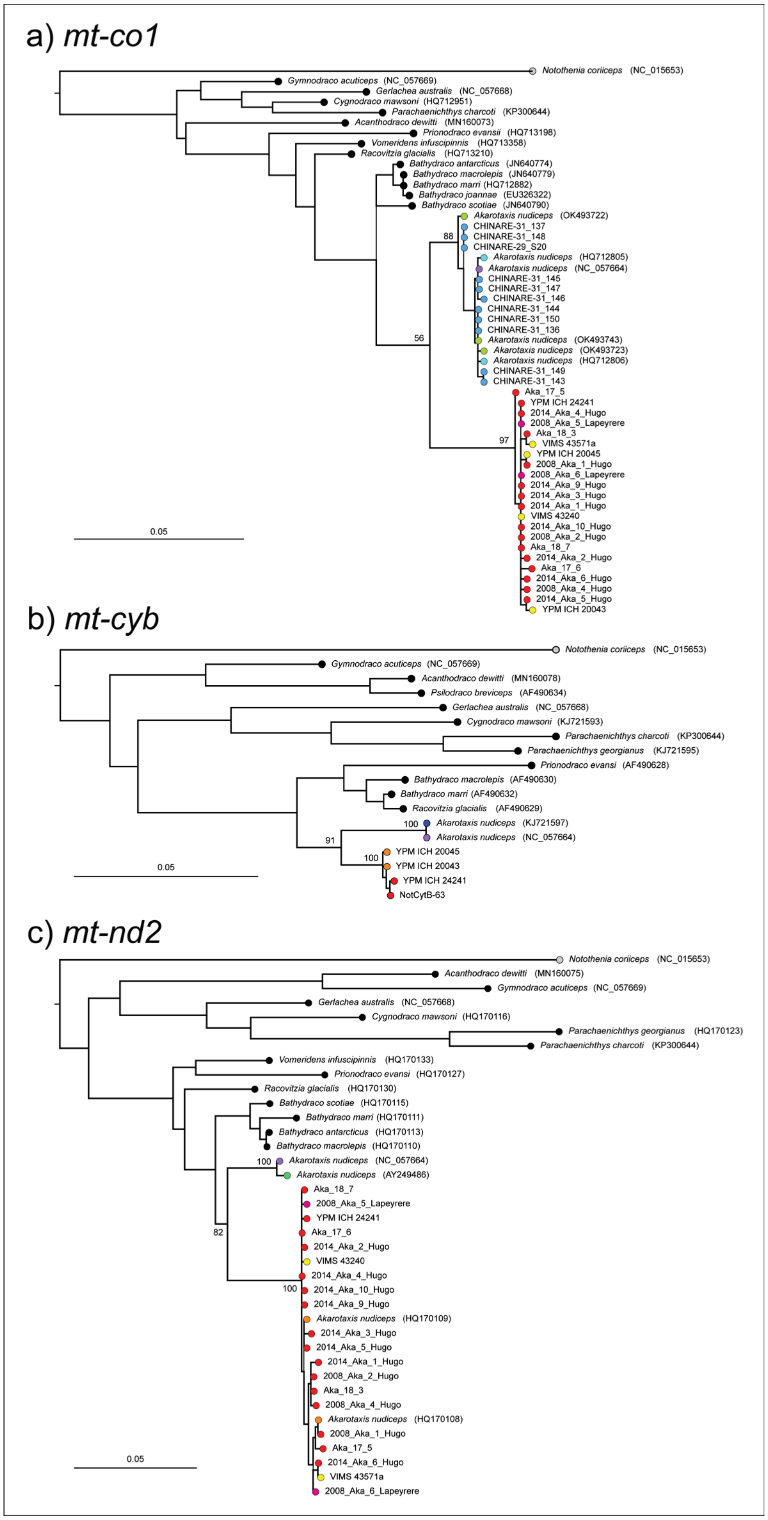

Supplemental Figure 1. Maximum likelihood estimated phylogenetic trees for mitochondrial genes used in this study. Circles corresponding to *Akarotaxis* spp. in the trees are colored to match the haplotype diagrams (Fig 7d-h) and distribution map (Fig 7g). Scale bars indicate substitution rate.

CHAPTER 5
Biotic and abiotic factors that shape the phenology of an Antarctic larval fish assemblage

This chapter is in preparation for submission as: Corso AD, Steinberg DK, Conroy JA, Moffat C, Nolan M, Nardelli S, Klink J, Dinniman M, and Hilton EJ. Biotic and abiotic factors that shape the phenology of an Antarctic larval fish assemblage.

Abstract

Seasonal fluctuations of sunlight and sea ice in polar regions present unique constraints on the life histories of marine organisms. The western Antarctic Peninsula (WAP) has experienced long-term increase in ocean temperature and reduction in the duration of sea ice coverage. We investigated the phenology of larval fishes at two coastal stations in the northern WAP during austral spring and summer in two years of contrasting sea ice conditions (2017-2018 and 2018-2019). We quantified the abundance, taxonomic composition, and growth of larval fishes collected in weekly net tows. A multivariate model incorporating phytoplankton, zooplankton, and physical forcing was used to elucidate biotic and abiotic drivers influencing larval fish phenology. Output from a high-resolution regional numerical model back-calculated the dispersion pathways of yolk-sac larvae to approximate adult spawning locations. The larval fish assemblage was dominated by five taxa belonging to the family Nototheniidae: *Lindbergichthys nudifrons, Trematomus newnesi*, *Nototheniops larseni*, *Trematomus scotti*, and *Lepidonotothen squamifrons.* The taxonomic composition was relatively consistent between years, although we observed a large inerannual shift in the total abundance of *T. newnesi* and *L. nudifrons*. Results of the multivariate model suggest this shift was influenced by the phenology of the copepod *Calanus propinquus* and diatoms, which was driven by changes in sea ice dynamics. We also observed significant correlations between larval fish abundance and ocean temperature and salinity. All five fish species were captured earlier in 2018 – 2019 which we theorize is due to increased light availability from reduced sea ice coverage. Finally, the dispersion model identified potential spawning areas for *T. newnesi* in the WAP region. This study offers insights into current phenological trends in this unique larval fish assemblage, while providing a roadmap for future surveys of adult notothenioid reproduction in the Anvers Island region.

1. Introduction

Characterizing seasonal environmental factors that impact the timing of organisms' periodic life-history events (i.e., phenology) is a foundational component of ecology (Sydeman and Bograd 2009; Pau et al. 2011). Phenological studies initially focused on terrestrial and lacustrine ecosystems (Sydeman and Bograd 2009; Asch 2015), but over the last 25 years there has been increasing focus on climate-mediated phenological impacts in the marine environment (Edwards and Richardson 2004; Burrows et al. 2011; Asch 2015). In their global meta-analysis, Chmura *et al.* (2019) show marine species generally shift their phenology more frequently, more rapidly, and in greater magnitude than terrestrial species when exposed to similar changes in temperature (Poloczanska et al. 2013; Chambers et al. 2013). However, generalizing phenological trends across marine taxa must be done cautiously as an array of variables, such as life history, habitat latitude, physiological tolerances, evolutionary history, and community composition, can impact phenological plasticity (Poloczanska et al. 2016; Chmura et al. 2019).

The spawning period of temperate fishes is thought to be relatively fixed, and therefore mortality of larval fishes is regulated by the timing of the spring phytoplankton bloom and in turn resulting abundance of zooplankton (e.g., copepods), the main prey of many larval fishes (Cushing 1972; Cushing 1990; Kristiansen et al. 2011). However, the lack of ichthyoplankton time series with concurrent data on lower trophic levels and relevant physical variables hinders efforts to test this match-mismatch theory, especially in pelagic ecosystems outside the temperate Atlantic and Pacific oceans (Robert et al. 2014). Light availability in high-latitude ecosystems limits the duration of phytoplankton blooms (Vernet et al. 2008; Joy-Warren et al. 2019), which results in shortened growing seasons for zooplankton and fishes compared to low-latitude ecoystems. Consequently, the phenology of polar organisms is hypothesized to be primarily driven by environmental factors (e.g., sea ice, light, and temperature) (Pau et al. 2011).

High-latitude ecosystems are disproportionally impacted by climate change (Hoegh-Guldberg and Bruno 2010) and therefore are where phenological responses to climate changes may be pronounced. The region surrounding the western Antarctic Peninsula (WAP) has experienced widespread environmental perturbation due to climate change. Over the last 30 years, ocean continental shelf temperatures along the WAP have warmed by 0.1 to 0.3° C per decade (Schmidtko et al. 2014) resulting in a 3-month reduction in annual sea ice coverage since the 1970s (Stammerjohn et al. 2008; Stammerjohn et al. 2012; Parkinson 2019). Long-term and interannual changes in WAP community composition at all trophic levels are tied to these changes, including phytoplankton (Schofield et al. 2017; Lin et al. 2021), zooplankton (Steinberg et al. 2015), fishes (Corso et al. 2022), sea birds (Cimino et al. 2016), and whales (Pallin et al. 2023). Recently, seasonal and phenological changes in plankton community structure nearshore have also been examined. Nardelli *et al.* (2023) described the dynamics and environmental drivers of seasonal phytoplankton succession patterns during a short sea ice season with rapid retreat (2017 – 2018) and a long sea ice season with slow retreat (2018 – 2019). In addition, Conroy *et al.* (2023) characterized regional phenology of copepods and other zooplankton during these two contrasting years, while Cimino *et al.* (2023) analyzed three decades of phenological metrics in relation to Adélie penguin reproduction. However, few prior studies have investigated the phenology of larval fishes along the WAP (Loeb et al. 1993; Kellermann 1996).

Fishes of the suborder Notothenioidei dominate the species diversity in the WAP region. Adult notothenioids typically inhabit the benthos of the coast and continental shelf (Daniels and Lipps 1982; Gon and Heemstra 1990; Casaux et al. 2003; Jones et al. 2009; Trokhymets et al. 2022), while larval and juvenile notothenioids are pelagic (Loeb et al. 1993; Donnelly and Torres 2008). The spawning and early life history characteristics of notothenioids vary widely across taxa and regions, but many notothenioids in the WAP region spawn during the austral winter (June – August) and larvae hatch at the beginning of summer (November – December) during the peak in phytoplankton productivity. Hatching succession in the most abundant notothenioid species of the WAP area was documented by Loeb *et al.* (1993). These larvae co-occur spatially and consume similar prey, which primarily consists of all life stages of calanoid and cyclopoid copepods, krill eggs, and diatoms. Therefore, Loeb *et al.* (1993) posit temporal succession in hatching is an important evolutionary development to limit competition for prey. Kellermann (1996) observed a similar hatching succession, and further postulated that an early sea ice retreat will likely cause mismatches between larval fishes and their prey. Several calanoid copepods emerge from diapause immediately following sea ice retreat and ascend to the near-surface waters to feed, molt, and spawn (Kellermann 1996; Schnack-Schiel 2002). The extent and duration of winter sea ice also impacts the spawning success of Antarctic krill (*Euphausia superba*), with greater sea ice duration leading to more diatoms which facilitates higher *E. superba* egg production (Saba et al. 2014).

In this study, we investigate phenology of larval fishes near Anvers Island, a coastal site on the WAP, during the same two years of contrasting sea ice conditions studied for other taxa. We first describe the taxonomic composition, seasonal succession, and growth of larval fishes.

We then develop a multivariate model that incorporates phytoplankton, zooplankton, and physical forcing to examine the biotic and abiotic drivers influencing fish phenology in the context of the 'match-mismatch' hypothesis. Finally, we model the dispersion pathways of yolk-sac larvae of *T. newnesi* to back-calculate approximate spawning locations. We discuss the possible consequences of continued and intensifying climate change on the future of this unique assemblage of fishes.

2. Materials and Methods

Data and sample collection

Data and samples were collected from two coastal locations (Stations B and E) near Anvers Island, along the western Antarctic Peninsula (Fig 1). The two stations were usually sampled twice weekly using a rigid-hulled inflatable boat, at approximately the same time of day (between 10:00 to 15:00 local time) over two consecutive years: 17 November 2017 – 12 March 2018 and 6 November 2018 – 11 March 2019.

Physical data

Ocean temperature and salinity were determined using a SeaBird Electronics Seacat SBE 19plus sensor (CTD) deployed to 65m at both stations. We included temperature and salinity from the surface (5m), 20m, and 50m depths in our analysis. Sea ice dynamics were determined by Nardelli *et al.* (2023) following methods from Stammerjohn et al. (2008). Satellite-derived daily sea ice concentration was calculated using the Goddard Space Flight Center Bootstrap algorithm (v3.1) and extracted for the 25km x 25km satellite pixel closest to Palmer Station to determine sea ice metrics, including day of ice-edge advance and day of ice-edge retreat

(Nardelli et al. 2023). Local tidal regime did not impact zooplankton taxonomic structure over these two seasons at Stations B and E (Conroy *et al.* 2023) and was thus excluded in our multivariate analysis.

Larval fish and zooplankton collection and processing

Plankton net tows for sampling larval fishes and zooplankton were performed as described in Conroy et al. (2023). A 1-m^2 frame Metro net (700-µm mesh) was used to quantify larval fishes and krill (*E. superba* and *Thysanoessa macrura*) and a 1-m diameter circular ring net (200-µm mesh) for larval fishes and copepods. Both nets were towed obliquely to 50m, and duplicate samples were collected with the 1-m^2 frame Metro net at each station. A General Oceanics flowmeter was placed at the opening of both nets to calculate water volume filtered by the net and a Star-Oddi Data Storage Tag (DST) centi-TD was attached to record tow depth.

Larval fishes were preserved in 95% ethanol at Palmer Station and archived in the Nunnally Ichthyology Collection at the Virginia Institute of Marine Science (VIMS). Fishes were identified and measured from the upper jaw to the end of the notochord (SL) to the hundredth of a millimeter using a stage micrometer mounted on a Zeiss dissecting microscope. Several larvae were also photographed using Zeiss Discovery V20 stereomicroscope and used Z-stacking to increase the depth of field. Adobe Photoshop was used to adjust color, contrast, and background of the images, but no alterations to the subjects were made. Adobe Illustrator © was used to assemble images.

Zooplankton collected at each station were processed as described in Conroy et al. (2023). Briefly, zooplankton collected in one of the replicate ring net tows at each station were preserved in 4% buffered formaldehyde and later processed at VIMS. The ring net samples were size-fractionated with nested mesh sizes into five size classes: 0.2 – 0.5, 0.5 – 1, 1 – 2, 2 – 5, and > 5mm. All copepods in the three largest size classes (>1mm) were identified and counted. The smaller two size classes (0.2 – 1mm) were divided using a Folsom plankton splitter and subsamples of at least 1/64 of the total copepods were identified and counted. The > 1mm size class consisted primarily of three copepod taxa: *Calanoides acutus*, *Calanus propinquus*, and *Rhincalnus gigas*. The 0.2 – 1mm size class consisted primarily of two taxa: *Oithona* spp. and small calanoids.

Phytoplankton data collection and processing

Five phytoplankton groups (diatoms, cryptophytes, prasinophytes, haptophytes, and mixed flagellates) were determined with high-performance liquid chromatography (HPLC) as described in Nardelli *et al.* (2023) following methods from Carvalho *et al.* (2020). Immediately following collection, water samples were filtered onto 25mm GF/F filters and flash frozen in liquid nitrogen. Samples were processed using an Agilent 1100/12000 series system with a Diode Array Detector (Model G1315C, scanning wavelengths 275–800 nm) with a Zorbax Eclipse Plus C18 column to separate pigments. HPLC output data was separated into the five phytoplankton groups using CHEMTAX V1.95 and pigment ratios derived from phytoplankton collected in a similar region of the WAP (Kozlowski et al. 2011; Nardelli et al. 2023).

Multivariate model and ridgeline plot

To evaluate abiotic and biotic drivers of larval fish phenology, we developed generalized linear latent variable models (GLLVMs; Moustaki & Knott, 2000; Niku *et al.*, 2017) in the statistical program R (R Core Team 2022). Latent variable models, which are a form of Joint Species Distribution Models, are a function of both measured and unmeasured (latent) predictors (Warton et al. 2015). In LVMs, latent predictors can account for between-species and spatial correlations (Hui et al. 2022). GLLVMs expand on the structure of single-species generalized linear model (GLM) framework to include latent variables with a factor analytic approach to model multivariate data (Hui et al. 2017; Niku et al. 2019; van der Veen et al. 2021). In the recently developed R package gllvm, there are several distributions that accommodate zero-inflated multivariate abundance data (e.g., zero-inflated Poisson) and the inclusion of an autoregressive component to account for temporal correlation (Niku et al. 2019). Therefore, we opted to proceed with a GLLVM framework for this study.

We selected the five most abundant larval fish taxa across both years to include as response variables in the GLLVM (see Results – Community composition). We used untransformed abundance data for these species with tow volume included as an offset variable. To account for the temporal autocorrelation on the time series, we applied an autoregressive(1) [AR(1)] correlation structure to tow date. As the abundance data of the larval fishes is zero-inflated, we used a zero-inflated Poisson (ZIP) distribution in the GLLVM. We first selected a baseline model with ocean temperature and salinity based on the lowest Akaike information criterion (AIC). Then, we progressively added zooplankton and phytoplankton covariates to candidate models (Supp. Table 1). We selected the final model based on hypothesis testing, parsimony, and AIC.

To visualize peaks in the abundance of the five dominant larval fish taxa, we constructed a ridgeline plot in R using the package ggridges (Wilke 2022). The start of weekly net tows was slightly different between seasons, with the first quantitative net tow (i.e., fully processed) in 2017 – 2018 starting on November 24 and the first tow in 2018 – 2019 starting on November 8. To standardize this visualization, we removed all abundance data collected before December.

Larval fish dispersion model

We used output from a high-resolution regional numerical model (Haidvogel et al. 2008) to evaluate possible hatching sites and dispersion pathways for the yolk-sac larvae of *Trematomus newnesi* Boulenger 1902 captured at Station E. The Regional Ocean Modeling System (ROMS) was configured to encompass the entire WAP shelf with a 1.5 km horizontal resolution and 24 vertical levels that are distributed to provide higher resolution near the surface and the bottom. Details of the configuration of the model can be found in Graham *et al.* (2016) and Hudson et al (2021). Simluated releases of neutrally buoyant particles around Palmer Deep Canyon were modelled every two days from November 1, 2008 to the end of March, 2009 at 10, 120 and 300 m. From these, a subset of particles was selected for further study.

We focused this analysis on the smallest and youngest larvae captured, with adequate information on larval growth, to reduce uncertainty in the model. Swimming speeds of yolk-sac larvae are difficult to measure but are assumed to be relatively weak, especially in high latitude regions (Moyano et al. 2016). Based on the maximum sustained horizontal swimming speed of similarly sized Atlantic herring yolk-sac larvae (< 0.6 cm s^{-1}), we assumed yolk-sac larvae in the model to be freely drifting. We collected two *T. newnesi* yolk-sac larvae at Station E on 30 Nov. 2017 (7.5 mm SL) and 04 Dec. 2017 (7.3 mm) (Fig 3b). Based on the estimated age of *T. newnesi* yolk-sac larvae collected in the WAP region (Radtke et al. 1989), we determined the two yolk-sac larvae to be approximately 14 to 17 days old. Based on hatching observations and larval distributions, we also assumed larvae immediately transition to the epipelagic zone (≤150 m) after hatching (Hourigan and Radtke 1989).

To study potential pathways for larval advection, we analyzed the particles that reach an area within 3 km (or roughly two model grid points) from Station E during November and December. To match the depths of net tows, only particles that reached depths ≤ 120m were considered. We then analyzed the paths of this subset 17 days prior to the arrival time of each particle. We created a heatmap in Matlab using the package geodensityplot to highlight dense clusters of particles. The package uses Kernal Density Estimate to calculate the density of points within a 10 km radius.

3. Results

Larval fish community composition, growth, and seasonal dynamics

During the 2017 – 2018 sampling season, a total of 277 larval fishes were captured at Stations B and E (n = 239 and 38, respectively). In the 2018 – 2019 season, 281 total larval fishes were collected (n = 224 and 57, respectively) (Table 1). The larval fish assemblages of both seasons were primarily composed of five species: *Lindbergichthys nudifrons* (Lönnberg

1905), *Trematomus newnesi*, *Nototheniops larseni* (Lönnberg 1905), *Lepidonotothen squamifrons* (Günther, 1880), and *Trematomus scotti* (Boulenger, 1907) (Table 1; Figs 2a, 3). *Trematomus newnesi* was the most abundant taxon in 2017-2018, while *L. nudifrons* was the most abundant species during 2018 – 2019 (Fig 2a).

Several other taxa were rarely captured during both seasons, including the harpagiferid *Harpagifer antarcticus* Nybelin 1947, the myctophid *Electrona antarctica* (Günther, 1878), the chanichthyids *Champsocephalus gunnari* (Lönnberg 1905) and *Psuedochaenichthys georgianus* Norman 1937, the nototheniids *Trematomus pennellii* Regan 1914 and *Trematomus lepidorhinus* (Pappenheim 1911), the paralepidid *Notolepis coatsorum* Dollo 1908, and the muraeonlepidid *Muraenolepis spp*. Gunther 1880 (Table 1; Fig 2b). Larvae of *E. antarctica* were all preflexion (Fig 4a,b) and three larval *H. antarcticus* collected on 5 and 8 March 2018 had their yolk-sacs intact (Fig 4c,d).

The abundance distributions for *L. nudifrons* and *T. newnesi* shifted similarly between seasons, with *L. nudifrons* mean, or peak, abundance occurring 15 days earlier and *T. newnesi* 26 days earlier in the 2018 – 2019 season (Fig 5). Although *N. larseni*, *T. scotti*, and *L. squamifrons* also occurred earlier in the 2018 – 2019 season, their shifts were not as pronounced as those of *L. nudifrons* and *T. newnesi* (Fig 5). The 2018 – 2019 season (178d duration) had an ice advance 16 days earlier and an ice retreat 24 days later than the 2017 – 2018 season (138d duration). We fit linear regressions to the measurement series of the five most abundant species (Fig 6) and used linear coefficients as an approximation of daily growth rates (mm day $^{-1}$) (Table 2). Daily growth rates changed little between years for all taxa except *T. newnesi*, which had its growth rate double (0.100 ± 0.03 SE mm day $^{-1}$) in 2018 – 2019 compared to 0.052 ± <0.001 SE mm day $^{-1}$ in 2017 – 2018, but standard error also greatly increased with the 2018 – 2019 estimate (Table 2; Fig 6). *Lindbergichthys nudifrons* and *N. larseni* both had larger intercepts in 2018 – 2019.

Environmental and biotic factors affecting larval fish abundance

In baseline multivariate models used to examine potential biotic and abiotic factors affecting larval abundance, we found ocean temperature at 20m and salinity at 50m minimized AIC (Supp. Table 1). In the final model (see Supp. Table 1 for selection process), we found the copepods *C. propinquus* and *Oithona spp.*, the krill *T. macrura*, and diatoms to be important covariates. Although the addition of diatoms slightly increased our AIC by a value of 1 (Supp. Table 1), we included it in our model based on hypothesized interactions. We also included one latent variable in the final model (Supp. Table 1), as described below in script notation:

> gllvm(abundance ~ 20m temperature + 50m salinity + *C. propinquus* density (den.) + *Oithona* spp. den. + *T. macrura* den. + diatom den., family = zero-inflated Poisson[link = log])

The final model supported several significant correlations between fishes and covariates. Among environmental variables, *L. nudifrons*, *T. newnesi*, and *N. larseni* all negatively correlate with ocean temperature, while *L. squamifrons* has a positive correlation with temperature (Fig 7). Additionally, *T. scotti* has a positive correlation with salinity. For phytoplankton, *L. nudifrons* and *N. larseni* increase with increasing diatom density, although the correlation was non-significant (Fig 7). For copepods, *T. scotti* has a negative correlation with *Oithona* spp., and *L. squamifrons* has a negative correlation with *C. propinquus*, while *T. newnesi* has a positive correlation with *C. propinquus*. Finally, *L. squamifrons* abundance increased with increased abundance of the krill *T. macrura* (Fig 7). Covariate estimates, standard errors, and *p* values from the final GLLVM model can be found in Supplemental Table 2.

Larval fish dispersion model

Overall, 3524 particles released satisfied the selection criteria (Fig 8a). The mean distance traveled by particles was 182 ± 47 km (±1 Standard Deviation) (Supp. Fig 1). The heatmap of particle origins (Fig 8b) shows higher values along the northwest coast of Anvers Island, and secondarily on the northern coast of Palmer Deep Canyon (Fig 8b), which is consistent with the regional circulation patterns (see Discussion).

4. Discussion

Factors impacting larval fish phenology

The significant interannual changes in timing and peak abundance of the two most prevalent larvae, *T. newnesi* and *L. nudifrons,* are indicative of the extreme interannual variability associated with this system. The two abundant species have relatively similar biogeography; both are widely distributed demersal fishes in the Antarctic Peninsula (AP) region occurring at depths from 5 to 400 m (Hourigan and Radtke 1989; Gon and Heemstra 1990; Llompart et al. 2015; Eastman 2017; Deli Antoni et al. 2019). In the AP region, *T. newnesi* spawns from March to April in shallow (<160 m) depths, with hatching occurring from September to October (Radtke et al. 1989; Kellermann 1990; Kock and Kellermann 1991). Spawning of *L. nudifrons* likely occurs between March to July in shallow (< 80 m) depths, with males nest guarding for approximately four months of egg incubation (Hourigan and Radtke

1989; Gon and Heemstra 1990; Kellermann 1990; Kock and Kellermann 1991; Novillo et al. 2021). In the South Shetland Island region, *L. nudifrons* hatching occurs from winter to early spring (La Mesa et al. 2017). Despite these similarities, *T. newnesi* abundance decreased by an order of magnitude in 2018 – 2019, while *L. nudifrons* abundance increased to a similar degree (Table 1).

Increased larval *T. newnesi* abundance during 2017 – 2018 may be, in part, a result of high *C. propinquus* copepod abundance due to reduced sea ice conditions that year. *Trematomus newnesi* larvae, which are estimated to be about 9 mm at hatching, consume calanoid copepodites, the copepod *C. propinquus*, and eggs of *E. superba*–all of which range in size from 0.6 to 4.3 mm (Kellermann 1990b). *Trematomus newnesi* consumption of *C. propinquus* is supported by the results of our GLLVM analysis, with larval *T. newnesi* abundance positively related to *C. propinquus* density, and by a single gut dissection (Fig 9). The omnivorous copepod *C. propinquus* feeds on ice algae after it is released from sea ice (Gradinger and Schnack-Schiel 1998) but is less reliant on diatoms than other *Calanus* spp. (Pasternak and Schnack-Schiel 2001). *Calanus propinquus* is also more abundant in ice-free areas in the Weddell Sea (Burghart et al. 1999; Voronina et al. 2001) and the Bellingshausen Sea (Atkinson and Shreeve 1995). Furthermore, *C. propinquus* density in the low sea-ice 2017 – 2018 season was about an order of magnitude greater than the high sea-ice 2018 – 2019 season (Supp. Fig. 2)(Conroy et al. 2023). Plentiful feeding opportunities for nototheniid larvae delays their yolk-sac absorption (Kellermann 1996). Concordantly, we only captured yolk-sac *T. newnesi* during the 2017 – 2018 season, which might suggest an abundance of prey (Fig 3b). *Trematomus newnesi* grew faster in the 2018-2019 season (Table 2), but its scarcity that year limits certainty in the estimated growth rate.

Abundance of *L. nudifrons* appears more closely tied to diatoms than to copepods. We found a positive correlation ($p = 0.09$) with diatom density in the GLLVM, and concordantly, diatoms formed a higher percent of total phytoplankton biovolume in the 2018 – 2019 season compared to 2017 – 2018, which was partially attributed to the greater sea ice duration in 2018 - 2019 in the Anvers Island region (Nardelli *et al.*, 2023). Although there are no reports on larval *L. nudifrons* diet, diatoms are an important prey item for other larval nototheniid species (Koubbi et al. 2007; Koubbi et al. 2009). *Nototheniops larseni*, which also had a positive, but non-significant correlation with diatom density, was more abundant in 2018 – 2019. Moline *et al.* (2008) also proposed a relationship between abundance of *L. nudifrons* and sea ice, theorizing survivorship of *L. nudifrons* would increase following an earlier sea ice retreat due to an associated increase in secondary production and early stages of copepods. Although we observed this trend under different sea ice conditions, it is evident that *L. nudifrons* larval abundance is tied to primary production.

Although some shifts were more evident than others, the mean abundance dates for all five of the most abundant taxa were earlier in 2018 – 2019 than in 2017 – 2018. This may be tied to interannual difference in sea ice cover, light levels, or timing of the spring phytoplankton bloom. Although sea ice duration was longer in 2018 – 2019 with a more delayed retreat, Nardelli *et al.* (2023) found the initial phytoplankton bloom began earlier in 2018 – 2019 than in 2017 – 2018. November sea ice coverage (~30%) was lower and patchier in 2018 – 2019 compared to ~50% coverage in November of 2017 – 2018. As a result, phytoplankton in 2018 –

2019 were exposed to more light and began growing earlier, despite the overall later retreat. In captivity, notothenioid larvae, including *L. nudifrons*, are positively phototactic, swimming towards light sources following hatching (Hourigan and Radtke 1989; Evans et al. 2005). Kellermann (1996) suggested that nototheniid larvae could fine-tune their hatching dates with sea ice retreat based on light availability; i.e., increased light accelerates egg metabolic rate. The earlier appearance dates for the five larval fish taxa in 2018 – 2019 therefore suggest that light availability due to reduced sea ice coverage may be an especially important cue for hatching nototheniid larvae.

Ocean temperature was an important predictor of larval abundance, with significant relationships in four of the five species. The association of *L. nudifrons*, *T. newnesi*, and *N. larseni* with colder water temperature is indicative of their stenothermy; Hardewig *et al.* (1999) suggested a temperature of 8 – 9°C is likely lethal for adult *L. nudifrons*. The only taxa we examined with significantly higher abundance in warmer ocean temperatures was *L. squamifrons*, a finding supported by the relatively high metabolic acclimation potential of this species compared to other nototheniids (Strobel et al. 2013). *Lepidonotothen squamifrons* is an abundant nototheniid that occurs in the sub-Antarctic Islands and the northern AP region at depths ranging from 5 to 900 m, with our sampling location near the poleward extent of their range (Gon and Heemstra 1990; Eastman 2017). It is likely that adult *L. squamifrons* commonly encounters summer temperatures over 3.5 °C in its sub-Antarctic range (Strobel *et al.* (2013). Furthermore, *L. squamifrons* lacks measurable antifreeze glycoprotein (AFGP) in its blood, one of the few examples of this trait loss among Antarctic nototheniids (Miya et al. 2016). *Lepidonotothen squamifrons* appears latest in the season, during January and February, which is also the warmest period. Our GLVVM should incorporate this temporal autocorrelation, suggesting that larval *L. squamifrons* are also more abundant on warmer days during the later season.

We captured only three channichthyid larvae and no *Pleuragramma antarctica* (Boulenger 1902) larvae in our study. However, both groups were previously reported to be primary components of this regional larval fish assemblage (Loeb et al. 1993). Channichthyid larvae hatch at especially large sizes, as they specialize in the predation of other nototheniid larvae and euphausiids (Kellermann 1990; Loeb et al. 1993; Kellermann 1996), thus their absence may represent a sampling bias due to the small size of our plankton nets coupled with slow towing speeds. As *P. antarctica* larvae are similar in size to other nototheniids we routinely sampled, we attribute their absence to the lack of suitable sea ice spawning habitat in the vicinity of Anvers Island due to recent sea ice loss and warming (Parker et al. 2015; Corso et al. 2022). As the WAP region continues to warm, it will be important to document long-term trends in *T. newnesi*, *L. nudifrons*, and other members of the larval assemblage, in addition to their phenology, to determine how multi-decadal ocean temperature variability may be impacting their population dynamics.

The occasional presence of mesopelagic fish larvae (including myctophids, paralepidids, and muraenolepidids) was unexpected, as these larvae are associated with deeper regions farther offshore (Konstantinidis et al. 2016). For the myctophid *E. antarctica*, Greely *et al.* (1999) proposed a larval stage lasting 30 to 47 d using otolith microincrement analysis. Hatch date is estimated to occur sometime between June to August in the Scotia Sea (Kellermann 1989; Saunders et al. 2014), and much later during late November to December off Wilkes Land, East

Antarctica (Moteki et al. 2017). We found larvae of *E. antarctica* smaller than 7mm SL from 17 November 2017 to 8 March 2018 (Fig 4a,b). The presence of these small preflexion stages spanning four months suggests this species is likely spawning in the region over a wide period, with hatching occurring anywhere from October through February.

We are also able to draw insights on the spawning behavior of *H. antarcticus* due to the presence of yolk-sac larvae (Fig 4c,d). In the South Orkney Islands, *H. antarcticus* eggs were observed to develop for up to 150 days (White and Burren 1992), with larvae taking up to 35 days to fully absorb their yolk-sac (Daniels 1978). Together this suggests larvae we collected hatched sometime in early February or late January, and spawning occurred between August to early September. Also around Anvers Island, Daniels (1978) observed *H. antarcticus* laying eggs from mid-June through late August. Using histological analysis, Novillo *et al.* (2021) found *H. antarcticus* were likely spawning during January – February in Paradise Bay on the WAP. These studies, combined with the occurrence of yolk-sac larvae during our sampling, indicates *H. antarcticus* likely has at least two spawning events in the WAP region, which was also suggested by Novillo *et al.* (2021).

Growth rate variability

Prior studies indicate significant differences between daily length and otolith-based methods for determining larval nototheniid growth rates, which adds an element of uncertainty to our length-based rates (La Mesa et al. 2017). For example, our daily growth rates for *L. nudifrons*, 0.078 and 0.074 mm day $^{-1}$, for the 2017 – 2018 and 2018 -2019 seasons, respectively, are each about 50% slower than those calculated by La Mesa *et al.* (2017). While our daily growth estimates for *T. scotti* (0.048 and 0.036 mm day $^{-1}$) are similar to the estimate of 0.05 mm day $^{-1}$ determined using length frequency distributions over a summer season by Loeb (1991), they are 3-5 times slower than the rate of 0.17 mm day $^{-1}$ determined by otolith microstructure analysis (La Mesa et al. 2015). It is also important to note there is intraspecific, interspecific, and geographic variation in the growth rates of larval nototheniids (Kellermann 1990; La Mesa et al. 2015; La Mesa et al. 2017). We report length-based estimates here to illustrate changes in growth between years. In the future, it will be important to focus future efforts on completing otolith analyses to more accurately describe the larval development for these fishes.

Dispersion model

Our dispersion model provides the first estimation of potential spawning areas for *T. newnesi*, which helps to better understand the early life history of these species. Based on larval length and the presence of yolk-sac stages, we estimate *T. newnesi* larvae hatch sometime in October through early November in the Anvers Island region. To our knowledge, nests of *T. newnesi* have not been observed.

Particle release (spawning) locations are in general agreement with other ongoing studies (Dinniman, Pers. Comm, 2023). Particles generally moved in a southerly direction, likely influenced by the Antarctic Peninsula Coastal Current (APCC) (Moffat and Meredith 2018). These pathways are consistent with key circulation features of this region. Submarine troughs (or canyons) are bathymetric features are areas of enhanced transport of water across the shelf (e.g., Moffat *et al.*, 2009; Moffat & Meredith, 2018; Schofield *et al.*, 2013). Also, the near-shore circulation is heavily influenced by the discharge of freshwater from the coast, which along the

WAP favors flow towards the south (Moffat et al. 2008; Schubert et al. 2021). This analysis suggests that the nearshore region north of Palmer Deep as well as Palmer Canyon provide the most likely source regions for the larvae found at Station E.

Several of the particles were retained in the subsurface eddy (K. Hudson et al. 2021) in the Palmer Deep Canyon (Fig 8b). Hudson *et al.*, (2021b) found diel vertical migration (DVM) influences particle retention in the Palmer Canyon region, but we opted not to include DVM in the model as presumably yolk-sac stage *T. newnesi* are not actively vertically migrating their first weeks of life. Particle release depth (e.g., 10m, 120m, or 300m) slightly impacted results. Particles that were originally released deeper did not travel as far likely due to current speeds, which generally are slower at greater depths, and thus particle release locations occupied a smaller area. We selected the 10m release depth as it eliminated the additional variability of *T. newnesi* nest depth, which likely fluctuates from near shore to at least 160m (Gon and Heemstra 1990).

Because the area where particles were released is smaller than the full model domain, this analysis does not capture all possible paths a larva might have followed before arriving at Station E. Particles that originated outside of the seeding area and took less than 17-19 days to reach Station E will not be captured in our analysis. Additionally, interannual variability in current speeds and directions is not accounted for. Despite these limitations, the model provides an important source of information to locate spawning habitat more precisely and can serve as a guide for any future survey efforts in the region (e.g., with towed cameras).

Conclusion

Climate-driven changes in phenology will perpetuate effects throughout food webs (Sydeman et al. 2015). With increasingly severe climate change continuing to impact sea ice dynamics and other components of the WAP ecosystem, it is important to understand the phenology of this region before it is irreversibly altered. Continued seasonal monitoring of this larval fish assemblage, a rigorous diet analysis, and otolith measurements to verify larval growth patterns are necessary to further develop the trends we present. Nevertheless, this study offers insights into current phenological trends in this unique larval fish assemblage, while providing a roadmap for future surveys of adult notothenioid reproduction in the Anvers Island region.

Acknowledgments

We thank Kharis Schrage, Maya Thomas, and Leigh West for assistance in the field, Joseph Cope for data management and field expertise, Ross Nichols for figure development, and the support of marine technicians, laboratory managers, and all other personnel at Palmer Station, Antarctica. We also thank the captains, crew, and support staff of the ASRV *Laurence M. Gould* and the Leidos Antarctic Support Contractors. This work was funded by the National Science Foundation Office of Polar Program (OPP-1440435, 2026045, and 1543383 for specimen and environmental data collection) and Division of Biological Infrastructure (DBI-1349327 for specimen preservation and analysis), the Explorers Club, and the VIMS John Olney Fellowship.

References

Asch RG. 2015. Climate change and decadal shifts in the phenology of larval fishes in the California Current ecosystem. Proceedings of the National Academy of Sciences. 112(30):E4065–E4074. https://doi.org/10.1073/pnas.1421946112

Atkinson A, Shreeve RS. 1995. Response of the copepod community to a spring bloom in the Bellingshausen Sea. Deep Sea Research Part II: Topical Studies in Oceanography. 42(4–5):1291–1311.

Auger-Méthé M, Newman K, Cole D, Empacher F, Gryba R, King AA, Leos-Barajas V, Mills Flemming J, Nielsen A, Petris G, Thomas L. 2021. A guide to state–space modeling of ecological time series. Ecological Monographs. 91(4):e01470. https://doi.org/10.1002/ecm.1470

Boulenger GA. 1902. Pisces. In: In: Report on the collections of natural history made in the Antarctic regions during the voyage of the “Southern Cross” [ix, 344 p, 53 leaves of plates]. https://www.marinespecies.org/aphia.php?p=sourcedetails&id=348394

Burghart SE, Hopkins TL, Vargo GA, Torres JJ. 1999. Effects of a rapidly receding ice edge on the abundance, age structure and feeding of three dominant calanoid copepods in the Weddell Sea, Antarctica. Polar Biology. 22(4):279–288. https://doi.org/10.1007/s003000050421

Burrows MT, Schoeman DS, Buckley LB, Moore P, Poloczanska ES, Brander KM, Brown C, Bruno JF, Duarte CM, Halpern BS, et al. 2011. The Pace of Shifting Climate in Marine and Terrestrial Ecosystems. Science. 334(6056):652–655. https://doi.org/10.1126/science.1210288

Carvalho F, Fitzsimmons JN, Couto N, Waite N, Gorbunov M, Kohut J, Oliver MJ, Sherrell RM, Schofield O. 2020. Testing the Canyon Hypothesis: Evaluating light and nutrient controls of phytoplankton growth in penguin foraging hotspots along the West Antarctic Peninsula. Limnology and Oceanography. 65(3):455–470. https://doi.org/10.1002/lno.11313

Casaux R, Barrera-Oro E, Baroni A, Ramón A. 2003. Ecology of inshore notothenioid fish from the Danco Coast, Antarctic Peninsula. Polar Biol. 26(3):157–165. https://doi.org/10.1007/s00300-002-0463-y

Chambers LE, Altwegg R, Barbraud C, Barnard P, Beaumont LJ, Crawford RJM, Durant JM, Hughes L, Keatley MR, Low M, et al. 2013. Phenological Changes in the Southern Hemisphere. PLOS ONE. 8(10):e75514. https://doi.org/10.1371/journal.pone.0075514

Chmura HE, Kharouba HM, Ashander J, Ehlman SM, Rivest EB, Yang LH. 2019. The mechanisms of phenology: the patterns and processes of phenological shifts. Ecol Monogr. 89(1):e01337. https://doi.org/10.1002/ecm.1337

Cimino MA, Conroy JA, Connors E, Bowman J, Corso A, Ducklow H, Fraser W, Friedlaender A, Kim HH, Larsen GD. 2023. Long-term patterns in ecosystem phenology near Palmer Station, Antarctica, from the perspective of the Adélie penguin. Ecosphere. 14(2):e4417.

Cimino MA, Lynch HJ, Saba VS, Oliver MJ. 2016. Projected asymmetric response of Adélie penguins to Antarctic climate change. Scientific Reports. 6(1):28785. https://doi.org/10.1038/srep28785

Conroy JA, Steinberg DK, Thomas MI, West LT. 2023. Seasonal and interannual changes in a coastal Antarctic zooplankton community. Marine Ecology Progress Series. 706:17–32. https://doi.org/10.3354/meps14256

Corso AD, Steinberg DK, Stammerjohn SE, Hilton EJ. 2022. Climate drives long-term change in Antarctic Silverfish along the western Antarctic Peninsula. Communications biology. 5(1):1–10.

Cushing DH. 1972. The production cycle of and the numbers of marine fish. In: Symp Zool Soc London. Vol. 29. p. 213–232.

Cushing DH. 1990. Plankton Production and Year-class Strength in Fish Populations: An Update of the Match/Mismatch Hypothesis. In: Blaxter JHS, Southward AJ, editors. Advances in Marine Biology. Vol. 26. Academic Press; p. 249–293. https://doi.org/10.1016/S0065-2881(08)60202-3

Daniels RA. 1978. Nesting Behaviour of *Harpagifer bispinis* in Arthur Harbour, Antarctic Peninsula. Journal of Fish Biology. 12(5):465–474. https://doi.org/10.1111/j.1095-8649.1978.tb04190.x

Daniels RA, Lipps JH. 1982. Distribution and ecology of fishes of the Antarctic Peninsula. Journal of Biogeography.:1–9.

Deli Antoni MY, Delpiani SM, González-Castro M, Blasina GE, Spath MC, Depiani GE, Ashikaga FY, Cruz VP, Oliveira C, de Astarloa JMD. 2019. Comparative populational study of *Lepidonotothen larseni* and *L. nudifrons* (Teleostei: Nototheniidae) from the Antarctic Peninsula and the South Shetland Islands, Antarctica. Polar Biolgy. 42(8):1537–1547. https://doi.org/10.1007/s00300-019-02540-1

Dollo L, Traquair MRH. 1908. V.—*Notolepis Coatsi*, Poisson pélagique nouveau recueilli par l'Expédition Antarctique Nationale Ecossaise. Proceedings of the Royal Society of Edinburgh. 28:58–65. https://doi.org/10.1017/S0370164600011561

Donnelly J, Torres JJ. 2008. Pelagic fishes in the Marguerite Bay region of the West Antarctic Peninsula continental shelf. Deep Sea Research Part II: Topical Studies in Oceanography. 55(3–4):523–539.

Eastman JT. 2017. Bathymetric distributions of notothenioid fishes. Polar Biolgy. 40(10):2077–2095. https://doi.org/10.1007/s00300-017-2128-x

Edwards M, Richardson AJ. 2004. Impact of climate change on marine pelagic phenology and trophic mismatch. Nature. 430(7002):881–884. https://doi.org/10.1038/nature02808

Evans CW, Cziko P, Cheng C-HC, Devries AL. 2005. Spawning behaviour and early development in the naked dragonfish *Gymnodraco acuticeps*. Antartic science. 17(3):319–327. https://doi.org/10.1017/S0954102005002749

Gon O, Heemstra PC. 1990. Fishes of the Southern Ocean. JLB Smith Institute of Ichthyology, Grahamstown.

Gradinger R, Schnack-Schiel SB. 1998. Potential effect of ice formation on Antarctic pelagic copepods: salinity induced mortality of *Calanus propinquus* and *Metridia gerlachei* in comparison to sympagic acoel turbellarians. Polar Biology. 20(2):139–142. https://doi.org/10.1007/s003000050288

Graham JA, Dinniman MS, Klinck JM. 2016. Impact of model resolution for on-shelf heat transport along the West Antarctic Peninsula. Journal of Geophysical Research: Oceans. 121(10):7880–7897.

Greely TM, Gartner Jr JV, Torres JJ. 1999. Age and growth of *Electrona antarctica* (Pisces: Myctophidae), the dominant mesopelagic fish of the Southern Ocean. Marine Biology. 133(1):145–158. https://doi.org/10.1007/s002270050453

Günther A. 1878. II.—Preliminary notices of Deep-Sea Fishes collected during the Voyage of HMS ‘Challenger.’ Journal of Natural History. 2(7):17–28.

Gunther A. 1880. Report on the shore fishes procured during the voyage of HMS Challenger, in the years 1873-1876. Rep Sci Res Voy HMS Challenger Zool. 1:32-pls.

Haidvogel DB, Arango H, Budgell WP, Cornuelle BD, Curchitser E, Di Lorenzo E, Fennel K, Geyer WR, Hermann AJ, Lanerolle L, et al. 2008. Ocean forecasting in terrain-following coordinates: Formulation and skill assessment of the Regional Ocean Modeling System. Journal of Computational Physics. 227(7):3595–3624. https://doi.org/10.1016/j.jcp.2007.06.016

Hardewig I, Pörtner HO, Peck LS. 1999. Thermal sensitivity of mitochondrial function in the Antarctic Notothenioid *Lepidonotothen nudifrons*. Journal of Comparative Physiology B: Biochemical, Systemic, and Environmental Physiology. 169(8):597–604. https://doi.org/10.1007/s003600050260

Hoegh-Guldberg O, Bruno JF. 2010. The impact of climate change on the world’s marine ecosystems. Science. 328(5985):1523–1528.

Holmes EE, Ward EJ, Kellie W. 2012. MARSS: multivariate autoregressive state-space models for analyzing time-series data. R J. 4(1):11.

Hourigan TF, Radtke RL. 1989. Reproduction of the Antarctic fish *Nototheniops nudifrons*. Marine Biology. 100:277–283.

Hudson K, Oliver MJ, Kohut J, Dinniman MS, Klinck JM, Moffat C, Statscewich H, Bernard KS, Fraser W. 2021. A Recirculating Eddy Promotes Subsurface Particle Retention in an Antarctic Biological Hotspot. Journal of Geophysical Research: Oceans. 126(11):e2021JC017304. https://doi.org/10.1029/2021JC017304

Hudson KL, Oliver MJ, Kohut J, Cohen JH, Dinniman MS, Klinck J, Statscewich H, Bernard KS, Fraser W. 2021. Subsurface Eddy Facilitates Retention of Diel Vertical Migrators in a Biological Hotspot. Oceanography. https://doi.org/10.1002/essoar.10506863.1

Hui FKC, Hill NA, Welsh A h. 2022. Assuming independence in spatial latent variable models: Consequences and implications of misspecification. Biometrics. 78(1):85–99. https://doi.org/10.1111/biom.13416

Hui FKC, Warton DI, Ormerod JT, Haapaniemi V, Taskinen S. 2017. Variational Approximations for Generalized Linear Latent Variable Models. Journal of Computational and Graphical Statistics. 26(1):35–43. https://doi.org/10.1080/10618600.2016.1164708

Jones CD, Damerau M, Deitrich K, Driscoll R, Kock K-H, Kuhn K, Moore J, Morgan T, Near T, Pennington J. 2009. Demersal finfish survey of the South Orkney Islands. NOAA Technical Memorandum NMFS SWFSC. 445:49–66.

Joy-Warren HL, van Dijken GL, Alderkamp A-C, Leventer A, Lewis KM, Selz V, Lowry KE, van de Poll W, Arrigo KR. 2019. Light Is the Primary Driver of Early Season Phytoplankton Production Along the Western Antarctic Peninsula. Journal of Geophysical Research: Oceans. 124(11):7375–7399. https://doi.org/10.1029/2019JC015295

Kellermann A. 1989. The larval fish community in the zone of seasonal pack-ice cover and its seasonal and interannual variability. Arch FischWiss Beih 1. 39:81–109.

Kellermann AK. 1990. Identification key and catalogue of larval Antarctic fishes. Ber Polarforsch.(67):1–138.

Kellermann AK. 1996. Midwater fish ecology. Foundations for ecological research west of the Antarctic Peninsula. 70:231–256.

Kock K-H, Kellermann A. 1991. Reproduction in Antarctic notothenioid fish. Antarctic Science. 3:125–150. https://doi.org/10.1017/S0954102091000172

Konstantinidis P, Hilton EJ, Matarese AC. 2016. New records of larval stages of the eel cod genus *Muraenolepis* Günther 1880 (Gadiformes: Muraenolepididae) from the western Antarctic Peninsula. Journal of Fish Biology. 89(2):1494–1500.

Koubbi P, Duhamel G, Hecq J-H, Beans C, Loots C, Pruvost P, Tavernier E, Vacchi M, Vallet C. 2009. Ichthyoplankton in the neritic and coastal zone of Antarctica and Subantarctic islands: a review. Journal of Marine Systems. 78(4):547–556.

Koubbi P, Vallet C, Razouls S, Grioche A, Hilde D, Courcot L, Janquin MA, Vacchi M. 2007. Condition and diet of larval *Pleuragramma antarcticum* (Nototheniidae) from Terre Adélie (Antarctica) during summer.

Kozlowski WA, Deutschman D, Garibotti I, Trees C, Vernet M. 2011. An evaluation of the application of CHEMTAX to Antarctic coastal pigment data. Deep Sea Research Part I: Oceanographic Research Papers. 58(4):350–364.

Kristiansen T, Drinkwater KF, Lough RG, Sundby S. 2011. Recruitment Variability in North Atlantic Cod and Match-Mismatch Dynamics. PLoS One. 6(3):e17456. https://doi.org/10.1371/journal.pone.0017456

La Mesa M, Catalano B, Jones CD. 2015. Early life history traits of *Trematomus scotti* in the Bransfield Strait. Antarctic Science. 27(6):535–542.

La Mesa M, Riginella E, Catalano B, Jones CD, Mazzoldi C. 2017. Maternal contribution to spawning and early life-history strategies of the genus *Lepidonotothen* (Nototheniidae, Perciformes) along the southern Scotia Arc. Polar Biolgy. 40(7):1441–1450. https://doi.org/10.1007/s00300-016-2068-x

Lin Y, Moreno C, Marchetti A, Ducklow H, Schofield O, Delage E, Meredith M, Li Z, Eveillard D, Chaffron S, Cassar N. 2021. Decline in plankton diversity and carbon flux with reduced sea ice extent along the Western Antarctic Peninsula. Nature Communications. 12(1):4948. https://doi.org/10.1038/s41467-021-25235-w

Llompart F, Delpiani M, Lattuca E, Delpiani G, Cruz-Jiménez A, Orlando P, Ceballos S, Astarloa JMDD, Vanella F, Fernández D. 2015. Spatial patterns of summer demersal fish assemblages around the Antarctic Peninsula and South Shetland Islands. Antarctic Science. 27(2):109–117. https://doi.org/10.1017/S0954102014000352

Loeb VJ. 1991. Distribution and abundance of larval fishes collected in the western Bransfield Strait region, 1986–87. Deep Sea Research Part A Oceanographic Research Papers. 38(8):1251–1260. https://doi.org/10.1016/0198-0149(91)90105-O

Loeb VJ, Kellermann AK, Koubbi P, North AW, White MG. 1993. Antarctic larval fish assemblages: a review. Bulletin of Marine Science. 53(2):416–449.

Lönnberg E. 1905. The fishes of the Swedish South Polar expedition. Lithographisches Institut des Generalstabs.

Miya T, Gon O, Mwale M, Cheng C-HC. 2016. Multiple independent reduction or loss of antifreeze trait in low Antarctic and sub-Antarctic notothenioid fishes. Antarctic Science. 28(1):17–28. https://doi.org/10.1017/S0954102015000413

Moffat C, Beardsley RC, Owens B, van Lipzig N. 2008. A first description of the Antarctic Peninsula Coastal Current. Deep Sea Research Part II: Topical Studies in Oceanography. 55(3):277–293. https://doi.org/10.1016/j.dsr2.2007.10.003

Moffat C, Meredith M. 2018. Shelf–ocean exchange and hydrography west of the Antarctic Peninsula: a review. Phil Trans R Soc A. 376(2122):20170164. https://doi.org/10.1098/rsta.2017.0164

Moffat C, Owens B, Beardsley RC. 2009. On the characteristics of Circumpolar Deep Water intrusions to the west Antarctic Peninsula Continental Shelf. Journal of Geophysical Research: Oceans. 114(C5). https://doi.org/10.1029/2008JC004955

Moline MA, Karnovsky NJ, Brown Z, Divoky GJ, Frazer TK, Jacoby CA, Torres JJ, Fraser WR. 2008. High Latitude Changes in Ice Dynamics and Their Impact on Polar Marine Ecosystems. Annals of the New York Academy of Sciences. 1134(1):267–319. https://doi.org/10.1196/annals.1439.010

Moteki M, Fujii K, Amakasu K, Shimada K, Tanimura A, Odate T. 2017. Distributions of larval and juvenile/adult stages of the Antarctic myctophid fish, *Electrona antarctica*, off Wilkes Land in East Antarctica. Polar Science. 12:99–108. https://doi.org/10.1016/j.polar.2017.02.004

Moustaki I, Knott M. 2000. Generalized latent trait models. Psychometrika. 65(3):391–411. https://doi.org/10.1007/BF02296153

Moyano M, Illing B, Peschutter P, Huebert KB, Peck MA. 2016. Thermal impacts on the growth, development and ontogeny of critical swimming speed in Atlantic herring larvae. Comparative Biochemistry and Physiology Part A: Molecular & Integrative Physiology. 197:23–34.

Nardelli SC, Gray PC, Stammerjohn SE, Schofield O. 2023. Characterizing coastal phytoplankton seasonal succession patterns on the West Antarctic Peninsula. Limnology & Oceanography. 12314. https://doi.org/10.1002/lno.12314

Niku J, Hui FK, Taskinen S, Warton DI. 2019. gllvm: Fast analysis of multivariate abundance data with generalized linear latent variable models in R. Methods in Ecology and Evolution. 10(12):2173–2182.

Niku J, Warton DI, Hui FKC, Taskinen S. 2017. Generalized Linear Latent Variable Models for Multivariate Count and Biomass Data in Ecology. JABES. 22(4):498–522. https://doi.org/10.1007/s13253-017-0304-7

Norman JR. 1937. LV.—Diagnoses of new Nototheniiform fishes collected by the 'Discovery' Expedition. Annals and Magazine of Natural History. 20(118):475–476. https://doi.org/10.1080/00222933708655368

Novillo M, Moreira E, Macchi G, Barrera-Oro E. 2021. Histological analysis provides further insights into *Harpagifer antarcticus* reproductive biology at the western Antarctic Peninsula. Polar Biology. 44(11):2165–2175.

Nybelin O. 1947. Antarctic fishes. Scientific Results of the Norwegian Antarctic Expeditions (1927-1931). 26(2):1–76.

Pallin LJ, Kellar NM, Steel D, Botero-Acosta N, Baker CS, Conroy JA, Costa DP, Johnson CM, Johnston DW, Nichols RC. 2023. A surplus no more? Variation in krill availability impacts reproductive rates of Antarctic baleen whales. Global Change Biology.

Pappenheim P. 1911. Sitzungsberichte der Gesellschaft Naturforschender Freunde zu Berlin 1911. :382.

Parker ML, Fraser WR, Ashford J, Patarnello T, Zane L, Torres JJ. 2015. Assemblages of micronektonic fishes and invertebrates in a gradient of regional warming along the Western Antarctic Peninsula. Journal of Marine Systems. 152:18–41.

Parkinson CL. 2019. A 40-y record reveals gradual Antarctic sea ice increases followed by decreases at rates far exceeding the rates seen in the Arctic. Proceedings of the National Academy of Sciences. 116(29):14414–14423. https://doi.org/10.1073/pnas.1906556116

Pasternak A, Schnack-Schiel S. 2001. Seasonal feeding patterns of the dominant Antarctic copepods *Calanus propinquus* and *Calanoides acutus* in the Weddell Sea. Polar Biology. 24(10):771–784. https://doi.org/10.1007/s003000100283

Pau S, Wolkovich EM, Cook BI, Davies TJ, Kraft NJB, Bolmgren K, Betancourt JL, Cleland EE. 2011. Predicting phenology by integrating ecology, evolution and climate science. Global Change Biology. 17(12):3633–3643. https://doi.org/10.1111/j.1365-2486.2011.02515.x

Poloczanska ES, Brown CJ, Sydeman WJ, Kiessling W, Schoeman DS, Moore PJ, Brander K, Bruno JF, Buckley LB, Burrows MT. 2013. Global imprint of climate change on marine life. Nature Climate Change. 3(10):919–925.

Poloczanska ES, Burrows MT, Brown CJ, García Molinos J, Halpern BS, Hoegh-Guldberg O, Kappel CV, Moore PJ, Richardson AJ, Schoeman DS, Sydeman WJ. 2016. Responses of Marine Organisms to Climate Change across Oceans. Frontiers in Marine Science. 3. https://www.frontiersin.org/articles/10.3389/fmars.2016.00062

R Core Team. 2022. R: A language and environment for statistical computing. https://www.R-project.org/

Radtke RL, Targett TE, Kellermann A, Bell JL, Hill KT. 1989. Antarctic fish growth: profile of *Trematomus newnesi*. Marine Ecology Progress Series.:103–117.

Regan CT. 1914. II.—Diagnoses of new marine fishes collected by the British Antarctic (‘Terra Nova’) Expedition. Annals and magazine of Natural History. 13(73):11–17.

Robert D, Murphy HM, Jenkins GP, Fortier L. 2014. Poor taxonomical knowledge of larval fish prey preference is impeding our ability to assess the existence of a “critical period” driving year-class strength. ICES Journal of Marine Science. 71(8):2042–2052. https://doi.org/10.1093/icesjms/fst198

Saba GK, Fraser WR, Saba VS, Iannuzzi RA, Coleman KE, Doney SC, Ducklow HW, Martinson DG, Miles TN, Patterson-Fraser DL, et al. 2014. Winter and spring controls on the summer food web of the coastal West Antarctic Peninsula. Nat Commun. 5(1):4318. https://doi.org/10.1038/ncomms5318

Saunders RA, Collins MA, Foster E, Shreeve R, Stowasser G, Ward P, Tarling GA. 2014. The trophodynamics of Southern Ocean *Electrona* (Myctophidae) in the Scotia Sea. Polar Biol. 37(6):789–807. https://doi.org/10.1007/s00300-014-1480-3

Schmidtko S, Heywood KJ, Thompson AF, Aoki S. 2014. Multidecadal warming of Antarctic waters. Science. 346(6214):1227–1231.

Schnack-Schiel SB. 2002. Aspects of the study of the life cycles of Antarctic copepods. In: Lopes RM, Reid JW, Rocha CEF, editors. Copepoda: Developments in Ecology, Biology and Systematics. Vol. 156. Dordrecht: Kluwer Academic Publishers. p. 9–24. https://doi.org/10.1007/0-306-47537-5_2

Schofield O, Ducklow H, Bernard K, Doney S, Patterson-Fraser D, Gorman K, Martinson D, Meredith M, Saba G, Stammerjohn S, et al. 2013. Penguin Biogeography Along the West Antarctic Peninsula: Testing the Canyon Hypothesis with Palmer LTER Observations. Oceanography. 26(3):204–206.

Schofield O, Saba G, Coleman K, Carvalho F, Couto N, Ducklow H, Finkel Z, Irwin A, Kahl A, Miles T. 2017. Decadal variability in coastal phytoplankton community composition in a changing West Antarctic Peninsula. Deep Sea Research Part I: Oceanographic Research Papers. 124:42–54.

Schubert R, Thompson AF, Speer K, Schulze Chretien L, Bebieva Y. 2021. The Antarctic coastal current in the Bellingshausen Sea. The Cryosphere. 15(9):4179–4199.

Stammerjohn S, Massom R, Rind D, Martinson D. 2012. Regions of rapid sea ice change: An inter-hemispheric seasonal comparison. Geophysical Research Letters. 39(6). https://doi.org/10.1029/2012GL050874

Stammerjohn Sharon E., Martinson DG, Smith RC, Iannuzzi RA. 2008. Sea ice in the western Antarctic Peninsula region: Spatio-temporal variability from ecological and climate change perspectives. Deep Sea Research Part II: Topical Studies in Oceanography. 55(18):2041–2058. https://doi.org/10.1016/j.dsr2.2008.04.026

Stammerjohn S. E., Martinson DG, Smith RC, Yuan X, Rind D. 2008. Trends in Antarctic annual sea ice retreat and advance and their relation to El Niño–Southern Oscillation and Southern Annular Mode variability. Journal of Geophysical Research: Oceans. 113(C3). https://doi.org/10.1029/2007JC004269

Steinberg DK, Ruck KE, Gleiber MR, Garzio LM, Cope JS, Bernard KS, Stammerjohn SE, Schofield OME, Quetin LB, Ross RM. 2015. Long-term (1993–2013) changes in macrozooplankton off the Western Antarctic Peninsula. Deep Sea Research Part I: Oceanographic Research Papers. 101:54–70. https://doi.org/10.1016/j.dsr.2015.02.009

Strobel A, Graeve M, Poertner HO, Mark FC. 2013. Mitochondrial Acclimation Capacities to Ocean Warming and Acidification Are Limited in the Antarctic Nototheniid Fish, *Notothenia rossii* and *Lepidonotothen squamifrons*. PLOS ONE. 8(7):e68865. https://doi.org/10.1371/journal.pone.0068865

Sydeman W, Bograd S. 2009. Marine ecosystems, climate and phenology: introduction. Mar Ecol Prog Ser. 393:185–188. https://doi.org/10.3354/meps08382

Sydeman WJ, Poloczanska E, Reed TE, Thompson SA. 2015. Climate change and marine vertebrates. Science. 350(6262):772–777. https://doi.org/10.1126/science.aac9874

Trokhymets V, Savytskiy O, Zinkovskyi A, Gupalo O, Dykyy I, Lutsenko D, Berezkina A, La Mesa M. 2022. Species composition, distribution and relative abundance of the inshore fish community off the Argentine Islands, Bellingshausen Sea. Polar Biol. 45(5):845–855. https://doi.org/10.1007/s00300-022-03040-5

van der Veen B, Hui FKC, Hovstad KA, Solbu EB, O'Hara RB. 2021. Model-based ordination for species with unequal niche widths. Methods in Ecology and Evolution. 12(7):1288–1300. https://doi.org/10.1111/2041-210X.13595

Vernet M, Martinson D, Iannuzzi R, Stammerjohn S, Kozlowski W, Sines K, Smith R, Garibotti I. 2008. Primary production within the sea-ice zone west of the Antarctic Peninsula: I—Sea ice, summer mixed layer, and irradiance. Deep Sea Research Part II: Topical Studies in Oceanography. 55(18):2068–2085. https://doi.org/10.1016/j.dsr2.2008.05.021

Voronina N, Kolosova E, Melnikov I. 2001. Zooplankton life under the perennial Antarctic Sea ice. Polar Biology. 24(6):401–407. https://doi.org/10.1007/s003000100224

Warton DI, Blanchet FG, O'Hara RB, Ovaskainen O, Taskinen S, Walker SC, Hui FKC. 2015. So Many Variables: Joint Modeling in Community Ecology. Trends in Ecology & Evolution. 30(12):766–779. https://doi.org/10.1016/j.tree.2015.09.007

White MG, Burren PJ. 1992. Reproduction and larval growth of *Harpagifer antarcticus* Nybelin (Pisces, Notothenioidei). Antartic science. 4(4):421–430. https://doi.org/10.1017/S0954102092000622

Wilke CO. 2022. ggridges: Ridgeline Plots in “ggplot2”. https://wilkelab.org/ggridges/

Table 1. Larval fish species collected near Anvers Island, Antarctica at Stations B and E.

Taxa	Family	2017-2018 individuals	2018-2019 individuals
Trematomus newnesi	Nototheniidae	197	22
Lindbergichthys nudifrons	Nototheniidae	15	181
Lepidonotothen squamifrons	Nototheniidae	18	24
Nototheniops larseni	Nototheniidae	12	23
Trematomus scotti	Nototheniidae	12	21
Harpagifer antarcticus	Harpagiferidae	12	4
Electrona antarctica	Myctophidae	8	2
Champsocephalus gunnari	Channichthyidae	1	1
Trematomus pennellli	Nototheniidae	1	0
Trematomus lepidorhinus	Nototheniidae	1	0
Peudochaenichthys georgianus	Channichthyidae	0	1
Notolepis coatsorum	Paralepididae	0	1
Muraenolepis sp.	Muraenolepididae	0	1
Total		**277**	**281**

Table 2. Larval fish growth estimated from linear models. Linear model (LM) starting values, coefficients, and standard errors (SE) of the coefficients for the five most abundant taxa collected during both seasons. Linear coefficients are used as estimates of larval growth in mm day^{-1}.

Taxa	Season	LM intercept (mm)	Coefficient (mm day^{-1})	SE
L. nudifrons	2017 - 2018	9.93	0.078	0.010
L. nudifrons	2018 - 2019	10.53	0.074	0.007
T. newnesi	2017 - 2018	8.57	0.052	<0.001
T. newnesi	2018 - 2019	7.57	0.100	0.030
N. larseni	2017 - 2018	6.52	0.030	0.010
N. larseni	2018 - 2019	7.63	0.040	0.011
T. scotti	2017 - 2018	4.63	0.048	0.039
T. scotti	2018 - 2019	4.40	0.036	0.014
L. squamifrons	2017 - 2018	6.20	0.039	0.023
L. squamifrons	2018 - 2019	5.55	0.034	0.019

Supplemental Table 1. Model selection table for generalized linear laten variable (GLLVM) models. Assemblage is the five nototheniid species of interest (*L. nudifrons, T. newnesi, N. larseni, T. scotti, and L. squamifrons*). Model development and selection was based on hypothesis testing, parsimony, and AIC (Akaike's information criterion). Model t3 did not converge (NC). The final model format is bolded.

Model	Formula	AIC	dAIC
t1	assemblage ~ sea surface temperature (temp.)	920.5	33.7
t2	assemblage ~ 20m temp.	911.1	24.4
t3	assemblage ~ 50m temp.	NC	NC
s1	assemblage ~ 20m temp. + sea surface salinity (sal.)	914.1	27.3
s2	assemblage ~ 20m temp. + 20m sal.	916.7	29.9
s3	assemblage ~ 20m temp. + 50m sal.	908.4	21.6
c1	assemblage ~ 20m temp. + 50m sal. + C. acutus	908.7	21.9
c2	assemblage ~ 20m temp. + 50m sal. + C. propinquus	892.3	5.5
c3	assemblage ~ 20m temp. + 50m sal. + R. gigas	919.2	32.4
c4	assemblage ~ 20m temp. + 50m sal. + Small calanoids	909.7	22.9
c5	assemblage ~ 20m temp. + 50m sal. + Oithona spp.	915.9	29.1
c6	assemblage ~ 20m temp. + 50m sal. + C. propinquus + C. acutus	899.4	12.6
c7	assemblage ~ 20m temp. + 50m sal. + C. propinquus + Oithona spp.	895.3	8.6
c8	assemblage ~ 20m temp. + 50m sal. + C. propinquus + Small calanoids	896.1	9.3
c9	assemblage ~ 20m temp. + 50m sal. + C. propinquus + C. acutus	899.4	12.6
c10	assemblage ~ 20m temp. + 50m sal. + C. propinquus + R. gigas	907.3	20.5
c11	assemblage ~ 20m temp. + 50m sal. + C. propinquus + Oithona spp. + Small calanoids	899.5	12.7
k1	assemblage ~ 20m temp. + 50m sal. + C. propinquus + E. superba	898.0	11.2
k2	assemblage ~ 20m temp. + 50m sal. + C. propinquus + T. macrura	895.7	8.9
k3	assemblage ~ 20m temp. + 50m sal. + C. propinquus + Oithona spp. + E. superba	891.4	4.6
k4	assemblage ~ 20m temp. + 50m sal. + C. propinquus + Oithona spp. + T. macrura	886.8	0.0
p1	**assemblage ~ 20m temp. + 50m sal. + C. propinquus + Oithona spp. + T. macrura + diatoms**	**887.8**	**1.0**
p2	assemblage ~ 20m temp. + 50m sal. + C. propinquus + Oithona spp. + T. macrura + mixed flagellates	890.3	3.5
p3	assemblage ~ 20m temp. + 50m sal. + C. propinquus + Oithona spp. + T. macrura + cryptophytes	889.2	2.4
p4	assemblage ~ 20m temp. + 50m sal. + C. propinquus + Oithona spp. + T. macrura + prasinophytes	901.6	14.8
p5	assemblage ~ 20m temp. + 50m sal. + C. propinquus + Oithona spp. + T. macrura + haptophytes	895.3	8.5
p6	assemblage ~ 20m temp. + 50m sal. + C. propinquus + Oithona spp. + T. macrura + diatoms + cryptophytes	898.4	11.6
l1	**p1 + 1 latent variable**	**887.8**	**1.0**
l2	p1 + 2 latent variables	895.8	9.0

Supplemental Table 2. Estimates (est.), standard errors (std. error), and *p* values (with values < 0.1 bolded) from the final GLLVM model (See Supp. Table 1).

Taxa	Diatom density (est., std. error, *p*)	*Oithona* spp. density (est., std. error, *p*)	*C. propinquus* density (est., std. error, *p*)	Salinity (est., std. error, *p*)	Temperature (est., std. error, *p*)	*T. macrura* density (est., std. error, *p*)
L. nudifrons	0.58, 0.35, **0.09**	0.22, 0.32, 0.50	-0.35, 0.51, 0.49	0.18, 0.34, 0.60	-1.34, 0.39, **<0.01**	-13.39, 14.34, 0.35
T. newnesi	0.058, 0.41, 0.88	-0.27, 0.30, 0.36	0.76, 0.38, **0.05**	-0.07, 0.30, 0.83	-0.17, 0.37, **<0.01**	-2.09, 3.82, 0.59
N. larseni	0.47, 0.26, **0.07**	0.06, 0.24, 0.81	-0.12, 0.39, 0.77	0.37, 0.29, 0.21	-0.93, 0.28, **<0.01**	-0.26, 0.45, 0.57
T. scotti	0.21, 0.26, 0.42	-0.74, 0.36, **0.04**	-0.23, 0.35, 0.51	0.96, 0.34, **<0.01**	-0.05, 0.35, 0.88	-0.18, 0.28, 0.53
L. squamifrons	0.30, 0.21, 0.15	0.24, 0.25, 0.34	-0.82, 0.37, **0.03**	0.57, 0.39, 0.14	2.21, 0.73, **<0.01**	0.58, 0.16, **<0.01**

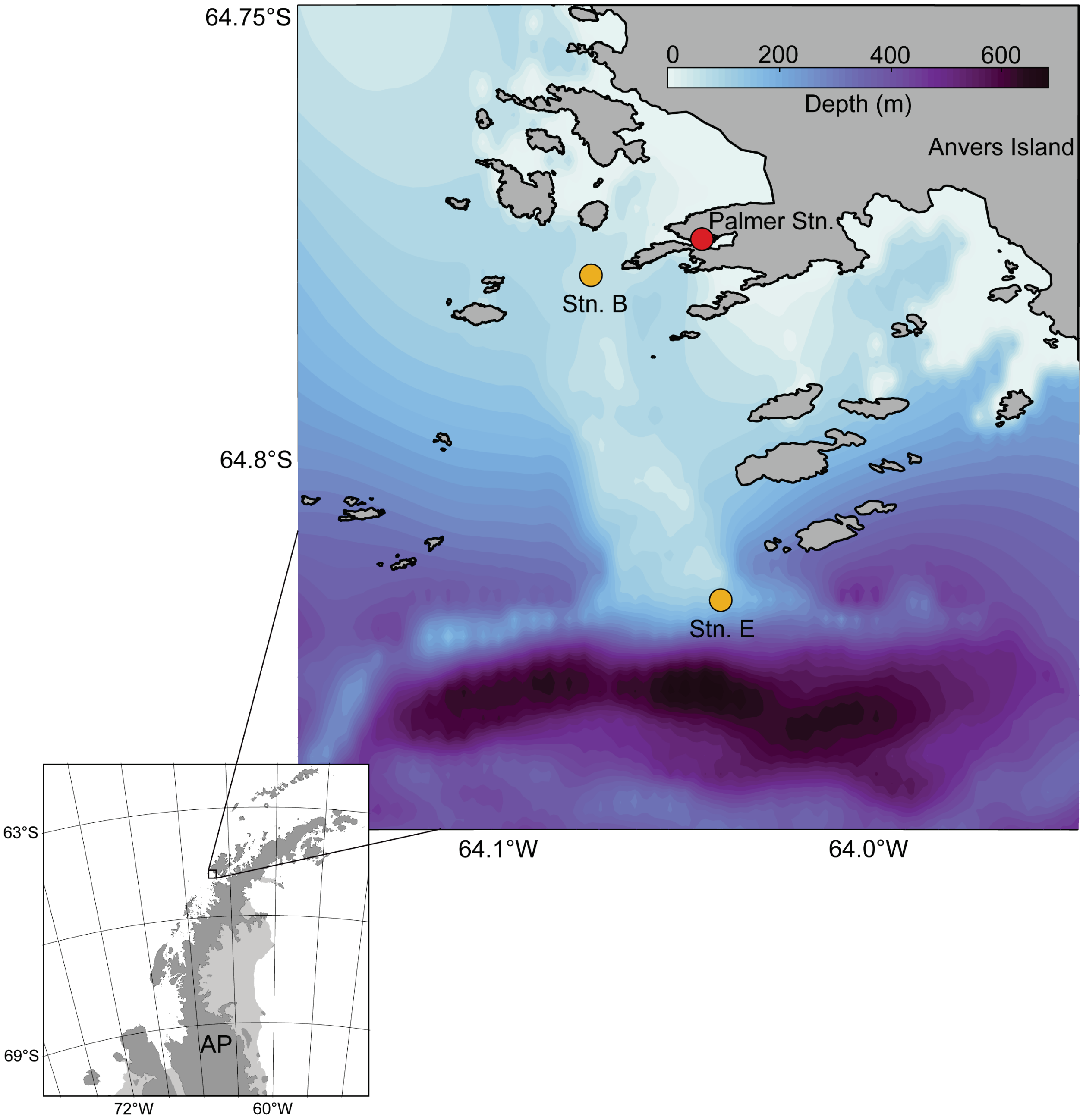

Figure 1. Study area near Palmer Station on Anvers Island, western Antarctic Peninsula. Map indicates Palmer Station (red dot) and sampling sites, Stations B and E (yellow dots) in the Anvers Island area. The inset shows the greater Antarctic Peninsula (AP) region. The map was created using Matlab and ArcGIS Pro (Version 3.1.1, Environmental Systems Research Institute).

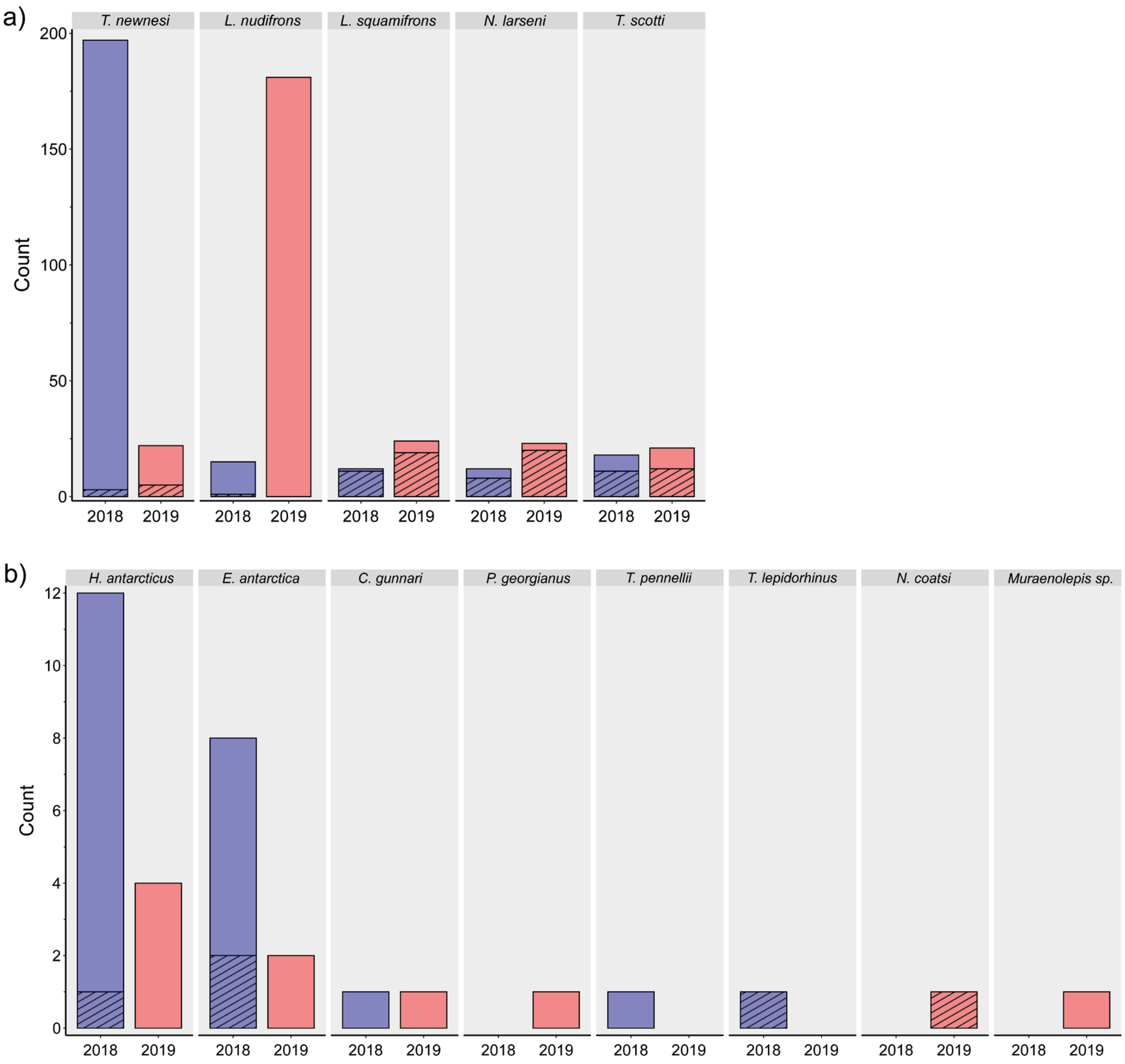

Figure 2. Total counts of a) of the five most abundant larval fish taxa and b) the less abundant larval fish taxa collected near Anvers Island, Antarctica during the 2017 – 2018 (blue) and 2018 – 2019 (red) seasons. Stations B and E are combined, with fishes collected at Station E cross-hatched. See Table 1 for full species names.

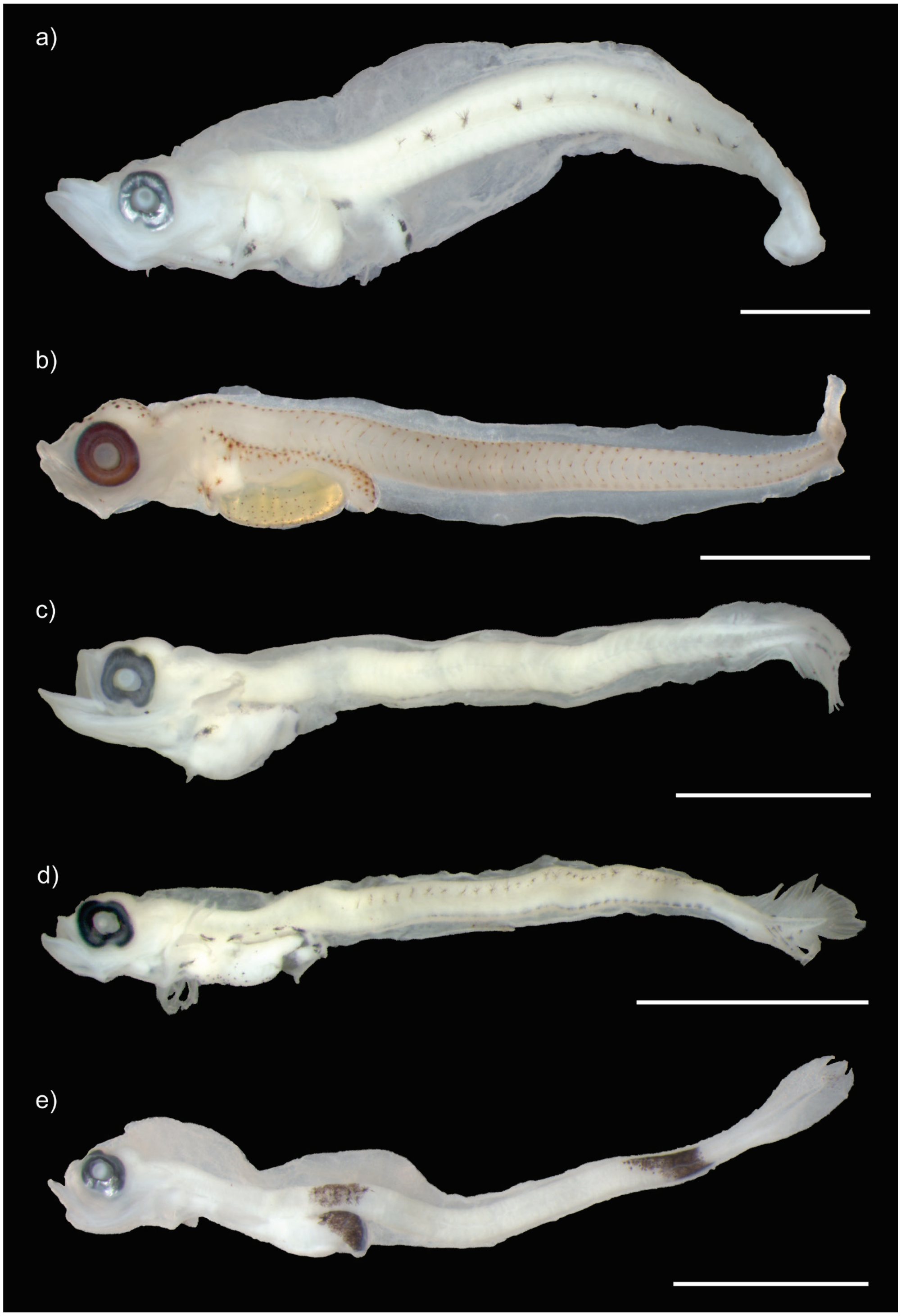

Figure 3. Images of the five most abundant larval fish species collected during this analysis. a) *Lindbergichthys nudifrons* (Lönnberg 1905), b) *Trematomus newnesi* (Boulenger 1902), c) *Nototheniops larseni* (Lönnberg 1905), d) *Trematomus scotti* (Boulenger, 1907), and e) *Lepidonotothen squamifrons* (Günther, 1880). Images are of preserved specimens; scale bars are 2mm.

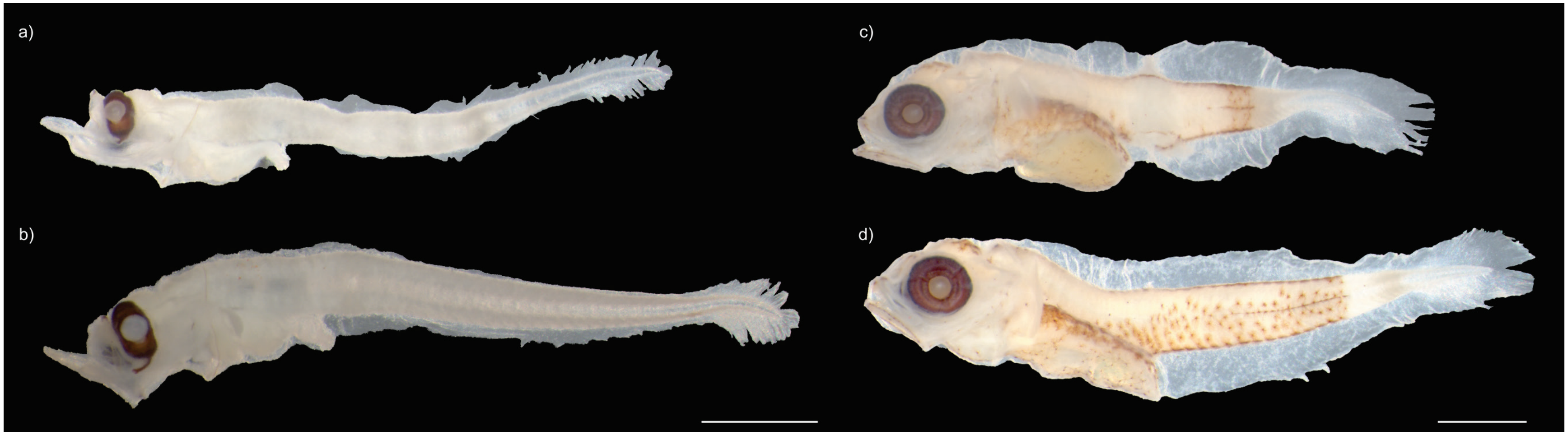

Figure 4. Larval stages of a, b) – the myctophid *Electrona antarctica* (Günther, 1878) and c, d) – the harpagiferid *Harpagifer antarctcus* Nybelin, 1947. Scale bars for each species are both 1 mm.

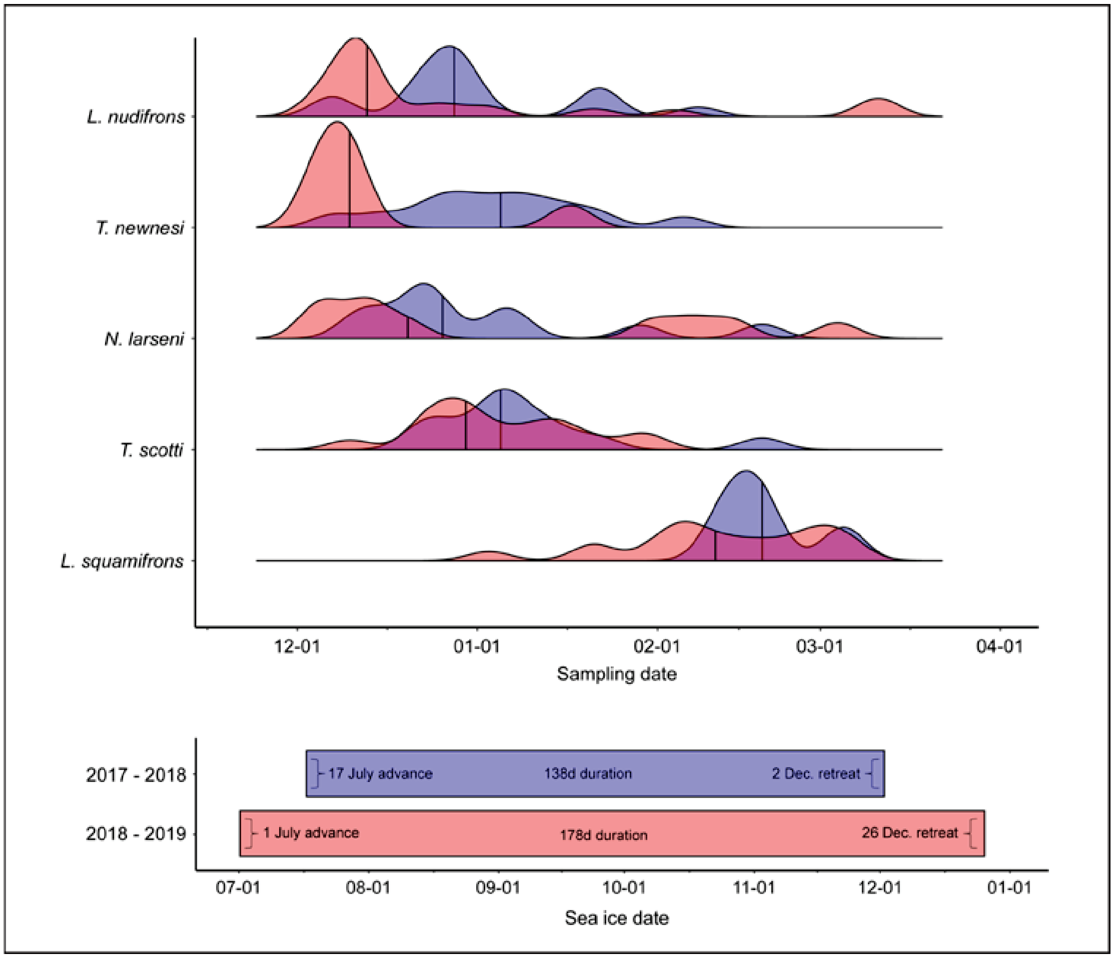

Figure 5. Ridgeline plots of the five most abundant larval fish taxa at Stations B and E near Anvers Island, Antarctica during 2017 – 2018 (blue) and 2018 – 2019 (red). Y-axes are scaled to frequency and vertical black lines represent mean, or peak, abundance dates. Sea ice dynamics include the day of advance, duration in days (d), and day of retreat for both seasons.

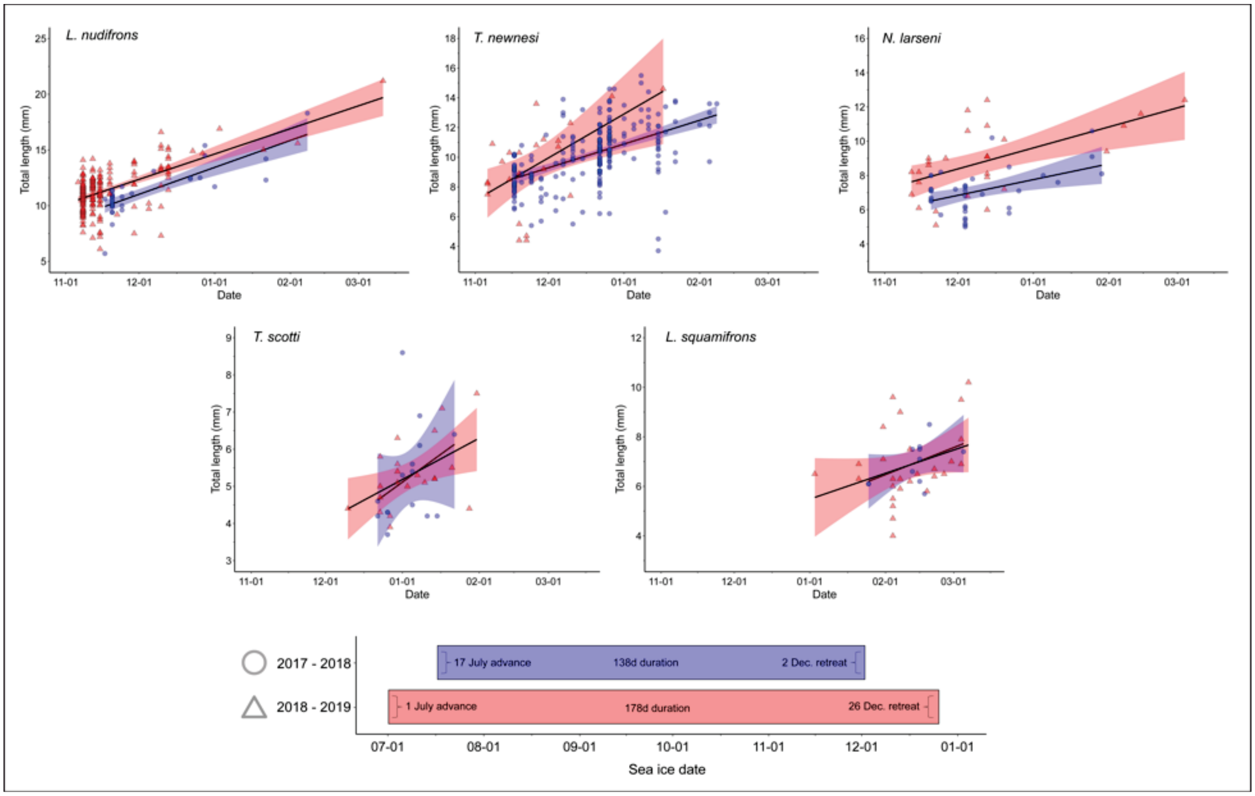

Figure 6. Standard length (SL) of the five most abundant larval fishes collected at Stations B and E near Anvers Island, Antarctica during 2017 – 2018 (blue circles) and 2018 – 2019 (red triangles). Sea ice dynamics include the day of advance, duration in days (d), and day of retreat for each season. Black fitted lines represent linear regressions surrounded by 95% error (colored shading).

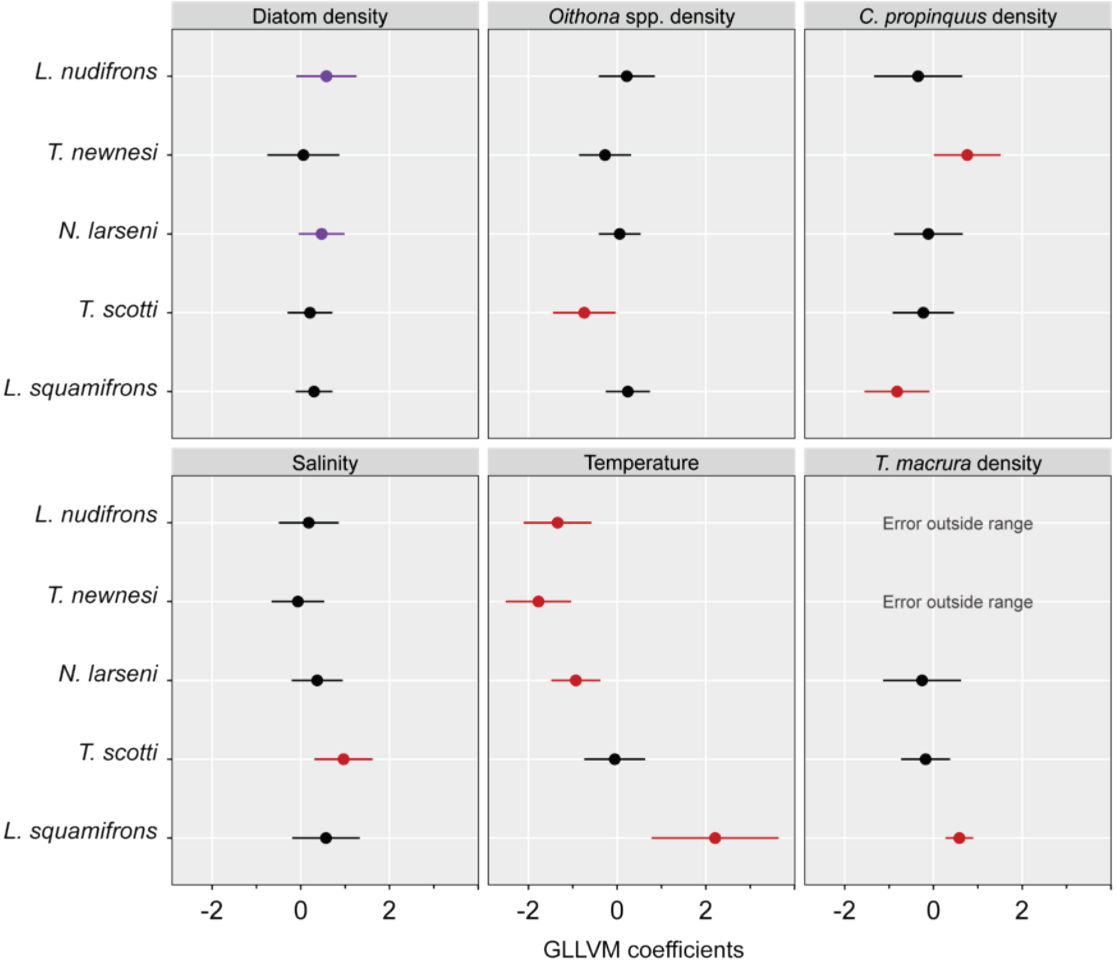

Figure 7. Coefficients (circles) and 95% error (lines) estimated from the final GLLVM model. All parameters are z-scored to aid in model convergence. Red indicates significant relationships ($p < 0.05$); purple $p < 0.10$, and black non-significant. The estimates for *L. nudifrons* (-13.39 +/- 28.11) and *T. newnesi* (-2.09 +/- 7.49) with the parameter *T. macrura* were extremely outside the range of all other estimates and not significant; they are not displayed to improve interpretation of all other coefficients.

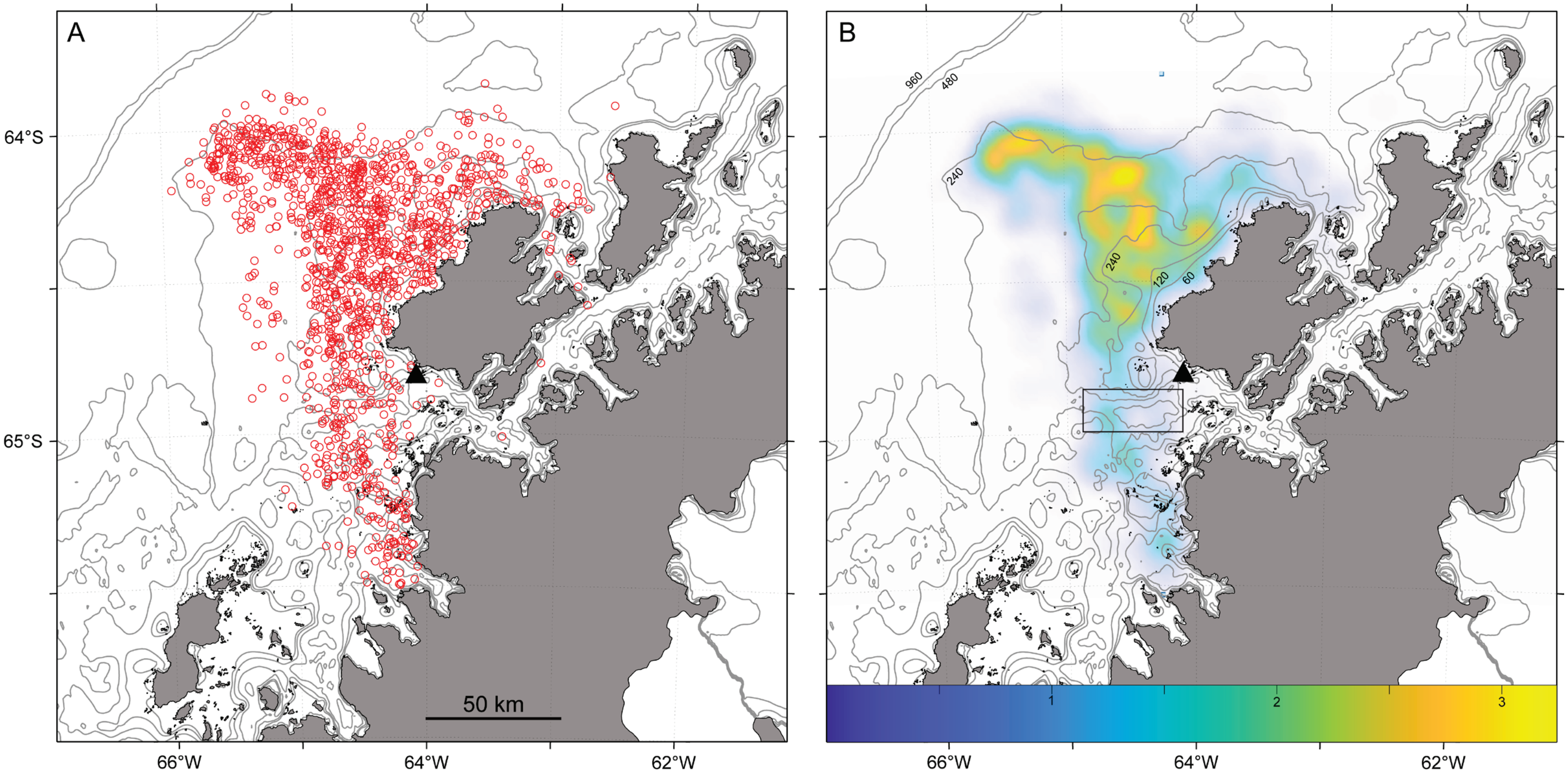

Figure 8. Larval fish dispersion model. A. Origin locations (red circles) of the particles originally released at 10 m that reached the upper 120 m at Station E (black triangle) after 17 days of drift. B. Heatmap illustrating concentrations of particle origins, with colors corresponding to kernel densities and the black box outlining Palmer Deep Canyon. Bathymetric intervals are the same for both maps - 0, 60, 120, 240, 480, 960m.

Figure 9. Larval *T. newnesi* and copepod prey. This specimen (top) had a full gut that contained this copepod (bottom), likely *C. propinquus*.

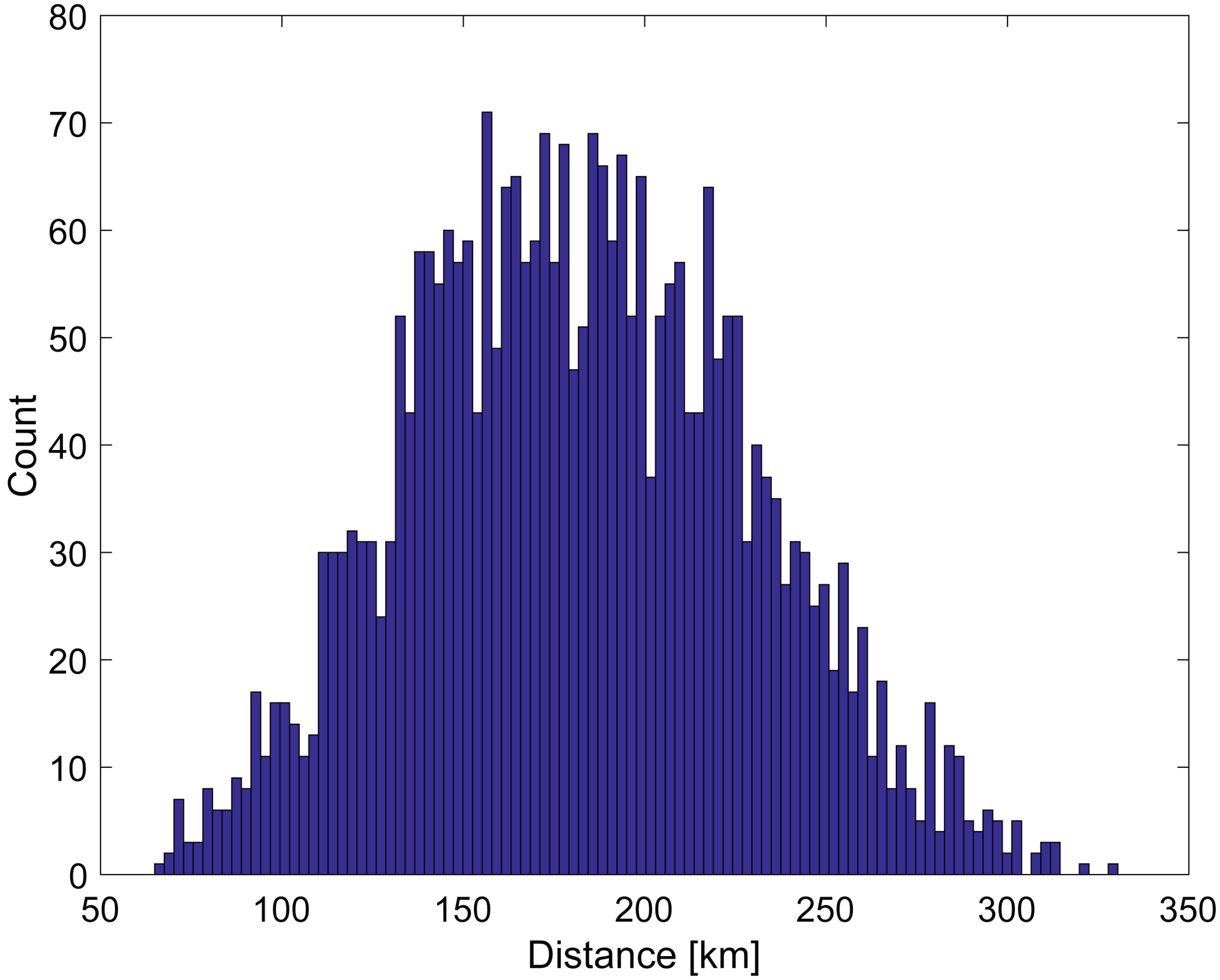

Supplemental Figure 1. Travel distance of the 3524 particles selected in the dispersion model (Fig 8a).

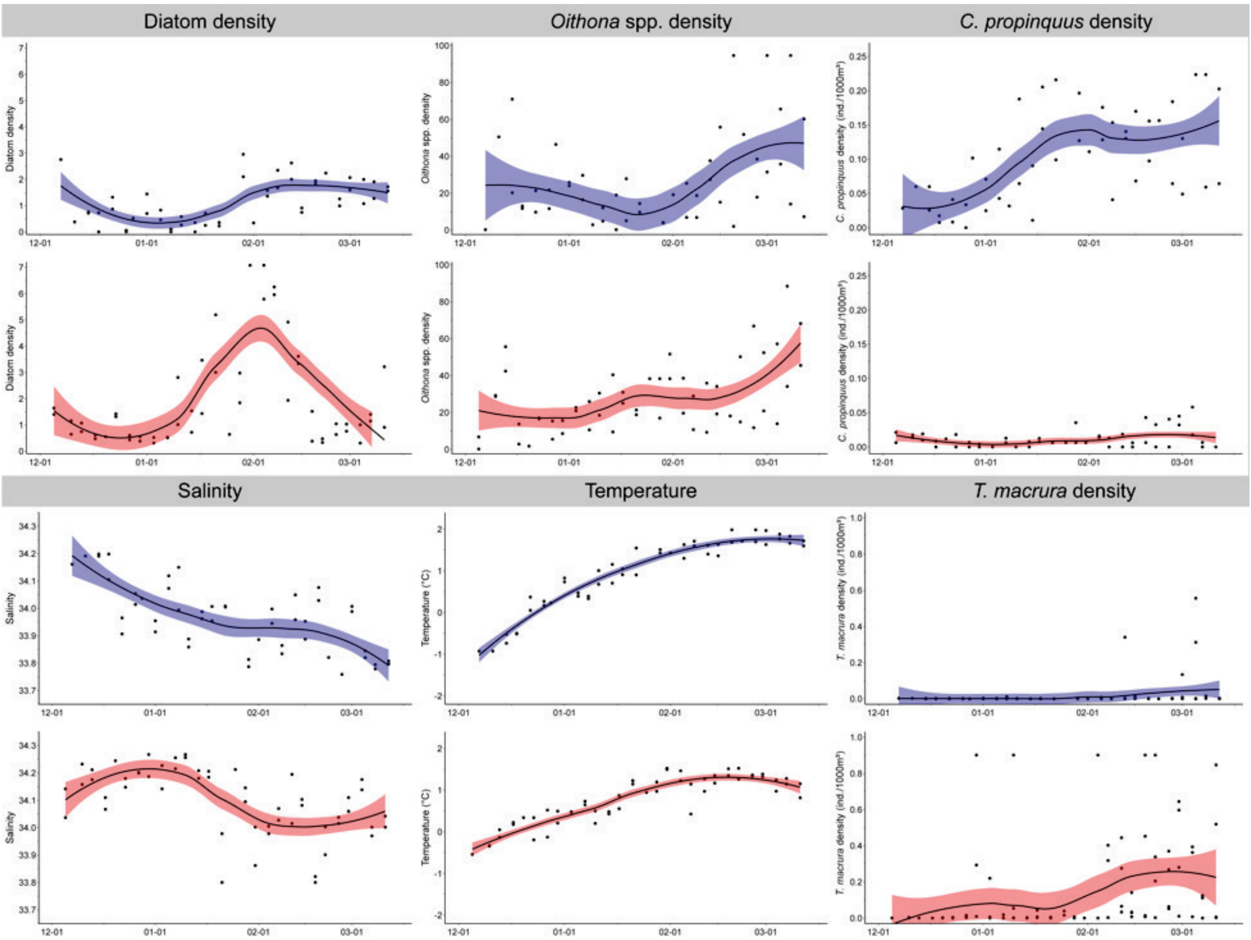

Supplemental Figure 2. Covariates selected from the final GLLVM model (see Supp. Table 1) plotted over each season, with 2017 – 2018 in blue and 2018 – 2019 in red. Each variable is fit with a generalized additive model (GAM; black lines) surrounded by 95% error (colored shading).

CHAPTER 6
Thermal tolerance of larval Antarctic cryonotothenioid fishes

This chapter is in preparation for submission as: Corso AD, Mowatt-Larssen T, Brill RW, Steinberg DK, Hilton EJ. Thermal tolerance of larval Antarctic cryonotothenioid fishes.

Abstract

Cryonotothenioids constitute a subgroup of notothenioid fishes endemic to the Southern Ocean that are specialized to exist in a narrow range of near-freezing environmental temperatures. Due to the challenges of reliably collecting and maintaining larval cryonotothenioids in good condition, most studies of their thermal tolerance have been limited to adult and juvenile stages. With increasing environmental pressures from climate change in Antarctic ecosystems, it is important to elucidate the potential impacts of warming on larval stages as well. In this study, we determine the critical thermal maxima (CTmax) of cryonotothenioid larvae collected in pelagic net tows during three research cruises near the western Antarctic Peninsula. We sampled larvae from three families – Nototheniidae, Channichthyidae, and Artedidraconidae. Channichthyid and nototheniid CTmax ranged from 8.6 – 14.9 ° C, and was positively correlated with body length, suggesting that younger, less motile larval channichthyids may be especially susceptible to rapid warming events such as marine heatwaves. Additionally, to our knowledge, this is the first published test of artedidraconid acute thermal tolerance, with CTmax ranging from 13.2 – 17.8°C, which did not correlate with body length. Of the two artedidraconid species we collected, *Neodraco skottsbergi* showed remarkable tolerance to warming and was the only species to resume normal swimming following trials. We offer two hypotheses as to why *N. skottsbergi* has such an elevated thermal tolerance – 1) their unique green coloration serves as camouflage within near-surface phytoplankton blooms, suggesting they occupy an especially warm near-surface niche and 2) recent insights into their evolutionary history links ancestral taxa that may have occupied warm tide-pool habitat. Collectively, these results establish *N. skottsbergi* and larval channichthyids as groups of interest for future physiological studies to gain further insights on the health of cryonotothenioids in a warming ocean.

1. Introduction

The perciform suborder Notothenioidei, which dominates fish diversity and accounts for nearly 90% of the fish biomass in the Southern Ocean's coastal and shelf regions (Gon and Heemstra 1990), is regarded as the most stenothermal group of marine fishes (Dahlke et al. 2020). The unprecedented pace of ocean warming in regions of the Southern Ocean poses risks to notothenioid fishes, especially those endemic to Antarctic waters (i.e., members of the five families included in the Cryonotothenioidea) (Mintenbeck et al. 2012; Beers and Jayasundara 2015). During just the latter half of the 20th century, mid-depth Southern Ocean temperatures rose 0.17° C on average (Gille 2002), with sea-surface temperature (SST) in the highly impacted western Antarctic Peninsula (WAP) warming over 1° C (Meredith and King 2005). Precise estimates of future warming scenarios in the Southern Ocean are currently limited by interdecadal variability, geographically asymmetrical responses, and data paucity (Kennicutt et al. 2019). Despite this uncertainty, it is likely that the Southern Ocean will continue to warm in the coming decades, primarily as a result of anthropogenic influence (Rintoul et al. 2018; Swart et al. 2018). It is therefore important to determine the thermal tolerance of cryonotothenioids at different life stages to better predict how these fish populations will respond to current and future environmental change.

Most research on cryonotothenioid thermal tolerance is focused on adult notothenioids from the families Nototheniidae, Channichthyidae, and Bathydraconidae (Bilyk and DeVries 2011; Beers and Sidell 2011). Initial studies suggested that these fishes have remarkably low Upper Incipient Lethal Temperatures, ranging from 5 – 7° C in *Pagothenia borchgrevinki*, *Trematomus bernacchii*, and *Trematomus hansoni* (Somero and DeVries 1967). Subsequent studies suggest that nototheniid thermal tolerance may be influenced by habitat, with nototheniids inhabiting the northerly Seasonal Pack Ice Zone (SPZ) having higher thermal tolerance compared to closely related species that inhabit the more southerly, cooler High-Antarctic Zone (HAZ) (Bilyk and DeVries 2011). During austral summer, shallow waters (< 20m) of the SPZ can reach temperatures exceeding 2° C for nearly one month (Cárdenas et al. 2018), while shallow-water temperatures rarely exceed -0.5° C in the HAZ (Hunt et al. 2003; Bilyk and DeVries 2011). Several nototheniids from SPZ areas show a higher capacity for metabolic acclimation under warming conditions, suggesting that phylogenetic history also contributes to thermal tolerance (Todgham & Mandic 2020). Studies on the thermal tolerance and physiology of larval and juvenile cryonotothenioids are limited to just two Antarctic nototheniid species and one bathydraconid species, all of which were collected from the McMurdo Sound HAZ region (Table 1). We have summarized current information on thermal tolerance for juvenile, larval, and egg stages of cryonotothenioids and one sub-Antarctic larval nototheniod in Table 1.

A method commonly used to describe the thermal tolerance of adult cryonotothenioid fishes is the difference between the critical thermal minimum (CTmin) and critical thermal maximum (CTmax), which are the temperatures below and above, respectively, at which an individual loses its ability to swim (Lutterschmidt and Hutchison 1997; Beers and Jayasundara 2015). The temperature that cryonotothenioids freeze (approximately -2.2° C) is defined as their CTmin (Bilyk and DeVries 2011). To determine CTmax, fishes are exposed to rising temperatures in aquaria at a fixed rate (usually 0.3° C min^{-1}) and monitored for behavioral changes. The temperature at which a fish is unable to maintain its ability to right itself, an indicator for loss of swimming capability, is recorded as the CTmax (Morgan et al. 2018).

In this study, we follow the methods of Bilyk & DeVries (2011) to determine the CTmax of larvae of several species of cryonotothenioids. These results are compared to the CTmax of adults determined by Bilyk & DeVries (2011). We then discuss potential future research priorities to better understand the thermal limits and physiology of several groups of cryonotothenioids.

2. Materials and Methods

Collection of larval fishes

Larval cryonotothenioids were collected during January 2020 and January 2023 aboard the ASRV *Laurence M. Gould* and November – December 2021 aboard the ASRV *Nathaniel B. Palmer* as part of the Palmer Antarctica Long-Term Ecological Research (Palmer LTER) program. Sampling was conducted in the Bellingshausen Sea along the western Antarctic Peninsula (WAP) shelf (**Fig 1a**). Larvae were captured opportunistically from epipelagic oblique net tows targeting zooplankton, using a 2-m^2 frame (700-µm mesh; 120m target depth) or 1-m^2 frame (333-µm mesh; 300m target depth) Metro net (Steinberg et al. 2015). The contents of these tows were immediately transferred from the cod end to a large holding tank where larval cryonotothenioids were identified and evaluated for condition. Postflexion larvae swimming normally with no signs of body trauma were chosen either for control or CTmax trials.

CTmax and control trials

Selected larvae were transferred to 11.4-liter polycarbonate tanks filled with seawater supplied from a hull-mounted flow through system. Tanks were aerated with an air pump to maintain adequate high oxygenation and prevent thermal stratification. The control tank was incubated in a flow through seawater bath to maintain ambient sea water temperature (-1 to 3° C; Fig 2b). Larval behavior was monitored in the control tanks to ensure the results of the CTmax trials were not artifacts of trauma sustained during net tows.

Fishes in the CTmax tank were immediately warmed at a fixed rate of 0.3° C min^{-1}. Moyano et al. (2017) suggested that a slower heating rate is potentially more suitable for larval fishes. However, the primary goal of our study is to compare CTmax of larvae with that of adults reported in Bilyk & DeVries (2011), therefore we chose to replicate their heating rate of 0.3° C min^{-1}, as changes in heating rate can impact CTmax in notothenioids (Peck et al. 2014). Water temperature in the control and experimental tanks was recorded using a NIST-traceable thermistor thermometer (Digi-Sense, USA).

Larvae were monitored continuously for the duration of each CTmax trial. Consistent heating was continued until a fish was unable to right itself for one minute after rolling on its side, indicating "persistent loss of equilibrium" (Bilyk and DeVries 2011). After the CTmax temperature was recorded, larvae were transferred to a tank held at the environmental temperature where their recovery was evaluated. Larvae were then measured (standard length [SL] mm), euthanized by overdose of methanosulfanate (MS-222), preserved in 95% ethanol, and cataloged into the Virginia Institute of Marine Science (VIMS) Nunnally Ichthyology Collection.

We used box and whisker plots to illustrate and interpret CTmax data. Larvae with similar characteristics were then grouped to analyze the correlations between length and SST at collection location, (determined by a SBE38 Digital Thermometer), with CTmax using linear regressions. All plots were created in R (R Core Team 2022). We also plot collection sites for larvae along the WAP using ArcGIS Pro Version 3.1.1. (Environmental Systems Research Institute Inc.).

Ethical approval

This research involved contact with live animals, all experiments were conducted in compliance with William & Mary Institutional Animal Care and Use Committee (IACUC) permits 2019-11-04-13894, 2021-10-05-15162, and 2022-09-15-15848.

3. Results

We collected 37 larvae that were in suitable condition for this study. Of these, 31 were used for CTmax trials (Table 2), and six larvae were monitored as controls (no warming). The group of experimental fishes included three cryonotothenioid families: Channichthyidae (n = 13 larvae), Artedidraconidae (n = 14), and Nototheniidae (n = 4). Artedidraconids possessed the highest average CTmax (15.4° C ± 1.6), followed by nototheniids (13.9° C ± 1.2), and then channichthyids (10.9° C ± 1.4) (Table 2; Fig 1b). *Neodraco skottsbergi* Lönnberg 1905 (Artedidraconidae) possessed the highest average CTmax (16.8° C ± 1.0), with one individual attaining a CTmax of 17.8° C, which is among the highest values reported for any adult or larval cryonotothenioid (Bilyk and DeVries 2011; Beers and Sidell 2011). Three *Chionodraco rastrospinosus* DeWitt and Hureau 1980(Channichthyidae) larvae had CTmax values ranging from 8.6 – 9.2 ° C (Fig 1b), which are among the lowest values of any cryonotothenioid tested to date (Bilyk and DeVries 2011; Beers and Sidell 2011). Of all species, only *N. skottsbergi* were able to resume normal swimming behavior following experimental trials. This behavior was briefly monitored (<10 min) before larvae were euthanized; therefore, it is unclear how long this behavior would have persisted nor the long-term effects of exposure to acute thermal stress on these larvae. All control larvae (four artedidraconids, one nototheniid, and one channichthyid) maintained normal swimming behavior for at least 7.2 hours, while the longest CTmax trial was 59 minutes.

There is a positive linear relationship (coefficient [coef] = 0.76, mean squared error [MSE] = 2.6, $p = 0.058$) between length and CTmax among grouped channichthyid and nototheniid larvae (Fig 2a). There is also a positive relationship (coef = 0.74, MSE = 2.6, $p = 0.067$) between tow location SST and CTmax among the grouped channichthyids and nototheniids (Fig 2b). Due to their anomalously high CTmax, artedidraconids were excluded from both regressions.

5. Discussion

Artedidraconids

Little is known regarding the thermal tolerance of artedidraconids of any life stage. The high-Antarctic *Artedidraco orianae* (Regan 1914) appears to have limited metabolic capacities at elevated temperatures based on cellular energy budgets, but insufficient data prevented any firm conclusions from this analysis (Mark et al. 2005). The impact of acclimation time on oxygen consumption in *Pogonophryne scotti* has also been tested (Saint-Paul et al. 1988). We are unaware of any studies on the whole-body thermal tolerance of any artedidraconid species. Therefore, it is unclear if the abnormally high thermal tolerances we observed in *N. skottsbergi*, and to a lesser degree *Doliodraco longedorsalis* (Roule 1913) (Table 2; Fig 1b), are unique to larval stages. Also, the rapid recovery of all larval *N. skottsbergi* following CTmax trials may indicate that the physiological damage of the acute heat exposure is, at least temporarily, reversible (Ern et al. 2023).

The biology of adult *N. skottsbergi* does not explain the unusually high thermal tolerance of their larval stages. This species has a circumpolar distribution, found in both SPZ and HAZ regions, and possesses antifreeze glycoproteins (Miya et al. 2016; Baalsrud et al. 2018). Similar to other artedidraconids, they are benthic, generalist feeders consuming primarily amphipods and polychaetes (Gon and Heemstra 1990; La Mesa et al. 2015). Small (10.0 – 14.5 mm SL) *N. skottsbergi* larvae with remnants of their yolksac have been found around Joinville Island, WAP from early November to early December, which suggests that hatching in this area occurs from October – November (Kellermann 1990). They are only captured in the epipelagic zone during the austral summer (January to late February); afterwards, they likely begin their descent to the benthos (Kellermann 1990). Thus, their biogeographic and ecologic traits do not generally differ from other more stenothermal cryonotothenioids; however, one aspect of their larval biology is unusual and described below.

All *N. skottsbergi* larvae we captured possessed a unique vibrant green color (Fig 3a). We are unaware of any other cryonotothenioid larvae with similar green pigmentation and there is no mention of this trait in Kellermann (1990) or any other publication. Although there is little information on the coloration of postlarvae and juveniles, *N. skottsbergi* are dark brown with a yellowish hue as adults (Gon and Heemstra 1990). Most cryonotothenioid larvae have a pelagic stage lasting at least two months during the austral summer, which temporally overlaps with peak phytoplankton production (Kock and Kellermann 1991). All *N. skottsbergi* in this study were collected in neritic areas near marine-terminating glaciers in Dalgleish Bay (Fig 1a). The freshwater layer associated with glacial meltwater stratifies the upper water column during the summer, which leads to warmer sea surface temperatures, while the macro- and micro-nutrients found in the stable meltwater promote the growth of several Antarctic phytoplankton species (Pan et al. 2020). The green coloration of the larvae could help them blend in with phytoplankton concentrated in near-surface (< 1m depth) waters, which may provide cover to escape predation (Coston-Clements et al. 1991). During daylight and marginal wind conditions, the upper meter of the water column can be twice as warm as at 10 m depth (Minnett and Kaiser-Weiss 2012). At these shallow depths, *N. skottsbergi* would routinely experience warmer temperatures than other notothenioids that are normally found in deeper areas (20 – 500 m; Loeb et al. 1993), which could partially explain their elevated CTmax. This explanation aligns with an analysis of eight adult nototheniid species which found cardio-respiratory control is correlated with ecotype (e.g., benthic, epibenthic, or pelagic)(Campbell et al. 2009). All larval *N. skottsbergi* in our study were captured by oblique tows covering 0 – 120m; thus, we are unaware of their exact collection depth. Future research should evaluate the exact depth horizon larval *N. skottsbergi* occupy, their prey field, and intraspecific variability in their green coloration.

Recent research on artedidraconids has focused on their evolutionary history and phylogenetic relationships, which can drive species trait patterns and thermal tolerance (Felsenstein 1985; Todgham and Mandic 2020) . In their phylogenetic analysis, Parker and Near (2022) recovered artedidraconids as a group within Harpagiferidae as the subfamily Artedidraconinae (Andriashev 1965). One harpagiferid species, *Harpagifer bispinis* (Foster 1801), is found in the Magellan region of South America (Duhamel et al. 2014), where summer ocean temperatures can exceed 11°C. Although experimental fishes were acclimated to aquaria before trials, *H. bispinis* has a CTmax of 23.6 °C (Llompart et al. 2020; Giménez et al. 2021). Several harpagiferid species are also routinely found in shallow tide pools in the SPZ (Duarte and Moreno 1981; Casaux 1998; Eastman 2017), where temperatures can exceed 5°C depending on sunlight intensity (Mintenbeck et al. 2012; Clarke and Beaumont 2020). Evolutionary history is known to correlate strongly with CTmax in freshwater fishes, with the retention of plesiomorphic characters contributing to thermal tolerance (Comte and Olden 2017). Therefore, occupying habitats such as the warm tide pools inhabited by closely related harpagiferids could also contribute to the CTmax of *N. skottsbergi*; whether this reflects a plesiomorphic habitat association for artedidraconids is unknown. Future study of their physiological responses to warming will contribute to the understanding of the evolution of this outlying condition within cryonotothenioids.

Channichthyids and nototheniids

Channichthyids are among the most stenothermal of all cryonotothenioids (Beers and Sidell 2011). These fishes completely lack hemoglobin, the protein in red blood cells that binds to oxygen and facilitates its transport throughout the circulator system. The absence of hemoglobin, and in some cases myoglobin (which stores oxygen in muscular tissue), in white-blooded channichthyids limits their oxygen carrying capacity to 10% that of red-blooded nototheniids (Holeton 1970; Beers and Sidell 2011). Beers and Sidell (2011) evaluated the CTmax of several channichthyids and nototheniids, finding hematocrit (i.e., the proportion of red-blood cells within a circulatory system) positively correlates with CTmax. Two channichthyid species (*Chionodraco rastrospinosus* and *Chaenocephalus aceratus* (Lönnberg 1906)) possess the lowest mean CTmax in that analysis (Beers and Sidell 2011).

Results of our linear regression suggest that thermal tolerance in some larvae of channichthyids increases with ontogeny and environmental SST. Although larval nototheniids were included in the regression, we hesitate to draw similar conclusions regarding their relationships without a larger sample size of individuals in experimental trials. However, our results (mean of 13.9° C) align closely with the only known CTmax for larval nototheniids (14.6° C; Table 1) (Evans et al. 2012). The positive correlation with SST is consistent with results obtained by Bilyk and DeVries (2011), who report that several adult cryonotothenioids have a level of plasticity in their upper thermal limit depending on the ocean temperature of their environment. Previous studies have reported CTmax values for the adult counterparts for two of our study species: *C. rastrospinosus* (Beers and Sidell 2011) and *L. squamifrons* (Bilyk and DeVries 2011). The average CTmax for both species is lower in larvae than that reported for adults (Table 2).

Ontogeny is known to impact thermal tolerance in fishes, although few experiments have been conducted on the early life stages of cryonotothenioids (Table 1). Studies of other marine fishes suggest heat tolerance is positively correlated with the development of the cardiorespiratory system (Dahlke et al. 2020). For example, *Boreogadus saida* (Lepechin 1774), or Arctic Cod, larvae have an upper thermal tolerance that is 40% less than that of adults based on cardiac response (Drost et al. 2016). The limited aerobic capacity of early life stages can result in a compromised ability to deliver oxygen to tissues during unusually warm temperatures (Rombough 1988; Pörtner et al. 2006). Given that channichthyids are already functioning with limited oxygen carrying capacity, the early larval stages of this group may be especially vulnerable to thermal extremes as their cardiorespiratory systems develop.

Increased stenothermy during early life stages has been proposed as a possible trade-off, such that larval fishes are more dependent on ideal environmental temperatures and thus may invest more energy into growth (Pörtner et al. 2006). Pre-flexion larvae are also less motile than older fishes, which limits their ability to escape incursions of warm water (Downie et al. 2020). In addition to the long-term ocean warming observed in the WAP region of 0.1 to 0.3° C per decade (Schmidtko et al. 2014), increasing frequency of extreme heatwaves may pose a serious risk to pre-flexion channichthyid larvae (Robinson et al. 2020; Robinson 2022; Morrison et al. 2022; González-Herrero et al. 2022). The long-term abundance of the larval nototheniid *Pleuragramma antarctica* (Boulenger 1902) is negatively correlated with sea surface temperature (Corso et al. 2022), but there are no long-term analyses of channichthyid abundance in relation to ocean temperature during any life stage. Such analyses will be needed to model population dynamics accurately.

In conclusion, results of this study indicate that additional research on the physiology and ecology of artedidraconids and channichthyids should be prioritized to determine potential “winners” and “losers” of climate change in the Southern Ocean. Future *in vivo* research is especially necessary to better understand the impact that warming may have on all cryonotothenioid fishes, particularly during sensitive larval stages. Together, these efforts will explicate a clearer projection for the future Southern Ocean ecosystem.

Acknowledgements

We thank Kharis Schrage, Meredith Nolan, Joseph Cope, Maya Thomas, and Kristen Sharpe for assistance with experimental trials, Ann Tarrant for loaned experimental equipment, Chuck and Maggie Amsler for experimental design input, and Thomas Desvignes for discussion. We thank the captains, crew, and support staff of the R/V *Polar Duke*, ARSV *Laurence M. Gould* and RVIB *Nathaniel B. Palmer*, the support of personnel at Palmer Station, Antarctica, and the Leidos Antarctic Support Contractors. This work was funded by the National Science Foundation Office of Polar Program (OPP-1440435 and 2026045 for specimen and environmental data collection and OPP-1947040) and Division of Biological Infrastructure (DBI-1349327 for specimen preservation and analysis), and the VIMS John Olney Fellowship.

References

Andriashev AP. 1965. A General Review of the Antarctic Fish Fauna. In: van Mieghem J, van Oye P, editors. Biogeography and Ecology in Antarctica. Dordrecht: Springer Netherlands. p. 491–550. https://doi.org/10.1007/978-94-015-7204-0_15

Baalsrud HT, Tørresen OK, Solbakken MH, Salzburger W, Hanel R, Jakobsen KS, Jentoft S. 2018. De novo gene evolution of antifreeze glycoproteins in codfishes revealed by whole genome sequence data. Molecular Biology and Evolution. 35(3):593–606.

Beers JM, Jayasundara N. 2015. Antarctic notothenioid fish: what are the future consequences of 'losses' and 'gains' acquired during long-term evolution at cold and stable temperatures? Journal of Experimental Biology. 218(12):1834–1845.

Beers JM, Sidell BD. 2011. Thermal Tolerance of Antarctic Notothenioid Fishes Correlates with Level of Circulating Hemoglobin. Physiological and Biochemical Zoology. 84(4):353–362. https://doi.org/10.1086/660191

Bilyk KT, DeVries AL. 2011. Heat tolerance and its plasticity in Antarctic fishes. Comparative Biochemistry and Physiology Part A: Molecular & Integrative Physiology. 158(4):382–390.

Boulenger GA. 1902. Pisces. In: Report on the collections of natural history made in the Antarctic regions during the voyage of the "Southern Cross" [ix, 344 p, 53 leaves of plates]. https://www.marinespecies.org/aphia.php?p=sourcedetails&id=348394

Campbell H, Davison W, Fraser KPP, Peck LS, Egginton S. 2009. Heart rate and ventilation in Antarctic fishes are largely determined by ecotype. Journal of Fish Biology. 74(3):535–552. https://doi.org/10.1111/j.1095-8649.2008.02141.x

Cárdenas CA, González-Aravena M, Santibañez PA. 2018. The importance of local settings: within-year variability in seawater temperature at South Bay, Western Antarctic Peninsula. PeerJ. 6:e4289. https://doi.org/10.7717/peerj.4289

Casaux R. 1998. The contrasting diet of *Harpagifer antarcticus* (Notothenioidei, Harpagiferidae) at two localities of the South Shetland Islands, Antarctica. Polar Biology. 19(4):283–285. https://doi.org/10.1007/s003000050246

Clarke A, Beaumont JC. 2020. An extreme marine environment: a 14-month record of temperature in a polar tidepool. Polar Biology. 43(12):2021–2030. https://doi.org/10.1007/s00300-020-02762-8

Comte L, Olden JD. 2017. Evolutionary and environmental determinants of freshwater fish thermal tolerance and plasticity. Global Change Biology. 23(2):728–736. https://doi.org/10.1111/gcb.13427

Corso AD, Steinberg DK, Stammerjohn SE, Hilton EJ. 2022. Climate drives long-term change in Antarctic Silverfish along the western Antarctic Peninsula. Communications biology. 5(1):1–10.

Coston-Clements L, Settle LR, Hoss DE, Cross FA. 1991. Utilization of the Sargassum Habitat by Marine Invertebrates and Vertebrates, a Review. U.S. Department of Commerce, National Oceanic and Atmospheric Administration, National Marine Fisheries Service, Southeast Fisheries Science Center, Beaufort Laboratory.

Dahlke FT, Wohlrab S, Butzin M, Pörtner H-O. 2020. Thermal bottlenecks in the life cycle define climate vulnerability of fish. Science. 369(6499):65–70. https://doi.org/10.1126/science.aaz3658

DeWitt HH, Hureau JC. 1980. Fishes collected during" Hero" cruise 72-2 in the Palmer Archipelago, Antarctic, with the description of two new general and three new species. Bulletin du Museum National d'Histoire Naturelle Zoologie (France).

Downie AT, Illing B, Faria AM, Rummer JL. 2020. Swimming performance of marine fish larvae: review of a universal trait under ecological and environmental pressure. Reviews in Fish Biology and Fisheries. 30(1):93–108. https://doi.org/10.1007/s11160-019-09592-w

Drost HE, Fisher J, Randall F, Kent D, Carmack EC, Farrell AP. 2016. Upper thermal limits of the hearts of Arctic cod *Boreogadus saida*: adults compared with larvae. Journal of Fish Biology. 88(2):718–726. https://doi.org/10.1111/jfb.12807

Duarte WE, Moreno CA. 1981. The specialized diet of *Harpagifer bispinis*: its effect on the diversity of Antarctic intertidal amphipods. Hydrobiologia. 80:241–250.

Duhamel G, Hulley P-A, Causse R, Koubbi P, Vacchi M, Pruvost P, Vigetta S, Irisson J-O, Mormede S, Belchier M. 2014. Biogeographic patterns of fish. 328-362.

Eastman JT. 2017. Bathymetric distributions of notothenioid fishes. Polar Biology. 40(10):2077–2095. https://doi.org/10.1007/s00300-017-2128-x

Ern R, Andreassen AH, Jutfelt F. 2023. Physiological Mechanisms of Acute Upper Thermal Tolerance in Fish. Physiology. 38(3):141–158. https://doi.org/10.1152/physiol.00027.2022

Evans CW, Williams DE, Vacchi M, Brimble MA, DeVries AL. 2012. Metabolic and behavioural adaptations during early development of the Antarctic silverfish, *Pleuragramma antarcticum*. Polar Biology. 35(6):891–898. https://doi.org/10.1007/s00300-011-1134-7

Felsenstein J. 1985. Phylogenies and the Comparative Method. The American Naturalist. 125(1):1–15.

Gille ST. 2002. Warming of the Southern Ocean Since the 1950s. Science. 295(5558):1275–1277. https://doi.org/10.1126/science.1065863

Giménez EM, Barrantes ME, Fernández DA, Lattuca ME. 2021. Thermal responses of two sub-Antarctic notothenioid fishes, the black southern cod *Patagonotothen tessellata* (Richardson, 1845) and the Magellan plunderfish *Harpagifer bispinis* (Forster, 1801), from southern South America. Polar Biology. 44(6):1055–1067. https://doi.org/10.1007/s00300-021-02852-1

Gon O, Heemstra PC. 1990. Fishes of the Southern Ocean. JLB Smith Institute of Ichthyology Grahamstown.

González-Herrero S, Barriopedro D, Trigo RM, López-Bustins JA, Oliva M. 2022. Climate warming amplified the 2020 record-breaking heatwave in the Antarctic Peninsula. Communications Earth and Environment. 3(1):1–9. https://doi.org/10.1038/s43247-022-00450-5

Holeton GF. 1970. Oxygen uptake and circulation by a hemoglobinless Antarctic fish (*Chaenocephalus aceratus* Lonnberg) compared with three red-blooded Antartic fish. Comparative biochemistry and physiology. 34(2):457–471.

Hunt BM, Hoefling K, Cheng C-HC. 2003. Annual warming episodes in seawater temperatures in McMurdo Sound in relationship to endogenous ice in notothenioid fish. Antartic Science. 15(3):333–338. https://doi.org/10.1017/S0954102003001342

Kellermann AK. 1990. Identification key and catalogue of larval Antarctic fishes. Ber Polarforsch.(67):1–138.

Kennicutt MC, Bromwich D, Liggett D, Njåstad B, Peck L, Rintoul SR, Ritz C, Siegert MJ, Aitken A, Brooks CM, et al. 2019. Sustained Antarctic Research: A 21st Century Imperative. One Earth. 1(1):95–113. https://doi.org/10.1016/j.oneear.2019.08.014

Kock K-H, Kellermann A. 1991. Reproduction in Antarctic notothenioid fish. Antarctic Science. 3(2):125–150.

La Mesa M, Castelli A, Eastman JT, Riginella E. 2015. Factors involved in prey resource partitioning in the genus *Artedidraco* (Notothenioidei, Artedidraconidae) from the western Ross Sea. Hydrobiologia. 761(1):249–259. https://doi.org/10.1007/s10750-015-2206-4

Llompart FM, Fernández DA, Aureliano D, La Mesa M. 2020. Life-history traits of the Magellan plunderfish *Harpagifer bispinis* (Forster, 1801) in the Beagle Channel (Tierra del Fuego, South America). Polar Biology. 43(10):1643–1654. https://doi.org/10.1007/s00300-020-02735-x

Lönnberg E. 1905. The fishes of the Swedish South Polar expedition. Lithographisches Institut des Generalstabs.

Lönnberg E. 1906. Contributions to the fauna of South Georgia. Almqvist & Wiksells.

Lutterschmidt WI, Hutchison VH. 1997. The critical thermal maximum: history and critique. Canadian Journal of Zoology. 75(10):1561–1574.

Mark FC, Hirse T, Pörtner HO. 2005. Thermal sensitivity of cellular energy budgets in some Antarctic fish hepatocytes. Polar Biology. 28(11):805–814. https://doi.org/10.1007/s00300-005-0018-0

Meredith MP, King JC. 2005. Rapid climate change in the ocean west of the Antarctic Peninsula during the second half of the 20th century. Geophysical Research Letters. 32(19). https://doi.org/10.1029/2005GL024042

Minnett P, Kaiser-Weiss A. 2012. Near-surface oceanic temperature gradients. GHRSST Discussion Doc. 7.

Mintenbeck K, Barrera-Oro ER, Brey T, Jacob U, Knust R, Mark FC, Moreira E, Strobel A, Arntz WE. 2012. Impact of climate change on fishes in complex Antarctic ecosystems. In: Advances in ecological research. Vol. 46. Elsevier; p. 351–426.

Miya T, Gon O, Mwale M, Cheng C-HC. 2016. Multiple independent reduction or loss of antifreeze trait in low Antarctic and sub-Antarctic notothenioid fishes. Antarctic Science. 28(1):17–28. https://doi.org/10.1017/S0954102015000413

Morgan R, Finnøen MH, Jutfelt F. 2018. CTmax is repeatable and doesn’t reduce growth in zebrafish. Sci Rep. 8(1):7099. https://doi.org/10.1038/s41598-018-25593-4

Morrison AL, Heyblom KB, Singh HA, Rasch PJ. 2022. Projected Antarctic extreme heat events in a warming world. *Authorea Preprints*. https://doi.org/10.1002/essoar.10510941.1

Moyano M, Candebat C, Ruhbaum Y, Alvarez-Fernandez S, Claireaux G, Zambonino-Infante J-L, Peck MA. 2017. Effects of warming rate, acclimation temperature and ontogeny on the critical thermal maximum of temperate marine fish larvae. PLoS One. 12(7):e0179928.

Pan BJ, Vernet M, Manck L, Forsch K, Ekern L, Mascioni M, Barbeau KA, Almandoz GO, Orona AJ. 2020. Environmental drivers of phytoplankton taxonomic composition in an Antarctic fjord. Progress in Oceanography. 183:102295.

Parker E, Near TJ. 2022. Phylogeny Reconciles Classification in Antarctic Plunderfishes. Ichthyology & Herpetology. 110(4). https://doi.org/10.1643/i2021126

Peck LS, Morley SA, Richard J, Clark MS. 2014. Acclimation and thermal tolerance in Antarctic marine ectotherms. Davies SA, Dow JAT, Lukowiak K, editors. Journal of Experimental Biology. 217(1):16–22. https://doi.org/10.1242/jeb.089946

Pörtner HO, Bennett AF, Bozinovic F, Clarke A, Lardies MA, Lucassen M, Pelster B, Schiemer F, Stillman JH. 2006. Trade-Offs in Thermal Adaptation: The Need for a Molecular to Ecological Integration. Physiological and Biochemical Zoology. 79(2):295–313. https://doi.org/10.1086/499986

R Core Team. 2022. R: A language and environment for statistical computing. https://www.R-project.org/

Regan CT. 1914. II.—Diagnoses of new marine fishes collected by the British Antarctic (‘Terra Nova’) Expedition. Annals and magazine of Natural History. 13(73):11–17.

Rintoul SR, Chown SL, DeConto RM, England MH, Fricker HA, Masson-Delmotte V, Naish TR, Siegert MJ, Xavier JC. 2018. Choosing the future of Antarctica. Nature. 558(7709):233–241.

Robinson SA. 2022. Climate change and extreme events are changing the biology of Polar Regions. Global Change Biology. 28(20):5861–5864. https://doi.org/10.1111/gcb.16309

Robinson SA, Klekociuk AR, King DH, Pizarro Rojas M, Zúñiga GE, Bergstrom DM. 2020. The 2019/2020 summer of Antarctic heatwaves. Global Change Biology. 26(6):3178–3180. https://doi.org/10.1111/gcb.15083

Rombough PJ. 1988. 2 Respiratory Gas Exchange, Aerobic Metabolism, and Effects of Hypoxia During Early Life. In: Hoar WS, Randall DJ, editors. Fish Physiology. Vol. 11. Academic Press. p. 59–161. https://doi.org/10.1016/S1546-5098(08)60199-5

Roule L. 1913. Deuxième expédition antarctique française (1908-1910), commandée par le Dr Jean Charcot: sciences naturelles : documents scientifique. Poissons. Paris: Masson et cie.

Saint-Paul U, Hubold G, Ekau W. 1988. Acclimation effects on routine oxygen consumption of the Antarctic fish *Pogonophryne scotti* (Artedidraconidae). Polar Biol. 9(2):125–128. https://doi.org/10.1007/BF00442040

Schmidtko S, Heywood KJ, Thompson AF, Aoki S. 2014. Multidecadal warming of Antarctic waters. Science. 346(6214):1227–1231.

Somero GN, DeVries AL. 1967. Temperature Tolerance of Some Antarctic Fishes. Science. 156(3772):257–258. https://doi.org/10.1126/science.156.3772.257

Swart NC, Gille ST, Fyfe JC, Gillett NP. 2018. Recent Southern Ocean warming and freshening driven by greenhouse gas emissions and ozone depletion. Nature Geosciences. 11(11):836–841. https://doi.org/10.1038/s41561-018-0226-1

Todgham AE, Mandic M. 2020. Understanding the Metabolic Capacity of Antarctic Fishes to Acclimate to Future Ocean Conditions. Integrative and Comparative Biology. 60(6):1425–1437. https://doi.org/10.1093/icb/icaa121

Table 1. Prior studies on cryonotothenioid thermal tolerance during early life stages. All study locations are in the Southern Ocean with the exception noted by asterisk (*).

Family	Species	n	Size	Stage(s)	Location	Procurement method	Relevant findings	Study
Nototheniidae	*Pleuragramma antarctica*	10	9mm SL	Larvae	Terra Nova Bay	Captured under sea ice	CTmax of 14.55 ± 0.87° C	Evans et al. 2012
Nototheniidae	*Trematomus bernacchii*	7 - 11 per treatment	41.7 ± 1.5mm SL	Juvenile	McMurdo Sound	Collected by SCUBA divers	Warming of 3° C (-1 to 2° C) increased heart rate, ventilation rate, and metabolic rate after 14 days. This increase also impacted fish behavior, with 12% reduced swimming activty. In the absence of elevated pCO2, fish showed some signs of warm acclimation by 28 days. However, elevated pCO2 (~1,200 uatm) prevented acclimation.	Davis et al. 2018
Nototheniidae	*Trematomus bernacchii*	7 - 11 per treatment	38.4 - 45.7 mm SL	Juvenile	McMurdo Sound	Collected by SCUBA divers	Warming (+3° C) increases growth rate of otoliths, while increased pCO2 level has no impact over 28 days	Naslund et al. 2021
Nototheniidae	*Patagonotothen cornucola*	10 per treatment	6.77–8.37 mm SL	Yolk-sac larvae	*Beagle Channel, Argentina	Collected by SCUBA divers	Larvae exposed to 12° C warming (4 to 16° C) over 4 days absorbed their yolk faster and grew more in length. CTmax of 18.5° C, which increased to 21.7° C after 4 days of warm (+12° C) acclimation	Bruno et al. 2022
Bathydraconidae	*Gymnodraco acuticeps*	5 - 25 per treatment	3.35 ± 0.01 egg diameter	Eggs	McMurdo Sound	Single clutch collected by SCUBA divers	Increased pCO2 (1000 uatm) and warming (+3° C) positively impact embryonic development rate over 3 weeks when they are seperately applied. However, when incresaed pCO2 and warming were applie together, development slowed and mortality increased.	Flynn et al. 2015
Bathydraconidae	*Gymnodraco acuticeps*	16 - 18 per treatment	Not provided	Eggs	McMurdo Sound	Single clutch collected by SCUBA divers	No evidence embryos exceeded thermal tolerance at 8°C. Greatest metabolic (Q10) thermal sensitivity exibited by embryos at the earliest developmental stage.	Flynn and Todgham 2018

Table 2. Mean critical thermal maxima (CTmax) and standard deviations (SD) of larval cryonotothenioids collected near the western Antarctic Peninsula during this study. Sample sizes (n), standard lengths (SL). Previously determined adult CTmax are reported for *C. rastrospinosus* and *L. squamifrons*.

Group	**n**	**SL (mm ± SD)**	**CTmax (C° ± SD)**	**Adult CTmax (C° ± SD)**
Channichthyidae	13	39.9 (± 12.2)	10.9 (± 1.4)	
Chionodraco rastrospinosus	10	36.9 (± 12.5)	10.6 (± 1.4)	13.3 (± 0.2)*
Chaenodraco wilsoni	2	49.9 (± 3.5)	11.7 (± 0.9)	
Cryodraco antarcticus	1	49.2	12.3	
Artedidraconidae	14	19.4 (± 2.9)	15.4 (± 1.6)	
Doliodraco longedorsalis	8	19.2 (± 3.6)	14.3 (± 1.0)	
Neodrao skottsbergi	6	19.6 (± 2.0)	16.8 (± 1.0)	
Nototheniidae	4	44.4 (± 9.6)	13.9 (± 1.2)	
Trematomus scotti	2	49.3 (± 13.5)	14.3 (± 0.9)	
Lepidonotothen squamifrons	2	39.6 (± 0.6)	13.6 (± 1.8)	15.38 (± 1.02)**

* (Beers and Sidell 2011)
** (Bilyk and DeVries 2011)

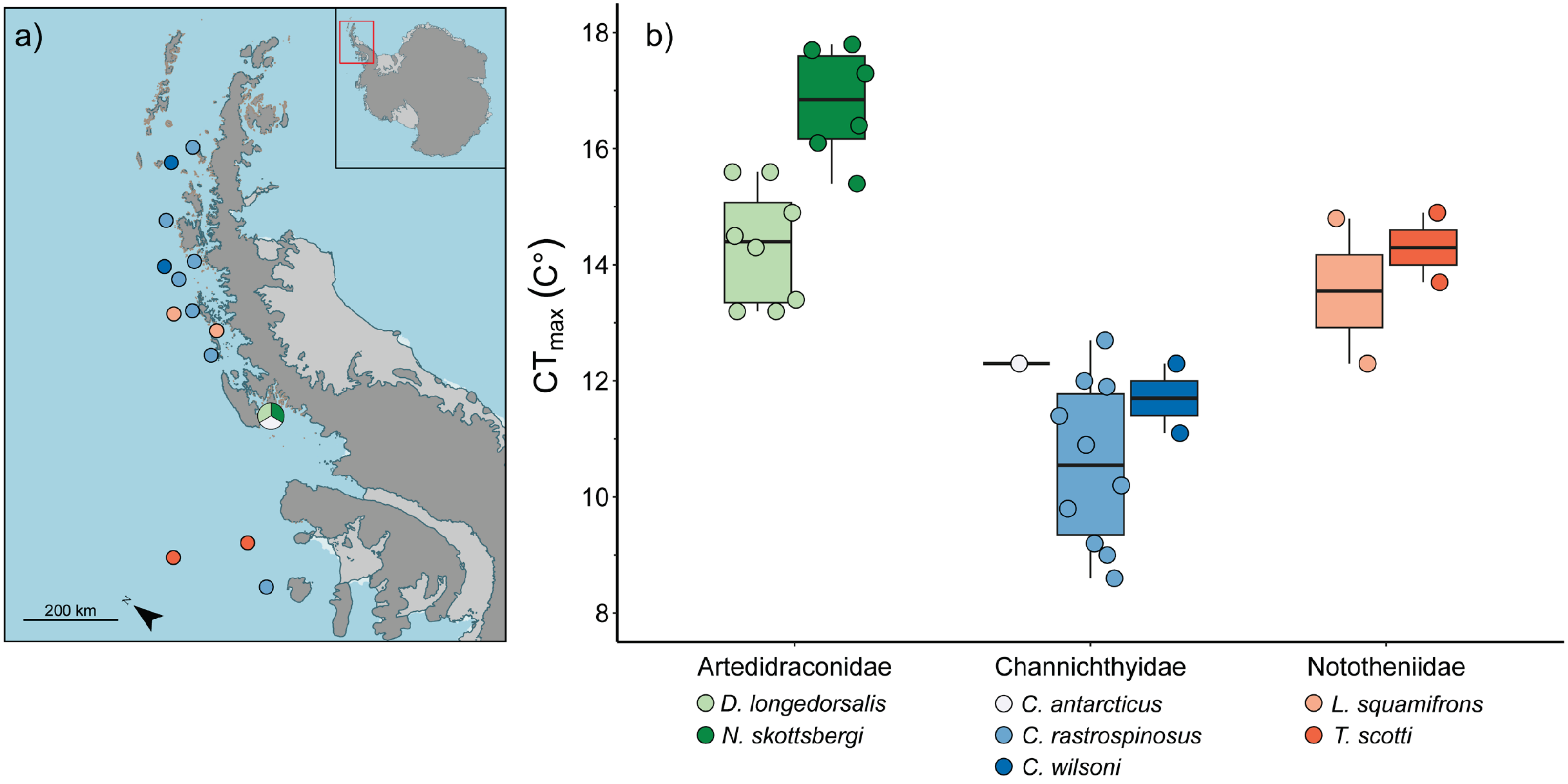

Figure 1. Larval fish collection sites and critical thermal maxima (CTmax). a) Map of the western Antarctic Peninsula (WAP) region indicating where larvae were collected on research cruises from 2020 – 2023 for experiments. Point color corresponds to the key in 1b. All artedidraconids and one *C. antarcticus* were collected in the same region in Dalgleish Bay over two cruises (2022 and 2023) and are represented by a tricolor circle. b) Box and whisker plots of cryonotothenioid CTmax values determined experimentally. Boxes are centered on median values (horizontal black lines) with vertical black lines extending to upper and lower extremes. The top and bottom of the boxes respectively correspond to the upper and lower quartiles. Each circle represents an individual experimental fish, color corresponds to species in the key below.

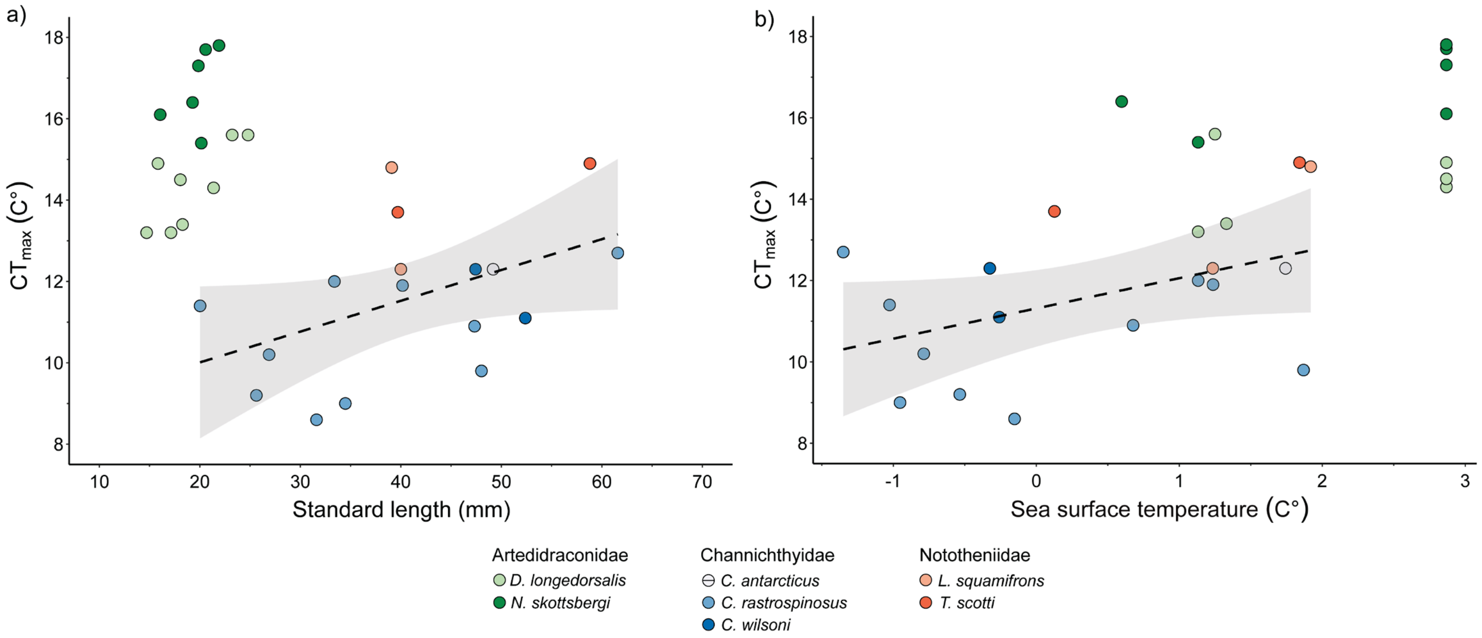

Figure 2. Relationship between a) standard length and b) sea surface temperature at collection location of all larvae in this study and CTmax. Linear regression (black dashed line) fitted only to fishes from Channichthyidae and Nototheniidae with species from Artedidraconidae (light and dark green circles) excluded. Grey shading represents 95% confidence intervals.

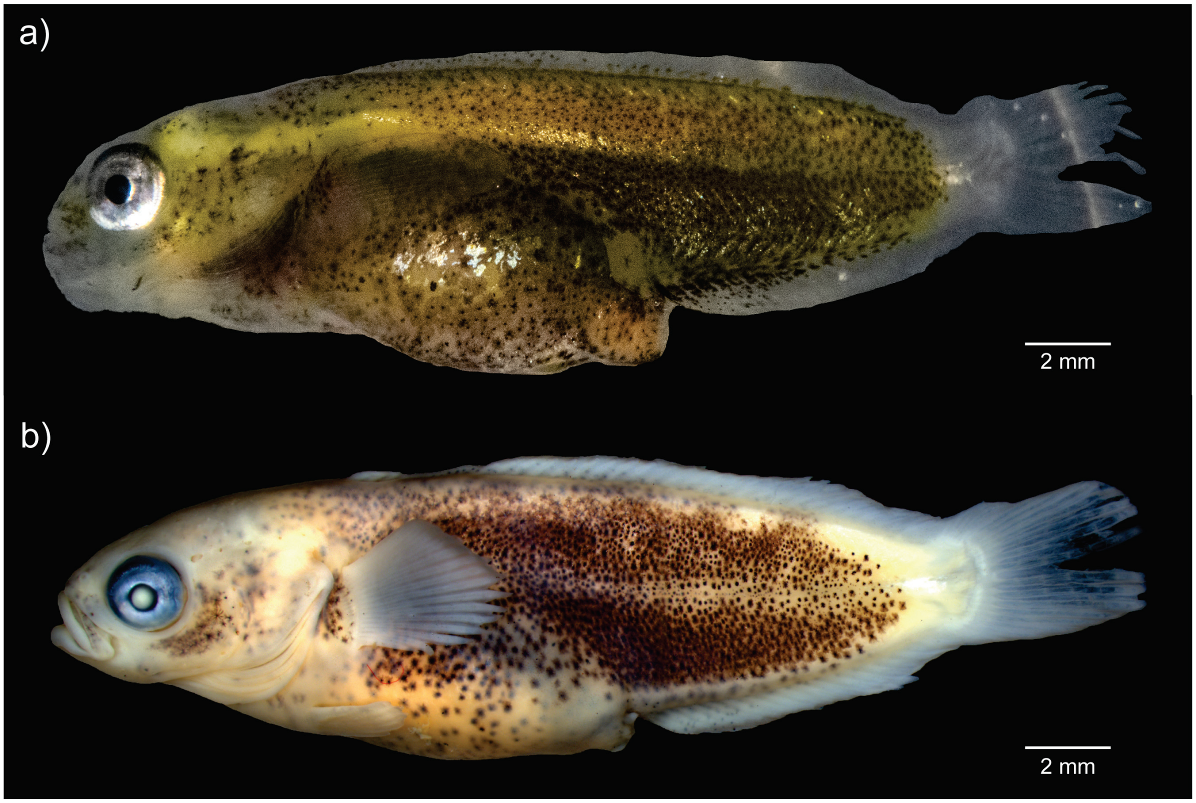

Figure 3. Post-flexion larva of *Neodraco skottsbergi* live (a) and preserved in 95% ethanol (b). VIMS 43504, SL 18.6 mm

CHAPTER 7
Summary and concluding remarks

This dissertation provides a multifaceted view on the vulnerable early life stages of fishes in a rapidly changing polar ecosystem. Chapter 2 shows that larval *Pleuragramma antarctica* abundance in the WAP is influenced by the amount of sea ice present during the adult spawning period; and is the first statistically significant relationship reported between sea ice and the abundance of any Antarctic fish species. Chapter 3 provides a description of the larval stages of *A. nudiceps*. In addition to advancing the biological and taxonomic understanding of the genus *Akarotaxis*, this study also led to the discovery of the species *Akarotaxis* n. sp. that is described in Chapter 4, the first newly described bathydraconid species since 1995. Chapter 5 explores the community composition and phenology of a coastal WAP larval fish assemblage during two seasons with contrasting sea-ice conditions, showing the influence of prey (copepods and diatoms) and sea ice on seasonal changes in larval nototheniid fish abundance. Chapter 5 also employs recent innovations in ocean modeling to determine the spawning region of an abundant nototheniid fish. Finally, Chapter 6 investigates the thermal tolerances of several larval notothenioid taxa, suggesting that larvae of the artedidraconid *N. skottsbergi* are among the most thermally tolerant Antarctic fishes based on CTmax values, while larval channichthyids are among the least tolerant. These combined results increase understanding of the ecology of notothenioids, with policy implications for the Southern Ocean, and also establish key future research objectives.

The impacts of anthropogenic climate change are now linked to the reproductive success of the keystone species *P. antarctica* (Chapter 2). Ongoing declines of sea ice (Eayrs et al. 2021) driven by the intensification and increased variability of climatic features such as the El Niño–Southern Oscillation (Cai et al. 2023) will likely have negative impacts on *P. antarctica* and the surrounding WAP ecosystem, including an imperiled population of Adélie penguins (Fraser and Hofmann 2003). This chapter also establishes the first correlation between the Amundsen Sea Low (ASL) and the abundance of any organism. Although the impacts of the ASL, the Southern Annular Mode (SAM), and other climatic teleconnections on Antarctic climate are an area of intense interest, few previous studies have considered ecosystem-level consequences of the strengthening and increased variability of these air-sea interactions. In addition to *P. antarctica*, the responses of other cryonotothenioids and WAP food web to shifts in the ASL should be evaluated in future analyses.

Due to the abundance and unique spawning strategy of *P. antarctica*, we focused our initial long-term analysis of the Palmer LTER ichthyoplankton time series on this keystone species. However, climate change is predictably impacting the population dynamics of other cryonotothenioid fishes. Results from thermal tolerance experiments in Chapter 6 identify larval channichthyids as the group to prioritize for future long-term modelling efforts of abundance and distribution. The fishes collected through Palmer LTER likely represent the longest and most complete time series of larval channichthyids and aspects of the population dynamics of the fishes should be examined. Analyses based on larval fishes collected and identified from another long-term time series, such as the California Cooperative Oceanic Fisheries Investigations (CalCOFI), have proved invaluable for the management of near-shore fisheries along the west coast of the United States (Moser et al. 2001). The Palmer LTER ichthyoplankton time series has similar value and potential as an important management tool.

Several additional years of continued Palmer LTER seasonal pelagic trawl surveys are also necessary to further resolve the influences of sea ice and prey on the phenology of the larval fish assemblage. In Chapter 5, changes in the abundance of prey items impact larval cryonotothenioids; therefore, copepod and diatom dynamics could magnify or dampen the effects of climate change on the larval fish assemblage. Although 2017 – 2018 was a low sea ice year, *T. newnesi* abundance increased by an order of magnitude, potentially due to a similar increase in the copepod *C. propinqus*, which prefers open water. Stomach content analysis of ichthyoplankton collected by the Palmer LTER can elucidate trophic niches of fish larvae, which will help determine the impacts of prey variability on abundance and growth of larval fishes.

Perhaps the most informative source of data collected by the Palmer LTER to elucidate additional impacts of climate change on growth, condition, and temperature sensitivity among larval cryonotothenioids has yet to be exploited. As described in Chapter 5, otoliths from preserved larvae can be used to more accurately estimate daily growth rates (La Mesa et al. 2017). Furthermore, oxygen isotope analysis of otoliths can be used to reconstruct daily temperatures that larvae experience (Reis-Santos et al. 2023). Correlations between environmental temperatures and metabolic rates of fishes can then be reconstructed using carbon isotope values (Chung et al. 2019; Reis-Santos et al. 2023). Limitated expertise in larval otolith removal, preparation, and microchemical analysis currently prevents the straightforward accomplishment of these studies. As a compliment to larval identification workshops that are offered annually by the American Fisheries Society, a larval fish otolith preparation and analysis workshop would facilitate the widespread use of these novel otolith analyses for the Palmer LTER time series and larval fish collections globally.

Together with the continued long-term monitoring of *P. antarctica* and other larvae by the Palmer LTER, annual surveys assessing the abundance and condition of adult *P. antarctica* in open water and under sea ice are urgently needed in the WAP region. These assessments would not only build upon our limited understanding of *P. antarctica* biology, but also improve ecosystem-based management (EBM) of the fishery for Antarctic toothfish (*Dissostichus mawsoni*), which relies on *P. antarctica* as prey. Under the pressures of a changing climate, EBM is the only acceptable method to manage fishing in the Southern Ocean (Fulton et al. 2019; Holsman et al. 2020; Cavanagh et al. 2021; Chavez-Molina et al. 2023). Standardized and frequent surveying of rarer notothenioids is also important for better characterization of the diversity and biology of the ichthyofauna, further supporting EBM.

The potential endemism of *Akarotaxis* n. sp. in the WAP region deepens our understanding of cryonotothenioid evolution and biodiversity, highlighting the likely role of deep coastal canyons as bastions of fish diversity during historic glacial maxima. These canyons should be prioritized as targets for benthic trawls to collect *Akarotaxis* n. sp. and other less-studied fishes. Diet analysis of *Akarotaxis spp.* is necessary to understand their ecology and additional drivers of speciation. Furthermore, non-lethal towed camera systems and automated underwater vehicles (AUVs) deployed in canyons could better elucidate the reproductive biology of *Akarotaxis* spp. and other deep-dwelling cryonotothenioids (Jones and Lockhart 2011; Xavier et al. 2016). The National Oceanic and Atmospheric Administration (NOAA) Antarctic Ecosystem Research Division (AERD) is tasked with the U.S. management of Antarctic marine living resources. However, due to funding reductions and shifting administrative priorities, the most recent finfish surveys conducted by NOAA AERD occurred in 2009 for benthic species

(Jones et al. 2009) and 2014 for mesopelagic species (Jones et al. 2014). Increasing the frequency and coverage of such surveys would significantly enhance our understanding of Antarctic fish fauna and facilitate their protection from human exploitation.

In 2019, approximately 90% (360,000 tons) of Antarctic krill harvested from the Southern Ocean were captured in the Antarctic Peninsula (AP) region, or the Commission for the Conservation of Antarctic Marine Living Resources (CCAMLR) subarea 48.1 (Hogg et al. 2020). As discussed in Chapter 4, Antarctic krill harvest results in the bycatch of larval fishes, the biology of many of which is still poorly known. The combined results of this dissertation, including climate-fish connections and novel fish diversity findings, will aid in the development of the regulations and boundaries of a proposed Marine Protected Area (MPA)(CCAMLR 2020) surrounding the AP that would restrict this krill harvest and subsequent fish bycatch.

Antarctic climate change is complex, variable, and alarming. As we are only beginning to untangle the intricate drivers of warming and sea ice loss in the WAP region, fish communities have already undergone shifts that could irreversibly alter the ecosystem. Studying aspects of these vulnerable communities can lead to pessimism regarding their long-term outlook. Associated impacts, such loss of biodiversity, diminished ecosystem services, and rising sea level from glacial melt, also appear bleak. However, through the continued long-term monitoring and interdisciplinary analyses of these fishes, we can begin to understand more accurately what is at risk from our societal choices. It is my hope that publishing and communicating these risks, through this dissertation and future efforts, might serve to inspire awareness and policy action to slow the looming changes that threaten one of the most pristine and unique places on Earth.

References

Cai W, Jia F, Li S, Purich A, Wang G, Wu L, Gan B, Santoso A, Geng T, Ng B, et al. 2023. Antarctic shelf ocean warming and sea ice melt affected by projected El Niño changes. Nature Climate Change. 13(3):235–239. https://doi.org/10.1038/s41558-023-01610-x

Cavanagh RD, Trathan PN, Hill SL, Melbourne-Thomas J, Meredith MP, Hollyman P, Krafft BA, MC Muelbert M, Murphy EJ, Sommerkorn M, et al. 2021. Utilising IPCC assessments to support the ecosystem approach to fisheries management within a warming Southern Ocean. Marine Policy. 131:104589. https://doi.org/10.1016/j.marpol.2021.104589

CCAMLR. 2020. Revised proposal for a conservation measure establishing a Marine Protected Area in Domain 1 (Western Antarctic Peninsula and South Scotia Arc) CCAMLR-39/08 Rev. 1. [accessed 2023 Jun 26]. https://meetings.ccamlr.org/en/ccamlr-39/08-rev-1

Chavez-Molina Vasco, Nocito ES, Carr E, Cavanagh RD, Sylvester Z, Becker SL, Dorman DD, Wallace B, White C, Brooks CM. 2023. Managing for climate resilient fisheries: Applications to the Southern Ocean. Ocean & Coastal Management. 239:106580. https://doi.org/10.1016/j.ocecoaman.2023.106580

Chung M-T, Trueman CN, Godiksen JA, Holmstrup ME, Grønkjær P. 2019. Field metabolic rates of teleost fishes are recorded in otolith carbonate. Communications Biology. 2:24. https://doi.org/10.1038/s42003-018-0266-5

Eayrs C, Li X, Raphael MN, Holland DM. 2021. Rapid decline in Antarctic sea ice in recent years hints at future change. Nature Geosciences. 14(7):460–464. https://doi.org/10.1038/s41561-021-00768-3

Fraser W, Hofmann E. 2003. A predator's perspective on causal links between climate change, physical forcing and ecosystem response. Marine Ecological Progress Series. 265:1–15. https://doi.org/10.3354/meps265001

Fulton EA, Punt AE, Dichmont CM, Harvey CJ, Gorton R. 2019. Ecosystems say good management pays off. Fish and Fisheries. 20(1):66–96. https://doi.org/10.1111/faf.12324

Hogg CJ, Lea M-A, Gual Soler M, Vasquez VN, Payo-Payo A, Parrott ML, Santos MM, Shaw J, Brooks CM. 2020. Protect the Antarctic Peninsula — before it's too late. Nature. 586(7830):496–499. https://doi.org/10.1038/d41586-020-02939-5

Holsman KK, Haynie AC, Hollowed AB, Reum JCP, Aydin K, Hermann AJ, Cheng W, Faig A, Ianelli JN, Kearney KA, Punt AE. 2020. Ecosystem-based fisheries management forestalls climate-driven collapse. Nature Communications. 11(1):4579. https://doi.org/10.1038/s41467-020-18300-3

Jones CD, Damerau M, Deitrich K, Driscoll R, Kock K-H, Kuhn K, Moore J, Morgan T, Near T, Pennington J. 2009. Demersal finfish survey of the South Orkney Islands. NOAA Technical Memorandum NMFS SWFSC. 445:49–66.

Jones CD, Koubbi P, Catalano B, Dietrich K, Ferm N. 2014. Mesopelagic and larval fish survey. NOAA Technical Memorandum NMFS SWFSC. 524:28–40.

Jones CD, Lockhart SJ. 2011. Detecting Vulnerable Marine Ecosystems in the Southern Ocean using research trawls and underwater imagery. Marine Policy. 35(5):732–736. https://doi.org/10.1016/j.marpol.2011.02.004

La Mesa M, Riginella E, Catalano B, Jones CD, Mazzoldi C. 2017. Maternal contribution to spawning and early life-history strategies of the genus *Lepidonotothen* (Nototheniidae, Perciformes) along the southern Scotia Arc. Polar Biology. 40(7):1441–1450. https://doi.org/10.1007/s00300-016-2068-x

Moser H, Charter R, Watson W, Ambrose D, Hill K, Smith P, Butler J, Sandknop E, Charter S. 2001. The CalCOFI ichthyoplankton time series: Potential contributions to the management of rocky-shore fishes. California Cooperative Oceanic Fisheries Investigations Report. 42:112–128.

Reis-Santos P, Gillanders BM, Sturrock AM, Izzo C, Oxman DS, Lueders-Dumont JA, Hüssy K, Tanner SE, Rogers T, Doubleday ZA, et al. 2023. Reading the biomineralized book of life: expanding otolith biogeochemical research and applications for fisheries and ecosystem-based management. Reviews in Fish Biology and Fisheries. 33(2):411–449. https://doi.org/10.1007/s11160-022-09720-z

Xavier JC, Brandt A, Ropert-Coudert Y, Badhe R, Gutt J, Havermans C, Jones C, Costa ES, Lochte K, Schloss IR, et al. 2016. Future Challenges in Southern Ocean Ecology Research. Frontiers in Marine Science. 3. https://www.frontiersin.org/articles/10.3389/fmars.2016.00094

VITA

Andrew Derik Corso was born in Long Branch, NJ, grew up in Pass Christian, MS, and graduated from Tuscarora High School, Leesburg, VA in August 2013. He was a visiting student at the Sea Semester Program in 2016 and graduated from William & Mary with a B.S. in Biology in January 2017. After a 6-month internship at the National Aeronautics and Space Administration Langley Research Center, Andrew entered the Masters program at the Virginia Institute of Marine Science (VIMS), William & Mary in August 2017 under the graduate co-advisors Drs. Eric J. Hilton and Deborah K. Steinberg. He bypassed into the Ph.D. program in 2021. At VIMS, he conducted research in Antarctica during four field seasons from 2017 – 2023. He is currently a Project Manager and Research Associate at the Coonamessett Farm Foundation, MA.